

## Durham E-Theses

---

### *The petrology and geochemistry of the north qoroq centre igaliko complex, south greenland*

Chambers, A. D.

#### How to cite:

---

Chambers, A. D. (1976) *The petrology and geochemistry of the north qoroq centre igaliko complex, south greenland*, Durham theses, Durham University. Available at Durham E-Theses Online:  
<http://etheses.dur.ac.uk/8342/>

#### Use policy

---

The full-text may be used and/or reproduced, and given to third parties in any format or medium, without prior permission or charge, for personal research or study, educational, or not-for-profit purposes provided that:

- a full bibliographic reference is made to the original source
- a [link](#) is made to the metadata record in Durham E-Theses
- the full-text is not changed in any way

The full-text must not be sold in any format or medium without the formal permission of the copyright holders.

Please consult the [full Durham E-Theses policy](#) for further details.

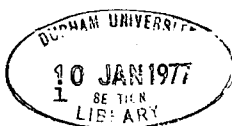
THE PETROLOGY AND GEOCHEMISTRY OF THE  
NORTH QÔROQ CENTRE  
IGALIKO COMPLEX, SOUTH GREENLAND

A.D. Chambers, B.Sc. (Dunelm)

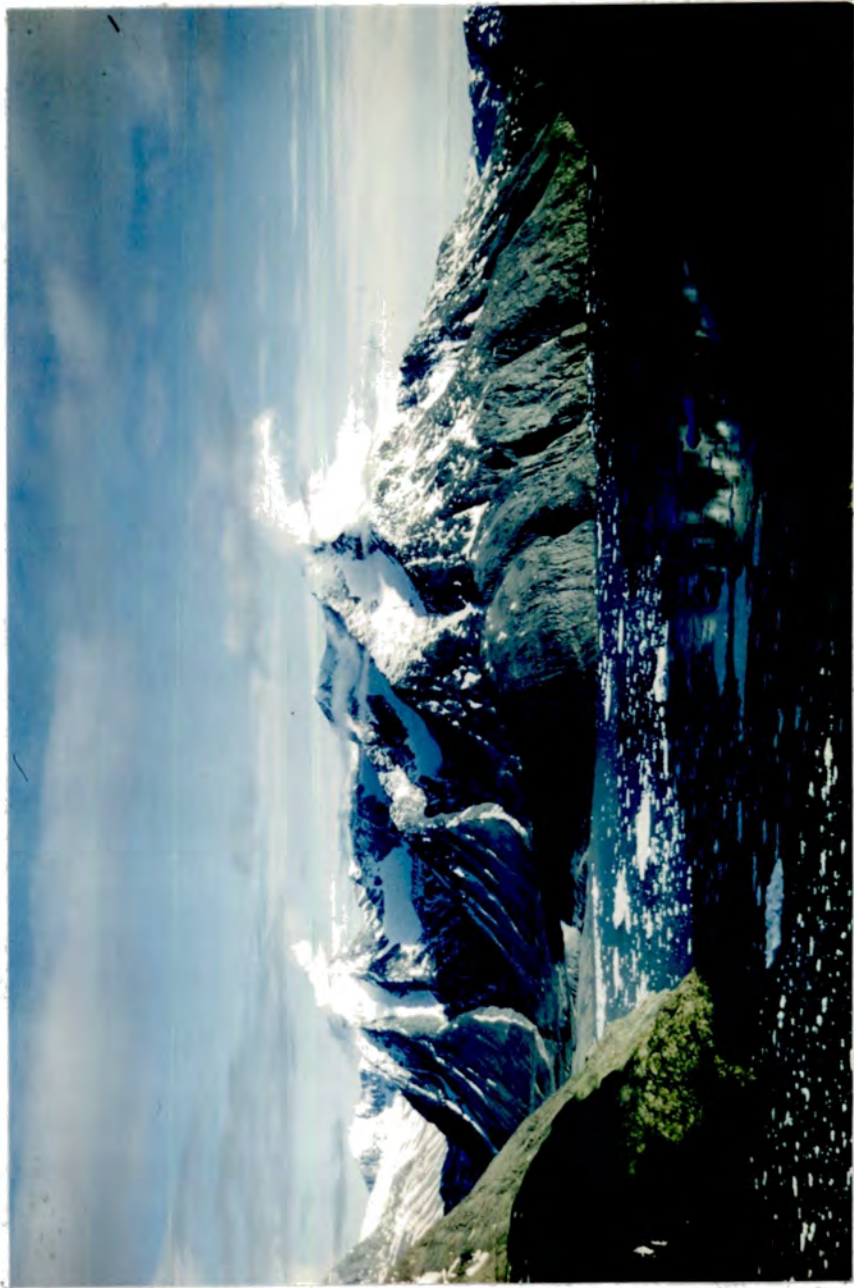
A thesis submitted for the Degree of Doctor  
of Philosophy in the  
University of Durham

September 1976

The copyright of this thesis rests with the author.  
No quotation from it should be published without  
his prior written consent and information derived  
from it should be acknowledged.



Frontispiece. View of the Igdlerfigssalik  
Centre taken from the North Qôroq Centre. July 1972.



## ABSTRACT

The North Qôroq Centre is one of four major intrusive centres comprising the Igaliko Nepheline Syenite Complex. The centre is composed of a number of syenitic bodies all showing undersaturated character. Emplacement of the bodies was probably by ring fracture and block subsidence, combined with a degree of stoping.

Petrographic, mineralogical and geochemical studies have demonstrated that the process of in situ fractionation accounts for the bulk of the variation in rock types seen in the centre. Clinopyroxene, olivine, Fe/Ti oxides and apatite were important early fractionating phases, followed by amphibole and biotite. The most important fractionating phase was, however, alkali feldspar. Its crystallization and separation resulted in peralkaline undersaturated syenites becoming more peralkaline and more undersaturated.

Probe work on the majority of major mineral phases, present in the syenites, has enabled values to be placed on a number of important physical and chemical parameters. The temperature of the magma as it evolved and the values and effect of steadily varying silica activity, oxygen fugacity, water fugacity, and activity of sodium disilicate have all been considered.

An alkali-rich aqueous phase probably co-existed with the more fractionated of the North Qoroq syenites. A

reasonable idea of the nature and composition of this phase has been obtained and a number of features exhibited by the syenites attributed to its action.

Influx of meteoric water at an early stage in the evolution of the magmas is suggested as an explanation for the common marginal pegmatites. This process could be instrumental in deciding whether magmas of trachytic composition proceed, with crystal fractionation, towards undersaturated or oversaturated residual compositions.

## ACKNOWLEDGEMENTS

Thanks are due to many people who assisted in the production and presentation of this thesis:

Dr. C.H. Emeleus for introducing me to the topic and for invaluable advice and discussion.

Professor G.M. Brown for providing research facilities at the University of Durham.

The Natural Environment Research Council for providing financial assistance during the study.

The Greenland Geological Survey for considerable assistance with field work and transportation of material.

Dr. M.D. Walker for acting as a field assistant during the summer of 1972.

Dr. A. Peckett for assistance with electron microprobe analysis.

Dr. J.G. Holland for assistance with X-ray fluorescence analysis.

Dr. B.G.J. Upton for providing rock powders used as X-ray fluorescence standards.

Drs. R. and M. Powell for instruction in the use of thermodynamic techniques.

Dr. I. Parsons and Dr. J.G. Anderson for much useful comment and discussion particularly with regard to the thermodynamics section of this thesis.

Dr. J.L. Knight, Dr. R.H. Pinsent, Mr. R. Hardy and Dr. F.W. Smith for discussion on various aspects of the thesis.

Dr. D. Stephenson whose work on the South Qôroq Centre contributed considerably to the present authors understanding of the geology of North Qôroq.

Mrs. M. Trewin and Mrs. C.L. Mines for typing the thesis.

My wife Kate for production of many of the diagrams and for considerable moral (and financial) support.



CHAPTER 3. PETROGRAPHY

3.1	Introduction	41
3.2	The major syenitic units	41
3.2.1	SN.1A	41
3.2.2	SN.1B	52
3.2.3	SN.2	56
3.2.4	?SN.3	57
3.2.5	SN.4A	58
3.2.6	SN.4B	64
3.2.7	SN.5	65
3.2.8	Conclusions from the major units	69
3.3	The minor units of North Qôroq	70
3.3.1	The microsyenite sheets	70
3.3.2	Carbonate Breccia Plug	71
3.4	The recrystallized rocks	73
3.4.1	Introduction	73
3.4.2	Textures	74
3.4.3	Mineralogical changes	78
3.4.4	Conclusions	82

CHAPTER 4. MINERALOGY

4.1	Olivines	85
4.1.1	Introduction	85
4.1.2	Major element variation	85
4.1.3	Minor element variation	89
4.2	Pyroxenes	93
4.2.1	Introduction	93
4.2.2	Major element variation	94
4.2.3	Minor element variation	98
4.2.4	Colour in North Qôroq pyroxenes	106
4.3	Amphiboles	108
4.3.1	Introduction	108
4.3.2	Classification and nomenclature	109
4.3.3	Chemical variation	116
4.4	Biotites	124
4.4.1	Introduction	124
4.4.2	Chemical variation	125
4.5	Fe/Ti Oxides	130
4.5.1	Introduction	130
4.5.2	Exsolution in the oxides	131
4.5.3	Chemical variation	133
4.6	Feldspars	136
4.6.1	Introduction	136
4.6.2	Structural state and exsolution	137
4.6.3	Major element variation	144
4.6.4	Trace element variation	148
4.6.5	The feldspar solvus, T and P.H <sub>2</sub> O	150

	Page
4.7 Nepheline	153
4.7.1 Introduction	153
4.7.2 Chemical variation	155
4.8 Cancrinite	159
4.9 Sodalite	160
4.10 Analcite	164
4.11 Natrolite	167
4.12 Aenigmatite	168
4.13 Rinkite	171
4.14 Other mineral phases	172
4.15 Conclusions from the mineralogy	172
4.16 Thermodynamic treatment of mineral data	174
4.16.1 Introduction	174
4.16.2 Lithostatic pressure ( $\approx$ P.T.)	178
4.16.3 Temperature (T)	179
4.16.4 Activity of silica in the magma (a.SiO <sub>2</sub> )	187
4.16.5 The fugacity of oxygen (f.O <sub>2</sub> )	194
4.16.6 The activity of sodium disilicate (a.Na <sub>2</sub> Si <sub>2</sub> O <sub>5</sub> ) and its mineral- ogical effects	205
4.16.7 Water vapour pressure (P.H <sub>2</sub> O)	209
4.16.8 Other volatile phases	212
4.16.9 Conclusions from the thermo- dynamic treatment of mineral data	212
 <u>CHAPTER 5. GEOCHEMISTRY</u>	
5.1 Introduction	214
5.2 Major element variation	216
5.3 Minor element variation	220
5.4 Geographical variation in trace element abundances	227
5.5 Normative mineralogy and the residua system	238
5.6 The peralkaline condition	249
 <u>CHAPTER 6. FENITIZATION AND THE AQUEOUS PHASE</u>	
6.1 Introduction	255
6.2 Fenitization of the country rocks around the North Qôroq Centre	257
6.2.1 Field relations	257
6.2.2 Petrography	257
6.2.3 Mineralogy	264
6.2.4 Geochemistry	274
6.2.5 The nature of the fenitizing fluid	284

	Page
6.3 The aqueous phase in the North Qôroq Centre	288
6.3.1 Metasomatism of the syenites	288
6.3.2 Co-existing vapour phase : presence or absence?	289
6.3.3 Marginal pegmatites	294
 <u>CHAPTER 7. CONCLUSIONS</u>	
7.1 Introduction	299
7.2 High level evolution and the state of North Qôroq magmas	299
7.2.1 Fractional crystallization	299
7.2.2 Other processes affecting North Qôroq rocks	305
7.2.3 Physical and chemical conditions of the evolving North Qôroq magmas	306
7.3 Oversaturated or Undersaturated nature of Gardar magmas	310
7.4 Evolution of the syenites at depth	317
7.4.1 Partial melting	317
7.4.2 Fractionation of basalt parent	320
7.4.3 Origin of North Qôroq Magmas	322
7.5 Global Setting of the Gardar Province	324
7.6 Summary	329
 <u>REFERENCES</u>	 330

## CHAPTER ONE: INTRODUCTION

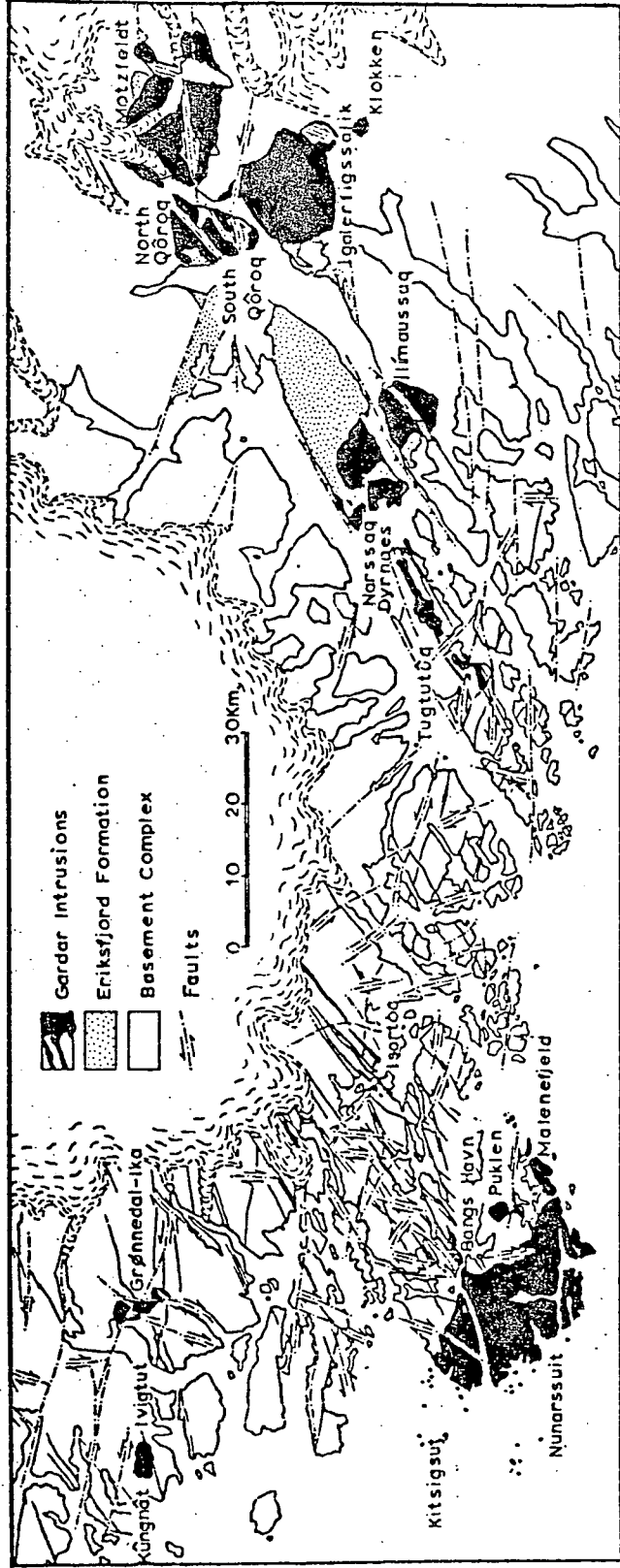
### 1.1. General setting

The Igaliko Nepheline Syenite Complex lies close to the head of Tunugdliarfik fjord in S.W. Greenland. It is one of a number of alkali igneous complexes outcropping in the area. Upton (1974) has produced a recent review of this alkaline province, and a further review, by Emeleus and Upton, is in preparation.

The North Qôroq Centre is the smallest, and most north-westerly, of the four major centres comprising the Igaliko Complex. The other centres are South Qôroq, Motzfeldt and Igdlerfigssalik. Each of these centres is made up of a number of syenitic units, and outside the centres are several small satellitic stocks. The North Qôroq Centre lies at  $61^{\circ}10'N.45^{\circ}20'W$ , close to Narssarssuaq Airport. Its position is indicated on Fig. 1.1, taken from Upton (op.cit.).

The close proximity of the centre to Narssarssuaq Airport made access a relatively simple matter. An excellent camp-site was established close to the reservoir at Narssarssuaq and from this base daily trips were made into the North Qôroq Centre. The prohibitive expense of helicopter hire meant that transportation of samples and equipment had to be on foot.

Fig.1.1 The Gardar Alkaline Igneous Province,  
showing the situation of the central  
complexes, rocks of the Eriksfjord  
Formation and the major faults.  
(Taken from Upton, 1974).



Weather in the summer of 1972 was generally good and little work time was lost. Rain and low cloud occasionally restricted work to the low lying ground around the 'old hospital' at Narssarssuaq. Density winds off the ice-cap were never sufficiently strong to interrupt work.

A constant irritation and annoyance during field-work was the persistent attention of mosquitoes, the larvae of which thrive in the numerous stagnant pools.

The lack of suitable soil in the area results in a sparsity of plant life. Geological exposure is generally good, although on the plateau between Qôroq and Narssarssuaq the rocks weather to give a coarse gravel.

## 1.2. General geology and terrain

The Igaliko Complex consists dominantly of Precambrian nepheline syenites (1310<sup>±</sup>31 - 1167<sup>±</sup>15 m.y. Blaxland et al., in press). It is cut by a variety of dykes and intrudes into basement granite/granite-gneisses (1780<sup>±</sup>20 m.y. van Breemen et al., 1974). The syenites form a number of high mountains (up to 1800 m.), often rising from fjord level and deeply dissected by glacial valleys. There is abundant evidence of the recent glacial activity with truncated spurs, hanging valleys, cirques,

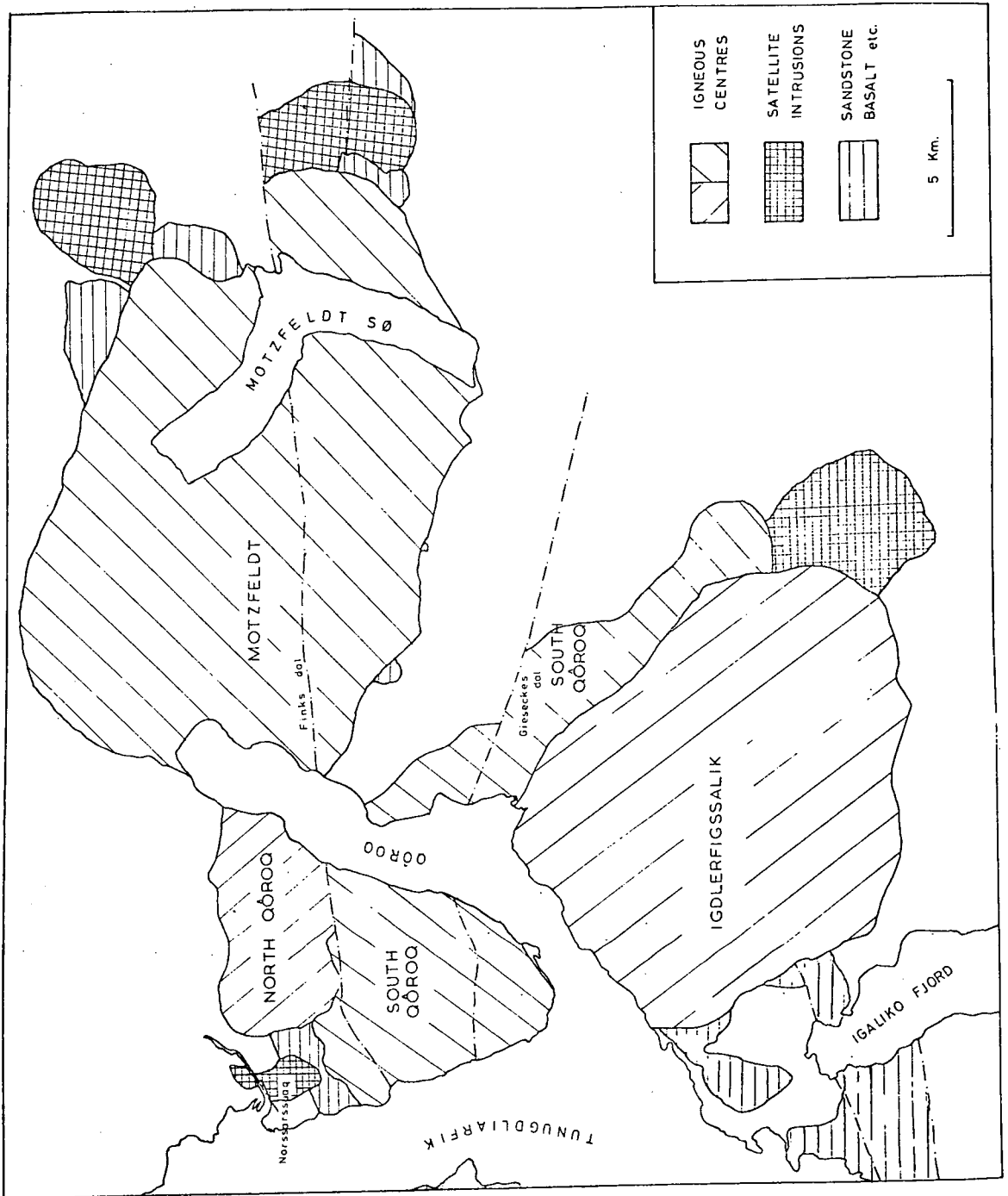
arêtes and pyramidal peaks being common. The North Qôroq Centre is the least mountainous and most easily accessible. Nevertheless, it proved impossible to survey and collect from the steep cliffs bounding Qôroq. In the summer of 1972, Qôroq was generally filled with ice as far south as Giesecke's dal and the cliff sections could not be studied by boat.

A simplified map of the area, with locations mentioned above marked on it, is given in Fig. 1.2.

### 1.3. Previous investigations

The nepheline syenites of the Igaliko Complex were known from the late nineteenth century and are mentioned by early workers such as Steenstrup and Kornerup (1881) and Flink (1898). The first detailed mapping of the syenites was undertaken by Ussing and Bøggild (Ussing, 1894; 1912). Ussing distinguished between the marginal augite syenites and the dominantly foyaitic nepheline syenites. Wegmann visited the area between Qôroq and Narssarssuaq in the 1930's (Wegmann, 1938), but the most detailed systematic mapping was done by the Greenland Geological Survey (G.G.U.). The Igaliko Complex was mapped by Emeleus and Harry in the summer field seasons of 1961, 1962, 1963 and 1966 (Emeleus and Harry, 1970). The bulk of the mapping of North Qôroq was carried out by Harry in

Fig.1.2 Simplified map of the Igaliko Complex,  
showing the four major centres, the  
satellite intrusions and the adjacent  
supracrustal rocks.  
(Modified from Emeleus and Harry, 1970).



1962 and 1963 and it is on his excellent interpretation of the field relations that the present author has relied.

The maps used in the field work were U.S. military maps. The A.M.S. grid found on these is given on the map showing the general geology of North Qoroq, in the back of the Appendix volume.

#### 1.4. Equipment and provisioning

The vast majority of equipment was generously provided by the Greenland Geological Survey. They also provided sample boxes and arranged for the collection of the rock samples from Narssarssuaq and their delivery to Copenhagen and from there to Durham.

Provisions were readily obtainable from the general store at Narssarssuaq and a quantity of cooked food was provided by the canteen kitchens catering for the staff at Narssarssuaq.

## CHAPTER TWO: FIELD RELATIONS

### 2.1 Introduction

A concise account of field relations found in North Qôroq, and in the Igaliko complex as a whole, was given by Emeleus and Harry (1970). This chapter summarizes the findings of these authors, and introduces observations made by the present author in the summer field season of 1972.

Of the four distinct major centres comprising the Igaliko complex, North Qôroq is the smallest. To the north the centre cuts Pre-Gardar granite/granite-gneisses (Julianehåb Granite), and to the west Gardar supracrustal rocks. The younger centre of South Qôroq forms the southern boundary, which is partially faulted. The eastern boundary with the Motzfeldt Centre is problematical, the critical area being concealed by a large fjord (Qôroq).

The North Qôroq Centre covers an area of approximately 25 sq.Km. and, prior to the intrusion of the South Qôroq Centre, was roughly oval in shape, being elongated in a north-westerly/south-easterly direction. It consists of six major units centering on the western side of the plateau between Qôroq and Narssarssuaq. These units frequently show a diversity of character. A further unit

(SN.3; Emeleus and Harry, 1970, p.41) is exposed only in the steep sides of Qôroq. The problematical nature of this unit is discussed later.

Also occurring in the area studied, are a carbonate-breccia plug, thin sheets of microsyenite and numerous dykes of varying character.

## 2.2. Country Rocks

### 2.2.1. Pre-Gardar basement

The basement in the area of North Qôroq is composed of the Keltidian Julianehåb Granite suite, and is described by Allaart (1964). It consists of granites and granite-gneisses, with variation towards dioritic and granodioritic types. In the area of North Qôroq, the Julianehåb Granite suite is mainly granitic in nature, with gneissose granodiorite developed to the west. A few amphibolite dykes cut through the Julianehåb Granite. Any foliations in the gneissose granite of the area are in a general north-easterly/south-westerly direction.

### 2.2.2. Gardar supracrustal rocks

To the west, the rocks of North Qôroq intrude into supracrustal rocks of the Eriksfjord Formation. These consist mainly of basic lavas and pyroclastics interbedded with clastic sediments. The formation, in the vicinity of North Qôroq, dips towards the south at angles between  $15^{\circ}$  and  $30^{\circ}$ .

## 2.3. The major syenitic units of North Qôroq (see Fig.2.1)

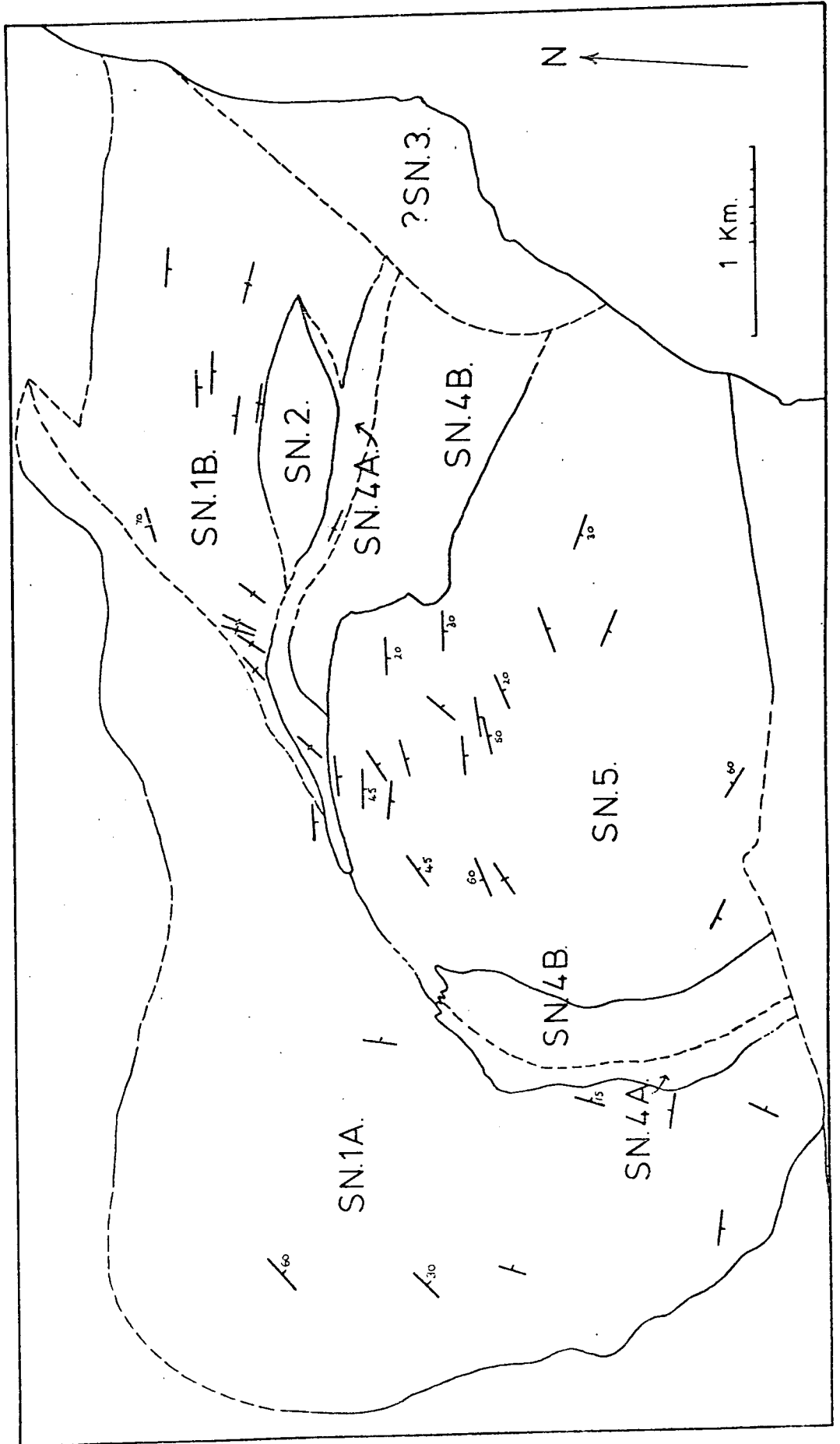
### 2.3.1. Unit SN.1 - the Outer Foyaite

This unit of the North Qôroq Centre occupies approximately half of the centre's present aerial extent and outcrops on the northern and western sides. It is especially well exposed in cliff sections overlooking the old hospital at Narssarssuaq. On the plateau between Qôroq and Narssarssuaq, it weathers to give a gravelly, rather featureless terrain, rendering systematic sampling difficult.

SN.1 is the oldest unit of the North Qôroq Centre. It is dominantly foyaitic but develops important variants near the margins. The typical foyaite of the western side of the area is coarse-grained and generally lacking in lamination. Where feldspar lamination does occur, it is at a gentle angle dipping towards the unit's centre. Fig. 2.1 shows mapped laminations for unit SN.1 and the other units of the North Qôroq Centre. The foyaite consists principally of tabular grey feldspars up to 2 cm. long, interstitial mafic areas composed mainly of alkali pyroxene, alkali amphibole and magnetite, small brown or white areas of nepheline and sporadic pink patches of natrolite.

To the east, this coarse foyaite passes into a finer-grained porphyritic rock type, with feldspars 1 cm. long, abundant nepheline and interstitial mafics consisting of alkali pyroxene and alkali amphibole, together with

Fig.2.1 Mapped laminations for all units of the North Qôroq Centre. Where measured, the dip of the laminations is noted.



magnetite. Unlike the coarser variety of SN.1 already described, this variant has a greater tendency to exhibit lamination, with aligned feldspars and occasional mafic bands. The problem is whether this finer-grained material is a separate intrusive body cutting out the earlier coarser foyaitic in the north-eastern part of North Qôroq, or whether there is a definite gradation from one type to the other. Evidence is scant, because of relatively poor exposure where the junction would occur, but numerous syenitic xenoliths are found in the finer-grained syenite and these may well represent inclusions of the coarser variety of SN.1. Also, laminations in the finer variety of SN.1 are discordant to the expected direction, unless the finer-grained variant is a separate intrusion. The most convincing evidence for SN.1 being formed by two separate intrusions comes from a petrographic study of the rocks. Rocks of the coarser SN.1, close to the possible contact, show very clear evidence of recrystallization (see section 3.4.). Hence, SN.1 is composed of two separate but similar units. The coarser unit to the west will be called SN.1A, and the finer-grained unit to the east SN.1B. SN.1B may be fine-grained because it is apparently close to the roof zone of the intrusion.

SN.1A develops a marked variant along its northern and western margins. This variant has a lateral extent of

only a few tens of metres. It is a medium-grained grey syenite with feldspars 1 cm. long and little, if any, nepheline. The interstitial mafic areas, unlike the rest of SN.1A, contain abundant olivine and biotite. There is field and petrographic evidence to suggest that this variant is a marginal phase, passing gradationally into the more typical foyaite.

Patches of pegmatite with feldspars up to 8 cm. long are common towards the outer margins of SN.1A (Plate 1), and in the margins and roof zone of the finer-grained foyaite SN.1B. This phenomenon is found in other units of North Qôroq, and in other centres of the Igaliko complex (see Fig. 2.2.). It is probably caused by the concentration of volatiles towards the edges and the roof zone of the intrusion. The stage at which this volatile transfer took place will be discussed later.

Xenoliths in SN.1A are uncommon. A block of un-laminated foyaite was, however, found in laminated foyaite (Plate 2) (grid reference 79668175). In the western part of the coarse foyaite, SN.1A, are found xenoliths of a fine-grained porphyritic rock. These xenoliths are generally rounded in outline and up to 2 m. across. SN.1B contains numerous xenoliths, often partly assimilated, of fine-grained syenite, Julianehåb Granite

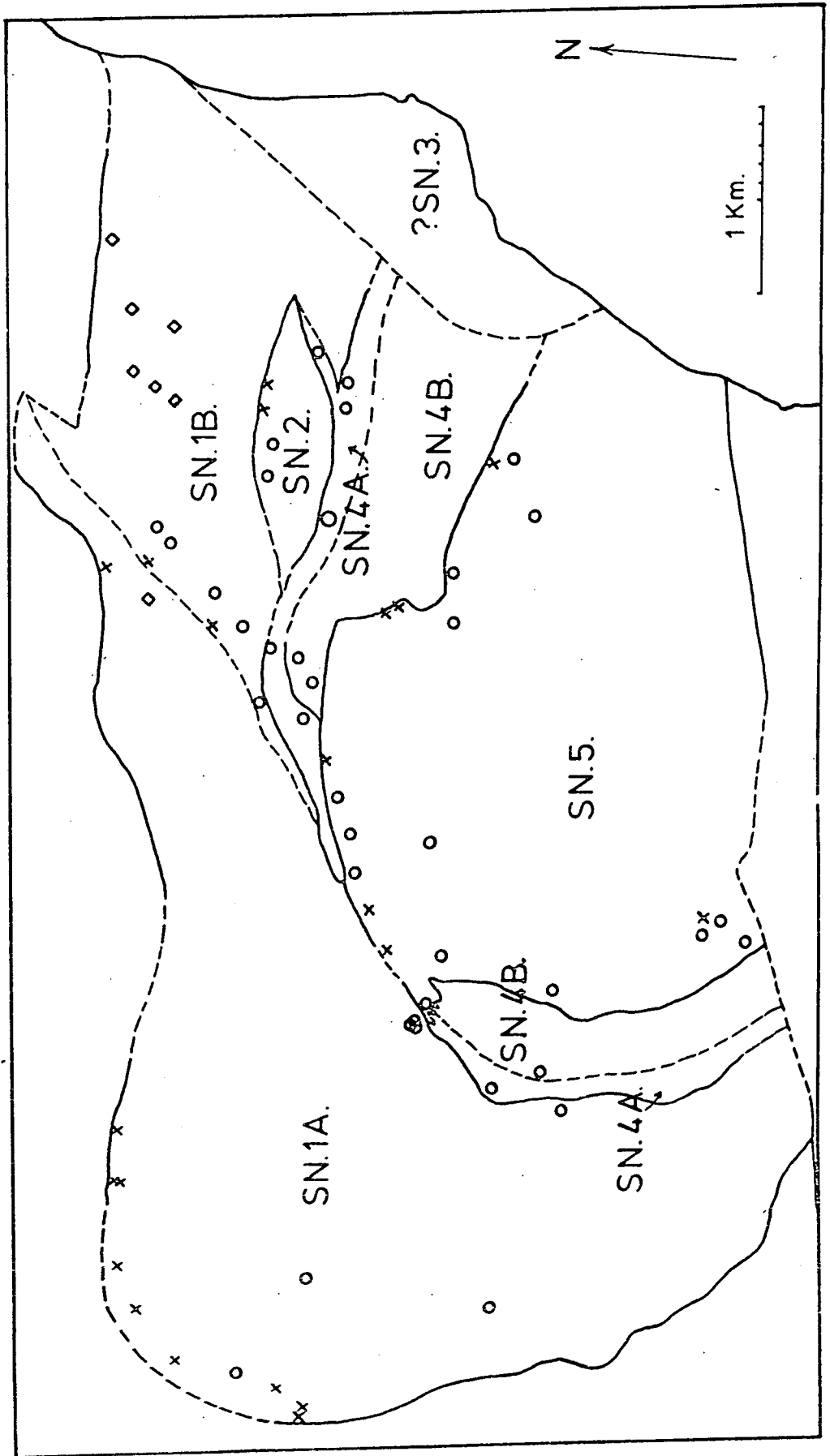
Plate 1. Patchy pegmatite in the outer margins of SN.1A, intimately associated with fine grained marginal rocks.

Plate 2. Xenolith of unlaminated SN.1A foyaite in laminated SN.1A.



Fig.2.2 The distribution of pegmatitic patches, syenite xenoliths and country rock xenoliths observed over the outcrop of the North Qôroq Centre.

- x - Pegmatitic patches
- o - Syenite xenoliths.
- ◊ - Country rock xenoliths.



and quartzite from the Gardar supracrustal rocks. A xenolith described as anorthosite by W.T. Harry, was misidentified, and proved to be Julianehåb Granite. A massive xenolith of quartzite 80 m. by 60 m. was found in the north-eastern corner of SN.1B (grid reference 84698307). The large number of xenoliths in SN.1B is to be expected if, as suggested, the foyaite here is close to the roof zone.

Fig. 2.2 shows the distribution of pegmatitic patches and xenoliths over the North Qôroq Centre.

It is thought that the marginal variants found in both SN.1A and SN.1B can be explained by the proximity to the country rock, i.e. rate of cooling, and to the action of volatiles.

### 2.3.2. Unit SN.2 - the Leucocratic Syenite

This unit occurs as a pod-shaped body of rock to the east of the long lake, in the north-eastern sector of North Qôroq. It occupies the highest ground in the centre and varies from coarse-grained to medium-grained, always exhibiting a characteristic pink colour. This colour resulted in the unit being termed the "Leucocratic Syenite" by Emeleus and Harry, although it is probably no more leucocratic than the other units in the centre.

The rock consists dominantly of prismatic feldspars up to 2 cm. long, occasional nepheline and subhedral

pyroxene and amphibole.

There is an absence in the unit of feldspar lamination mineral layering or xenoliths.

As with unit SN.1, pegmatitic patches are encountered around the margins of SN.2, where it comes into contact with the older unit. Here, the dominant mafic mineral is amphibole, which is strikingly poikilitic and occurs in crystals up to 10 cm. in length.

A suggested mechanism for the formation of SN.2 is presented later in the chapter.

### 2.3.3. Unit ? SN.3

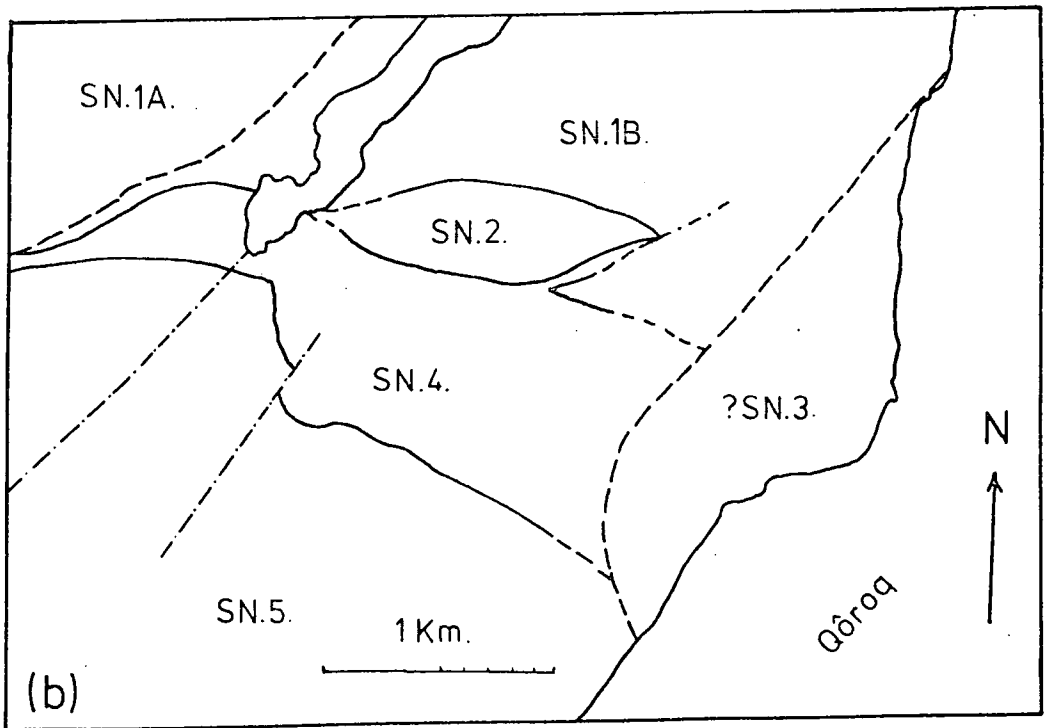
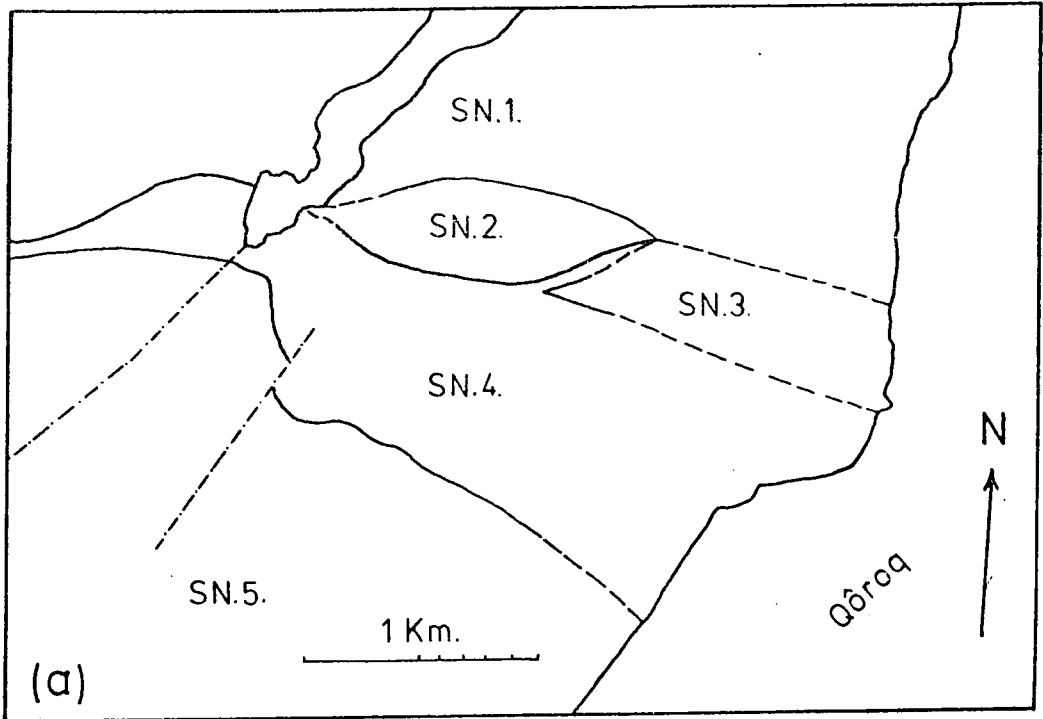
This unit, occurring to the east of SN.2, poses many problems because of its relative inaccessibility. It is only in this area that major modifications are proposed to the mapping of Emeleus and Harry. The previous and present interpretations of the eastern side of North Qôroq are shown in Fig. 2.3.

The rock, called SN.3 by Emeleus and Harry, is medium-grained, brittle and shows a purple discolouration. It was termed by them the "Altered Foyaite". It is now considered to be merely unit SN.1B, which has been crushed and sheared by movement along the proposed fault and recrystallized by the intrusion of SN.4. A limited traverse towards Qôroq fjord was made, and samples collected bore a marked petrographic and chemical similarity to specimens of SN.1B taken

Fig.2.3

- (a) The previous interpretation of the inter-unit relationships on the eastern side of the North Qôroq Centre.  
(After Emeleus and Harry, 1970).

- (b) The present interpretation of the field relations based on a short traverse towards Qôroq.



at a similar level.

Descending further towards Qôroq fjord, a new unit was encountered which cuts sharply across the proposed SN.1/SN.4 boundary and recrystallizes the porphyritic syenite, SN.4. This unit may be connected with North Qôroq, but if so, it cuts pre-existing boundaries almost at right angles. It is possible that it represents the outer unit of the Motzfeldt Centre. This would have the important implication of the Motzfeldt Centre being younger than the North Qôroq Centre, a perfectly possible state of affairs, considering the relatively similar ages which have been determined for the two Centres (Blaxland et al., in press). This new unit has been termed ?SN.3 in the rest of the account and the appendices. The exact nature of ?SN.3 and its relationships to surrounding rocks would not be able to be determined unless a traverse along the shore of Qôroq fjord were undertaken. In the area examined, ?SN.3 is a fresh syenite of medium grain size.

#### 2.3.4. Unit SN.4 - The Porphyritic Syenite

This unit, called the "Porphyritic Syenite" by Emeleus and Harry, outcrops to the south and east, on the higher ground of North Qôroq. The name is derived from the fact that all the varieties of SN.4 share the characteristic of having numerous feldspar phenocrysts up to 2 cm. in

length. The groundmass is generally fine-grained to medium-grained.

SN.4 is composed of a marginal fine-grained phase, with a maximum width of about 400 m. and an inner, coarser-grained phase. The strongly porphyritic marginal phase exhibits a decrease in size of the feldspar phenocrysts, as the margin is approached, and strongly resembles a number of dyke rocks cutting the area. In the field, the marginal phase can be seen to be in contact with the inner coarse-grained phase, although the contact is somewhat diffuse. It appears that the two phases represent separate intrusions of magma. However, these two intrusions, as they show such a close similarity to each other, were probably related to the same source at depth and were intruded almost contemporaneously. In the rest of the account the outer, earlier unit is termed SN.4A and the inner unit SN.4B. Both SN.4A and SN.4B show an absence of mineral lamination and no development of pegmatitic facies. Xenoliths are uncommon, although they do occur near the contact with other units. To the north and west of the unit's outcrop, a number of fine-grained, rounded xenoliths, similar to SN.4A, are found in SN.4B.

#### 2.3.5. Unit SN.5 - the Inner Foyaite

SN.5 is the youngest of the principal units. On its northern and western boundaries it cuts units SN.4 and SN.1A,

to the east it disappears towards Qôroq fjord, and to the south it is in faulted contact with the younger South Qôroq Centre.

The unit is of variable grain size, but is generally coarse to medium. This dominant variety is dull pink or red in hand specimen and weathers readily to give a gravelly land surface. Feldspars are up to 2 cm. long, and nepheline is abundant. Towards the margins of the unit a somewhat less coarse variety is encountered.

Lamination and mafic banding are occasionally encountered in SN.5 (Plates 3 and 4) and pegmatitic patches are developed near its contacts with SN.4 and SN.1A. Xenoliths are often extremely large and are exclusively of the units SN.4A and SN.4B, both of which are intruded by SN.5. They are frequently recrystallized to give a granular appearance. The present level of erosion may well be exposing the roof zone of SN.5, and many of the SN.4 xenoliths may be roof pendants and blocks fallen from the roof zone (see Fig. 2.5).

It is probable, as with other units, that variation in grain size in SN.5 can be explained by differential rates of cooling and differential distribution of volatiles.

## 2.4. External Contacts

### 2.4.1. Contact with the Julianehåb Granite

The contact of the syenites with the Julianehåb Granite

Plate 3. Rare mafic banding in unit SN.5. The mafic bands are thin, impersistent and composed dominantly of amphibole.

Plate 4. Mafic banding from the same locality in SN.5, showing the presence of a possible slump structure.



is best seen at the north-eastern margin of the area, where a 200 m. semi-vertical section shows it to be steep (c.  $70^{\circ}$ ) and outward dipping. At the contact the granite is often crushed and altered. A few metres from the contact, however, hand specimen examination shows SN.1B to have left the granite relatively unaffected. The Julianehåb Granite is veined by the syenite, which frequently shows the development of pegmatitic patches. Xenoliths of granite are often encountered in marginal SN.1B and occasionally in SN.1A.

#### 2.4.2. Contact with supracrustal rocks

The junction of unit SN.1A with basalts of the Eriksfjord Formation is exposed in a stream section, south-east of the Narssarssuaq reservoir site. SN.1A becomes progressively finer-grained towards the contact, where it is a pinkish grey rather altered rock. At the contact, the basalt is brecciated and extensively veined by syenitic material (Plate 5). Although the contact of the North Qôroq Centre with the clastic sediments of the Eriksfjord Formation was not found near Narssarssuaq, a large sheet of quartzite was encountered in SN.1B foyaite, near the north-eastern margin of the centre. This indicates the greater aerial extent of supracrustal rocks of the Eriksfjord formation at the time of intrusion, and that

part of the roof of the intrusion was probably formed by these supracrustal rocks.

#### 2.4.3. Contact with the South Qôroq Centre

The southern boundary of the North Qôroq Centre is in contact with unit SS.2 of the South Qôroq Centre. Over much of its length the contact is a faulted one, but in the south-west an intrusive contact can be seen. In this area both SS.2 and SN.1A are reddened and altered, but SS.2 can readily be seen to be the younger unit. As it approaches the contact with the North Qôroq Centre, SS.2 becomes finer-grained, and at the contact encloses numerous xenoliths of SN.1A. SN.1A, despite alteration, can frequently be seen to be extensively recrystallized, with the development of a rather granular rock type.

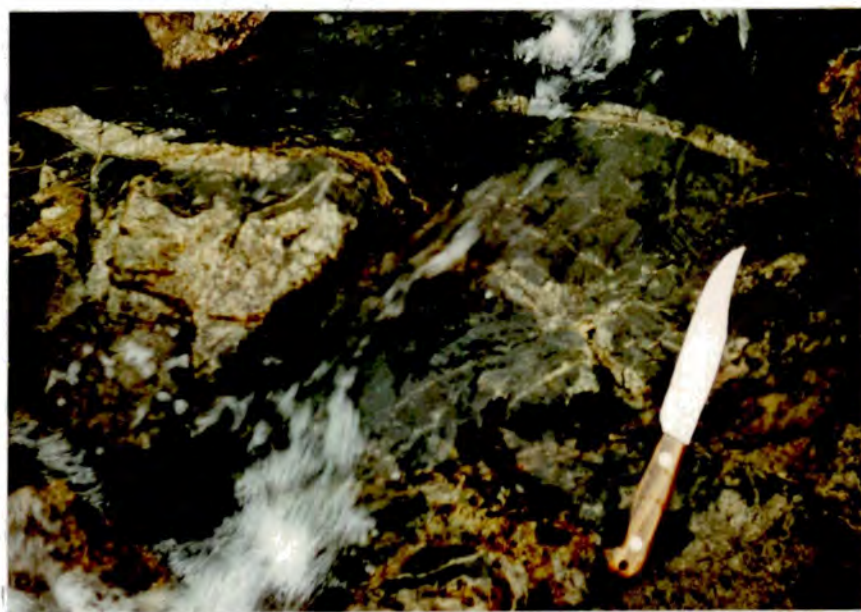
#### 2.5. Internal contacts

Most of the internal age relationships in North Qôroq can be established, in relative terms, by examination of the contacts between units (Plate 6).

The "Inner Foyaite", SN.5, would appear to be the youngest of the major units. The relationship of SN.5 to SN.1A can be established in the area just east of the breccia plug (grid reference 81528195. See map at end of appendix volume): Towards the contact, the "Outer Foyaite", SN.1A, shows no change in character, whereas the "Inner

Plate 5. The external contact of unit SN.1A with basaltic rocks of the Eriksfjord Formation. The syenite brecciates and extensively veins the basalt.

Plate 6. A typical internal contact relationship between syenite units. This contact is between the "Leucocratic Syenite", SN.2, (at bottom of plate) and the "Porphyritic Syenite", SN.4A, (at top of plate).



Foyaite", SN.5, generally decreases in grain size and develops pegmatitic patches. As seen before, this pegmatitic development tends to occur at a unit's outer (and upper) margins. SN.5 can also clearly be seen to be younger than SN.4. SN.5 becomes finer-grained as it approaches SN.4, develops pegmatitic patches, and encloses and veins numerous xenoliths of both SN.4A and SN.4B. Mention should be made here of the rock types described by Emeleus and Harry under the general term 'mélange'. This occurs in two principal areas at the northern end of SN.5. It is associated intimately with Porphyritic Syenites SN.4A and SN.4B, and is enclosed by medium- to coarse-grained SN.5. It seems likely that all the rock types of the 'mélange' can be accounted for by varying degrees of recrystallization and alteration of SN.4 by the later SN.5 intrusion. The area of 'variable syenite', at the south-west end of the SN.5 outcrop, probably also results from invading SN.5 reacting with earlier SN.4B.

Field relations readily show SN.4 to be younger than SN.1A, SN.1B, and SN.2. Xenoliths of these units can be found in the margins of SN.4A, which in turn develops a readily apparent 'chill' against the earlier units.

SN2/SN.1B field relations were less easy to establish. The development of pegmatitic patches towards the outer

margins of SN.2, and the absence of any change in character of SN.1B as the contact zone is approached, suggest that SN.2 is the younger unit. As mentioned earlier, SN.1B is clearly younger than SN.1A.

The contacts of the unit ?SN.3, on the west flanks of Qôroq fjord, proved inaccessible. However, although the actual contact was not seen, this unit clearly cuts the proposed SN.1/SN.4 and SN.4A/SN.4B boundaries almost at right angles and recrystallizes syenites of SN.4B. Apart from being younger than these two units, little more can be said about it at this stage.

## 2.6. Minor intrusive units

### 2.6.1. Carbonate-rich breccia plug

A minor intrusion of carbonatitic affinities occurs between two lakes, 4 km. east of Narssarssuaq Airport (Plate 7) (grid reference 81208189). The plug, about 40 m. in diameter, is of carbonate-rich brecciated material and closely resembles similar minor intrusives described from the Qagssiarssuq area (Stewart, 1964), and from north of Narssarssuaq (Walton, 1965). It cuts the SN.1A/SN.5 contact (Plate 8) and contains numerous angular fragments of syenite up to a metre in length. Fragments have been identified as coming from units SN.1A, SN.4 and SN.5 (Plate 9). A few fragments of basic xenolithic material also

Plate 7. The carbonate-rich breccia plug. This 'knobbly weathering' intrusion, about 40m in diameter, occurs between unit SN.5 (foreground) and unit SN.1A (middle distance). It is apparently the only body of its type to cut one of the major syenite centres.

Plate 8. Sheared contact between the breccia plug and unit SN.1A. The plug, to the right on the plate, can be seen to contain xenoliths of syenite.

Plate 9. An irregular xenolith of SN.5 syenite in the heavily jointed breccia plug.



occur within the plug, together with pyroxene and mica megacrysts. At its western edge, the plug can be seen to be in contact with sheared SN.1A material. This minor intrusion is significant, as it is the only one of its kind to cut a major syenitic centre. It obviously post-dates all the major intrusive units of North Qôroq, but is cut by a trachytic dyke, and thus probably predates the Mid-Gardar dyke swarm. The other plugs, described by Stewart and Walton, are similar to the one in North Qôroq and may well be of an equivalent age. Stewart suggests that plugs near Qagssiarssuq occurred at a late stage in the igneous activity.

#### 2.6.2. Microsyenite sheets

Two microsyenite sheets cut the major units of North Qôroq. The first occurs towards the outer margin of unit SN.2 and the second in unit SN.5. Both could be traced only impermissibly along their strike, because of the gravelly weathering of the terrain. The microsyenite sheets are only a few metres wide and dip at angles between  $30^{\circ}$  and  $60^{\circ}$  towards the south. They appear to have a curved outcrop and may have been injected as a cone-sheet type of intrusion. The most striking feature of both of the microsyenite sheets is the pronounced feldspar lamination and mafic banding (Plates 10-12). The fine mafic bands lie parallel to the contacts of the sheet, are formed mainly of amphibole, and

Plates 10-12. The feldspar lamination and mafic banding seen in the microsyenite sheet cutting unit SN.2. The top plate shows the steep attitude of the banding, and the other two plates the sharp base to the amphibole rich mafic bands and their much more diffuse and irregular upper boundaries.



probably result from crystals adhering to the cooling surfaces as the magma flowed along the cone-sheet fracture. Flow of the magma would cause crystals to be concentrated towards the centre of the sheet, in a similar manner to that suggested by Komar (1972). The temporary cessation of flow would result in these crystals falling to the lower cooling surface. Impersistent flow along the fracture would give the observed layering. The microsyenites postdate the major units of North Qôroq, and possibly occurred contemporaneously with the injection of trachytic and microsyenitic dykes.

#### 2.6.3. Dykes cutting the North Qoroq Centre

Numerous dykes cut the North Qôroq Centre, most of them showing the regional north-easterly trend. They are usually easily mapped, as they are more resistant to erosion than the syenites and, as a result, stand up as 'walls' of dyke material. They vary in thickness from less than a metre, to over 40 m., although most are between 2 m. and 10 m. thick. The dykes are sub-vertical, any dip tending to be in a north-westerly direction.

A variety of dykes are found, the most common types being trachytes and microsyenites. These vary in colour from grey-green to brown and usually contain feldspar phenocrysts, although they may be aphyric. Some of the microsyenites, as previously mentioned, closely resemble

the marginal phase of the "Porphyritic Syenite", SN.4A.

Dykes of a more basic character are also present. They can be termed dolerites or trachy-dolerites, and invariably contain large phenocrysts or xenocrysts of plagioclase and xenoliths of anorthosite. The feldspar crystals can be up to 12 cm. long and the anorthosite inclusions up to 30 cm. long. These "Big Feldspar Dykes", as they are called, are commonly encountered in the Gardar Province (Bridgwater and Harry, 1968).

Finally, a few thin dykes of a carbonatitic nature have been encountered in the area of North Qôroq.

Because of their parallel nature, the age relations of the dykes are difficult to determine. The carbonatitic dykes are impossible to place chronologically, but it seems likely, in the general area of Igaliko, that the "Big Feldspar Dyke" injection preceded the majority of dykes of a trachytic or microsyenitic character. All types of dyke cut the youngest major unit, SN.5, and hence, the intrusion of the major units preceded the major phase of dyke injection.

## 2.7. Structure

### 2.7.1. Faulting

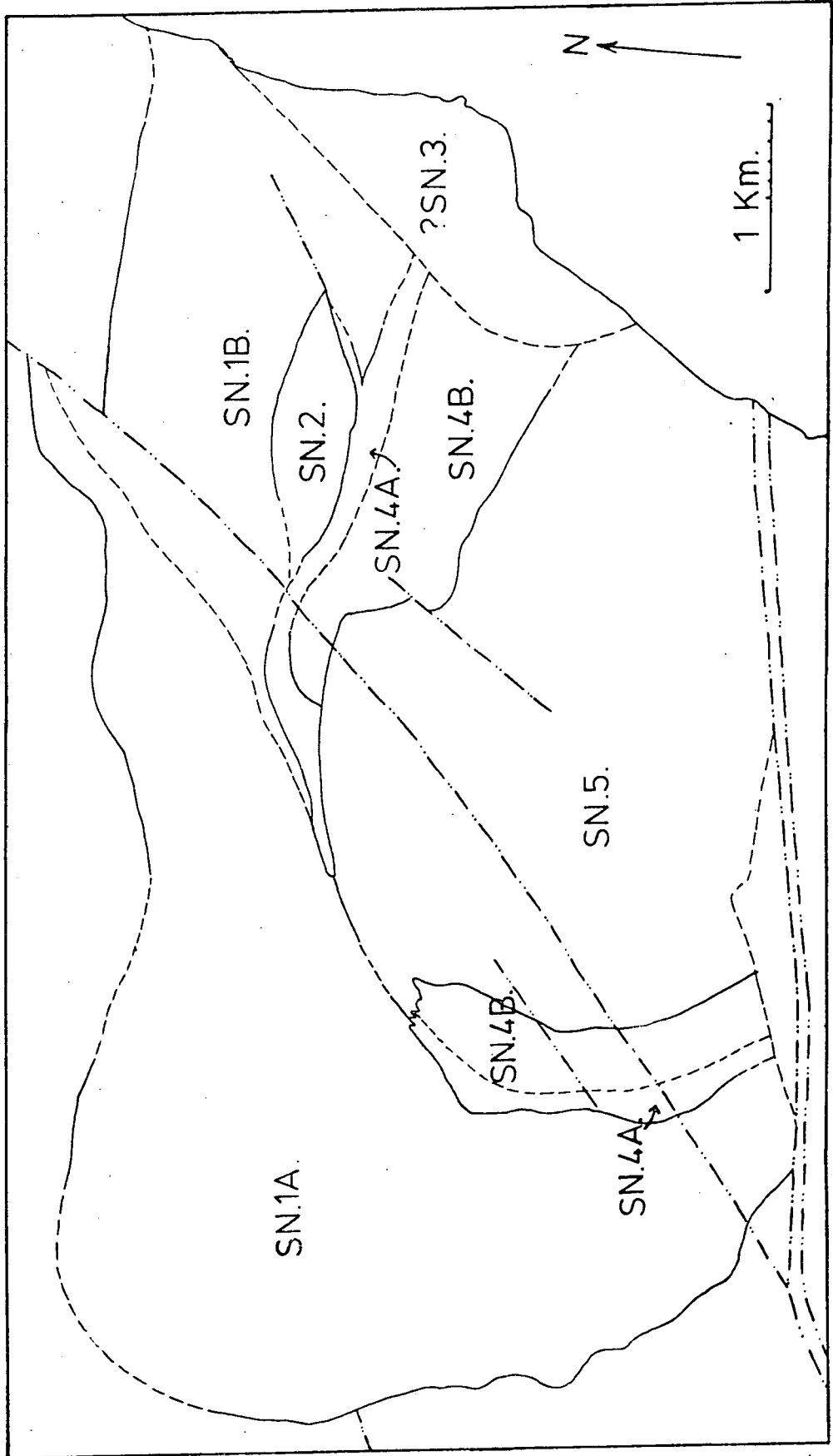
Two types of fault are found in the area of North Qôroq. One type is a roughly east-west trending fault with

a substantial strike slip component. The other trends in a north-easterly direction, generally with little apparent movement, and is often represented by crush zones. The faults cutting the area are shown in Fig. 2.4.

Crossing the peninsula between Qôroq and Narssarssuaq are two major east-west trending fault zones. The northernmost of these affects the North Qôroq Centre. It can be traced from just south of Akuliaruseq, across the peninsula to Qôroq, and into the broad U-shaped valley of Flinks Dal. On the peninsula it cuts through the South Qôroq Centre and, further eastwards, marks the boundary between North and South Qôroq. The fault zone brecciates and discolours the syenites through which it passes. The principal movement on the fault zone is horizontal, in a sinistral sense, and has been demonstrated to be of the order of 2 km. Any vertical displacement is uncertain, but there is probably a downthrow to the north.

Numerous north-easterly trending faults occur within North Qôroq. Frequently they are associated with little apparent movement and are represented by crushed and reddened syenites, which have subsequently been eroded into deep valleys, often filled with elongate lakes. One of these faults runs along the long lake in the north-east corner of North Qôroq and forms a well-marked valley, running south-west until truncated by the main east-west

Fig.2.4 The major faults affecting rocks  
of the North Qôroq Centre.



transcurrent fault zone. This fault appears to displace the outer contact of the syenites with the country rock, at the north end of the long lake, by several hundred metres, but does not displace the SN.4 and SN.5 contacts or the dyke rocks. A similar sub-parallel fault runs through the area of the altered foyaite, where a tongue of porphyritic syenite has apparently been injected along the fault line (grid reference 849824). Certain of the north-east/south-west trending faults, such as the two just mentioned, may postdate the earlier units of North Qôroq, but predate the later ones. A similar phenomenon can be seen in the Igdlérfigssalik Centre.

None of the north-east trending faults appear to displace the dykes. The major east-west transcurrent fault zone affects both major syenite units and dyke rocks, hence these transcurrent faults postdate the north-east trending faults.

A fault trending east-west, and downthrowing to the south, has been mapped downfaulting rock of the Eriksfjord Formation against Julianehåb Granite. It occurs between Narssarssuaq and the outer unit of the North Qôroq Centre, but has no affect on the syenites of the centre. It probably represents a phase of faulting which predates the major intrusive units.

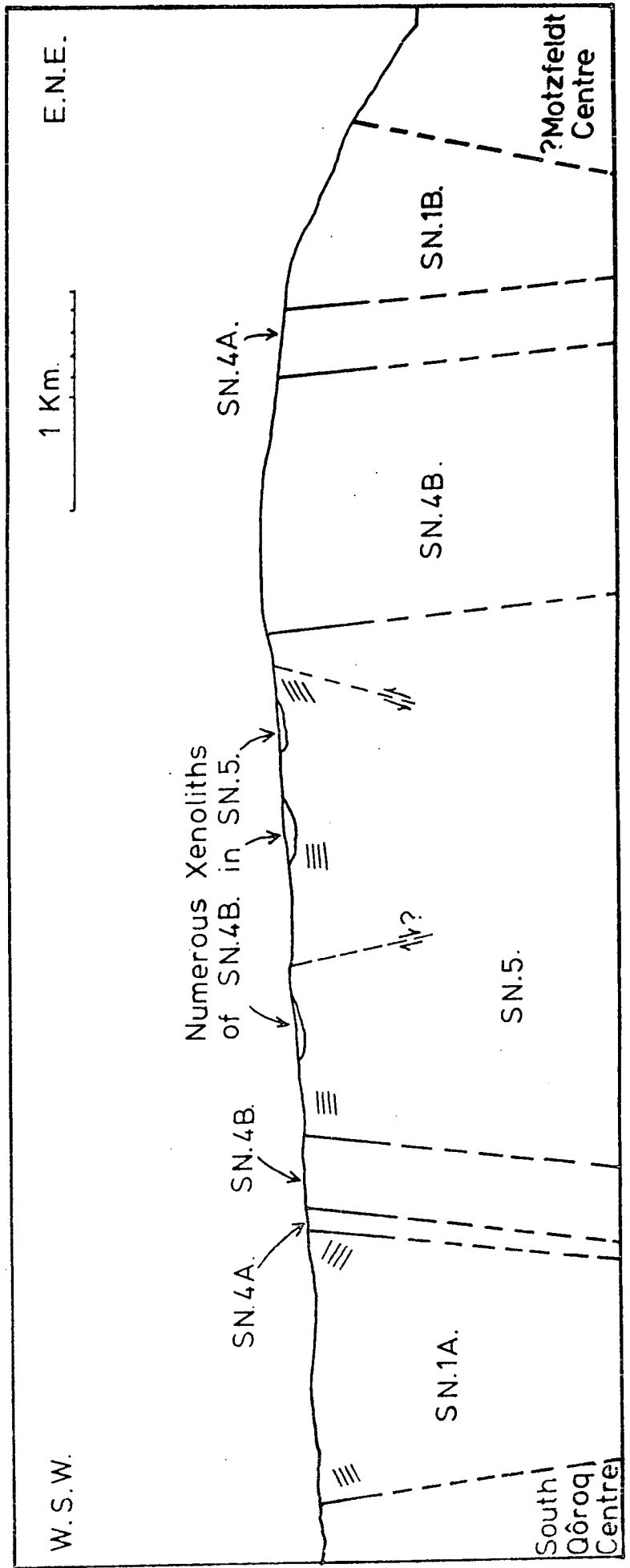
### 2.7.2. Tilting of the area

There is a strong possibility that the North Qôroq Centre has been tilted slightly, as a block, towards the south. Certainly, the supracrustal rocks just west of the centre, which were originally flat lying, now dip southwards at an angle of  $15^{\circ}$ . There is also a suggestion that the dyke rocks are not vertical but possess a steep north-westerly dip, in keeping with the proposed block tilting. This type of movement must have occurred late in the evolutionary history of North Qôroq, as it affects the dyke rocks. It may well be associated with either the considerable transcurrent movement along the major east-west fault zone, or the emplacement of the South Qôroq Centre. If tilting occurred, it has implications for the laminations noted in the rocks, the present orientations of which are shown in Fig. 2.1.

### 2.8. Mechanisms of intrusion

The present author agrees with Emeleus and Harry, that the majority of the syenitic units were formed by a process of ring fracture, and whether we now see a ring-dyke or a stock-like body depends on the level of erosion. Stoping may also have played a role in the evolution of the centre. Fig. 2.5 shows a section through North Qôroq based on this type of ring structure. The presence of

Fig.2.5 A schematic section through the North Qôroq Centre, showing the possible contact relationships between units, faulting, the attitude of laminations and the presence of numerous xenoliths of unit SN.4B in unit SN.5.



xenoliths and a finer-grained syenite in SN.1B suggest proximity to a roof zone. Hence, in SN.1B, the level of erosion has probably only proceeded as far as the stock zone. A similar erosional level is proposed for SN.1A. Indeed, considering the steep, outwardly dipping contacts SN.1A makes with the country rock, the central block would have to have subsided a considerable distance to cause a ring dyke of such dimensions. Unit SN.5 also appears to be exposed at a level near its roof, and to contain roof pendants of SN.4.

The one unit probably not intruded in this fashion is SN.2. It is proposed that shear movement occurred along two of the major north-easterly trending faults, one running along the long lake, and another running through the area of the altered foyaite. This shear stress resulted in an arcuate fracture forming in the pre-existing rocks, and in the intrusion of a sinusoidal body of magma along this fracture, so forming the unit SN.2. Hence, SN.2, which can be thought of as a mega-tension gash, was intruded as a pod-shaped body, and was not formed by a ring fracture mechanism.

### 2.9. Age Relations

The sequence of geological events affecting Igaliko stated in Emeleus and Harry's paper, is probably broadly

correct. There is, however, the possibility that the units of Motzfeldt may postdate those of North Qôroq, and that some of the north-easterly faults may have been active during the period of injection of the major units.

The relative ages must be considered together with the absolute age determinations on the Igaliko Complex, done using Rb/Sr isotopes (Blaxland *et al.*, in press). A summary of their findings with regard to the ages of the four major centres is presented in Table 1.

TABLE 1

<u>Centre</u>	<u>Age (million years)</u>
Motzfeldt	1310 $\pm$ 31
North Qôroq	1295 $\pm$ 61
South Qôroq	1185 $\pm$ 8
Igdlerfigssalik	1167 $\pm$ 15

It should be noted that the possible error on the ages of Motzfeldt and North Qôroq, especially the latter, is considerable. This error value is in excess of experimental error and poses problems, such as likely contamination by crustal material, which will be discussed in Chapter 7.

The most interesting result of the age dating is the huge time interval between the intrusion of the Motzfeldt/North Qôroq pair and the South Qôroq/Igdlerfigssalik pair. This also is further discussed in Chapter 7.

The ages agree with the relative ages observed from field relations. The close similarity in the ages of North Qôroq and Motzfeldt, and the large associated error, means that North Qôroq could well have preceded Motzfeldt. Therefore, as mentioned earlier in this chapter, the unit found on the western cliffs of Qôroq fjord (?SN.3), cutting earlier North Qôroq units, might be a representative of a later Motzfeldt Centre.

In the age dating, the assumption has been made that units in North Qôroq, and similarly those from the other centres, were intruded at approximately the same time. This perhaps is not the case, and if it were not so would help to explain the scatter on the North Qôroq isochron. From the Igdlerfigssalik Centre comes field evidence of a considerable gap between the early and late units. Dykes cutting early units are themselves cut by later ones. In North Qôroq, a small time gap between units is indicated by the 'chills' formed at internal contacts, and an even larger gap is perhaps indicated by the fault which displaces the outer boundary of SN.1 some 400 m. This fault is probably associated with the intrusion of SN.2, but does not appear to affect the SN.4/SN.5 contacts. Considering that, in a time interval of the order of 100 million years, the centre of activity has moved only a few kilometres

from North to South Qôroq, there is no reason why the units of North Qôroq might themselves not have been intruded over a considerable time span. There is, perhaps, a need for a detailed study of one centre, such as Igdlerfigssalik, where field relations indicate a time gap, to see if there is an identifiable range in ages for the units present in the centre.

## CHAPTER THREE: PETROGRAPHY

### 3.1. Introduction

The petrography of the major units is described, considering them in their sequence of intrusion. Of the minor units, only the microsyenite sheets and carbonate breccia plug are mentioned. A section is also included on rocks that have suffered metamorphism by the intrusion of later syenite units.

A detailed description of the largest unit, SN.1A, is given because of the considerable variation it shows. Other units, with less variation, are discussed more briefly.

### 3.2. The major syenitic units

#### 3.2.1. SN.1A

The margins of SN.1A show the common syneusis texture (Sørensen, 1974), with mafics, apatite and opaques grouped together in clusters. Moving towards the interior of the intrusion, mafics are more sporadic and usually interstitial.

Olivine is restricted to the marginal rocks, where it occurs as large rounded grains (Plate 13), often pseudomorphed by iddingsite or serpentine. In all samples olivine is rimmed by opaque material, which in turn may be rimmed by either pale green pyroxene or blue pleochroic

amphibole (X = blue, Y = dark blue, Z = blue-green).

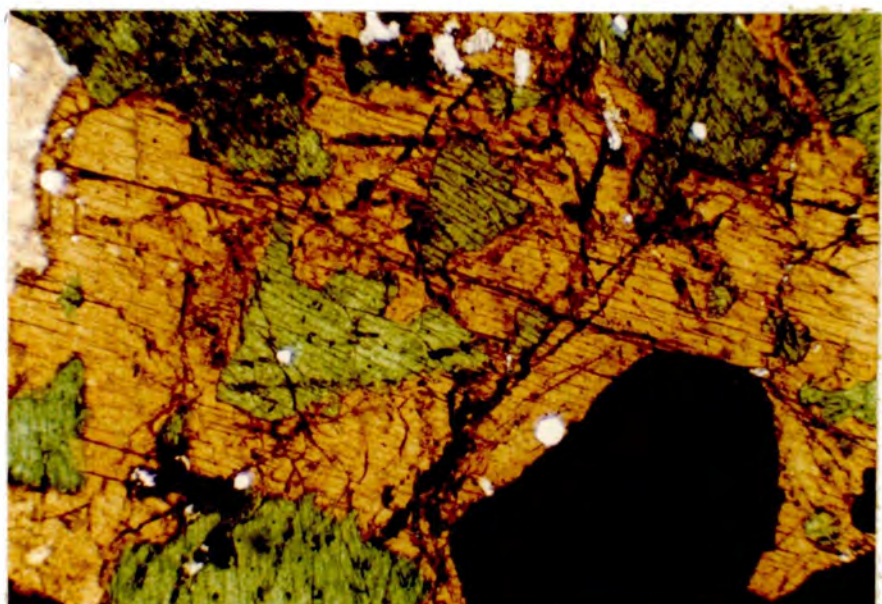
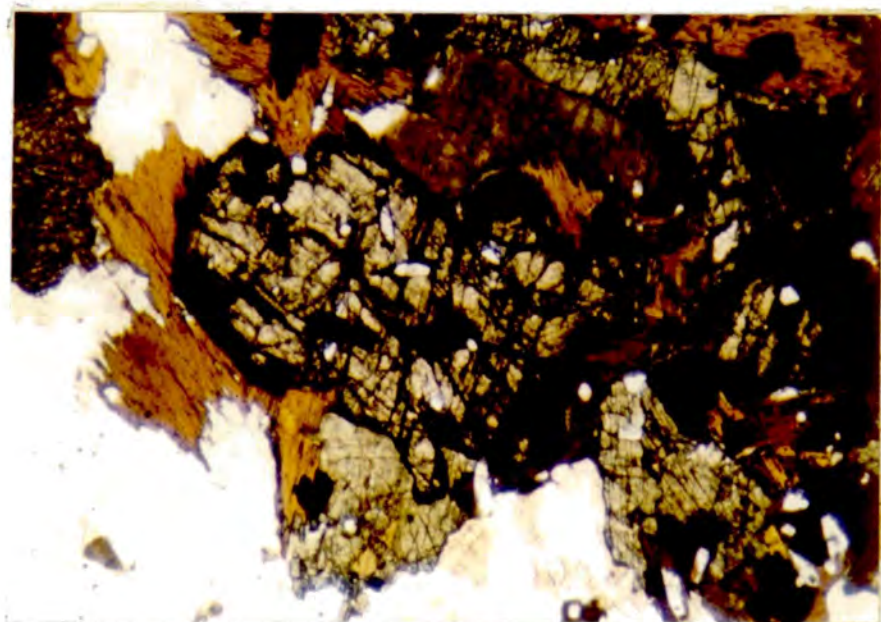
The abundant opaques of the marginal rocks are rounded magnetites with exsolved ilmenite lamellae, usually present as a fine-scale lattice. These Fe/Ti oxides become less abundant with an increase in height in the marginal rocks. Towards the centre of the unit the paragenesis of the oxides changes. They are less frequent, or absent, and occur as small disseminated grains or irregular patches, often associated with a sodic pyroxene. Aenigmatite occurs occasionally in the interior rocks of SN.1A. In some rocks the presence of aenigmatite may have been overlooked, as it is almost opaque and can only be confidently identified by using a combination of reflected and transmitted light techniques.

Apatite is common in the margins of SN.1A, but is rare or absent in the interior. It is obviously early formed, as stout prismatic needles are enclosed by all other phases (Plate 13).

Pyroxenes show a considerable variation. In the margins, there are numerous euhedral to subhedral crystals of pink-purple titan-augite or pale green ferro-augite. Occasional thin, bright green aegirine-augite rims may occur. Moving inwards from the margins, the dominant pyroxene is aegirine-augite (Plate 14). Often extensive zoning can be seen, with pale augite cores giving way to extensive

Plate 13. Rounded olivine grain extensively rimmed by opaque material, which in turn is rimmed by biotite. Early formed, stout, prismatic needles of apatite are enclosed by all other phases. (Unit SN.1A, Sp.No.52218, X30).

Plate 14. A rare mafic band, containing aegirine-augite rimmed by green-brown amphibole, rounded opaques and small needles of apatite. (Unit SN.1A, Sp.No.59786, X20).



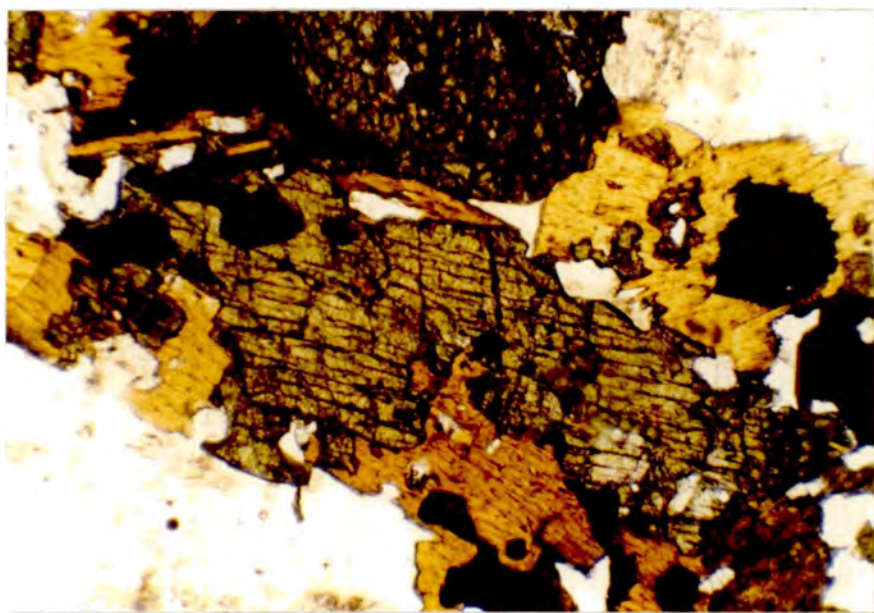
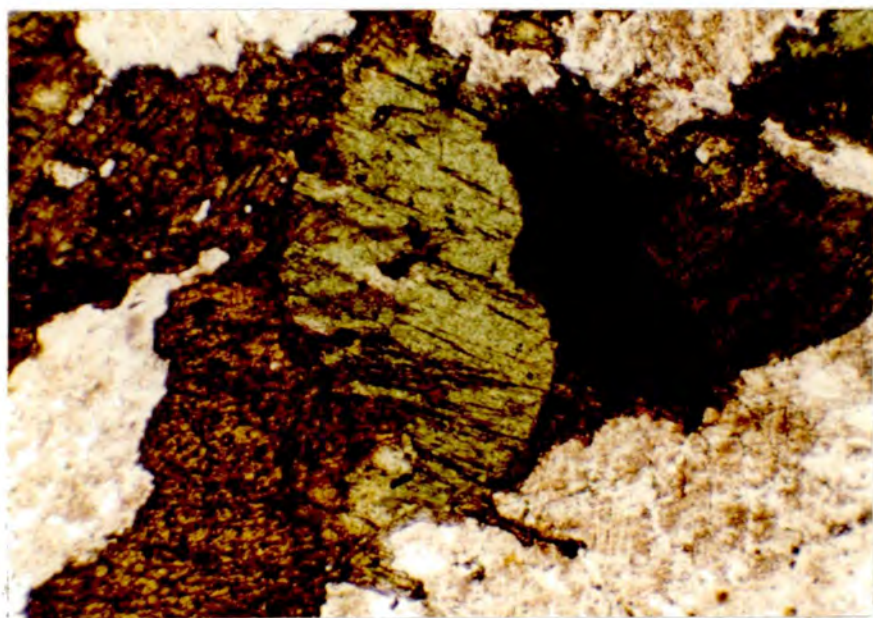
aegirine-augite rims. In contrast to the small cores, these rims are often interstitial to nepheline and feldspar. The unit's interior is characterised by the presence of a very Na-rich pyroxene. Both pale green aegirine and yellow-brown acmite occur (Plate 15), either as rims to amphibole, or as large interstitial wedges.

Amphibole occurs in variable quantities, and is always anhedral. It may be the dominant mafic mineral, or limited to thin rims on pyroxene. The brown pleochroic amphibole (X = straw yellow, Y = red-brown, Z = dark brown) of the marginal rocks rims augite (Plate 16). Further into the unit, this brown amphibole is replaced by a green variety (X = green-brown, Y = olive, Z = olive) and towards the centre the green variety is zoned to give rims of a grey-blue amphibole (?X = indigo, ?Y = grey-blue, ?Z = green-blue). This is the amphibole often found rimmed by sodic pyroxenes. In this central area, there is evidence of more extensive amphibole replacement, a mass of aegirine, opaques, biotite, analcite and carbonate completely pseudomorphing the amphibole. It is possible that certain of these areas reflect replacement of aegirine rather than amphibole. If so, the replacing minerals suggest reaction with a late stage aqueous fluid.

The final mafic phase in SN.1A, biotite, is abundant at the margins forming thick rims around opaque grains and

Plate 15. Khaki brown amphibole (far right)  
rimmed by dark green aegirine-augite,  
which in turn is rimmed by pale green  
aegirine and pale brown acmite (left).  
(Unit SN.1A, Sp.No. 155069, X30).

Plate 16. Pale green ferro-augite rimmed by brown  
amphibole. Plate also shows opaques  
rimmed by biotite.  
(Unit SN.1A, Sp.No. 52218, X30).



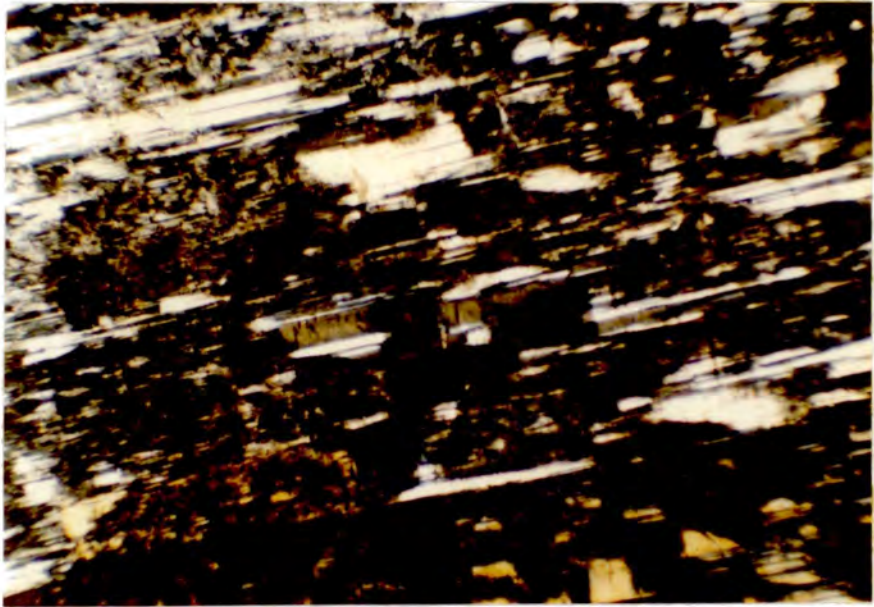
occurring as discrete crystals. The biotite here has the pleochroic scheme of lepidomelane (X = straw yellow, Y = Z = dark brown). Further into the unit, biotite rapidly becomes much less significant, and occurs as either a red variety (X = brown, Y = Z = red-brown), or a brown-green variety (X = brown, Y = Z = green-brown). It is most common in replacement areas as tiny flakes associated with opaques, analcite and aegirine.

Feldspar is the dominant mineral. At the unit's margins, it occurs as irregular crystals with interlocking rims, possibly indicating relatively rapid cooling. This is in agreement with the very fine scale perthitic textures developed (Plate 17). Further into the unit, the feldspars are tabular, showing Carlsbad or Manebach twinning. Here, the perthites are coarser (Plate 18), the Na-rich phase showing fine scale albite and occasionally pericline twins, and the K-rich phase tending to be cloudy with no obvious twinning. In terms of the albite/orthoclase ratio, these feldspars could be called antiperthites. Albite rims may be developed, but they are in optical continuity with the albitic phase in the feldspar core and represent exsolution.

Nepheline shows considerable variation between the marginal rocks and the interior. In the margins, it may be absent or occurs as small interstitial patches, indicating

Plate 17. Fine scale perthitic textures in the marginal rocks of unit SN.1A. The exsolution is on a coarser scale at grain margins and along fractures in the feldspars. (Unit SN.1A, Sp.No. 52218, crossed polars, X30).

Plate 18. Much coarser perthitic textures from the interior of unit SN.1A. (Unit SN.1A, Sp.No. 155005, crossed polars, X30).



late crystallization. A second mode of occurrence is as blebs and stringers in alkali feldspar. When fresh, these blebs can be seen to have the same optical orientation (Plate 19), suggesting formation by sub-solidus exsolution. Similar textures, also attributed to exsolution, have been described from the Oslo Larvikites (Widenfalk, 1972).

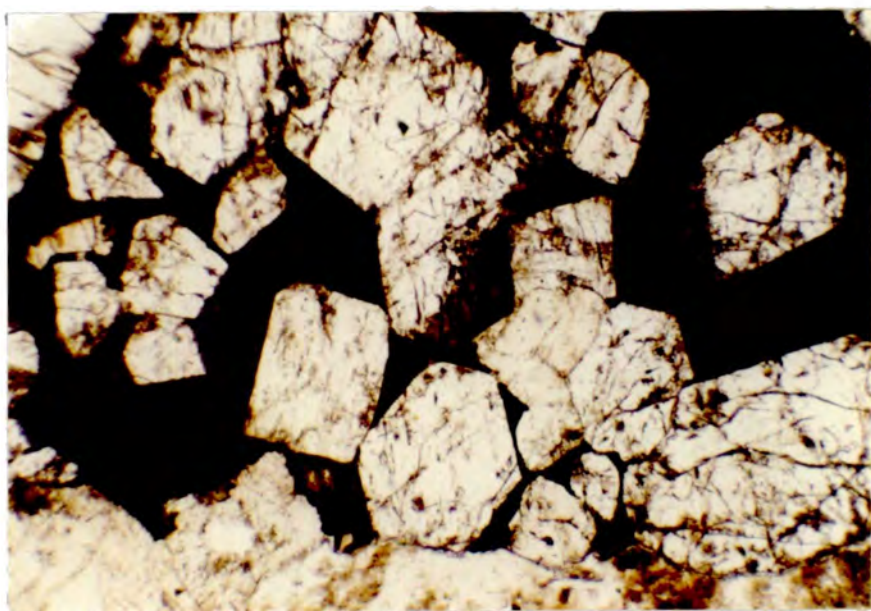
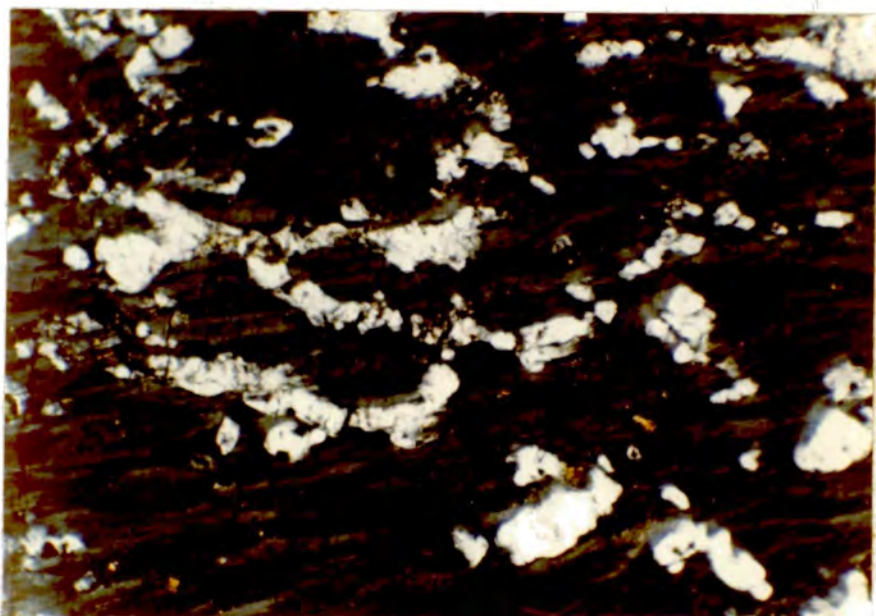
Towards the interior of the intrusion, nepheline rapidly assumes the status of a principal phase, euhedral crystals forming up to 20% of the rock (Plate 20). Both nepheline and feldspar were early formed minerals, mafic minerals occurring in the interstices between these phases.

Nepheline in all rocks of SN.1A may be altered to a fine-grained mass of gieseckite.

Cancrinite, sodalite, analcite and natrolite occur only very rarely in the marginal rocks, but are common in the interior, often forming a considerable proportion of the rock. Cancrinite may occur as a mosaic of crystals rimming and replacing nepheline, or together with analcite in interstitial patches. Sodalite, most easily identified by its orange fluorescence under ultra-violet light, is common either as interstitial wedges or as poikilitic patches enclosing nepheline and feldspar. Analcite, as well as occurring with cancrinite, also forms abundant interstitial areas. It can readily be identified and dis-

Plate 19. Nepheline blebs, apparently showing the same optical orientation, in perthitic alkali feldspar. (Unit SN.1A, Sp.No. 52221, crossed polars, X60).

Plate 20. Euhedral nepheline crystals set in brown interstitial amphibole. (Unit SN.1A, Sp.No. 155005, X30).



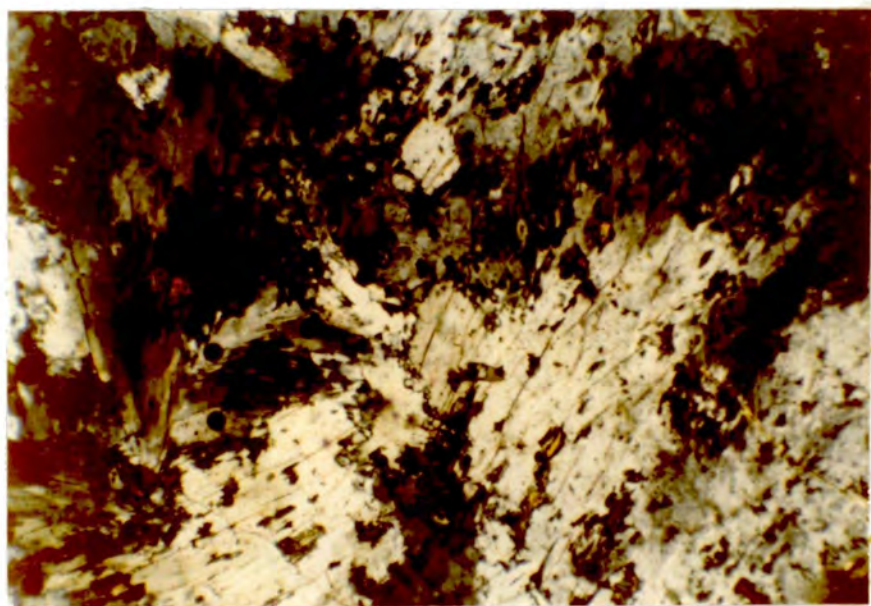
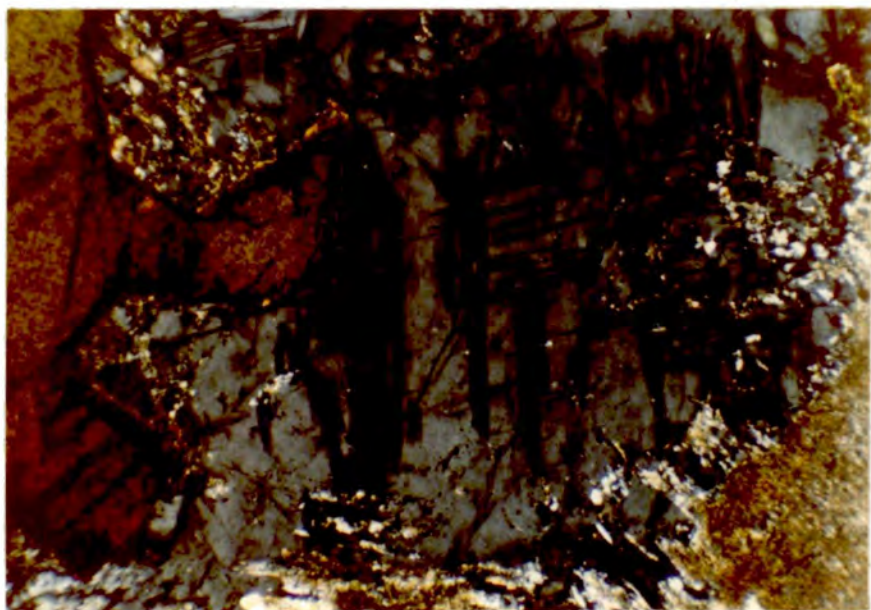
tinguished from sodalite by a low, but definite, birefringence. It also shows polysynthetic twinning (Plate 21), this variety of analcite having been described from Ilimaussaq (Sørensen, 1962) and other Gardar centres. Natrolite occurs sporadically as a late stage mineral in radiating fan-like patches (Plate 22). There appears to be an antipathy shown between natrolite and analcite probably reflecting replacement of the latter by the former.

Together with the major phases already mentioned, a number of minor phases occur in SN.1A. Calcite and fluorite form as alteration products and vein minerals, although fluorite is also present as a primary phase. Spene and zircon occur sporadically, especially in marginal rocks. Occasionally a colourless, euhedral, high relief mineral, identified as monazite, was found (Biaxial +ve,  $2V \ 10^\circ$ , small extinction angle, birefringence up to middle second order). Slightly higher contents of Th and La in the rocks containing this mineral supported the identification. One specimen of SN.1A contains a cluster of minute crystals, pleochroic from yellow to orange to violet-pink. This scheme suggests the mineral may be the Mn-rich epidote piedmontite.

The petrographic description of SN.1A shows there to be a considerable variation in rock type across the

Plate 21. Large area of analcite, interstitial to aegerine and nepheline. The analcite shows the characteristic polysynthetic twinning and very low birefringence. (Unit SN.1A, Sp.No. 46295, crossed polars, X30).

Plate 22. Typical radiating fan-like patches of the late stage mineral natrolite. (Unit SN.1A, Sp.No. 155018, crossed polars, X30).



outcrop, as already surmised from field observations. To see the geographical distribution of these types, SN.1A can be divided into three facies designated A, B and C. This division has been made on a number of mineralogical criteria outlined in Table 2. It must be emphasised that these three facies grade into each other, and that all intermediaries can be found.

Fig. 3.1 shows the distribution of these three facies. Fig. 3.2 shows the occurrence of (a) olivine and (b) cancrinite, two minerals used as criteria in placing rocks into a particular facies.

#### 3.2.2. SN.1B

This unit is finer-grained than SN.1A and has markedly porphyritic feldspars. However, apart from these features, it shows a strong petrographic resemblance to SN.1A. Whereas SN.1A showed mineralogical variation in a lateral sense, SN.1B is more inclined to show vertical variation, with the least fractionated rocks being exposed at the highest topographic levels. This is in accordance with observations from the field relations, that the level of erosion has exposed the roof zone of SN.1B.

In the highest levels of the unit, the rocks contain occasional pseudomorphs after olivine, pink augitic pyroxene, amphibole (X = brown-green, Y = green-brown, X = olive green), abundant Fe/Ti oxides rimmed by

TABLE 2

## Facies A: Marginal rocks of the unit.

1. Fayalitic olivine or pseudomorphs after olivine.
2. Pale pink or pale green euhedral or subhedral augites and ferro-augites.
3. Nepheline occurring as blebs in feldspar or as interstitial patches.
4. Amphibole pleochroic in shades of brown.
5. Abundant Fe/Ti oxides and apatite, occurring in mafic clusters.
6. Thick reaction rims of lepidomelane around the Fe/Ti oxides.
7. Little, if any, cancrinite, sodalite, analcite or natrolite.
8. Fine scale perthitic feldspars with irregular interlocking margins.

## Facies B: Intermediate between A and C.

1. Anhedral apple-green aegirine-augite.
2. Amphibole pleochroic in shades or green.
3. Nepheline more abundant.
4. Cancrinite, analcite, sodalite and natrolite becoming prominent.
5. Fe/Ti oxides and apatite becoming much less abundant.

## Facies C: Highly fractionated interior of SN.1A.

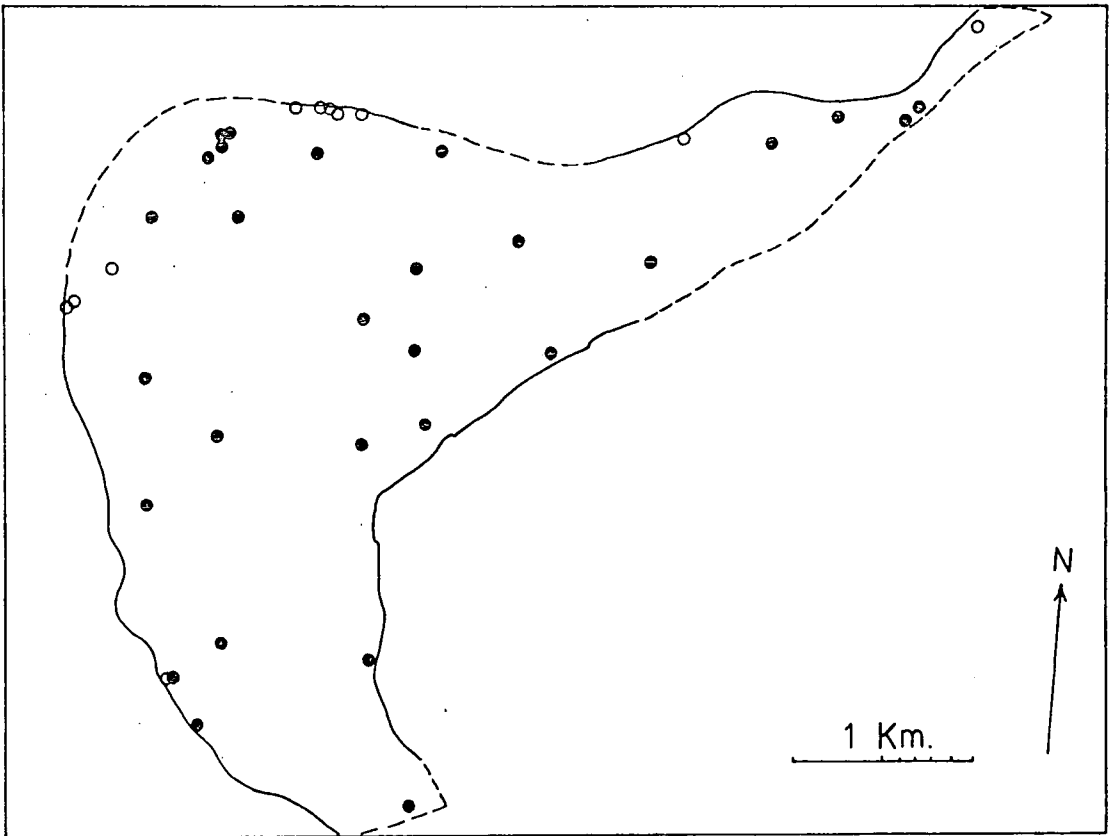
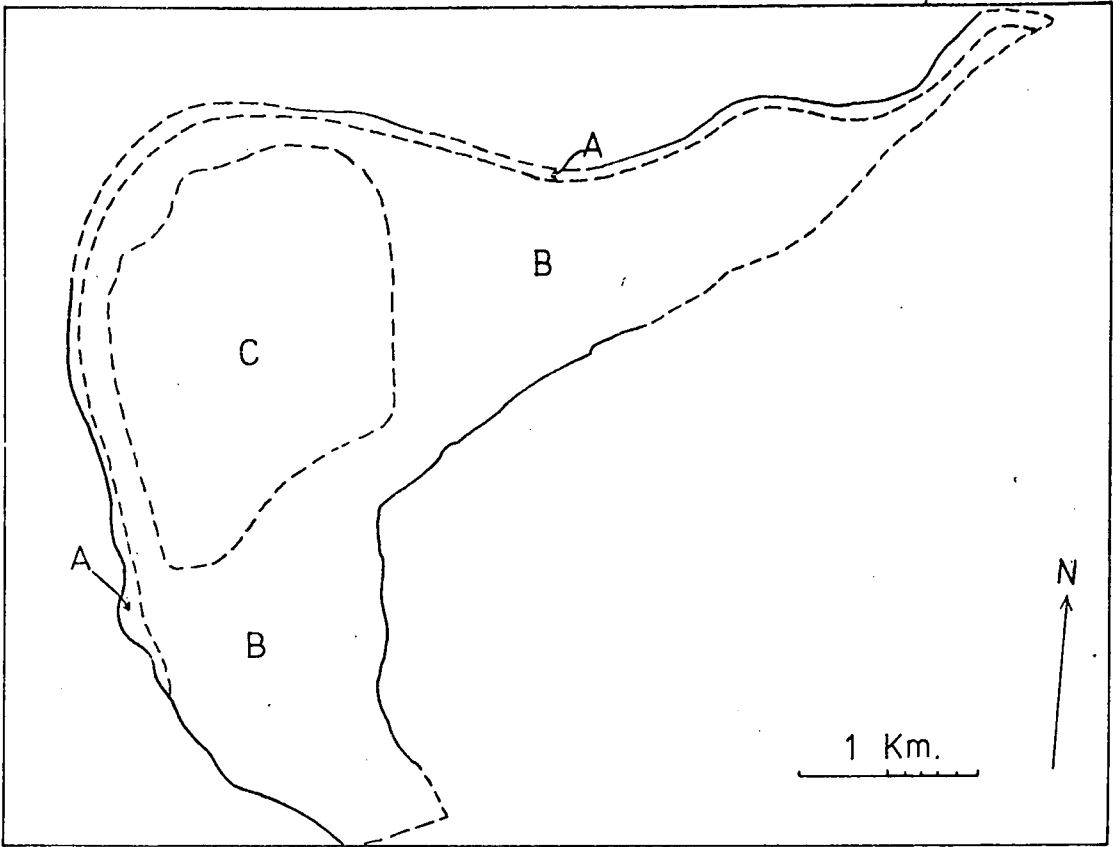
1. Pale green aegirine or brown acmite as the dominant mafic mineral.
2. Amphibole absent, or where present pleochroic in shades of blue and green, and rimmed by sodic pyroxene.
3. Nepheline euhedral, often rimmed by cancrinite.
4. Cancrinite, sodalite, analcite and natrolite forming up to 40% of the rock.
5. Occasional aenigmatite.
6. Fe/Ti oxides only present in small granular patches.
7. Apatite absent.

Fig.3.1 The distribution of the three 'facies' of unit SN.1A, outlined in Table 2.

Fig.3.2 The occurrence of olivine and cancrinite in unit SN.1A. These are two of the minerals used as criteria for dividing the unit into 'facies'.

○ - Olivine.

● - Cancrinite.



lepidomelane, and apatite. The feldspars are microperthitic and occur as subhedral, somewhat embayed crystals. Nepheline and other aluminosilicates are rare, and only occur as interstitial patches. In the roof zone the dominant mafic mineral is amphibole, although the amphibole to pyroxene ratio can be variable, even over small areas.

With decreasing height in SN.1B, the following changes are observed. Pyroxene becomes more sodic and occurs as late stage interstitial patches and small prismatic needles (Plate 23). Amphibole (X = blue, Y = grey, Z = blue-green) becomes scarcer and may disappear completely. Where present, it is rimmed by sodic pyroxene. Oxides are either absent or occur as granular patches, together with pyroxene, biotite and analcite, replacing amphibole. The biotite has a strong red colour (X = brown, Y = Z = red-brown), and is intimately associated with amphibole. Feldspar is again microperthitic, but now occurs as euhedral, tabular crystals. Nepheline also occurs as euhedral crystals, forming up to 20% of the rock, and shows extensive replacement, often by a mixture of analcite and cancrinite. The cancrinite occurs as 'peg-like' crystals orientated in two preferred directions, probably related to original crystallographic directions in the nepheline. The late stage aluminosilicates, sodalite, cancrinite, analcite and natrolite, are abundant, natrolite

giving the impression of being the last mineral to form, and tending to vein other minerals in a rather diffuse fashion.

Accessory minerals include fluorite, calcite, zircon and monazite.

### 3.2.3. SN.2

This relatively small unit shows little petrographic variation. Olivine is absent and pyroxene and amphibole occur, together with rounded opaques, in clusters. The opaques are magnetite with exsolved lamellae of ilmenite, and have occasional rims of biotite. The pyroxene occurs as large euhedral to subhedral augite crystals rimmed by a brown amphibole (X = yellow-brown, Y = red-brown, Z = dark brown), which itself zones outwards to a green-brown amphibole (X = brown-green, Y = olive-green, Z = olive-green). The unit's greatest variation is in the relative abundances of pyroxene and amphibole, amphibole being more abundant towards the margins, where it can occur as poikilitic crystals up to 10 cm. in diameter.

Alkali feldspar is present as large irregular micro-perthitic crystals, the Na-rich phase showing albite twins, and being enclosed in a cloudy K-rich host. Albite rims are common and occasional discrete grains of albite occur. A few crystals show a degree of compositional zoning, relatively small clear cores contrasting with thick, partly

altered, perthite rims. Nepheline is always present but never forms euhedral crystals. It is altered, either to gieseckite, or to a coarser-grained combination of mica and zeolite. SN.2 does not show any extensive development of the late stage aluminosilicates.

#### 3.2.4. ?SN.3

So few samples (5) could be collected of this unit, that it is impossible to say whether they are representative of the whole unit, or merely a marginal phase. The rocks show characteristics of derivation from a highly fractionated magma. Olivine is absent and both opaques and apatite uncommon. The pyroxene is typically anhedral aegirine-augite or 'blades' of aegirine. Aegirine may also rim a green amphibole (X = green, Y = grey-green, Z = blue-grey).

The biotite of ?SN.3 is a red-brown variety (X = brown, Y = Z = red-brown). It rims opaques and also occurs, with opaques, separating amphibole cores from rims of aegirine.

The feldspars are large laths of Carlsbad twinned microperthites with albite rims. Nepheline occurs as blebs in feldspar, but is more common as large subhedral crystals, forming up to 30% of the slide. The most distinctive feature of all the samples is the abundant presence of cancrinite. It occurs in radiating mosaics,

rimming and replacing embayed nepheline (Plate 24). The general impression is of a magma with a relatively high  $\text{CO}_2$  content, which, with fractionation, forms the carbonate bearing phase cancrinite at the expense of nepheline. This is supported by the occasional presence of calcite as a late stage phase, crystallising together with tiny blades of aegirine. Sodalite, analcite and fluorite were all found, in variable amounts, in the five specimens of ?SN.3.

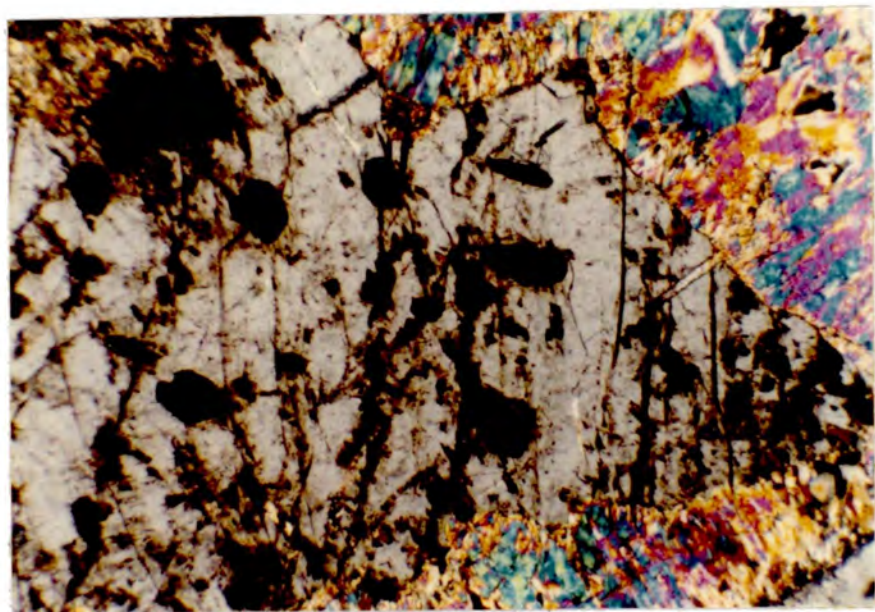
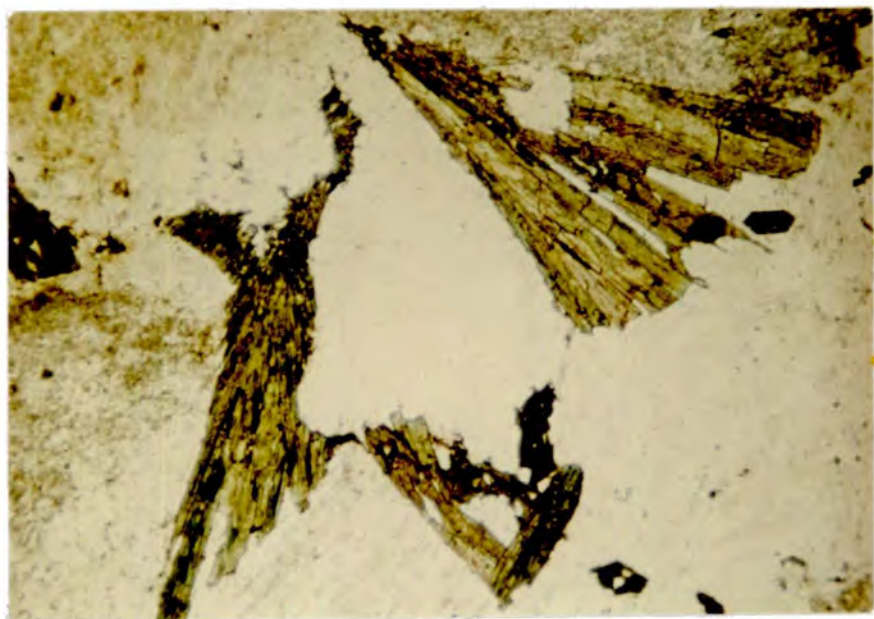
It is interesting to note that the five specimens collected, apart from a greater abundance of cancrinite, resemble in many petrographic features unit SM.4 of the Motzfeldt Centre. Perhaps, as suggested in the chapter on field relations, ?SN.3 is really a member of the Motzfeldt Centre, and the intrusion of Motzfeldt post-dates North Qôroq.

#### 3.2.5. SN.4A

This outer unit of SN.4 has a uniformly fine-grained groundmass and contains a number of types of phenocryst. Close to the margins with older units, the groundmass is so fine-grained that the rock must approximate to a 'chill', the phenocrysts indicating minerals on the liquidus at depth. The phenocrysts are of five types:

Plate 23. Prismatic needles of sodic pyroxene in unit SN.1B, associated with sodalite, analcite and natrolite. (Unit SN.1B, Sp.No. 155108, X60).

Plate 24. Nepheline crystal (grey) rimmed and extensively embayed by radiating mosaics of cancrinite (high birefringence). Section slightly thicker than normal. (Unit ?SN.3, Sp.No. 155180, crossed polars, X30).

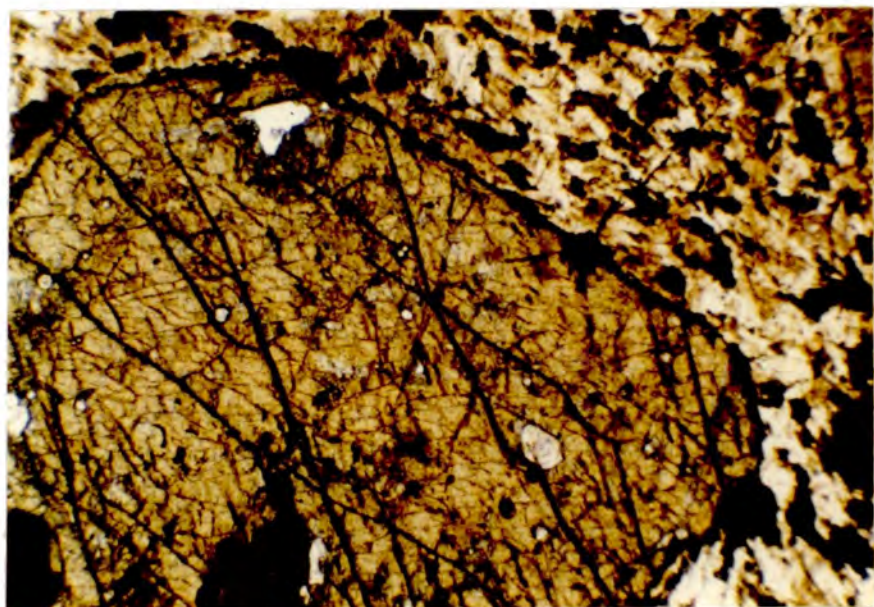
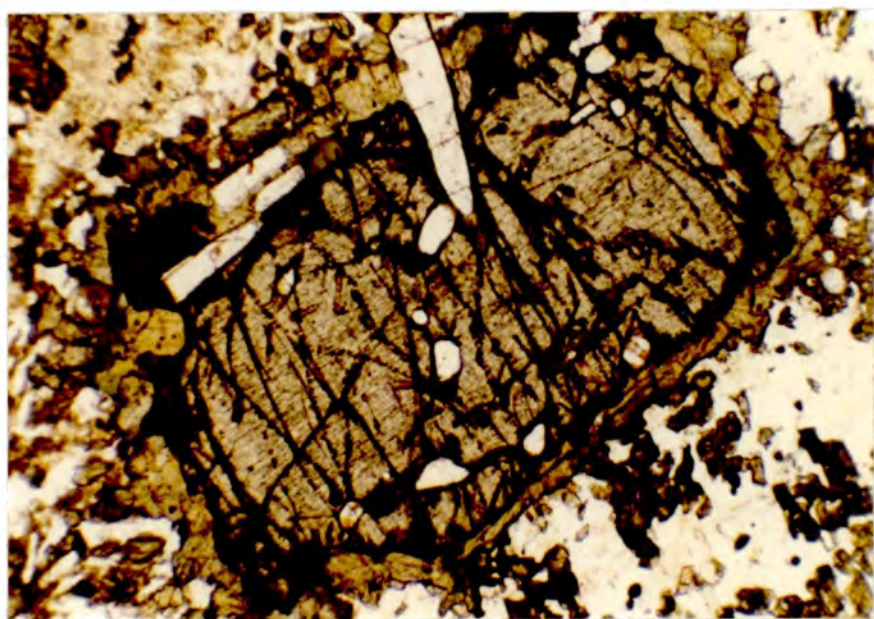


- a) Stout apatite needles up to 4 mm. in length.
- b) Rounded Fe/Ti oxides often rimmed by biotite.
- c) Olivine, rounded and rimmed by opaques, with an outer rim either of pale green pyroxene or blue-green amphibole (Plate 25).
- d) Euhedral pale pink augitic pyroxenes, with pale green ferro-augite rims (Plate 26).
- e) Numerous tabular feldspars up to 3 cm. in length.

The feldspar phenocrysts are the largest and most numerous, and are present even when other phenocrysts are not. They pose problems because of their variation. Some crystals are relatively unzoned, tabular and show perthitic exsolution on a fine scale. Other crystals, however, show a marked compositional zoning, borne out by probe work, with a definite core and contrasting rim. The rims may be extensive or narrow and again are composed of microperthite. The cores are distinctly different, being usually clear and free of obvious exsolution. Some crystal cores show a diffuse cross-hatch twinning, suggestive of anorthoclase, and resemble feldspars found in dyke rocks of the area. Other cores are apparently untwinned. The feldspar phenocryst cores may occur as clusters with a microperthitic rim surrounding the cluster. Whether the cores are single

Plate 25. Large olivine phenocryst enclosing stout prismatic needles of apatite. The olivine is rimmed and veined by Fe/Ti oxides and further rimmed by pale pyroxene and green-brown amphibole. (Unit SN.4A, Sp.No. 59758, X60).

Plate 26. Large, euhedral, pale pink augite phenocryst in fine grained groundmass of pyroxene, amphibole, Fe/Ti oxides and alkali feldspar. (Unit SN.4A, Sp.No. 155152, X60).



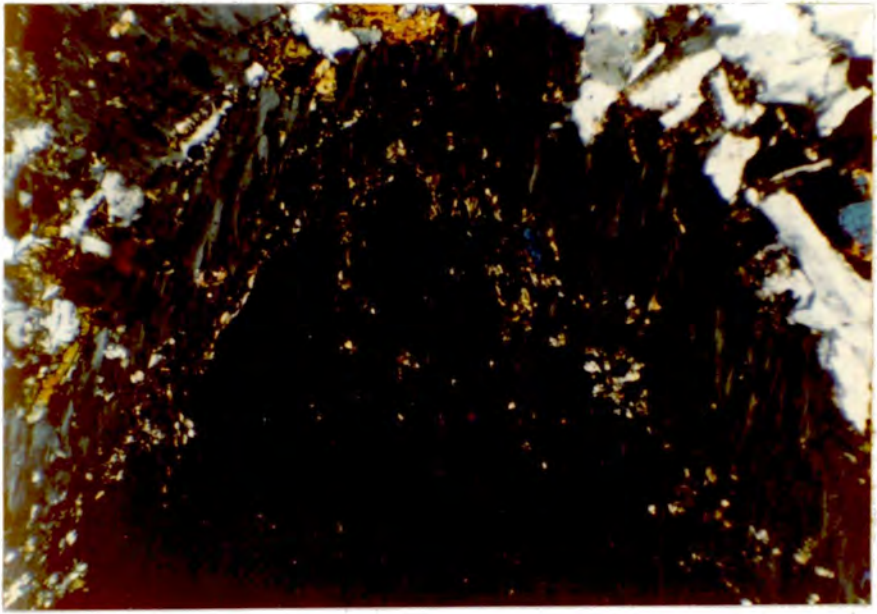
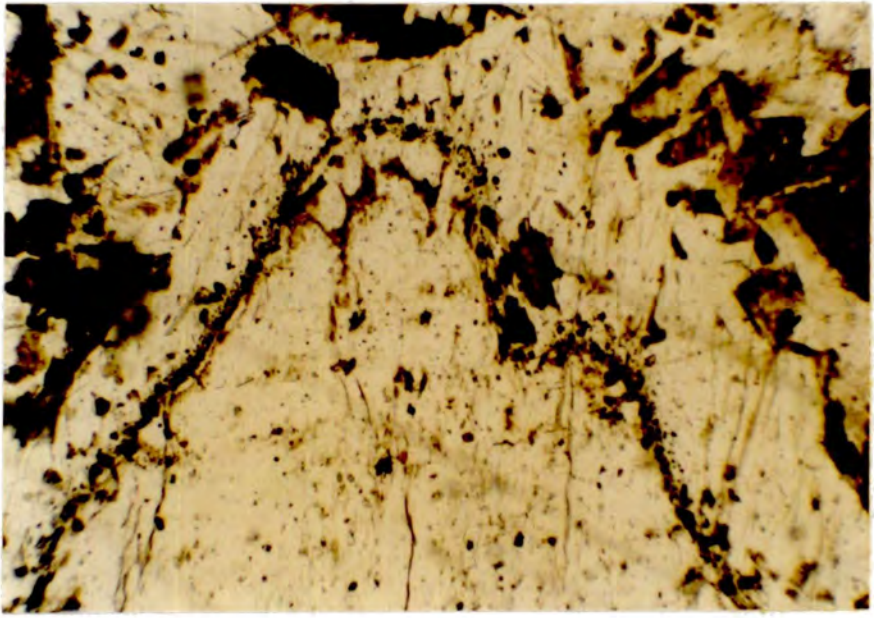
crystals or clusters, a thin line of tiny drop-like augite and/or amphibole crystals, similar to those found in the groundmass, separates core from rim (Plates 27 and 28). Occasional samples show feldspar patches with a myrmekitic intergrowth involving feldspar, nepheline and pyroxene (Plate 29). These are probably recrystallization textures. Many features of the feldspars of SN.4A closely resemble those found in feldspars of the Oslo Larvikites (Muir and Smith, 1956; Widenfalk, 1972).

As in the outer part of SN.1A, nepheline can be found as numerous exsolution blebs in feldspar.

The groundmass of SN.4A consists of an intimate intergrowth of small, well-formed laths of microperthitic feldspar, similar to the phenocryst rims, occasional small olivines and opaques, pale green ferro-augites and brown or brown-green amphibole. The amphibole occurs both rimming pyroxene, and as small poikilitic grains. The pyroxene/amphibole groundmass relationship is of interest. In some specimens pyroxene is the dominant groundmass phase, whereas in others it is amphibole, even to the complete exclusion of pyroxene. Specimens occur in which, over a distance of a few millimetres, there are patches rich in amphibole and other patches rich in pyroxene. This demonstrates that the water content of the magma is variable, even on a

Plate 27. Large feldspar phenocryst showing separation of core from rim by a thin line of tiny drop-like pyroxene and amphibole crystals. (Unit SN.4A, Sp.No. 59787, X60).

Plate 28. Same crystal, showing that the rim mentioned above separates a core showing faint diffuse twinning from a perthitic rim. (Unit SN.4A, Sp.No. 59787, crossed polars, X60).



microscopic scale. Nepheline, and to a lesser extent sodalite and analcite are present as very small and subordinate interstitial crystals.

#### 3.2.6. SN.4B

This unit develops a 'chill' against SN.4A, but quickly increases in grain size towards the centre of the intrusion, although always remaining finer grained than the other North Qôroq units. It shows the same petrographic features as SN.4A, containing phenocrysts of apatite, Fe/Ti oxides, pyroxene, olivine and feldspar. Moving towards the centre of the unit, a variation can be seen. The most noticeable feature is a decrease in the phenocryst content of the rock. Apatite, pyroxene, Fe/Ti oxide and olivine phenocrysts become noticeably less common and eventually absent, away from the margins of the unit, but feldspar phenocrysts persist, and it is only in exposures close to the unit's centre that they become rare. As the phenocryst content decreases, the groundmass crystals become larger and tend to show some changes in composition, when compared with the same phases at the unit's margins. Augitic pyroxene has thick rims of aegirine-augite and amphibole is pleochroic in shades of green rather than brown. Amphibole is also present in greater quantities than the pyroxene. Biotite occurs as

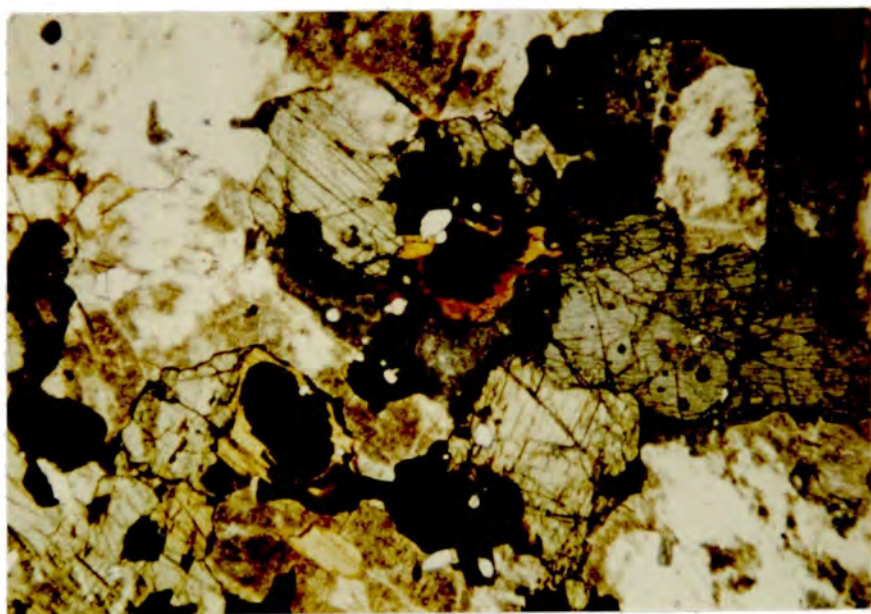
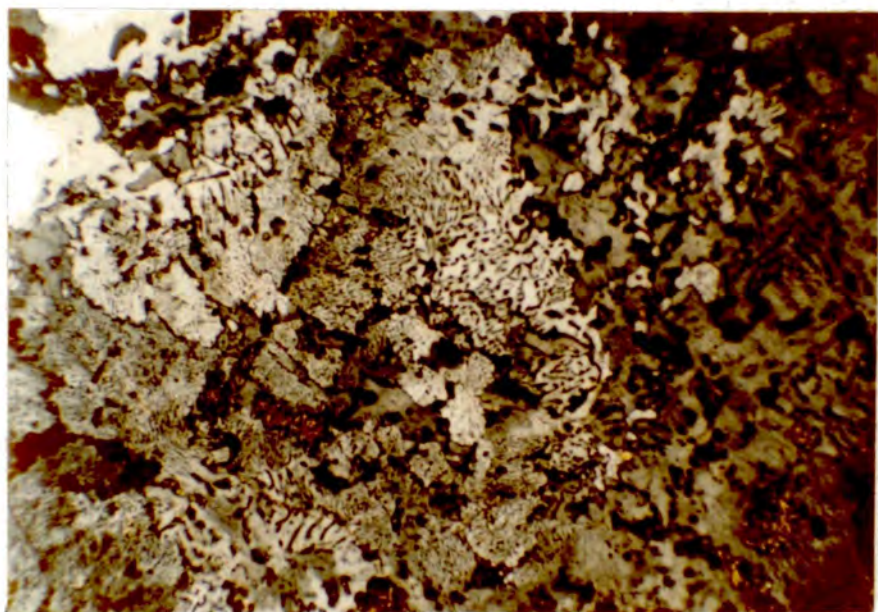
flakes in amphibole and as rims to rounded Fe/Ti oxides. These mafic minerals and opaques occur together in clusters (Plate 30). The dominant opaque is magnetite with fine scale exsolution lamellae of ilmenite. Occasional small, rounded blebs of pyrrhotite were identified. Much of the exposure in the interior has been lost by the intrusion of SN.5, but nepheline, although still interstitial, can be seen to form up to 10% of the rock, and sodalite, analcite and occasionally cancrinite are more prominent.

#### 3.2.7. SN.5

This innermost unit is coarse-grained, lacks abundant mafics and is foyaitic. Some variation can be seen in the unit, although not in a systematic sense (i.e. from margins to centre), due to the complex field relationships with SN.4. All samples show the unit to be highly fractionated. Olivine is absent and the typical pyroxene is a pale yellow-green aegirine, although, at contacts with earlier SN.4B, aegirine-augite can be found. Pyroxene crystals are frequently tabular and may show zoning at their rims from yellow-green, to blue-green, to extreme rims of pale brown acmite. Radiating needles of pyroxene are also present. Amphibole may be absent from SN.5, and when present occurs as anhedral crystals (?X = blue-green, ?Y = grey, ?Z = blue-grey), rimmed by sodic pyroxene (Plate 31). Just as in

Plate 29. Myrmekitic intergrowth involving feldspar, nepheline and pyroxene. Probably a re-crystallization texture. (Unit SN.4A, Sp.No. 59800, crossed polars, X60).

Plate 30. Typical mafic cluster in SN.4B, involving pale green ferro-augite, brown amphibole, Fe/Ti oxides and biotite. The phases surrounding the cluster are alkali feldspar and cloudy nepheline. (Unit SN.4B, Sp.No. 59788, X20).



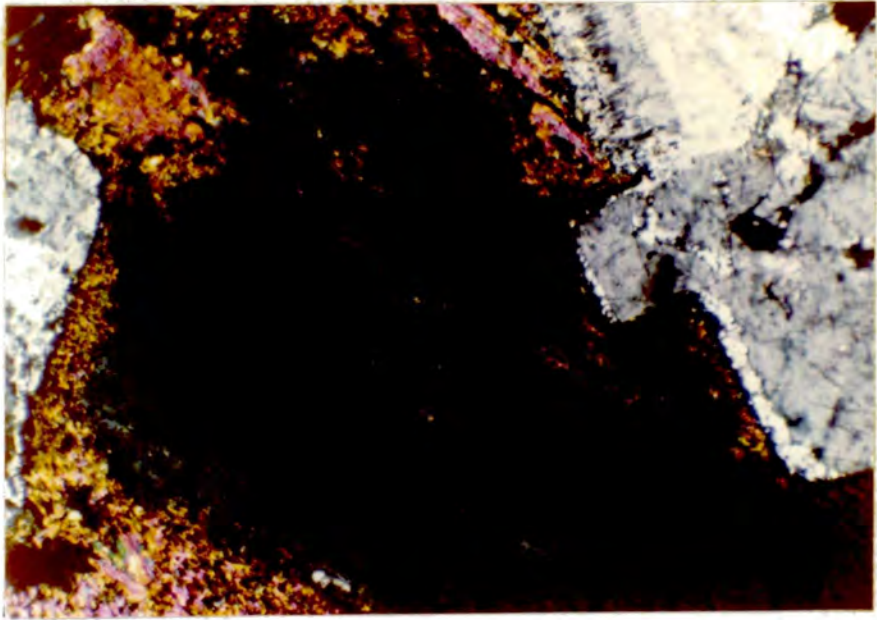
other highly fractionated rocks of North Qôroq, aegirine occurs, together with granular magnetite, biotite, calcite and analcite, probably replacing amphibole. Some areas, either originally of amphibole or sodic pyroxene, are now composed of calcite, analcite and fluorite. This may indicate late stage replacement by a volatile rich fluid, possibly an aqueous phase co-existing with the last dregs of SN.5 magma (see Chapter 6). Aenigmatite occurs occasionally in SN.5, although, as in SN.1A, positive identification is made difficult by the opaque character of the mineral.

The feldspars in SN.5 are tabular and often coarsely perthitic. Albite twins can clearly be seen in the exsolved blebs, and albite rims in optical continuity with these blebs are common. Small amounts of interstitial albite also occur, possibly not related to exsolution of an originally homogeneous feldspar, but to formation of albite from a late stage fluid. Nepheline is abundant and may be euhedral, although it is often embayed and rimmed by cancrinite. It frequently shows alteration to white mica crystals in an analcite background (Plate 32). Sodalite is prominent as interstitial wedges or poikilitically enclosing euhedral nepheline and feldspar (Plate 33). Both natrolite and analcite are abundant and, together with cancrinite and sodalite, may form 40% of the rock.

Plate 31. Sodic pyroxene, showing high birefringence colours, rimming blue-green amphibole. Also on the plate are euhedral nepheline crystals with a narrow rim of cancrinite. (Unit SN.5, Sp.No. 155194, crossed polars, X30).

Plate 32. Nepheline crystal, now altered to white mica crystals in a background of analcite, The orientation of the mica presumably reflects crystallographic directions in the original nepheline crystal. (Unit SN.5, Sp.No. 155187, crossed polars, X30).

Plate 33. Sodalite, poikilitically enclosing tiny feldspar and nepheline crystals. (Unit SN.5, Sp.No. 155103, crossed polars, X60).



Calcite occurs in SN.5, both as interstitial crystals and irregular patches. Of the rare minerals, monazite again is present and a late stage zeolitic mineral, which probe analyses show to be thompsonite.

### 3.2.8. Conclusions from the major units

Extensive discussion will be deferred until mineralogical and geochemical evidence has been presented (Chapter 4 and Chapter 5). A number of tentative conclusions can, however, be drawn at this stage.

1. Many of the units show marginal facies, and even 'chills', of a rock type akin to augite syenite.

2. There is a noticeable and systematic variation in petrographic character over the outcrop of certain units. This can be seen to be in a lateral sense, i.e. from margin to centre, for SN.1A and SN.1B, although much more marked for SN.1A. SN.1B shows variation in a vertical sense, as might be expected in the vicinity of a roof zone and SN.5 shows irregular variation, consistent with the complex field relations shown between this unit and SN.4.

3. The phenocryst content of SN.4B decreases from margin to centre of the unit, the effect being more noticeable for the denser phases, opaques, olivine and augite, and less noticeable for the less dense feldspar. A similar, but even more marked, decrease is suggested for SN.1A where the occurrence of olivine, augite etc. is

restricted to the extreme margins.

4. The variable quantities of amphibole and pyroxene over small distances in many units suggest variable contents of water in the magma. This is especially noticeable in both SN.4A and SN.4B, where the patchy distribution of groundmass amphibole and pyroxene occurs on a microscopic scale.

5. The mode of occurrence of late stage minerals such as analcite, sodalite and cancrinite indicates a magmatic origin. This would suggest that crystallization took place over a considerable temperature interval.

### 3.3. The minor units of North Qôroq

#### 3.3.1. Microsyenite sheets

Examination of mafic bands in the microsyenite sheets shows concentrations of amphibole (X = brown-green, Y = olive, Z = green-yellow). Opaques occur as rounded grains in the amphibole, and the amphiboles themselves may be replaced by sodic pyroxene and biotite along rims and patchily along cleavages.

Feldspars in the microsyenites are tabular Carlsbad twinned microperthites and show a strong lamination. Nepheline is abundant, but interstitial to feldspar and natrolite occurs sporadically, poikilitically enclosing earlier formed minerals.

### 3.3.2. Carbonate-rich breccia plug

The breccia plug shows a marked similarity in thin section to bodies described by Stewart (1970) and Walton (1965), occurring in the vicinity of Qagssiarssuq. All sections of the North Qôroq plug show extensive carbonate alteration. The dominant replacement mineral, apart from the carbonate, is a pale honey-coloured phlogopitic mica (X = yellow, Y = Z = brown-red). This occurs with carbonate, both in the groundmass and replacing pre-existing 'phenocrysts'. The groundmass also contains opaque material, serpentine and rare titaniferous augite or pale green ferro-augite. Megacrysts of both mica and pyroxene were encountered in hand specimens.

The large pseudomorphs altered to mica, carbonate and opaques are often difficult to identify. In sections showing less alteration, many can be seen to be micro-perthitic alkali feldspar. Usually these pseudomorphs after feldspar are euhedral. Smaller pseudomorphs of carbonate and opaques occur after what was probably pre-existing olivine, although nowhere does even a trace of the original olivine remain. Broad prismatic pseudomorphs with pointed terminations, found in the carbonate plugs at Qagssiarssuq, were interpreted by Stewart as representing original olivine. Pseudomorphs occurring in the North Qôroq

plug are similar in shape. Stewart also interpreted certain characteristically-shaped pseudomorphs as being after the minerals melilite and perovskite. This type of pseudomorph also occurs in North Qôroq and may well represent similar original material.

Rounded dark inclusions are abundant in the North Qôroq plug and in those at Qagssiarssuq. Examination shows them to consist, most frequently, of well-formed calcite crystals surrounded by rims of phlogopitic mica. It is tempting to suggest that these inclusions are in fact 'bubbles', indicating immiscibility between a silicate melt and a carbonate-rich fluid phase.

Numerous xenoliths of syenitic material, often identifiable as North Qôroq syenites, occur in the plug. Perhaps many, or all, of the partly pseudomorphed micro-perthite crystals are xenocrysts derived from the surrounding syenites. Indeed, their very variable and often partial replacement by carbonate and mica would support this.

Whether the original magma type could be described as a monchiquite or alnoite remains uncertain. Whatever the material, it has incorporated a mass of high level xenoliths and xenocrysts, and these, together with the original magma type, have undergone extensive carbonatization. It seems feasible that the ascending magma was

accompanied by a considerable quantity of an immiscible carbonate-rich fluid phase, which was responsible for the replacement and, by virtue of the high fluid pressure, for explosively brecciating the surrounding syenitic rocks.

### 3.4. The recrystallized rocks

#### 3.4.1. Introduction

This section deals with the recrystallization of major syenitic units by later similar units. Emeleus and Harry (1970) noted that the later Igdlérfigssalik Centre affected rocks of South Qôroq. Similar features are seen where South Qôroq cuts the older North Qôroq Centre. Recrystallization phenomena are not, however, restricted to areas where later centres cut earlier centres, but occur within the centres where later units intrude into, and undeniably metamorphose, earlier ones. The zone of recrystallization is never very extensive, the effect seldom occurring more than 100 m. from the contact. In North Qôroq the best developments of recrystallized rocks occur where South Qôroq cuts North Qôroq, where SN.5 intrudes SN.4 and where SN.1B intrudes SN.1A. Indeed, the obvious recrystallization of SN.1A by SN.1B was the primary reason for designating SN.1B as a separate unit.

### 3.4.2. Textures

Distinctive textures are one of the main criteria for identifying recrystallized rocks. One of the dominant textures is the formation of a granoblastic mosaic. Some distance from the contact the older rocks show a tendency for the groundmass minerals to form a fine-grained mosaic, with the rims of the larger feldspars and mafic minerals beginning to break up and contribute to it. As the contact is approached, the mosaic appears coarser, with simple intercrystal boundaries occurring between equigranular sodic pyroxene, feldspar, amphibole and opaques (Plate 34). In these rocks only a few larger crystals of perthite and nepheline resist the breakdown, and the net result is a rock with a porphyritic appearance. The occurrence, in other Gardar central complexes, of porphyritic syenites, especially when occurring as xenoliths, can perhaps be attributed to recrystallization of an earlier syenite, that may not have been porphyritic. Indeed, xenoliths of SN.1A in SN.1B show a distinct porphyritic tendency, whereas unaltered SN.1A is obviously non-porphyritic. Very close to the contact, or in xenoliths, the effect of recrystallization may have been such as to cause even the large resistant feldspars to breakdown, resulting in a fine-grained metamorphic syenite. Rocks described under the heading 'melange' in the North Qôroq Centre, where

SN.5 intrudes SN.4, are probably of this type. It is often difficult to tell whether originally perthitic feldspars are breaking down to separate crystals of a Na-rich and K-rich feldspar, because of the small grain size and general untwinned appearance of crystals in the mosaic. For some, this is not the case, as occasional small feldspar grains can be seen to be perthitic.

The second type of texture developed on metamorphism is a poikilitic, or more correctly poikiloblastic, texture. This texture is particularly shown by the recrystallized mafic minerals, but never by feldspar, which always occurs as part of the granoblastic mosaic, or as grains enclosed in the poikiloblastic crystals. Aegirine-augite, amphibole and newly formed aenigmatite may all be markedly poikiloblastic (Plates 35 and 36). Both analcite and sodalite can occasionally be seen as poikiloblastic crystals, and rims of large nepheline crystals may develop the texture (Plate 37), indicating secondary metamorphic growth. A final mineral which can occur poikiloblastically, is one which is rarely, if ever, observed in unrecrystallized rocks. It more commonly occurs in recrystallized rocks as prismatic, high relief crystals with ragged ends (Plate 38). Optical examination shows the crystals to be either colourless or very faintly pleochroic, from colourless to very

Plate 34. A recrystallized rock showing a typical granoblastic mosaic of alkali feldspar, amphibole, pyroxene and opaques. (Unit SN.4B, Sp.No. 59747, crossed polars, X30).

Plate 35. A recrystallization texture showing the development of poikiloblastic rims of aegirine-augite to pyroxene, and poikiloblastic aenigmatite (opaque). (Unit SN.1A, Sp.No. 155061, X20).

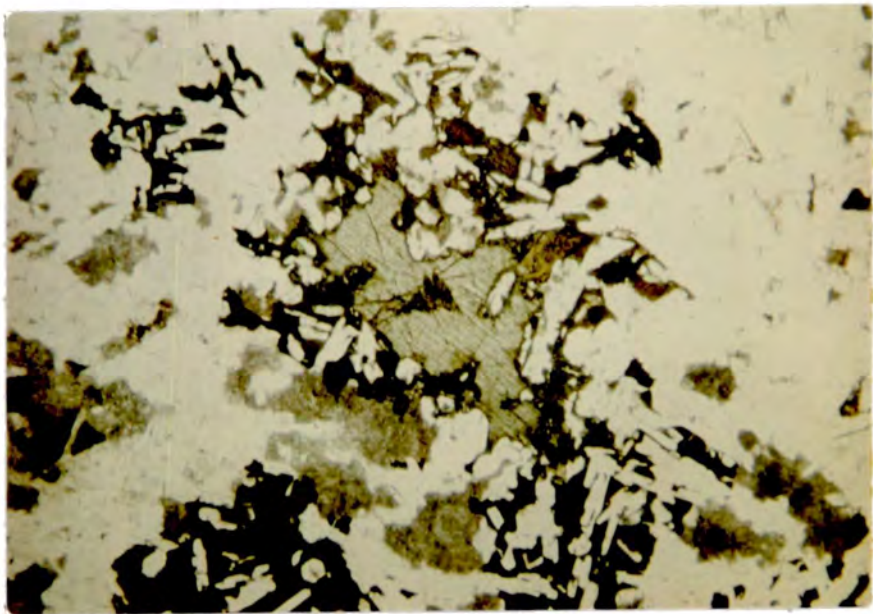
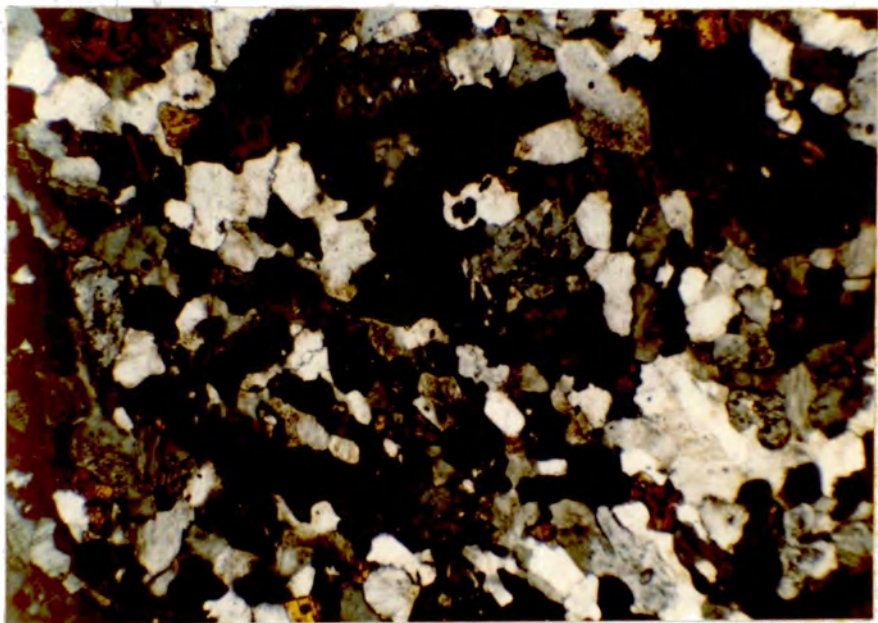
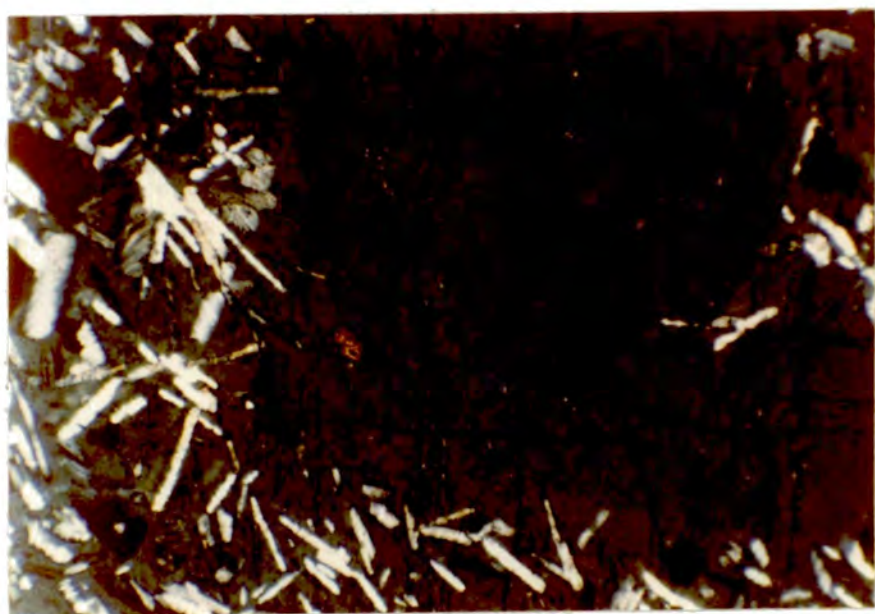
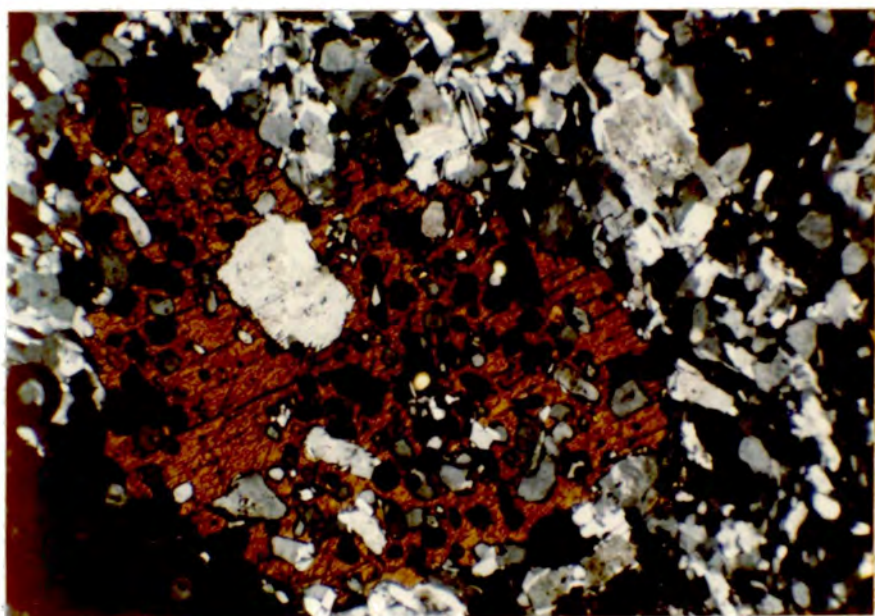


Plate 36. A recrystallization texture, showing poikiloblastic development of brown amphibole in a granoblastic groundmass, dominantly of alkali feldspar. (Unit SN.1A, Sp.No. 59751, crossed polars, X30).

Plate 37. A recrystallization texture, showing the development of a poikiloblastic rim to a large nepheline crystal. The unaffected core gives the rock a porphyritic appearance. (Unit SN.4B, Sp.No. 59739, crossed polars, X30).



pale yellow-brown. The crystals show polysynthetic twinning and a low birefringence, up to first order yellow. When the birefringent colour is grey, an anomalous blue tint is observed. The optical properties suggest that the mineral is a member of the rinkite group and partial probe analyses confirm it to be a zirconium-rich rinkite. The distribution of this mineral will be discussed later in the chapter.

#### 3.4.3. Mineralogical changes

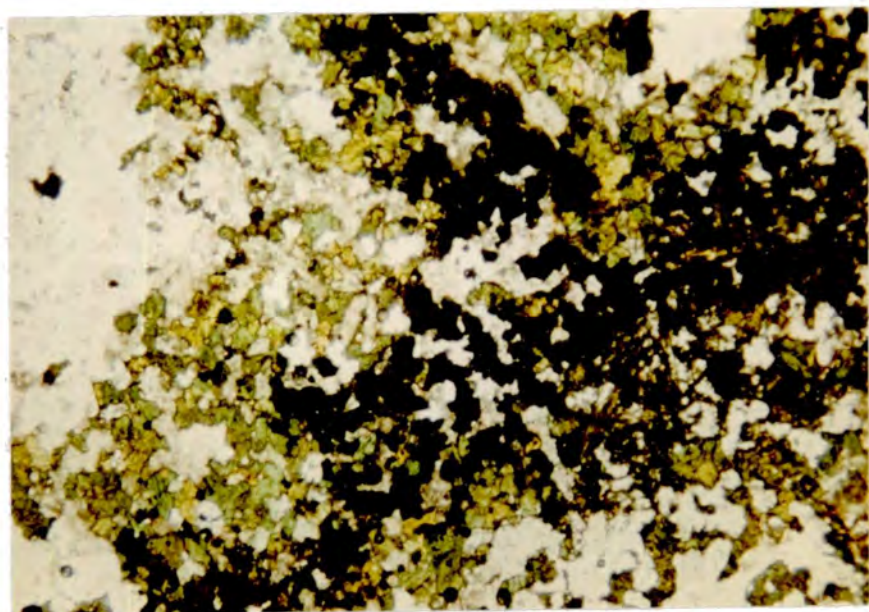
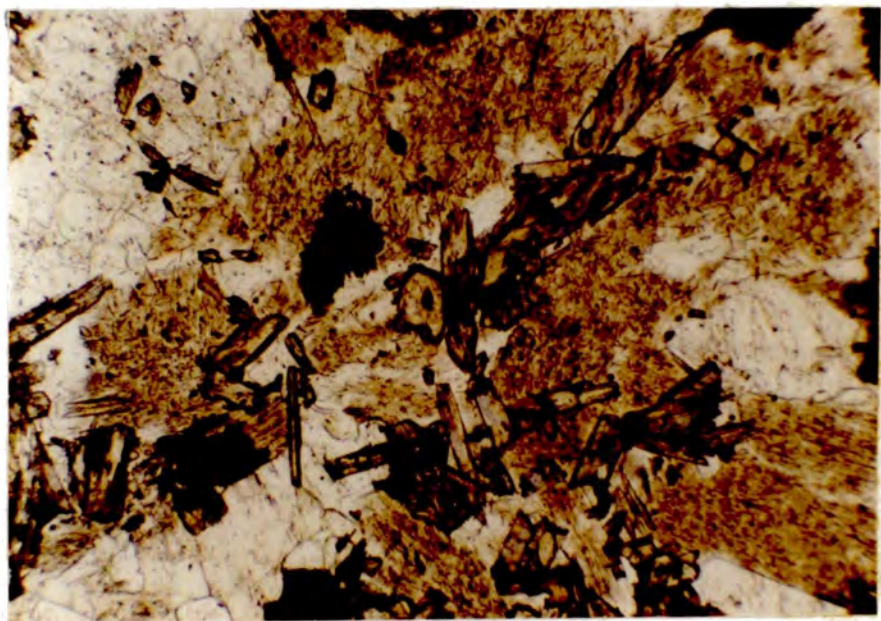
Metamorphism of the syenites of North Qôroq, as well as resulting in recrystallization, can cause a number of mineralogical changes. These changes often appear to involve a combination of metamorphism and metasomatism.

Evidence for metasomatism occurs in rocks some distance from the contact. The pyroxenes tend to be replaced along rims and cleavages by a more sodic pyroxene, the replacement occurring in an irregular and patchy manner. Similarly the brown-green or green amphiboles are patchily replaced by a blue, more sodic amphibole. The pyroxene and amphibole so formed are similar to those contributing to the granoblastic mosaic closer to the contact.

Some contact zones show breakdown of pre-existing amphibole, possibly already metasomatized, to a mosaic of magnetite, aegirine-augite and nepheline, with occasional biotite (Plate 39). This process may be represented by a

Plate 38. High relief, prismatic crystals of rinkite, developed a short distance from the contact of syenitic units, within the older unit. (Unit SN.1A, Sp.No. 59755, X60).

Plate 39. A recrystallization texture. Breakdown of pre-existing amphibole to give a mosaic of magnetite, aegirine augite and nepheline. (Unit SN.1A, Sp.No. 54221, X30).





igneous amphibole and pyroxene. They can perhaps be explained by reactions of the following type:

Igneous minerals	Process	Metamorphic minerals
Clinopyroxene	Metasomatism (Na <sup>+</sup> )	Sodic clinopyroxene
Clinopyroxene + Fe/Ti oxides	Metamorphism + metasomatism	Aenigmatite + sodic clinopyroxene
Amphibole	Metasomatism (Na <sup>+</sup> )	Sodic amphibole
Amphibole + Fe/Ti oxides	Metamorphism + metasomatism	Aenigmatite + sodic amphibole

The final mineralogical change may well be a retrogressive one. Around the rims, and along cleavages, of some of the poikiloblastic blue-green amphiboles a reaction rim of acmite + opaques  $\pm$  biotite  $\pm$  green amphibole is formed. This reaction mirrors that seen in certain unmetamorphosed syenites and may well be due to amphibole reacting and re-equilibrating with a late stage fluid. This rimming of amphibole could also be related to a local increase in oxygen fugacity. Ernst (1962) pointed out that the amphiboles of the riebeckite-arfvedsonite solid solution series are stable at relatively low partial pressures of oxygen and that at higher pressures acmite and opaques crystallize. Probe analyses show that the blue-green metamorphic amphibole found in the rocks is not far removed from arfvedsonite in composition.

#### 3.4.4. Conclusions

In xenoliths and at contact zones both metamorphic and metasomatic processes can be observed. Textural and mineralogical changes occur, depending on the nature of the newly intruded unit. The intrusions of SN.1B, SN.5 and South Qôroq (SS.2) were accompanied by marked metasomatism and the development of alkali pyroxene, alkali amphibole and aenigmatite. The main effect of the intrusion of SN.4, however, was to recrystallize the pre-existing minerals into a granoblastic mosaic. SN.4 may have been a drier body of magma, extensive metasomatism not accompanying its intrusion. The presence of a Na-rich fluid phase, associated with the intrusion of many of the other units, may also have facilitated metamorphic reactions by allowing greater mobility of the diffusing ions. It is interesting to note that Carmichael (1968) produced evidence that, under metamorphic conditions, the rate of diffusion of Al ions was an order of magnitude lower than that of many other common ionic species. Perhaps this explains the poikiloblastic nature of the Al-free or Al-poor phases aenigmatite, pyroxene and amphibole, and the much smaller tendency for the Al-rich phases, feldspar and nepheline, to occur poikiloblastically.

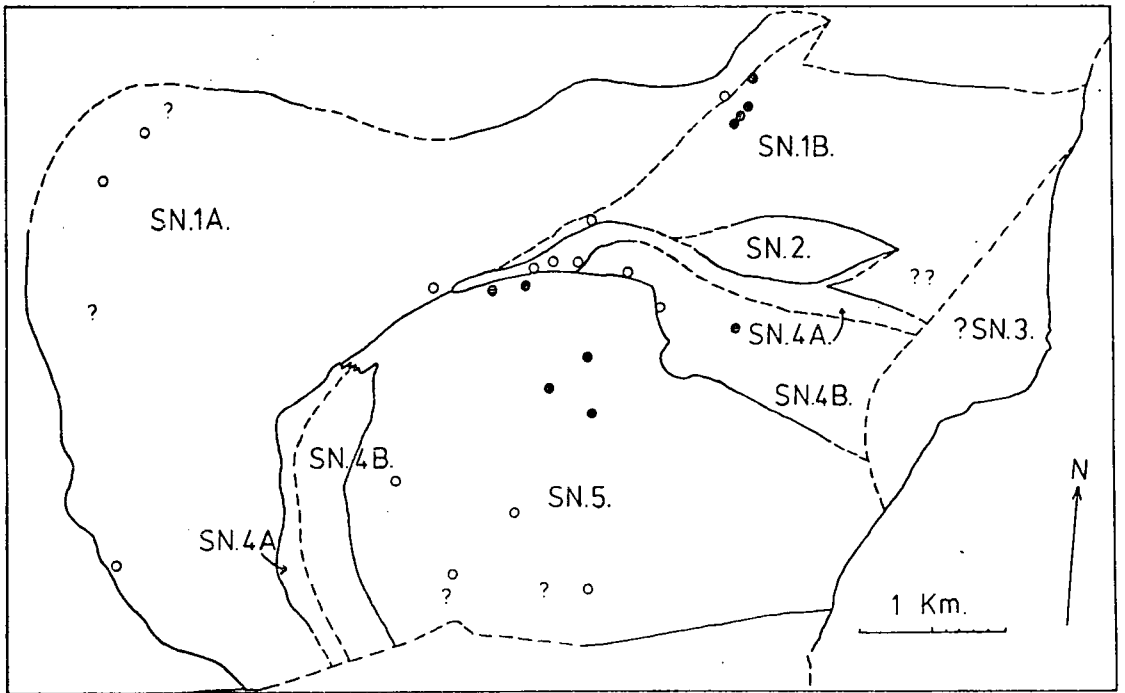
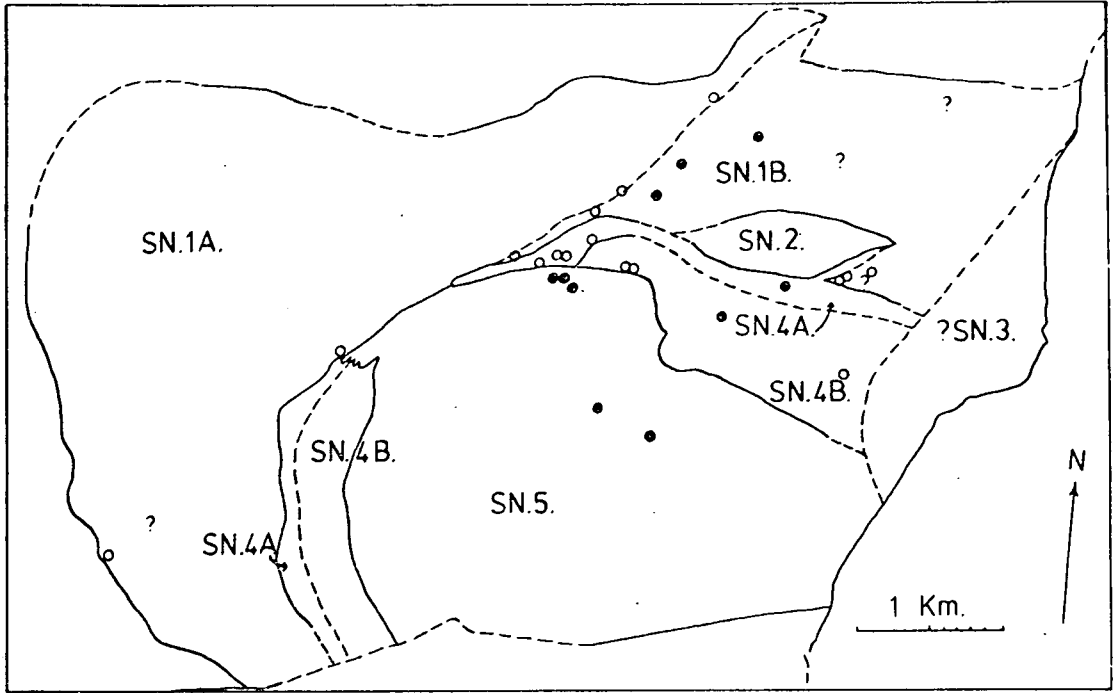
Comment must be made on the occurrence of the mineral

identified as rinkite. It is only commonly found in areas of recrystallization and tends to be concentrated some 50 m. or more away from the contact, usually as distinctive prismatic crystals. Probe traces along intercrystalline boundaries in unmetamorphosed syenites show sporadic, high concentrations of Zr and Nb, elements thought to be present in rinkite. The effect of a later intrusive unit on the rinkite in the earlier rocks has been to mobilize the microscopic grains, perhaps with the aid of a fluid phase, and recrystallize them as larger prismatic crystals some distance from the contact. Figs. 3.3 and 3.4 show the distribution of rinkite and aenigmatite over North Qôroq. Their proximity to contacts, i.e. their presence in recrystallized rocks, can be clearly seen. Aenigmatite can also be seen to occur occasionally in the more fractionated syenites. Compositions of the metamorphic/metasomatic phases are included in the mineralogy chapter.

Fig.3.3 The distribution of rinkite in the North Qôroq Centre. Concentrations of the mineral occur, close to younger intrusive units and in xenoliths.

- - Rinkite occurring in syenites, often recrystallized.
- - Rinkite occurring in xenoliths.
- ? - Uncertain identification of rinkite.

Fig.3.4 The distribution of aenigmatite in the North Qôroq Centre. Aenigmatite is concentrated close to younger intrusive units, in xenoliths and occasionally in highly fractionated rocks of units SN.1A, SN.1B and SN.5. Symbols as for Fig.3.3 (above).



## CHAPTER FOUR: MINERALOGY

### 4.1. Olivines

#### 4.1.1. Introduction

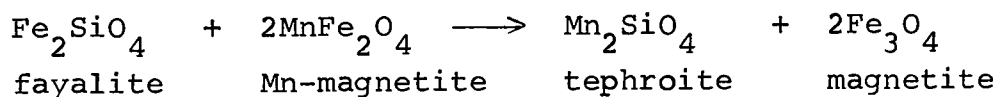
Olivine occurs in four major units of the North Qôroq Centre; SN.1A, SN.4A, SN.4B and rarely in SN.1B. It is absent from more highly fractionated units, and from the more highly fractionated parts of the units mentioned. Olivine occurs as an early formed phase, often in mafic aggregates. Rounded grains are always rimmed by opaque Fe/Ti oxides, which extend along fractures. Rims of pale green pyroxene or blue amphibole are occasionally present (see Chapter 3).

#### 4.1.2 Major element variation

Olivines from ten rock samples were analysed by electron microprobe. For each sample, several points on each crystal, and several crystals, were analysed (probe details in Appendix III).

Analyses showed all olivines to be extremely fayalitic indicating a relatively high state of fractionation for the parent magma, and to contain appreciable quantities of Mn. The olivines are similar to those described by Stephenson (1974), and to those from the Igdlarfigssalik centre (M. Powell, personal communication). The major element variation can be represented by the fayalitic portion of

the system Fosterite-Fayalite-Tephroite. The trends obtained can be seen in Fig.4.1 (a and b). No variation between SN.4A and SN.4B can be distinguished, consequently they are plotted together as SN.4. There is also little variation shown between SN.4 and SN.1A. A steady trend towards Fe-enrichment can be seen, together with a slight increase in Mn. Similar but more irregular trends can be seen in individual crystals from core to rim (see Fig.4.2). It is interesting to note that in both plots one sample shows a marked trend towards an increase in Mn with a decrease in Fe. Both these samples show evidence of recrystallization, due to the proximity of a younger intrusive unit. Perhaps the normal trend is controlled by crystal-magma equilibrium, whereas the trend towards Mn-enrichment may reflect appreciable diffusion in the solid state. The source of Mn may be the opaque material rimming the olivine. A simple ion-exchange reaction can explain the observed trend.



It is also possible that the trend can be explained by higher oxygen fugacity ( $f.O_2$ ). This would result in oxidation of  $\text{Fe}^{2+}$  to  $\text{Fe}^{3+}$  and the olivine following a trend towards Mn-enrichment earlier than rocks with

Fig.4.1

(a) Major element variation of olivines from unit SN.1A, shown in the fayalitic portion of the system Fosterite-Fayalite-Tephroite.

(b) Major element variation of olivines from units SN.4A and SN.4B, plotted together.

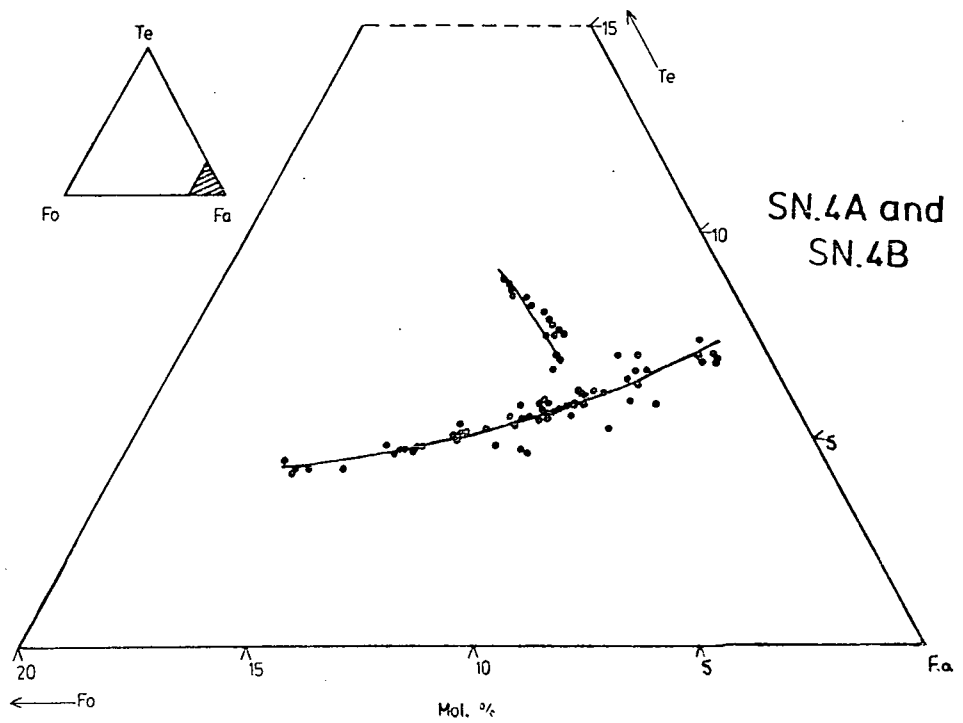
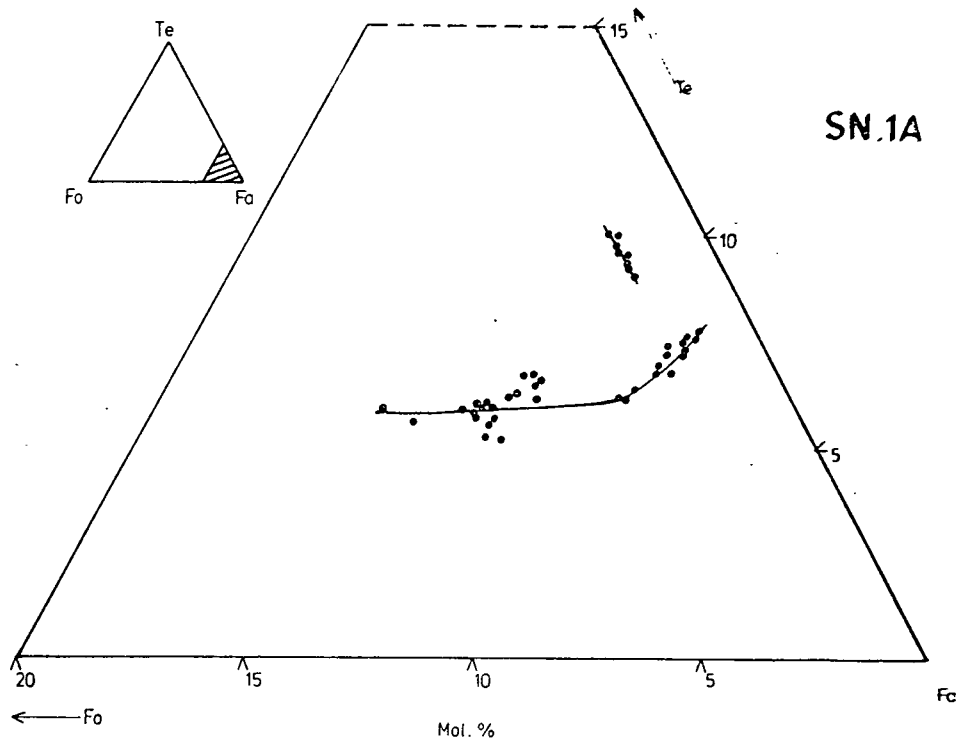
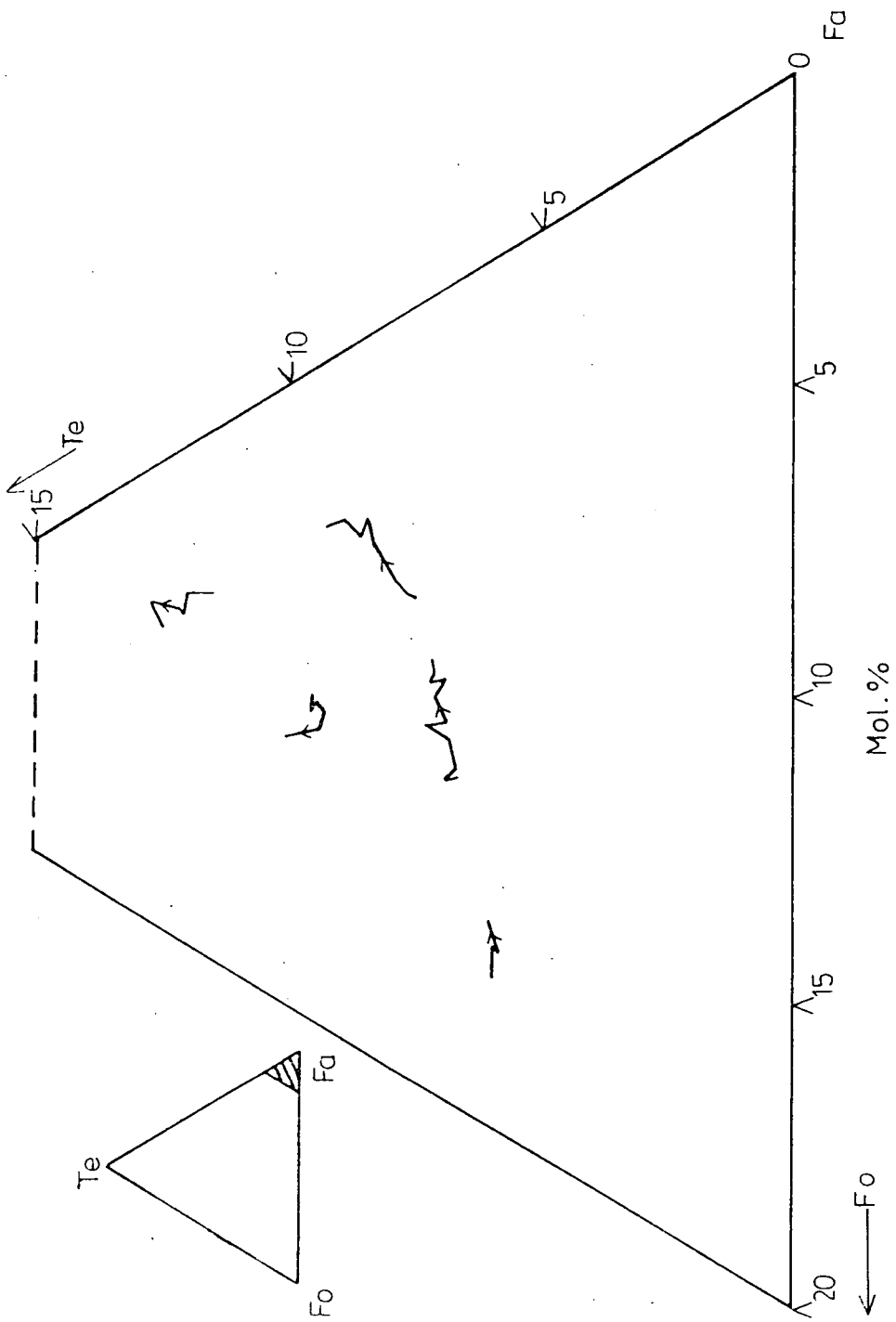
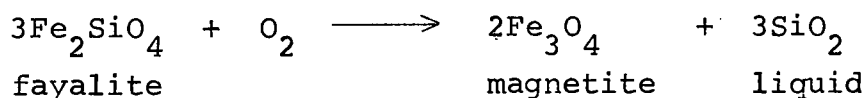


Fig.4.2 Irregular major element variation  
found in individual olivine crystals,  
from core to rim. Arrows indicate  
the direction to the rims.  
Represented in the system Fosterite-  
Fayalite-Tephroite.



a lower  $f.O_2$ .

The cause of the termination of olivine crystallization is indicated by the rims of oxide material, and can be represented by the reaction:

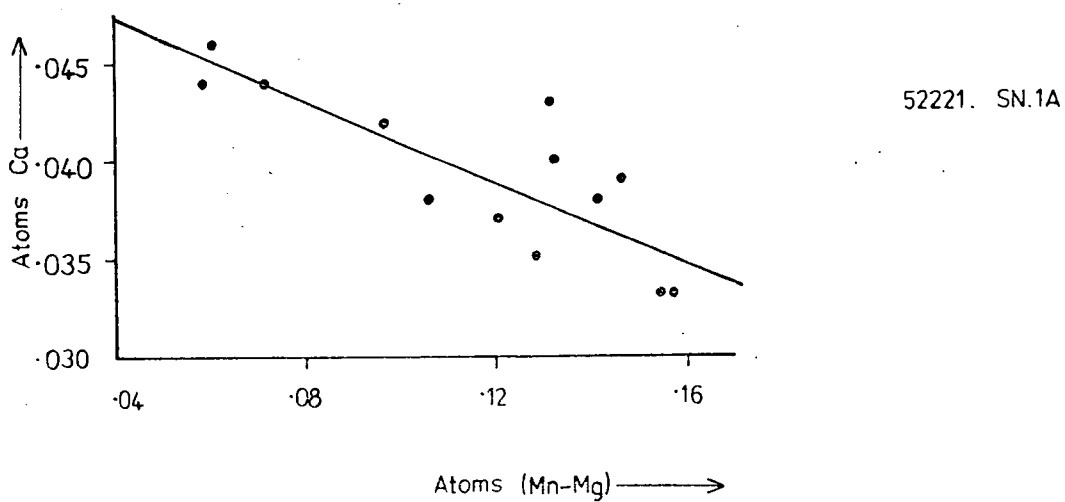
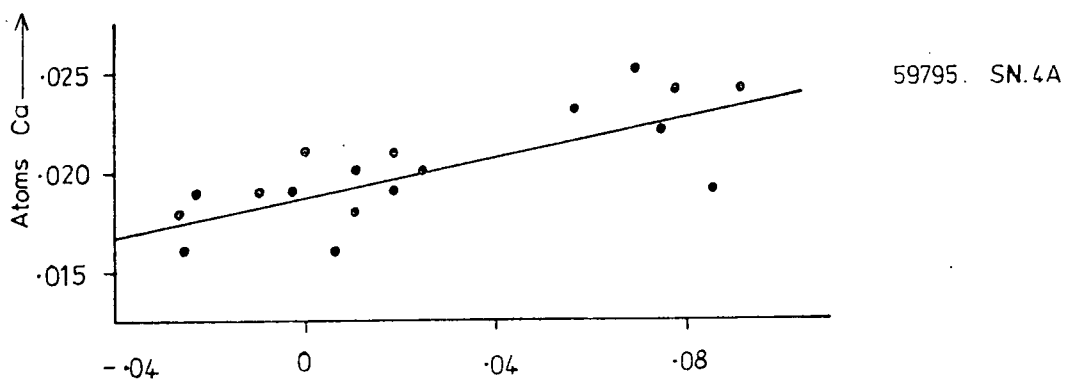
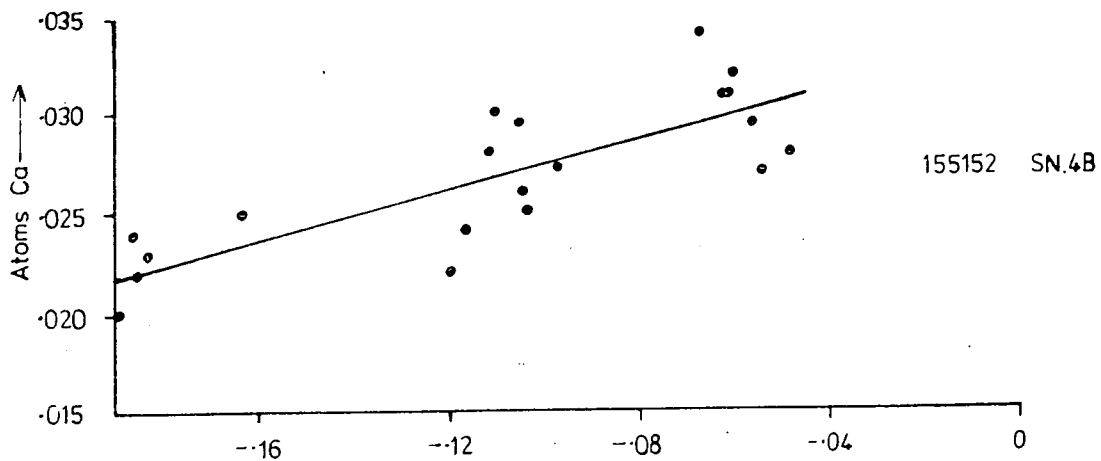


The termination may be caused by either an increase in  $f.O_2$ , as suggested by Stephenson (1974), or a decrease in silica activity ( $a.SiO_2$ ). These two parameters will be discussed later in the chapter.

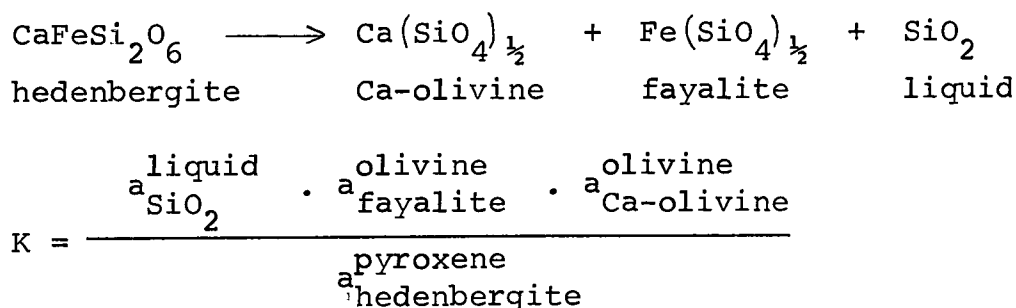
#### 4.1.3. Minor element variation

Neither Cr nor Ni were detected in the olivines and Ti and Al are only present in very small quantities. The only minor element of importance is Ca, and the olivines show Ca-contents ranging from 0.34 to 1.27 wt.%. Fig.4.3 shows the variation in Ca-content with fractionation in three samples, one from unit SN.1A and one from each of the SN.4 units, using a fractionation index of (Mn-Mg). A trend can be seen for Ca-depletion with fractionation in SN.1A, and enrichment in SN.4A and SN.4B. All analysed olivine samples showed comparable trends. Individual grains show variation in Ca-content from core to rim. Again, an irregular decrease in Ca from core to rim can be seen in SN.1A, and an increase in SN.4 units.

Fig.4.3 Typical Ca - zoning for olivines  
from various of the syenite units,  
with fractionation. Fractionation  
Index is  $(Mn - Mg)$  (atoms).



Simkin and Smith (1970) showed a positive correlation to exist between Ca-content of olivines and depth of formation. They also noted a weak positive correlation between Ca-content and degree of undersaturation (normative nepheline). Stormer (1975) expanded on their work and considered reactions involving the Ca-olivine component in olivine, clinopyroxene and silica in the liquid. Taking one of these reactions:



where K is the equilibrium constant for the reaction, and a is the activity of the species subscripted in the superscript phase (see section 4.16). Olivines from North Qôroq approximate to pure fayalite, hence the activity of fayalite in the olivine is close to unity. If pressure and temperature are constant, K is a constant, hence:

$$a_{\text{Ca-olivine}} \propto \frac{a_{\text{pyroxene hedenbergite}}}{a_{\text{liquid SiO}_2}}$$

For North Qôroq olivines the Ca content is dependent on

(a)  $a_{\text{SiO}_2}$  in the magma, and (b) activity of the hedenbergite

component in the pyroxene (at constant P.T.). It is likely that in the rocks examined  $a_{\text{SiO}_2}$  is buffered (see section 4.16.4). Stormer, considering the relationship between diopside, Ca-forsterite and silica, showed that in buffered rocks a decrease in temperature leads to a decrease in the Ca-content of the olivine, whereas a decrease in pressure, in either a buffered or unbuffered magma, results in an increase in the Ca-content. A more suitable reaction for the Mg-poor, North Qôroq syenites is the complementary one involving hedenbergite and fayalite, presented above. A further difference to Stormer's considerations is that the activity of hedenbergite in the pyroxene is variable, although not extensively so. Augites, probably in equilibrium with olivine, show small chemical variation, and no correlation of mole fraction hedenbergite in the pyroxene with Ca-content of the olivine was found. Use of the reaction involving hedenbergite and fayalite, and the slight variability of the activity of hedenbergite in the pyroxene, will not affect the trends towards Ca-depletion and enrichment with temperature drop and pressure drop respectively.

If the observed trends in the olivine can be explained by P.T. variation, as seems likely, then those observed for

both units of SN.4 would indicate a pressure control. All olivines analysed from these units are phenocrysts and growth of these olivines in an ascending magma, where pressure was decreasing, seems a reasonable explanation. In SN.1A the Ca-depletion with fractionation, both in a rock specimen and from core to rim of a single crystal, indicates a temperature control. This could be interpreted as growth of olivine in a high level (constant pressure), cooling magma body. The Ca may have been re-distributed by sub-solidus diffusion. The coarser grain size and greater volume of SN.1A, relative to both SN.4A and SN.4B, indicates slower cooling, which would have aided the diffusion process.

In conclusion, it appears that the high Ca-content of the North Qôroq olivines reflects the low  $a.\text{SiO}_2$  in the immediate parental magma, and that variation in the Ca-content can perhaps be attributed to variations in temperature and pressure.

## 4.2. Pyroxenes

### 4.2.1. Introduction

Pyroxenes are present as one of the principle mafic phases in all units of the North Qôroq Centre. In Chapter 3, optical properties showed them to possess considerable

compositional variation, both in and between units, even single crystals being extensively zoned.

Augitic pyroxene occurs, together with olivine, Fe/Ti oxides and apatite, as an early formed phase in the marginal parts of SN.1A and SN.1B, and in units SN.2, SN.4A and SN.4B. More hedenbergite-rich and acmite-rich pyroxenes are found in the inner parts of SN.1A and SN.1B, and in unit SN.5. The augites may be rimmed by amphibole, or may be zoned to apple-green aegirine-augite. Acmitic pyroxenes are found, either rimming blue amphibole, or in amphibole free rocks of a highly fractionated nature (inner parts of SN.1A and SN.5).

The present account is based on over 300 complete probe analyses (see Appendix III.4.), performed on 40 samples selected from the major North Qôroq units and the recrystallized rocks.

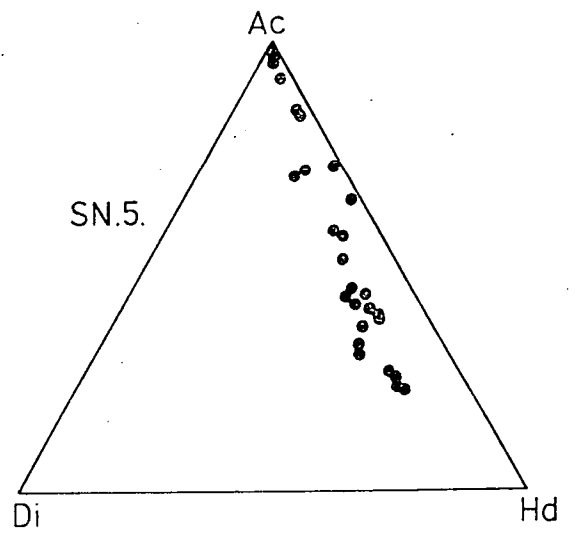
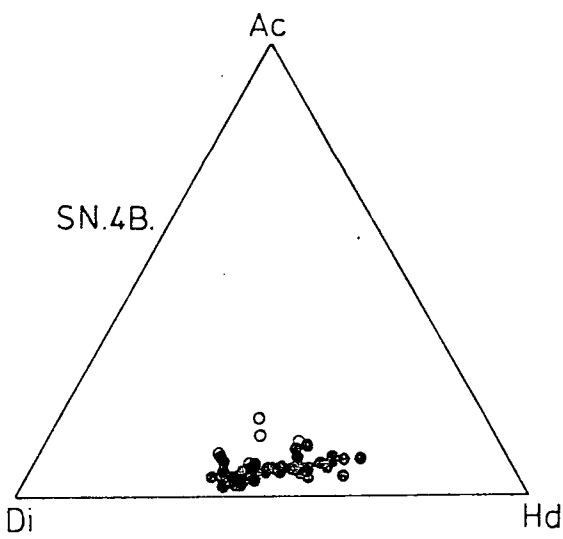
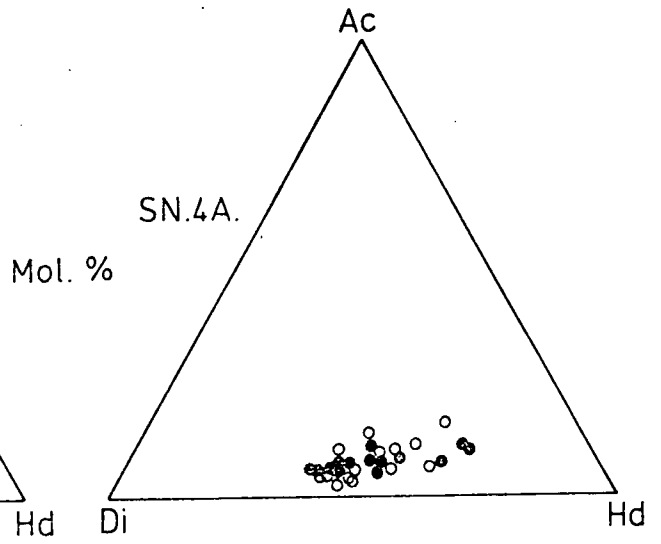
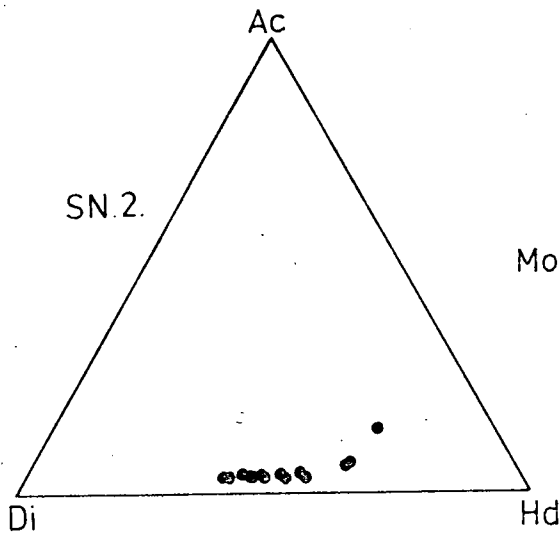
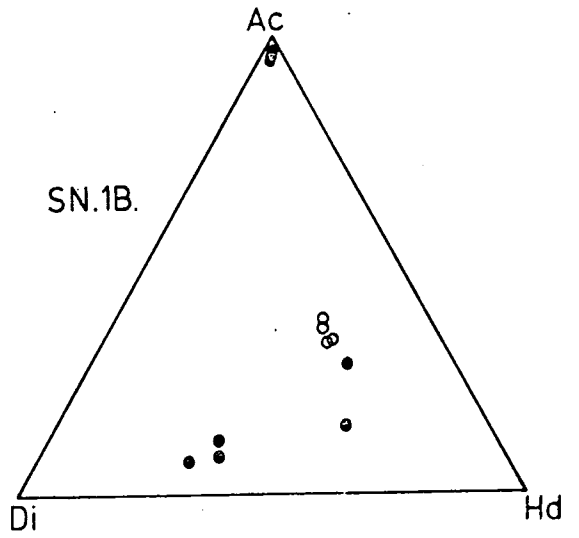
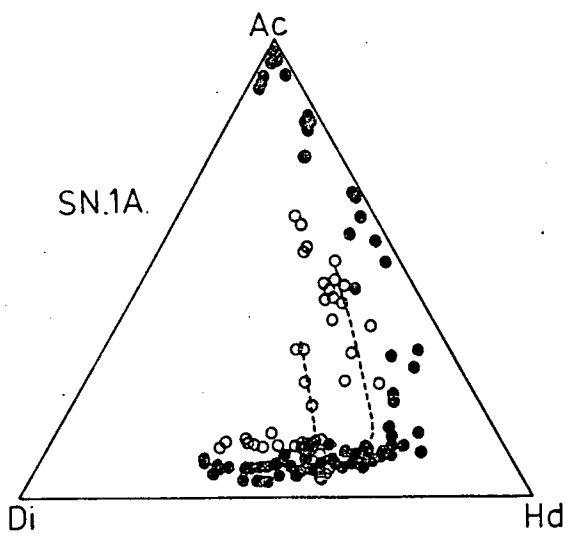
#### 4.2.2. Major element variation

The principal substitutions occurring as the pyroxenes evolve are firstly a replacement of Mg by  $\text{Fe}^{2+}$ , and secondly a coupled replacement of  $\text{Ca}(\text{Fe}^{2+}, \text{Mg})$  by  $\text{NaFe}^{3+}$ . This variation is expressed in Fig.4.4, where pyroxene analyses for each major unit are plotted separately, in terms of the end members Diopside-Hedenbergite-Acmite. For a discussion of the method of recalculation see

Fig.4.4 Pyroxene analyses from each of the major units of North Qôroq, plotted in terms of the end-members, Diopside-Hedenbergite-Acmite.

- - Pyroxenes from normal, unaltered syenites.
- - Pyroxenes from recrystallized syenites.

Dashed lines represent individual trends from two recrystallized samples of unit SN.1A.



Appendix III.2.2. In Fig.4.4, the solid circles represent pyroxenes from the typical syenite, whereas open circles represent pyroxenes from recrystallized rocks.

As mentioned in the chapter on petrography, unit SN.1A shows a considerable range in pyroxene composition from  $\text{Di}_{62}\text{Hd}_{30}\text{Ac}_{08}$  to  $\text{Di}_{01}\text{Hd}_{01}\text{Ac}_{98}$ . SN.1B, despite there being fewer analyses, would appear to show a similar range in compositions. Units SN.2, SN.4A and SN.4B have a more limited range, as was expected from petrographic observations. All the pyroxenes are augitic and only the most hedenbergite-rich show an increase in Na. Unit SN.5 is unusual in that the least evolved pyroxenes are Na-rich and there is a continuous series to almost pure acmite.

It is worthwhile to compare the trend shown by the two units showing greatest variation with that obtained from the adjacent South Qôroq Centre (Stephenson, 1972). Units SN.1A and SN.1B show a greater range in pyroxene compositions than any of the major syenitic units of South Qôroq. Whereas in South Qôroq acmitic pyroxenes are only present in pegmatites and as secondary minerals, in North Qôroq they occur as major, primary phases in the syenites themselves. Unlike South Qôroq, the compositional fields of the pyroxenes from the major units show a marked overlap. The fact that all units, apart from SN.5, have

similar initial pyroxene compositions suggests that, despite these units having evolved to differing extents, they originated from a common parental magma type. The implication of this is discussed in Chapter 7.

Pyroxenes from recrystallized rocks close to later intrusions tend to plot away from the field of 'normal pyroxenes'. As with South Qôroq, the recrystallized rocks appear to be following a trend towards acmite, a phenomenon discussed in the thermodynamics section of this chapter (section 4.16).

Zoning in individual crystals is shown in Fig.4.5, where several pyroxene analyses, taken from core to rim, are joined by an arrowed line, the arrow pointing towards the rim. Single crystals can show extensive, if irregular, compositional zoning. Crystals may be rimmed by amphibole before they get appreciably sodic or, in an adjacent sample, may zone right through to aegirine-augite. This suggests local variation, possibly in water pressure ( $P.H_2O$ ).

An important point to consider, when dealing with the major element variation, is what causes the pyroxene analyses to trend towards acmite, ie. why does the substitution  $NaFe^{3+} \rightleftharpoons Ca(Fe^{2+}, Mg)$  become dominant over the substitution  $CaFe^{2+} \rightleftharpoons CaMg$ ? Many workers (Aoki, 1964; Yagi, 1966; Nash and Wilkinson, 1970) have postulated that  $f.O_2$  is the controlling factor. From recent work on the

Nunarssuit complex, Anderson suggests that the pyroxene trend towards acmite is controlled by the Na/Ca ratio in the magma. Further discussion of this is made in the thermodynamics section of this chapter, but an appraisal of a relevant feature of the North Qôroq pyroxenes is worthwhile at this stage. Fig. 4.6 shows two clearly differing trends of Na enrichment shown by two samples of the same unit, SN.1A. The samples were taken only a short distance apart, and neither has undergone any re-crystallization. Both trends are closely defined, and demonstrate that whatever controls the tendency towards an increase in the acmite molecule is a variable parameter in a particular rock unit, as well as between units, and between different complexes. This suggests that the rocks evolved, at least in their later stages, in their own unique microsystem. A similar phenomenon was observed in rocks from Shonkin Sag Laccolith where the differing trends are even more apparent (Nash and Wilkinson, op.cit.). This feature of the pyroxenes means that it is not strictly valid to represent a 'trend' for a particular unit, or especially a particular centre, by a single line. The North Qoroq pyroxenes would be better represented by a 'field' of compositions.

#### 4.2.3. Minor element variation

The variation in selected minor elements is given in

Fig.4.5 Zoning shown by individual pyroxene crystals from core to rim, represented in the system Diopside-Hedenbergite-Acmite. Arrows indicate the direction to rims.

- a - Unit SN.1A, Sp.No. 155005
- b - Unit SN.1A, Sp.No. 52221
- c - Unit SN.1A, Sp.No. 52215
- d - Unit SN.4B, Sp.No. 54193
- e - Unit SN.5, Sp.No. 155159

Fig.4.6 Two clearly differing trends of Na enrichment shown by two samples of the same unit, SN.1A, neither having undergone any recrystallization.

- a - Sp.No. 155078
- b - Sp.No. 155005

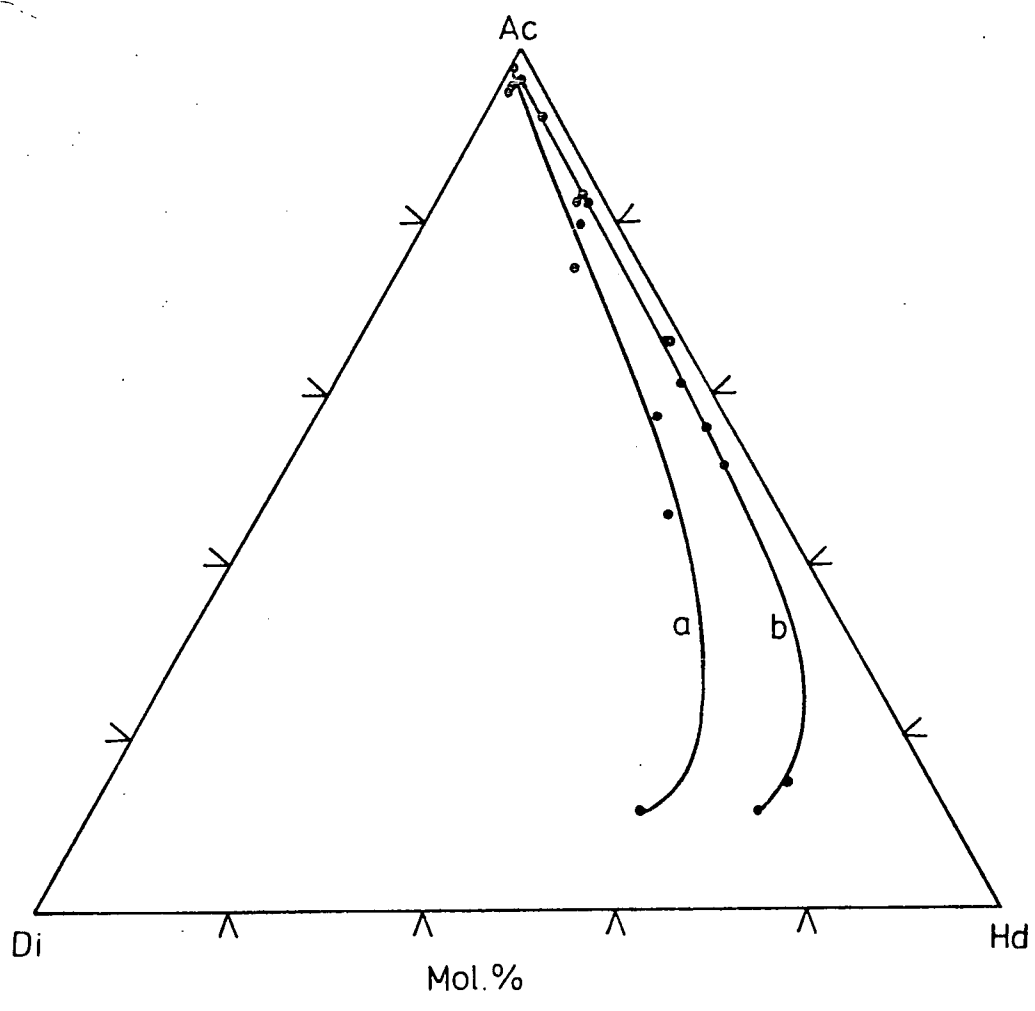
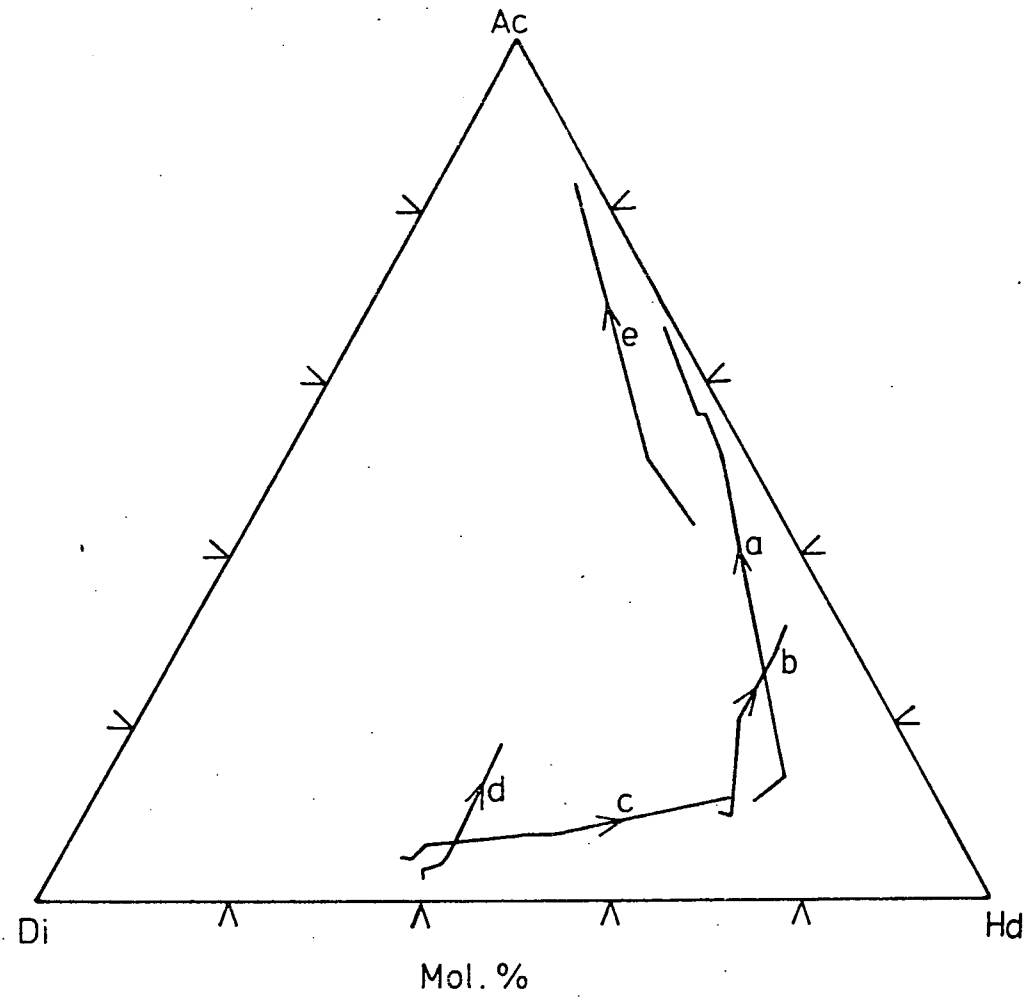


Fig. 4.7 (a-d). All elements are plotted as atoms per 6 oxygens, against a fractionation index of atoms (Na-Mg) (Stephenson, 1972).

Mn shows a steady build up in the least fractionated pyroxenes, reaches a peak, and then declines to almost zero in the acmites. The peak for Mn coincides with the general area where the pyroxene trend turns up towards acmite, i.e. where  $\text{Fe}^{2+}$  begins to decrease.  $\text{Mn}^{2+}$  obviously closely follows  $\text{Fe}^{2+}$  and has the ability to readily substitute for it in the pyroxene lattice.

The two dashed lines represent individual trends for two recrystallized rocks. Both these show Mn reaching a maximum value at a much earlier stage than occurs in the normal syenites, resulting from an earlier decrease in  $\text{Fe}^{2+}$  with the recrystallization trend towards acmite.

Four samples of interest are those from a recrystallized and sheared sample of SN.1B. They plot well above the other analyses and have approximately twice the Mn-content of a similar 'normal' pyroxene. The analyses come from aegirine-augite occurring in a mosaic of magnetite, nepheline, biotite and pyroxene, replacing original amphibole. It is interesting to note that the high Mn-content, while well above that in the normal pyroxenes, is approximately equivalent to that found in nearby amphibole, supporting the theory that these mosaics are

Fig.4.7 (two pages) The variation, with fractionation, shown by selected minor elements present in the pyroxenes. Fractionation Index (Na-Mg) (atoms).

○ - unit SN.1A

△ - unit SN.1B

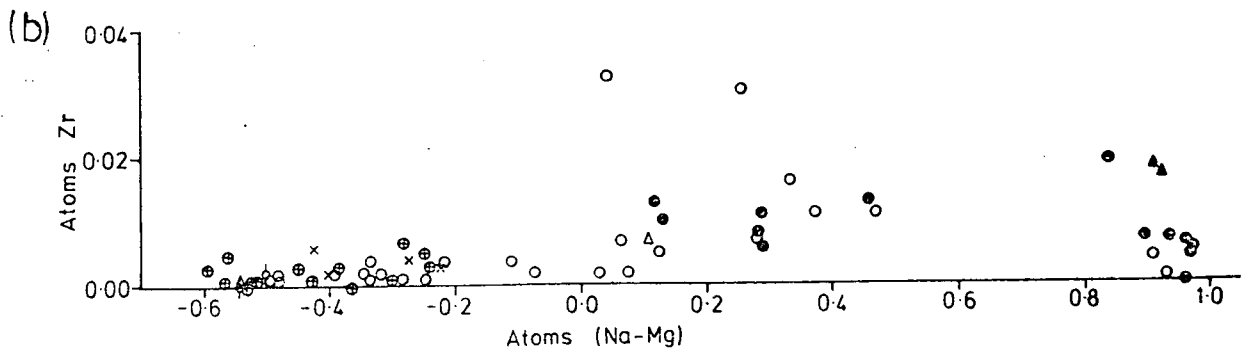
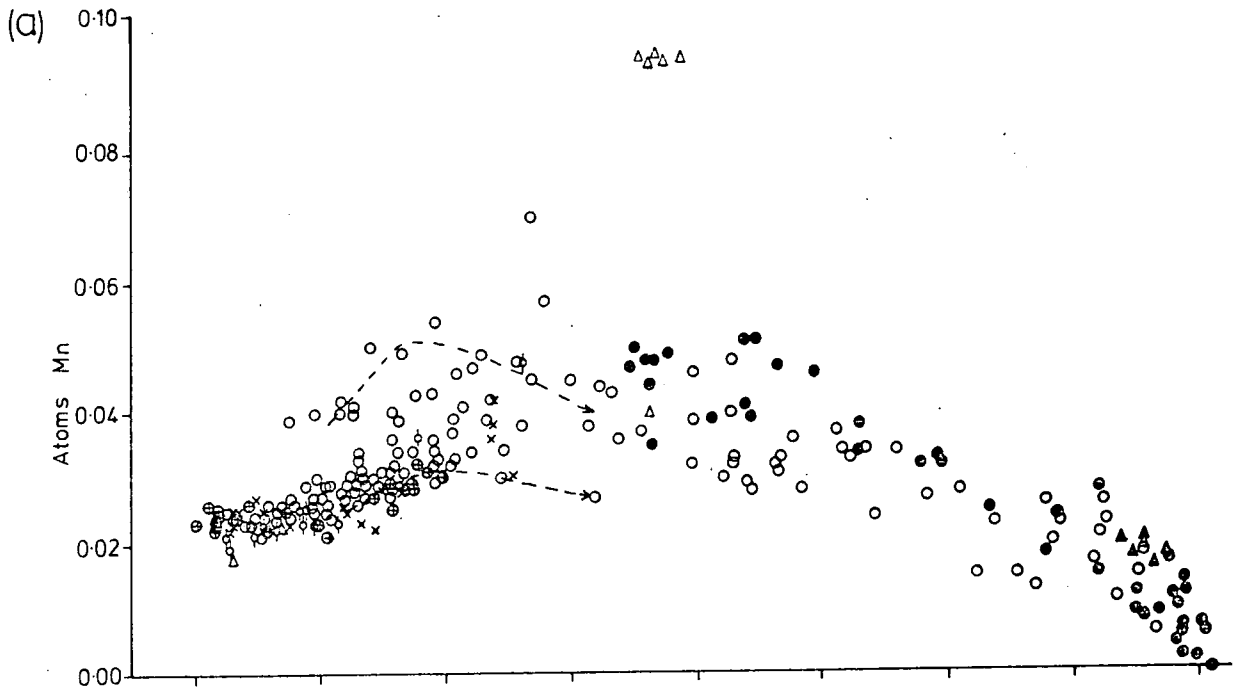
◊ - unit SN.2

▲ - unit ?SN.3

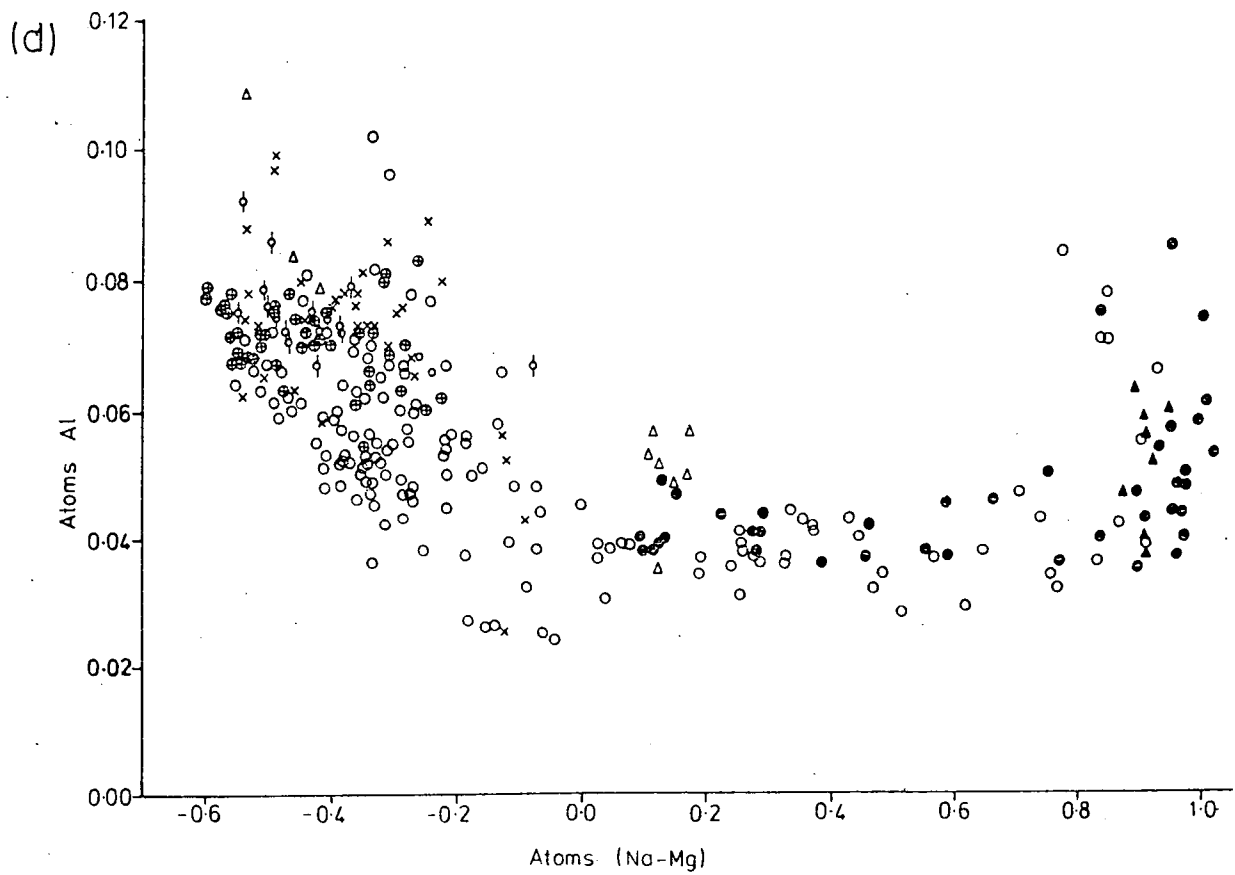
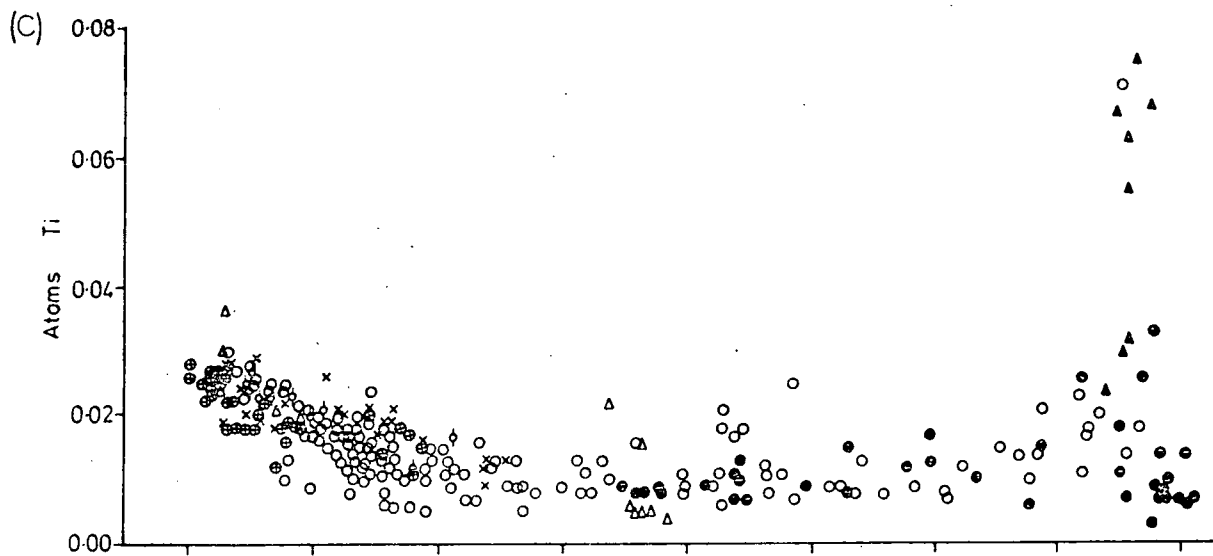
× - unit SN.4A

⊕ - unit SN.4B

● - unit SN.5



BURMA UNIVERSITY  
10 JAN 1977  
SECTION  
LIBRARY



areas of amphibole breakdown and not primary magmatic features.

Only a selected number of specimens were analysed for Zr. It was found to occur in varying amounts in almost all the pyroxenes analysed, but only in any quantity in the more sodic members. Occasionally the content of  $ZrO_2$  approached 1.5 wt.%. Zr probably resides in the Y-site, the charge excess being balanced by Na in the X-site and Al in the Z-site.

The distribution of Ti and Al in the various pyroxene types is particularly interesting. In the more basic rocks both are relatively concentrated and this concentration is in the ratio 2Al:1Ti, suggesting the molecule  $CaTiAl_2O_6$  (see Appendix III. 2.2). Both elements decrease rapidly as the pyroxenes become more  $Fe^{2+}$ -rich, and then continue at a low level of concentration until the pyroxenes become extremely acmitic. As can be seen from Fig. 4.7 (c and d), the acmitic pyroxenes show very variable contents of both Al and Ti. Values of up to 2.5 wt.%  $TiO_2$  and 1.4 wt.%  $Al_2O_3$  have been recorded. There is a negative correlation of Al with Ti and, almost certainly, the bulk of the Al is present as the jadeite molecule  $NaAlSi_2O_6$ , and the Ti as a titan-acmite  $NaTi^{4+}Fe^{3+}SiO_6$ .

Flower (1974) describes results obtained in the

system  $\text{Na}_2\text{O} - \text{Fe}_2\text{O}_3 - \text{Al}_2\text{O}_3 - \text{TiO}_2 - \text{SiO}_2$  at 1Kb.  $\text{P.H}_2\text{O}$ , and notes that there is extensive solid solution of the  $\text{NaTi}^{4+}\text{Fe}^{3+}\text{SiO}_6$  component in acmite. This varies with  $f.\text{O}_2$ , but is up to 28% at the  $\text{Mn}_2\text{O}_3 - \text{Mn}_3\text{O}_4$  buffer and up to 15% at the Ni-NiO buffer. The molecule  $\text{NaTi}^{4+}\text{AlSiO}_6$  also shows a moderate degree of solid solution with acmite. Flower goes on to suggest that  $f.\text{O}_2$  is one of the factors which controls whether Ti enters oxide phases, or silicates such as acmitic pyroxenes. He notes that published results from South Qôroq show no late stage increase of Ti in acmite and suggests that this indicates South Qôroq to have evolved under relatively low  $f.\text{O}_2$  conditions. If this were true it would mean that North Qôroq, which can show appreciable Ti enrichment in the acmites, must have formed under higher  $f.\text{O}_2$  conditions, at least in its late stages. Careful study of Stephenson's tabulated analyses for South Qôroq does, however, show that certain acmitic pyroxenes have high Ti values, but were not plotted on the published diagrams.

Examination of Fig. 4.7 shows the contents of both Ti and Al in the acmites to be extremely variable, a feature noticed even in individual specimens. This could be caused by sector zoning, which Leving (1974) has shown to be an important factor in the fractionation of trace elements. He showed that the  $11\bar{1}$  zone of a pyroxene

contained 3.1 wt.%  $\text{Al}_2\text{O}_3$  and 0.82 wt.%  $\text{TiO}_2$ , whereas the 100 zone of the same crystal contained 7.15 wt.%  $\text{Al}_2\text{O}_3$  and 1.95 wt.%  $\text{TiO}_2$ . Admittedly, this crystal was a titan-augite rather than a titan-acmite, but there seems no reason to suppose that the same process could not apply to the North Qôroq late stage pyroxenes, particularly as the volatile-rich liquid surrounding the crystals would have a low viscosity, which would aid ionic diffusion.

Apart from the possibility of sector zoning, there is a degree of irregular core to rim zoning with respect to Al and Ti.

Popp and Gilbert (1972) discussed the stability of acmite-jadeite pyroxenes at low pressure. They indicated that acmites from silica-undersaturated environments should have a higher proportion of the jadeite molecule than those from silica-saturated rocks. This is in accord with the relatively high jadeite component in the acmites of the undersaturated North Qôroq syenites. They derive an expression relating pressure of formation of pyroxenes to temperature, activity of albite in the feldspar and activity of jadeite in the pyroxene. A similar expression, they maintain, could be applied to undersaturated rocks. The great variation in the jadeite

content of adjacent North Qôroq acmites, which obviously formed under the same total pressure, suggests that the geobarometer is inapplicable.

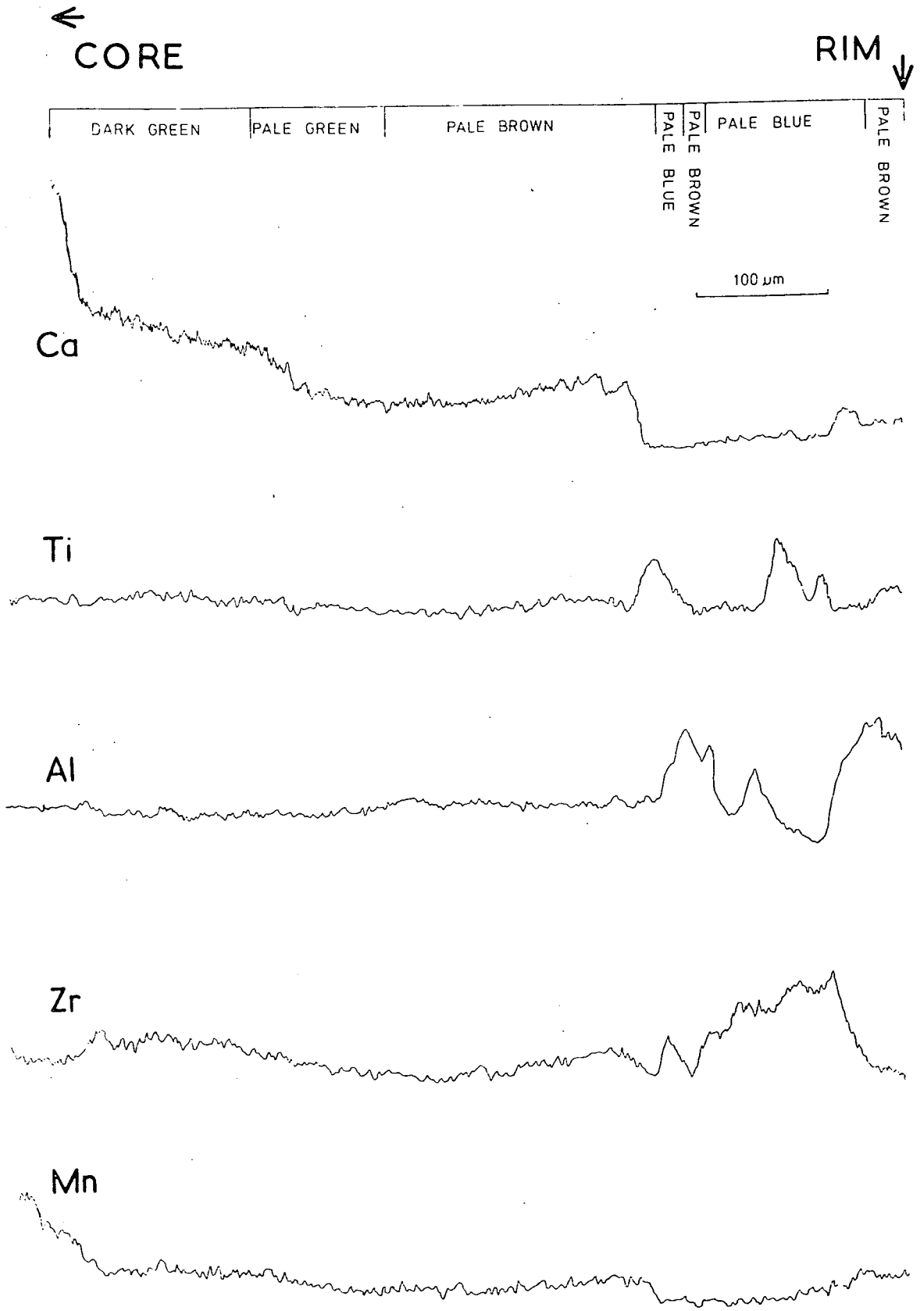
#### 4.2.4. Colour in North Qôroq pyroxenes

Pyroxenes from North Qôroq show a wide range of colours, and it is interesting to attempt to correlate colour with chemical composition.

In the least fractionated syenites, the pyroxenes show the pale pink or purple colours commonly described for titan-augites (Yagi, 1953). This, according to Burns (1970), is due to the presence of  $Ti^{3+}$  ions. The d-orbital electrons of these ions absorb radiation in the visible part of the spectrum (green) and the complementary colour is seen (pink or purple). The ferro-augites possess a pale green colour which deepens in the more sodic ferro-augites and aegirine-augites (X = apple green, Y = yellow green, Z = yellow brown). Many minerals with  $Fe^{2+}$  have a characteristic green colour, and the presence of both  $Fe^{2+}$  and  $Fe^{3+}$  facilitates charge transfer and results in strong colouration.

A marked variation in colour can be seen in the acmitic members of the North Qôroq pyroxene series. The normal colour is a pale green. This is the colour of pure acmite obtained experimentally (Bailey, 1969). Variants do occur, however, and Fig.4.8 shows a probe

Fig.4.8 Probe traverses, for selected elements, over the rim of an acmite crystal. Also shown is the colour appropriate to various parts of the crystal.



traverse, for selected elements, over the rim area of an acmite grain, together with the colour observed in various parts of the grain. In the extreme rim are zones rich in Ti and zones rich in Al. The two elements show an inverse correlation, Al reaching a maximum when Ti is at a minimum, and vice versa. The pale blue colour correlates with Ti, but in acmite, with its high  $\text{Fe}^{3+}/\text{Fe}^{2+}$  ratio, it is inconceivable that Ti should occur as  $\text{Ti}^{3+}$ . It must be present as  $\text{Ti}^{4+}$ .  $\text{Ti}^{4+}$ , however, has no d-orbital electrons and cannot absorb in the visible range of the spectrum. A strong correlation with the blue colour is also shown by Zr. Although Zr itself will not absorb in the visible, when occurring in pyroxenes it is frequently associated with small quantities of rare earth elements (Washington and Merwin, 1927). Certain of these possess f-orbital electrons capable of absorbing in the visible part of the spectrum. Colours produced by absorption by these rare earth elements are usually in pastel shades. Hence, the pale blue bands occurring in the acmite are probably caused by rare earth elements associated with Zr.

### 4.3. Amphibole

#### 4.3.1. Introduction

Amphiboles occur in all the syenitic rocks of North

Qôroq, except for highly fractionated members where the dominant, and at times only mafic phase is acmite.

The amphiboles vary in colour and chemical composition, depending on the state of fractionation of the parent rock. Those from the marginal augite syenites of SN.1A and SN.1B, and the syenites SN.2, SN.4A and SN.4B are dominantly pleochroic in shades of brown (X = straw yellow, Y = red-brown, Z = dark brown) or, if more highly evolved, in shades of green and brown (X = green-brown, Y = Z = olive). Where amphibole is present in the inner parts of SN.1A, SN.1B and SN.5, it typically shows blue-green pleochroism (?X = Indigo, ?Y = grey-blue, ?Z = green-blue).

Amphibole tends to rim pyroxene grains, brown amphiboles rimming augites, and green amphiboles rimming ferro-augite and aegirine-augite. The amphibole itself may have a rim of pale green acmite. This 'discontinuous reaction series' closely resembles that described from the syenites of Tugtutôq (Upton, 1964).

The present account is based on 130 amphibole analyses. All amphiboles were analysed for 10 major elements and a selected number for Zr and F.

#### 4.3.2. Classification and nomenclature

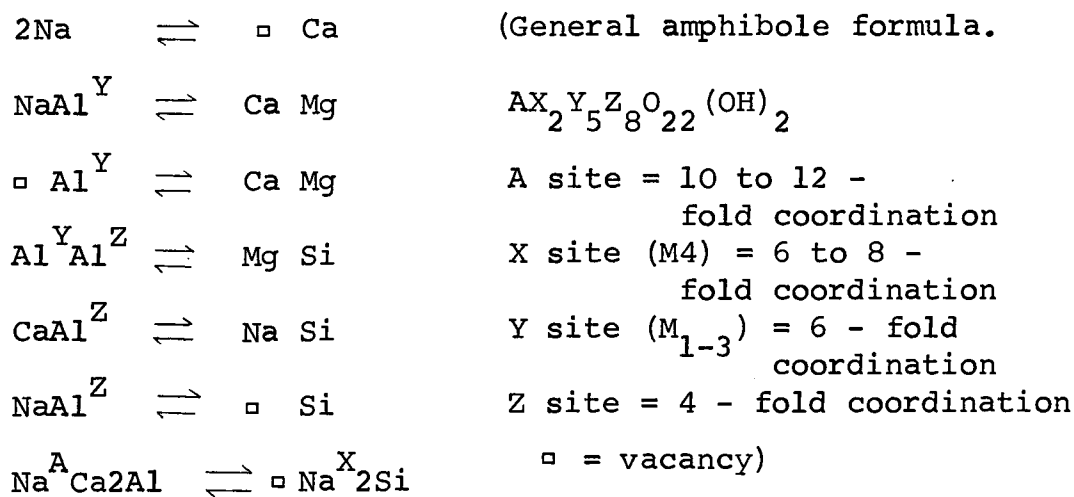
Previous workers on Gardar centres have tended to

avoid detailed discussion of the chemical variation which characterizes the amphiboles. Analytical work has often been restricted to partial analyses.

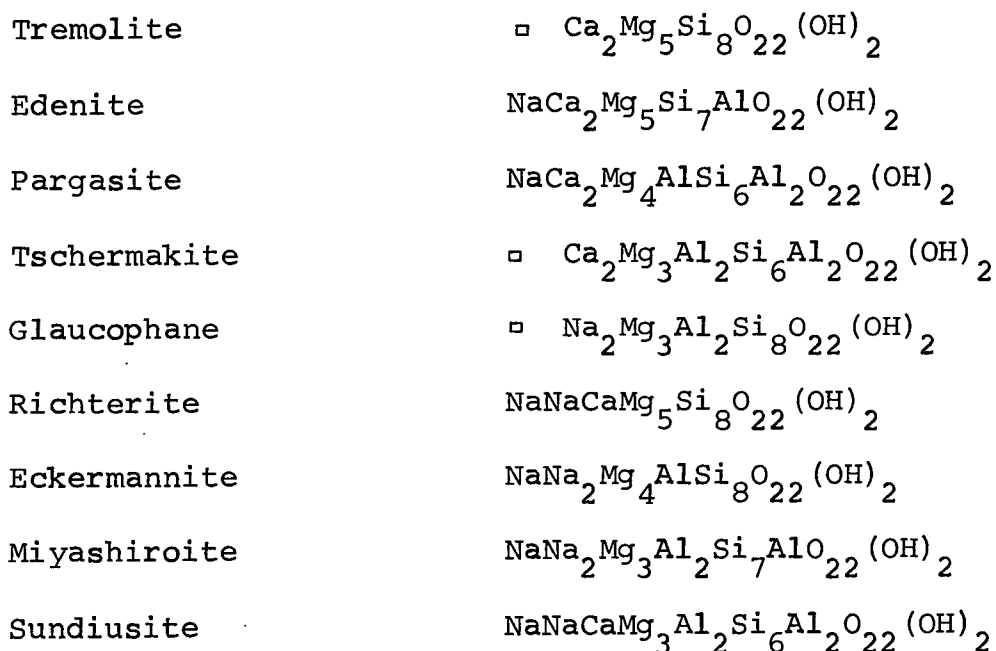
The dominant problem with the amphiboles is their complexity. In terms of chemical variation, amphiboles are the most complex and variable of all the rock forming minerals. This variability arises from the wide variety of cation sites in the amphibole structure, which allow a complex range of cation substitutions and the accommodation of ions showing a large range in ionic radii (Ernst, 1968).

Any attempt to understand amphibole variation is assisted by a sound classification scheme. Many workers have attempted to formulate such a scheme, with varying degrees of success. The most suitable method of classification is to place the analyses on to some form of 3-dimensional diagram. This approach was first attempted by Smith (1959). The scheme adopted in this account is that proposed by Phillips and Layton (1964) and Phillips (1966). It is one used by Stephenson (1973) and Rowbotham (1973) to describe amphiboles from other Gardar centres. Phillips and Layton took the tremolite composition and worked out possible ionic substitutions, taking account of charge, ionic size and available lattice sites in the amphibole. Substitutions involving cations of the same

charge and similar ionic radius, e.g.  $\text{Mg} \rightleftharpoons \text{Fe}^{2+}$ , were regarded as trivial for the purpose of establishing a general classification. This resulted in the following possible substitutions:



This in turn gave 9 amphibole end members:



The last two on the list were types that were not known in the natural state. Subsequent to publication, the

iron analogue of sundiusite was identified and called mboziite (Brock et al., 1964).

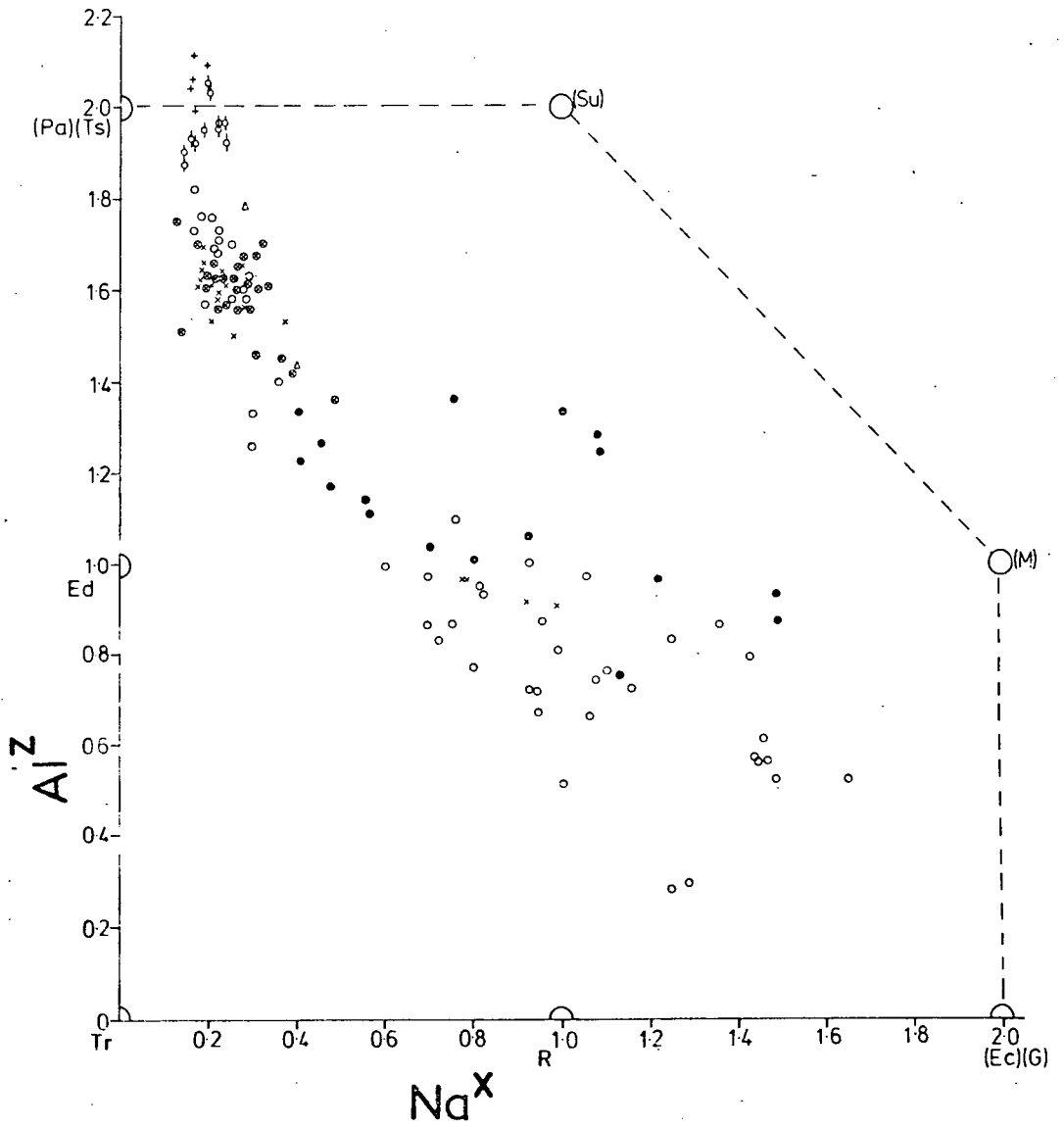
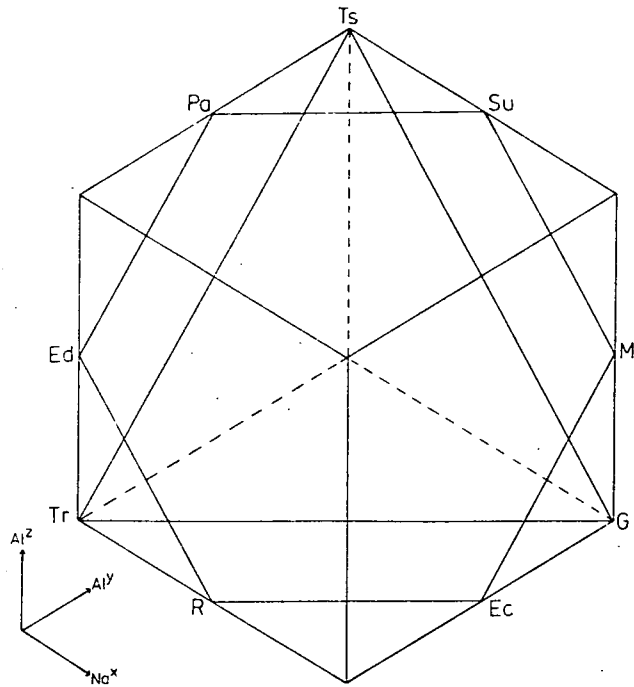
Phillips places the various end members on a 3-dimensional diagram. The three mutually perpendicular axes represent respectively, the number of Na ions in the X site, the number of Al ions in the Z site and the number of Al ions in the Y site. An alternative, but similar classification was proposed by Whittaker (1968). Whereas Phillips ignores vacancies in X and Z sites, Whittaker makes these sites up to whole numbers. 'Good' amphibole analyses plot on complementary points in both diagrams. The Phillips diagram used in this account is given in Fig. 4.9, the 9 end members being denoted by their first letters. Amphibole compositional space is a diagonal slice taken through the cube seen in the diagram. It is 'sandwiched' between the triangle Ts-Tr-G and the hexagon Ed-Pa-Su-M-Ec-R.

Figs. 4.10 is a view into the Phillips diagram along  $Al^Y$ , on which analyses of North Qôroq amphiboles are plotted. The dashed lines represent the limits of amphibole compositional space, and the vast majority of analyses plot inside it. Various symbols are used to differentiate between units. It must be remembered that the Phillips diagram reflects the Na, Mg, Al-analogues of the true amphiboles.

Fig.4.9 3-dimensional diagram (Phillips,1966) used in this account for the classification of the amphiboles. The 9 end-member amphibole compositions are denoted by their first letters (see text). 'Amphibole compositional space' is 'sandwiched', on this diagram, between the triangle Ts - Tr - G and the hexagon Ed - Pa - Su - M - Ec - R.

Fig.4.10 View into the Phillips diagram along the parameter  $Al^Y$  (see text). Amphibole analyses from North Qôroq rocks are plotted, showing the variation of Al content of the Z-site with the Na content of the X-site.

- - Unit SN.1A
- △ - Unit SN.1B
- ⊙ - Unit SN.2
- + - Unit ?SN.3
- × - Unit SN.4A
- ⊗ - Unit SN.4B
- - Unit SN.5



The amphibole analyses were recalculated, their ions assigned to sites, and named using the computer program MINDATA 5. Details of the procedure are given in Appendix III.2.3. An estimate of the  $\text{Fe}^{3+}/\text{Fe}^{2+}$  ratio is also made by the MINDATA 5 program. To obtain a true idea of the types of amphibole present, account is taken of the  $\text{Fe}^{2+}$  and  $\text{Fe}^{3+}$  substitutions, as demonstrated in Fig. 4.11. Here, amphiboles classed as eckermannites by MINDATA 5 are seen to lie close to the arfvedsonite end member composition. Likewise, those termed pargasites are in fact ferro-pargasites and ferro-hastingsites. The position of an analysis in Fig. 4.11 does depend on the  $\text{Fe}^{3+}/\text{Fe}^{2+}$  estimate. This estimate is thought to be reasonable, as it suggests that in the least evolved amphiboles  $\text{Fe}^{3+}$  is negligible, whereas in more highly evolved amphiboles  $\text{Fe}^{3+}$  is much more important. This late stage increase in  $\text{Fe}^{3+}$  with fractionation probably does occur, as with the pyroxenes, and the optical properties of the most fractionated amphiboles are in keeping with their being  $\text{Fe}^{3+}$ -rich arfvedsonites.

The North Qôroq amphiboles, with fractionation, follow a trend from Ti-rich ferro-pargasites and ferro-hastingsites, through ferro-edenites and ferro-richterites, to arfvedsonites.

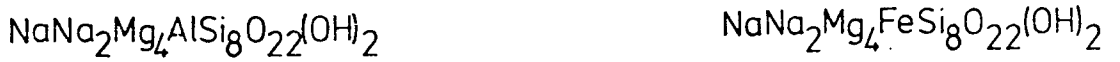
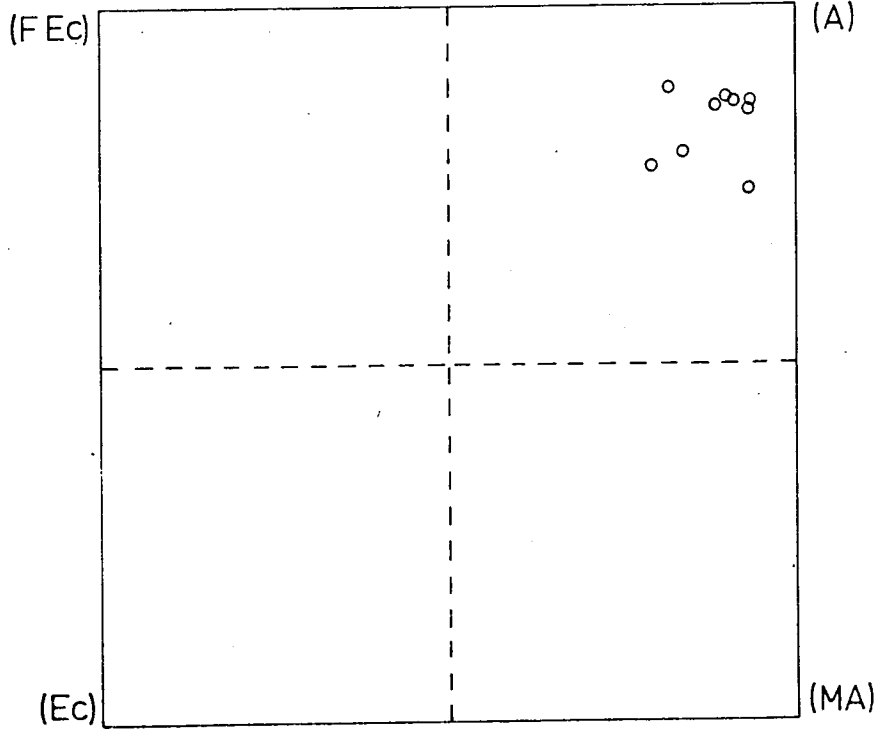
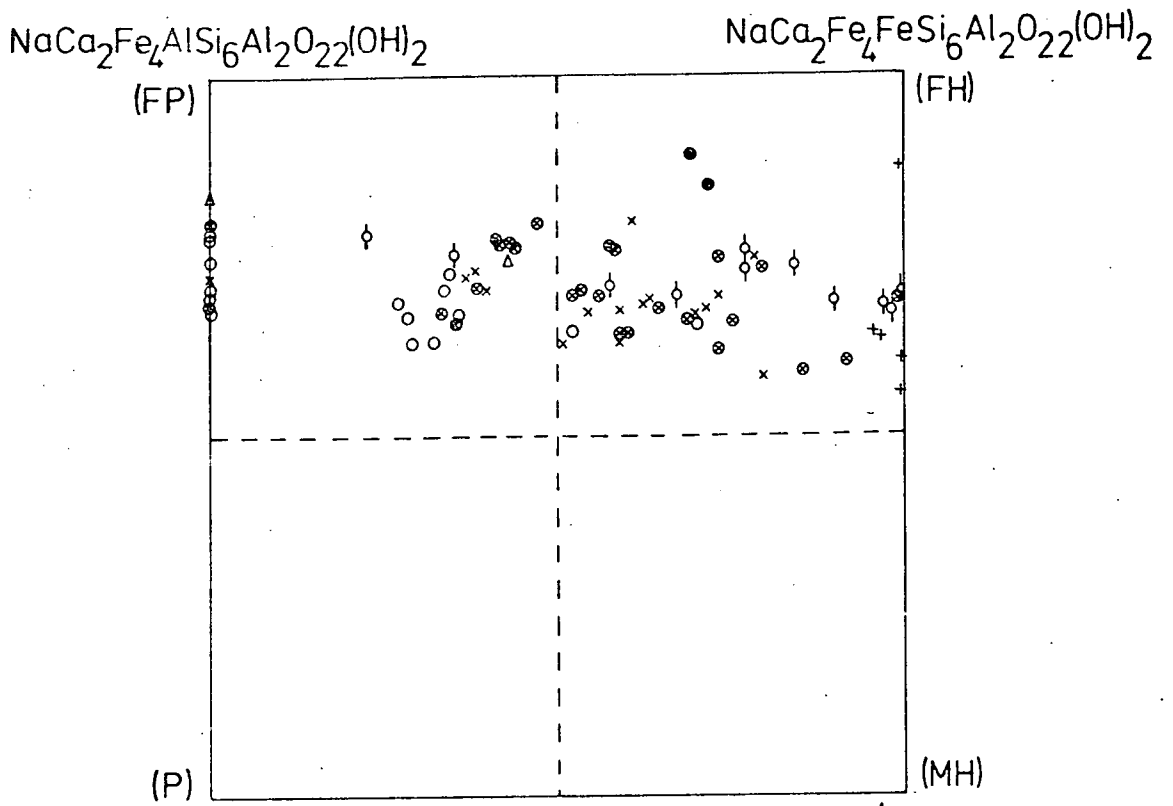
Fig.4.11 Diagram to show the effect of  $\text{Fe}^{2+}$  and  $\text{Fe}^{3+}$  substitutions on amphiboles classified by the 'Phillips system' as pargasites (top) and eckermannites (bottom).

Abbreviations used:

- P - Pargasite
- FP - Ferropargasite
- FH - Ferrohastingsite (hastingsite)
- MH - Magnesiohastingsite
- Ec - Eckermannite
- FEc - Ferroeckermannite
- A - Arfvedsonite
- MA - Magnesioarfvedsonite

Symbols used:

- - Unit SN.1A
- △ - Unit SN.1B
- ⊙ - Unit SN.2
- ⊕ - Unit ?SN.3
- × - Unit SN.4A
- ⊗ - Unit SN.4B
- - Unit SN.5



A detailed breakdown of the amphibole types from each unit is given below:

<u>UNIT</u>	<u>No. OF ANALYSES</u>	<u>AMPHIBOLE TYPES</u>
SN.1A	34	12 (FP) 2 (FH) 11 (FE) 5 (FR) 4 (A)
SN.1B	2	2 (FP)
SN.2	11	2 (FP) 9 (FH)
?SN.3	5	5 (FH)
SN.4A	28	12 (FP) 16 (FH)
SN.4B	20	4 (FP) 12 (FH) 2 (FE) 2 (FR)
SN.5	15	2 (FH) 6 (FE) 3 (FR) 4 (A)
Recrystallized rocks	15	10 (FR) 5 (A)

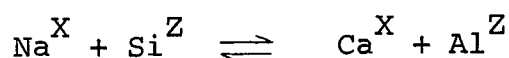
Abbreviations used: FP - ferro-pargasite  
 FH - ferro-hastingsite FE - ferro-edenite  
 FR - ferro-richterite A - arfvedsonite

#### 4.3.3. Chemical variation

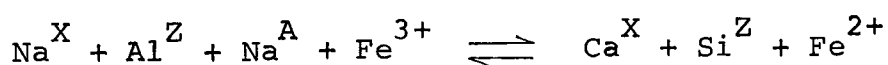
Previous Gardar workers have plotted amphibole analyses in terms of modified alkali pyroxene plot, plotting total  $Fe \propto Mg \propto (Na + K)$ . As will be shown below, of the two major substitutions simultaneously affecting North Qôroq amphiboles, one results in an increase in  $Fe^{2+}$  and one in an increase in Na. On the triangular plot the resultant is a trend at almost right angles to the pyroxene

trend, and one which fails to adequately indicate the relevant substitutions.

Fig. 4.10 shows North Qôroq analyses on a plot of  $\text{Na}^X \propto \text{Al}^Z$ . A systematic and extensive increase in  $\text{Na}^X$  and decrease in  $\text{Al}^Z$  can be seen, as the parent magma becomes more highly fractionated. This is a reflection of the major coupled substitution affecting the amphiboles:



This important substitution has been described from other Gardar centres as being of major importance. Rowbotham (op.cit.) indicates that amphiboles from Ilímaussaq show it, and Anderson (1974) describes it as the dominant substitution in certain of the Nunarssuit amphiboles. Stephenson (op.cit.) appears to have the same dominant substitution in South Qôroq, but has apparently misinterpreted his data. He suggests the complex substitution



This implies a decrease of  $\text{Si}^Z$  with decreasing  $\text{Ca}^X$ , whereas his data show the reverse to be the case.

On Fig. 4.10 amphiboles from SN.2 and ?SN.3 plot somewhat removed from the main trend, a feature seen on the majority of plots given in this section. Amphiboles of

these two units show little chemical variation, but possess a higher content of Al in the tetrahedral site ( $Al^Z$ ). Leake (1962), Boyd and England (1962), and earlier workers have suggested that high Al in tetrahedral coordination indicates a high temperature origin. It may be that both SN.2 and ?SN.3 amphiboles, with their high  $Al^Z$  values, crystallized at higher temperatures than those from the other North Qôroq units. Of the two units showing the largest variation in amphibole composition, SN.5 seems to have a higher content of tetrahedral Al than SN.1A, again possibly a temperature effect.

As the dominant coupled substitution is  $Na^X Si^Z \rightleftharpoons Ca^X Al^Z$ , the other elements present in the amphiboles have been plotted against a fractionation index of  $Na^X-Al^Z$  (atoms), reflecting this substitution (Fig. 4.12 (a)-(i)).

Figs. 4.12 (a) and (b) simply show the expected variation in Ca and Si for the above mentioned substitution. The virtual absence of any deviation from a straight line trend indicates that these elements are not participating in any other substitution, unless of a minor nature.

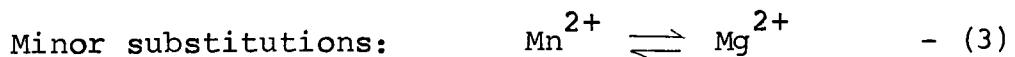
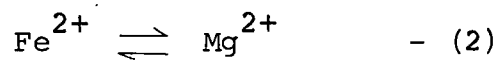
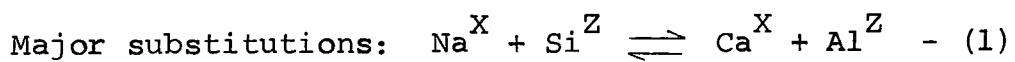
Figs. 4.12 (c) and (d) show that K tends to increase with amphibole fractionation, and that Na allocated to the A site increases, reaches a maximum, and then decreases in the more evolved amphiboles.

From Fig. 4.12(a) F can be seen to increase steadily with amphibole fractionation. It is particularly concentrated in some of the recrystallized amphiboles, reaching values up to 2.5 wt.%.

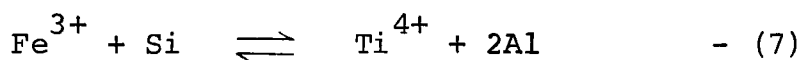
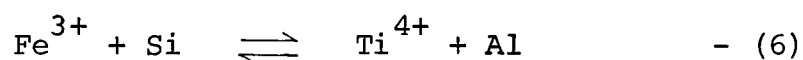
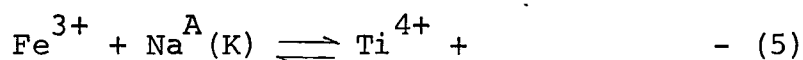
Figs. 4.12 (f)-(i) show how the remaining major elements vary (N.B. FeO = Total Fe as FeO). Total Fe increases steadily from 20 to 30 wt.% and Mn, which readily substitutes for  $\text{Fe}^{2+}$ , increases with it. Both Mg and Ti decrease, and only occur in very low concentrations in the more highly evolved amphiboles.

In many of the plots the amphiboles from units SN.2 and ?SN.3 are outlined with a dashed line and can be seen to differ from the other amphiboles in their chemistry. They are characterised by higher K, FeO and MnO, and lower  $\text{Na}^{\text{A}}$ , MgO and  $\text{TiO}_2$ .

The observed chemical variation for the North Qôroq amphiboles can be explained in terms of a number of major and minor ionic substitutions:



The decrease in Ti may be explained by one or more of the following substitutions:



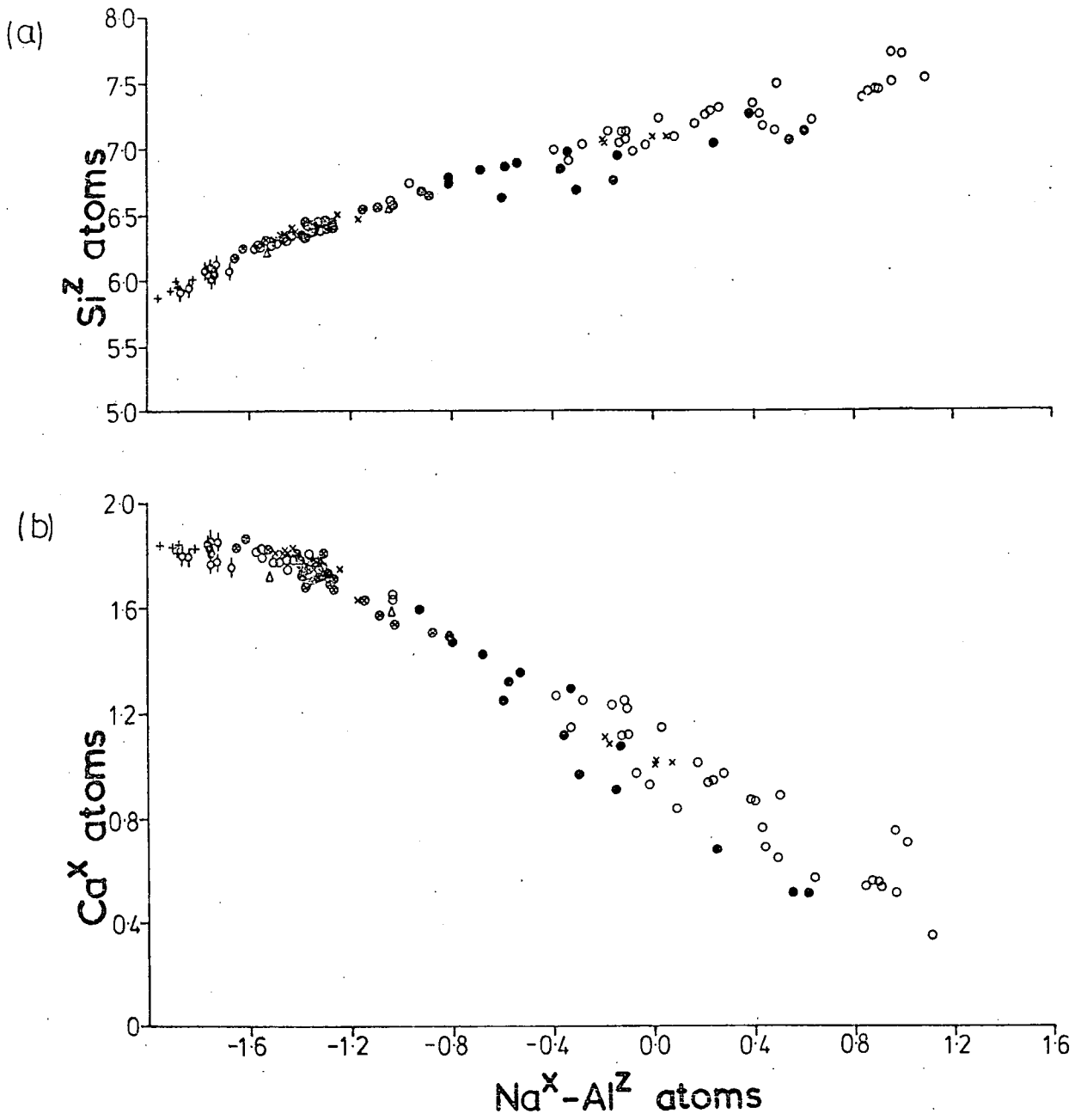
Substitution (5) is considered the most likely, as it is in accordance with the observed increase in  $\text{Na}^{\text{A}}(\text{K})$  and with the postulated increase in  $\text{Fe}^{3+}$ .

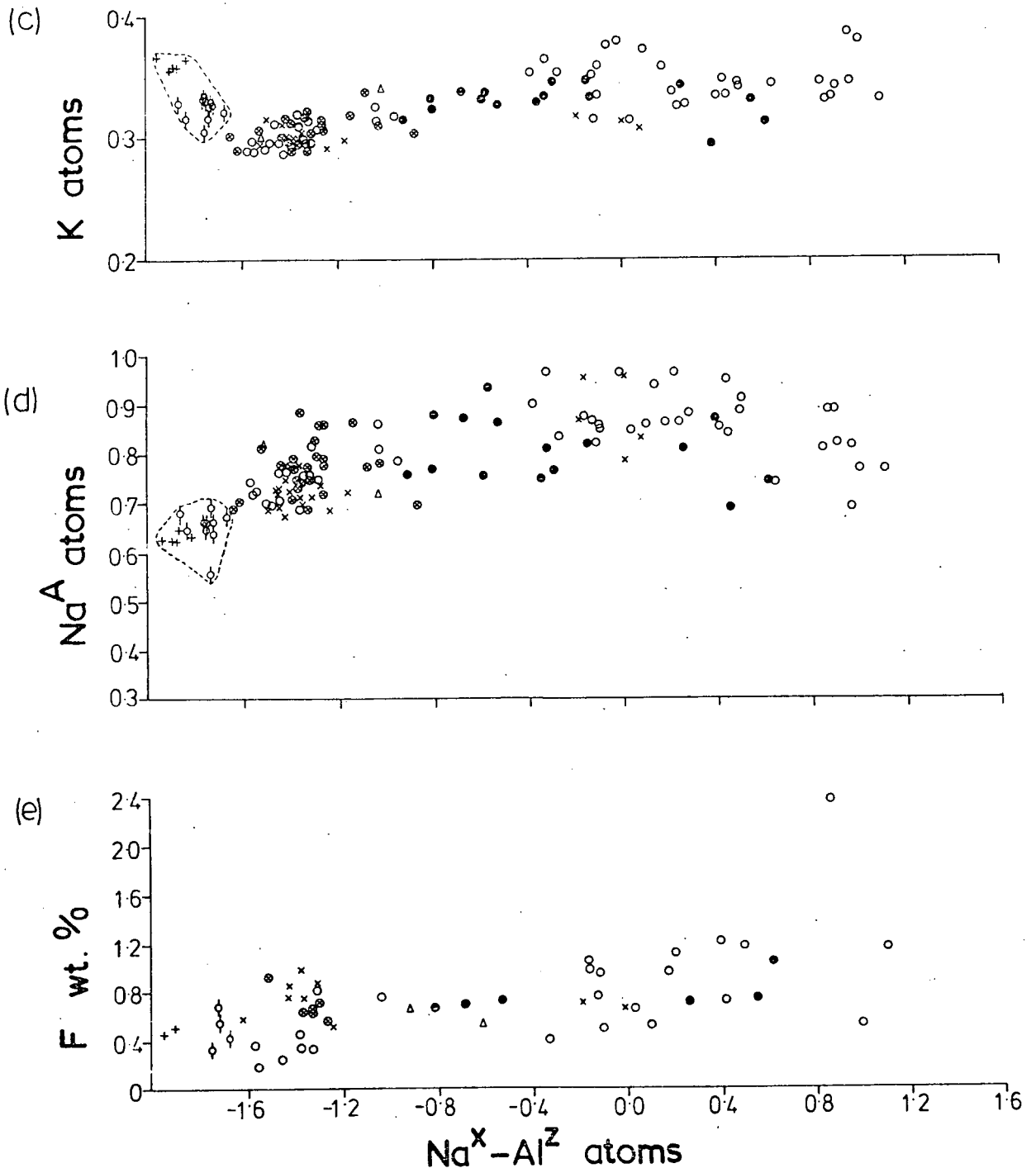
Mention should be made here of the amphiboles occurring in the recrystallized rocks. Just as with the pyroxenes, recrystallized amphiboles tend to lie off the dominant magmatic trend. In Figs. 4.12(f), (g) and (h) analyses of recrystallized amphiboles are outlined with a dotted line. Amphiboles from one recrystallized sample are outlined on all three diagrams, and amphiboles for a further two recrystallized rocks on the diagram showing MnO variation. It would appear that these amphiboles have a high Na-content in the X-site, while showing the Fe, Mn and Mg-contents of much less evolved amphiboles. This parallels the trend shown by the recrystallized pyroxenes, with their early enrichment in Na. The effect has been attributed to high oxygen fugacities in the pyroxenes. In the amphiboles, however, the increase in  $\text{Na}^{\text{X}}$  is not connected with an increase in the  $\text{Fe}^{3+}/\text{Fe}^{2+}$  ratio, but with the coupled substitution  $\text{Na}^{\text{X}}\text{Si}^{\text{Z}} \rightleftharpoons \text{Ca}^{\text{X}}\text{Al}^{\text{Z}}$ . Hence, it would appear that other factors must control the amphibole recrystallization

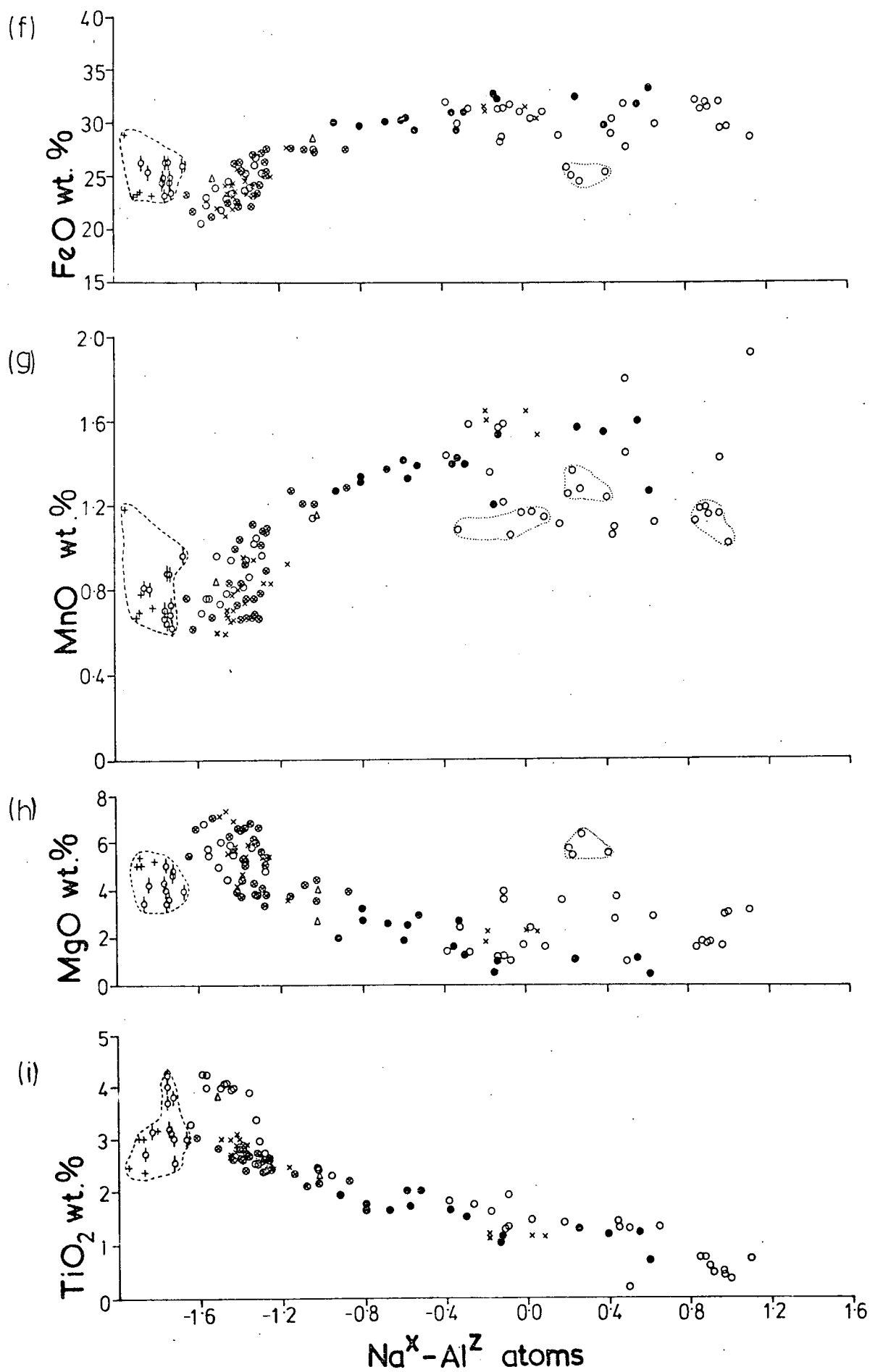
Fig.4.12 (three pages) The variation of selected major elements and minor elements with fractionation. The chosen Fractionation Index of  $\text{Na}^X - \text{Al}^Z$  (atoms) reflects the dominant substitution effecting North Qôroq amphibole compositions (see text). On certain of the diagrams, analyses from units SN.2 and ?SN.3 are outlined with a dashed line and those from recrystallized samples with a dotted line. Letters after the symbol for an element refer to the supposed site that the element resides in. The allocation of elements to sites is made using the computer program MINDATA 5 (see Appendix III.2.3.).

Symbols used:

- - Unit SN.1A
- △ - Unit SN.1B
- ⊙ - Unit SN.2
- + - Unit ?SN.3
- × - Unit SN.4A
- ⊗ - Unit SN.4B
- - Unit SN.5







trend, and these other factors may also have implications for the pyroxene trend. A discussion of these factors is given later.

No significant amounts of Al were allocated to the Y site. As  $Al^Y$  indicates a high pressure environment (e.g. glaucophane), this absence is consistent with the high level, low pressure environment that these amphiboles crystallized in.

Zr was found to be present in moderate amounts, but the concentration is variable and not related to amphibole type.

Two large amphiboles taken from late stage pegmatitic veins were analysed for trace elements by X-ray fluorescence analysis. Zr values of over 5000 p.p.m. were obtained, consistent with those obtained by microprobe analysis. Other elements present in quantity were Nb, 1000 p.p.m., and Zn, 2000 p.p.m. Although Zn was analysed for by microprobe, it was not encountered, and probably only reaches high concentrations in late stage pegmatites. This is in accordance with the findings of Rowbotham. He says that, although  $Zn^{2+}$  has the same ionic radius as  $Fe^{2+}$ , the Zn-O bond is less ionic than the Fe-O bond, and hence  $Zn^{2+}/Fe^{2+}$  will increase during fractionation. Values obtained by Rowbotham on late stage Ilímaussaq amphiboles

from lujavrites show Zn contents of around 2000 p.p.m., closely paralleling North Qôroq.

Amphibole stability fields and experimental work on amphiboles under varying T, P, H<sub>2</sub>O and f.O<sub>2</sub> conditions will be discussed in the thermodynamics section.

#### 4.4. Biotites

##### 4.4.1. Introduction

Biotite occurs in all units of the North Qôroq Centre. Unlike South Qôroq, where it is a common and important phase, its occurrence is usually very restricted. The exception to this is the marginal rocks of unit SN.1A, where biotite is abundant, forming up to 10 vol.% of the rock. Here, it shows the pleochroic scheme of an Fe-rich biotite (X = straw yellow, Y = Z = dark brown). It is found as extensive rims to Fe/Ti oxide grains, or as apparently discrete crystals. In the more highly fractionated interior of this unit, and in other units, biotite is much less abundant and occurs either as small interstitial crystals, as rims to opaques, or commonly as part of a patchy replacement mineralogy where biotite, pyroxene, opaques and analcite have replaced amphibole. Where biotite is a minor phase, the pleochroic scheme it shows is either X = brown, Y = Z = red-brown; or X = brown, Y = Z =

green-brown. According to Deer, Howie and Zussman (1962) high Ti content gives a red-brown colour while high  $\text{Fe}^{3+}$  gives green. No systematic variation of biotite colour with the presence or absence of other  $\text{Fe}^{3+}$  and Ti-bearing minerals, such as magnetite, aenigmatite or amphibole, was noted.

The present account is based on 28 analyses for 10 major elements and a selected number of Zr and F. Results of the probe analyses are given in Appendix III.4. As with other mineral groups, the  $\text{Fe}^{3+}/\text{Fe}^{2+}$  ratio was not determinable by the techniques employed, and all Fe in the biotites is expressed as  $\text{Fe}^{2+}$ . The possibility of the existence of biotites where  $\text{Fe}^{3+}$  in the octahedral site is balanced by  $\text{O}^{2-}$  substituting for  $\text{OH}^-$  is neglected.

#### 4.4.2. Chemical variation

A general formula for the micas is  $\text{X}_2\text{Y}_{4-6}(\text{Si,Al})_8\text{O}_{22}(\text{OH,F})_4$ , where X-site ions show 12-fold coordination, Y-site ions octahedral coordination and Si and Al ions tetrahedral coordination. Taking the analyses of biotite from North Qôroq, and allocating elements to lattice sites, a number of interesting points emerge.

The tetrahedral site total, to a base of 22 oxygens, is generally below 8 for biotites from units SN.1A, SN.1B, SN.4A and SN.4B (range 7.8-7.9). This may be a result of

true vacancies in the tetrahedral site, or the fact that some of the Fe, tabulated as octahedral  $\text{Fe}^{2+}$ , is in fact tetrahedral  $\text{Fe}^{3+}$ . In contrast to these tetrahedral deficient biotites, those from SN.2 and ?SN.3 show sufficient Al to fill the tetrahedral site and to contribute to the octahedral site. SN.5 biotites, although without tetrahedral vacancies, show the lowest content of Al for any of the syenites.

All the analyses show deficient octahedral sites totalling in the range 5.5-5.9. This is a common feature of biotites from all types of environment, and suggests that the minerals may be intermediate between dominant trioctahedral micas, with 6 octahedral cations, and dioctahedral micas, with 4 octahedral cations.

The 12-coordinated X-site usually contains 2 ions ( $\pm 0.1$ ). Ca is never present in more than trace amounts and Na constitutes between 0.1 and 0.3 ions per 22 oxygens. Biotites of SN.5 show a slightly higher X-site content (2.1), due to increased K.

All biotite analyses from the major syenitic units are plotted on Fig.4.13. This figure includes 4 end-members; phlogopite, annite, eastonite and siderophyllite, and assumes the micas to be of a trioctahedral nature. The 4 end-member composition positions are indicated on the figure by means of their first letters. All the analyses

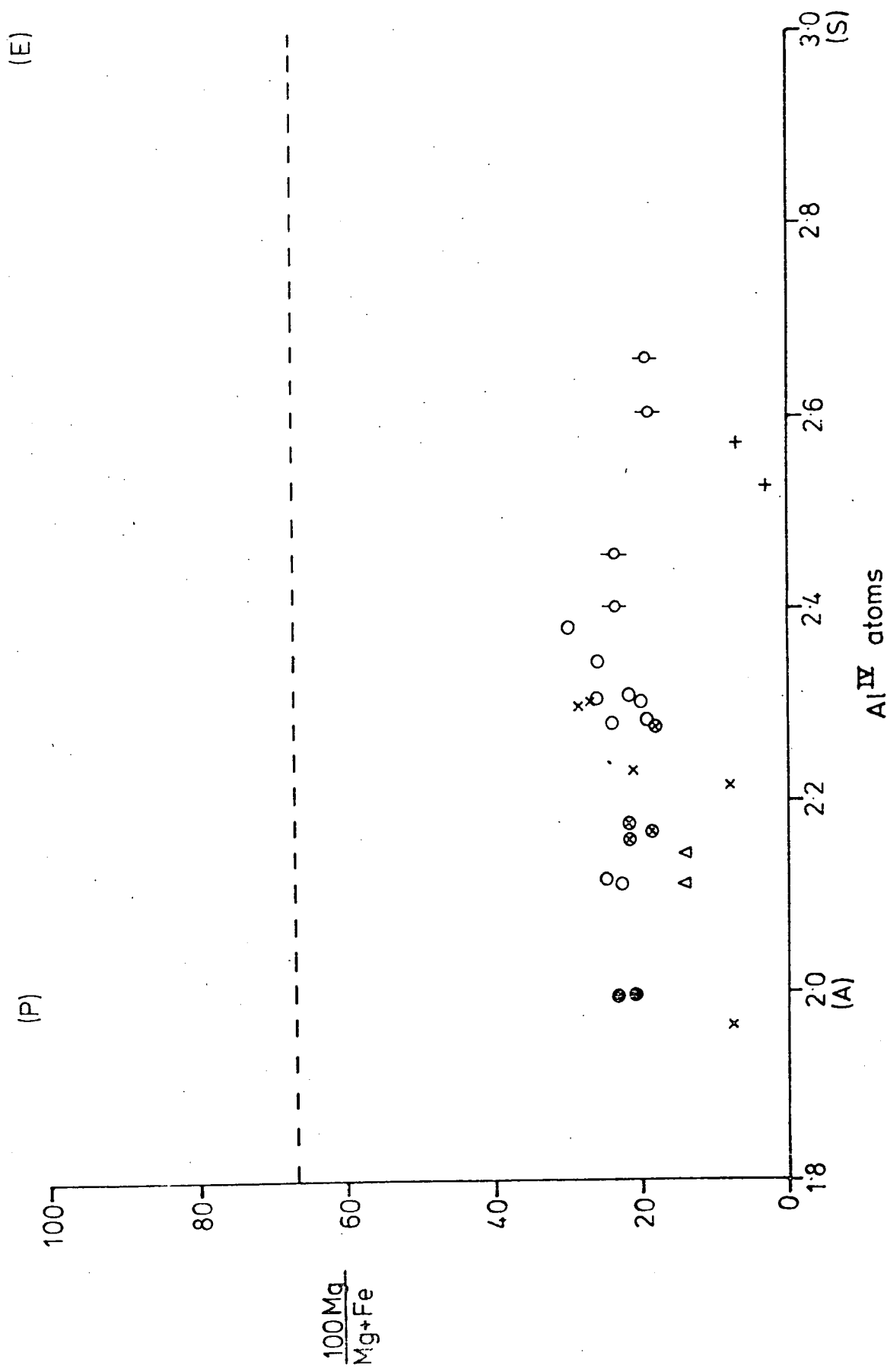
Fig.4.13 The variation in the composition of the biotites from the major units of North Qôroq. The 4 end-member compositions are indicated by their first letters.

Abbreviations used:

- P - Phlogopite
- E - Eastonite
- A - Annite
- S - Siderophyllite

Symbols used:

- - Unit SN.1A
- △ - Unit SN.1B
- ϕ - Unit SN.2
- + - Unit ?SN.3
- × - Unit SN.4A
- ⊗ - Unit SN.4B
- - Unit SN.5



can be seen to be low in Mg and high in total Fe (expressed as  $\text{Fe}^{2+}$  on this diagram). The biggest variation can be seen to be in the Al content of the tetrahedral sites. Although most analyses plot quite close to the annite end member, all analyses for units SN.2 and ?SN.3 contain appreciably more tetrahedral Al, causing them to plot between annite and siderophyllite. It is significant that, in both these units, the amphiboles also show high tetrahedral Al. As with the amphiboles, this could reflect a temperature effect, SN.2 and ?SN.3 biotites forming at higher temperatures than biotites from the other syenites.

In the other syenites, biotite appears to show a decrease in tetrahedral Al and an increase in Si with increased degree of fractionation of the parent rock.

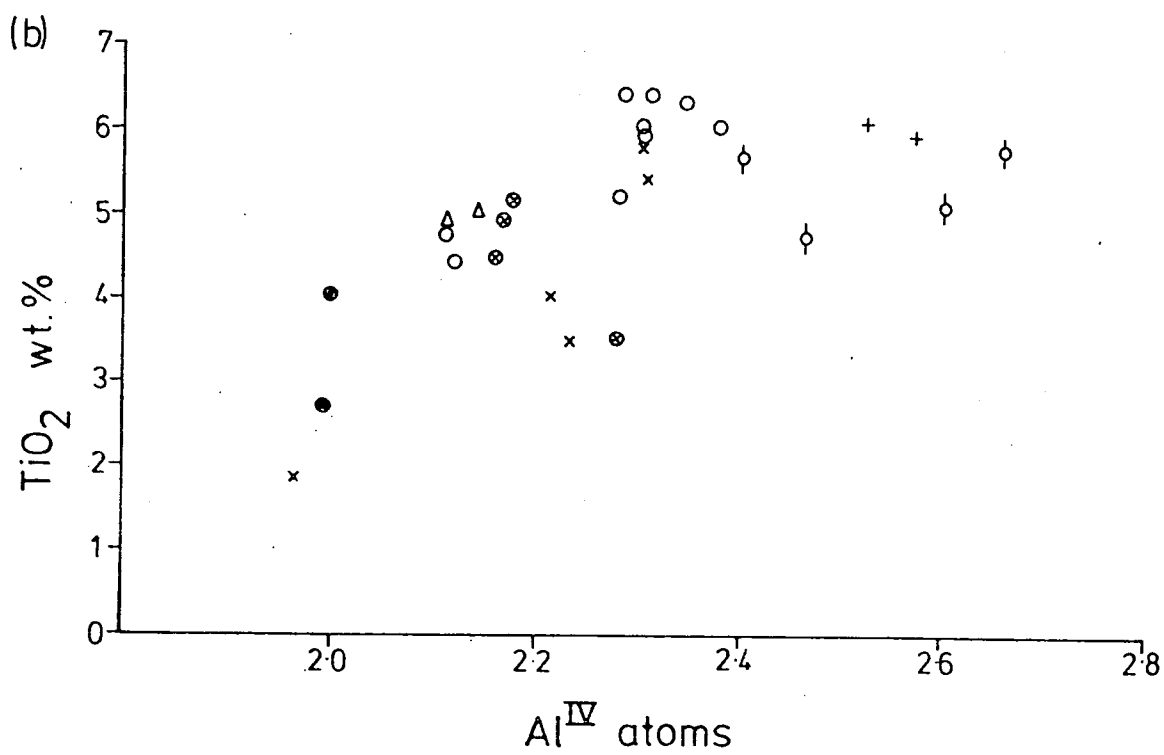
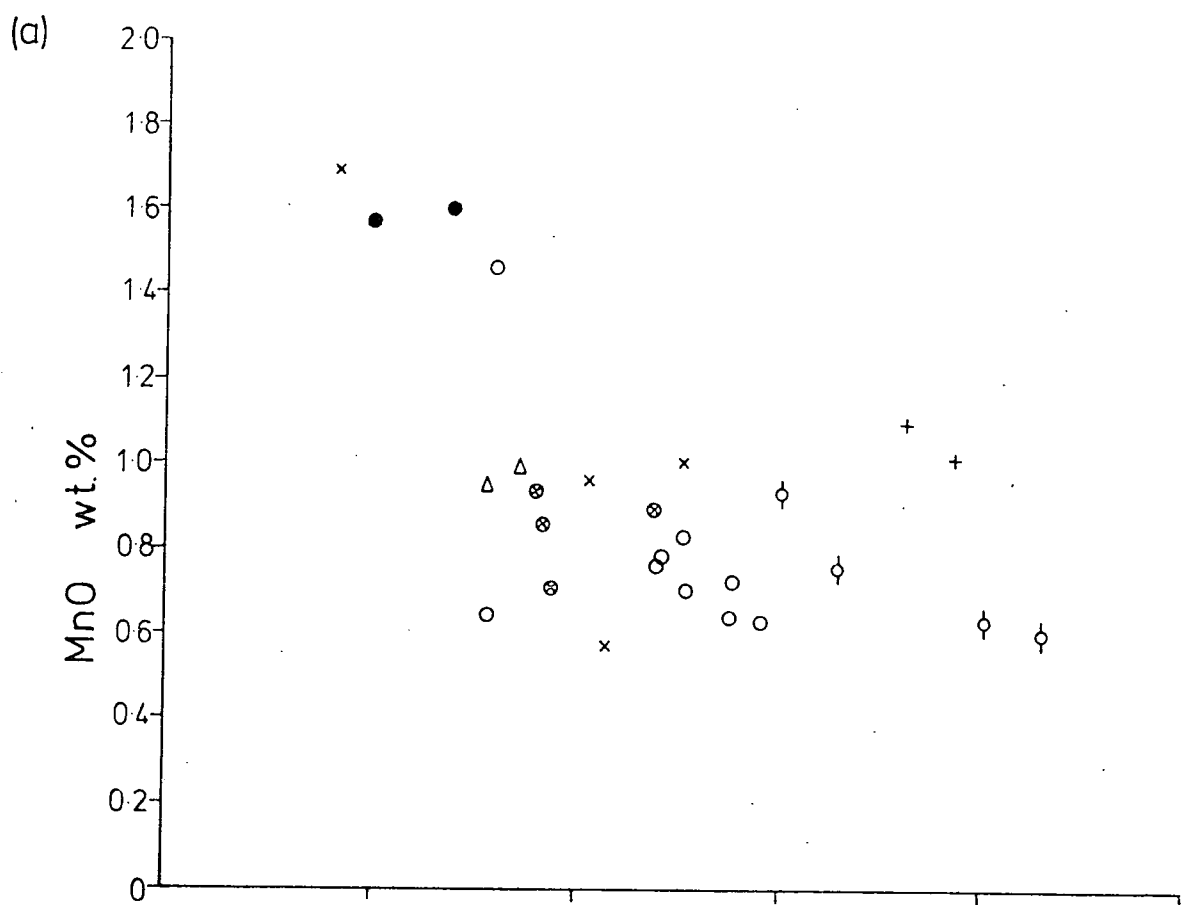
The only other elements to show systematic variation with fractionation (i.e. with decrease in tetrahedral Al) are Ti and Mn. Fig. 4.14(a) and (b) summarize this variation, showing Mn to increase and Ti to decrease.

F was analysed for in certain of the biotites, but only occurs in very small quantities, except for biotites from a recrystallized rock where 0.5 wt.% F was detected. Gillberg (1964) reports that biotites and amphiboles from Swedish granites have similar F contents. Biotite is known to participate in ion exchange with ground water much more

Fig.4.14 Variation in Mn and Ti contents of the North Qôroq biotites with variation in tetrahedral Al ( $Al^{iv}$ ).

Symbols used:

- - Unit SN.1A
- △ - Unit SN.1B
- ⊙ - Unit SN.2
- + - Unit ?SN.3
- × - Unit SN.4A
- ⊗ - Unit SN.4B
- - Unit SN.5



readily than amphibole, the  $F^-$  being replaced by  $OH^-$ .

This possibly happened to North Qôroq biotites, which now may contain somewhat less F than originally. The higher F content in the biotite from the recrystallized rocks may be a result of introduction of F by the metasomatic fluids that accompanied metamorphism (Chapter 6).

Zr never occurs in more than trace amounts in any of the analysed biotites.

Ba and Cl were analysed for. Although both can occur in significant amounts in biotites, they were not detected in those of North Qôroq.

A discussion of the stability field of biotite, with varying conditions of temperature,  $P.H_2O$  and  $f.O_2$ , is given in the thermodynamics section.

#### 4.5. Fe/Ti oxides

##### 4.5.1. Introduction

Fe/Ti oxides are present in all units of the North Qôroq Centre. In the least evolved rocks they occur as an early-formed major phase, associated with pyroxene and olivine, and frequently rimmed by biotite. In highly fractionated rocks they occur only as small interstitial crystals and granular patches, and are often associated with pyroxene, biotite and analcite as an 'amphibole replacement mineralogy'.

#### 4.5.2. Exsolution in the oxides

All the primary Fe/Ti oxides are magnetites with exsolved ilmenite lamellae. The exsolution takes place along the (111) planes in the magnetite resulting in a 'trellis texture'. Similar textures are described from oxides in the South Qôroq Centre (Stephenson, 1973) and in Nunarssuit syenites (Anderson, 1974). In the Alangorssuaq Gabbro, Anderson describes very fine scale exsolution of ulvôspinel along the (100) planes in the magnetite, a type of exsolution not encountered in North Qôroq oxides, because of too high an  $f.O_2$ . Buddington and Lindsley (1964) maintain that there is no solid solution between ilmenite and magnetite, and that the ilmenite represents ulvôspinel that has been oxidised. Duchesne (1970) favours direct oxidation-exsolution, occurring mainly at super-solvus temperatures, with (100) type ulvôspinel exsolution occurring at lower temperatures. It should be noted that the oxidation of ulvôspinel and the exsolution of ilmenite does not imply an increase in the fugacity of oxygen. This reaction must occur if the fugacity in the rock parallels the fayalite-magnetite-quartz buffer (F.M.Q.).

In North Qôroq oxides the scale of exsolution is variable. It is usually very fine in the marginal rocks

of SN.1A and in units SN.2, SN.4A and SN.4B, but on a coarser scale in the inner parts of SN.1A and in SN.5. Much of the variation can be interpreted as being caused by differing rates of cooling, slower cooled rocks showing much coarser scale exsolution. Another factor may be the presence of mineralizers (Ramdohr, 1969), possibly associated with a vapour phase co-existing with the magma (Buddington and Lindsley op.cit.). This would aid diffusion and favour coarse-scale exsolution. A combination of these two factors may explain the extremely coarse-scale exsolution seen in the Fe/Ti oxides from parts of North Qôroq.

Very occasional granular magnetite and ilmenite occur where samples were taken adjacent to younger units or to the younger South Qôroq Centre. Stephenson has attributed similar textures, shown by South Qôroq oxides from recrystallized rocks, to increased  $f.O_2$  and high diffusion rates.

Mention should be made here of certain samples which show haematite rimming the magnetite-ilmenite grains. It is uncertain at precisely what stage this oxidation took place, but it occurred late, and may even have been the result of weathering.

When analysing the Fe/Ti oxides of North Qôroq, the

technique employed was to defocus the electron beam and sum the counts obtained along several traverses. This resulted in combined bulk analyses of host and lamellae. The method has been employed by several other workers (Lindh, 1973; Elsdon, 1972; Simmons et al., 1974). Comparable results were obtained from different grains analysed in the same rock sample, suggesting that orientation effects are not an important factor. By employing this method, an analysis can be obtained of what was presumably an original titanomagnetite. The method of calculating the molecular proportion of ulvöspinel in this titanomagnetite is explained in Appendix III.2.4., and the results tabulated. The 41 bulk analyses thus obtained proved useful in calculating the  $f.O_2$  of the North Qôroq magmas (section 4.16).

#### 4.5.3. Chemical variation

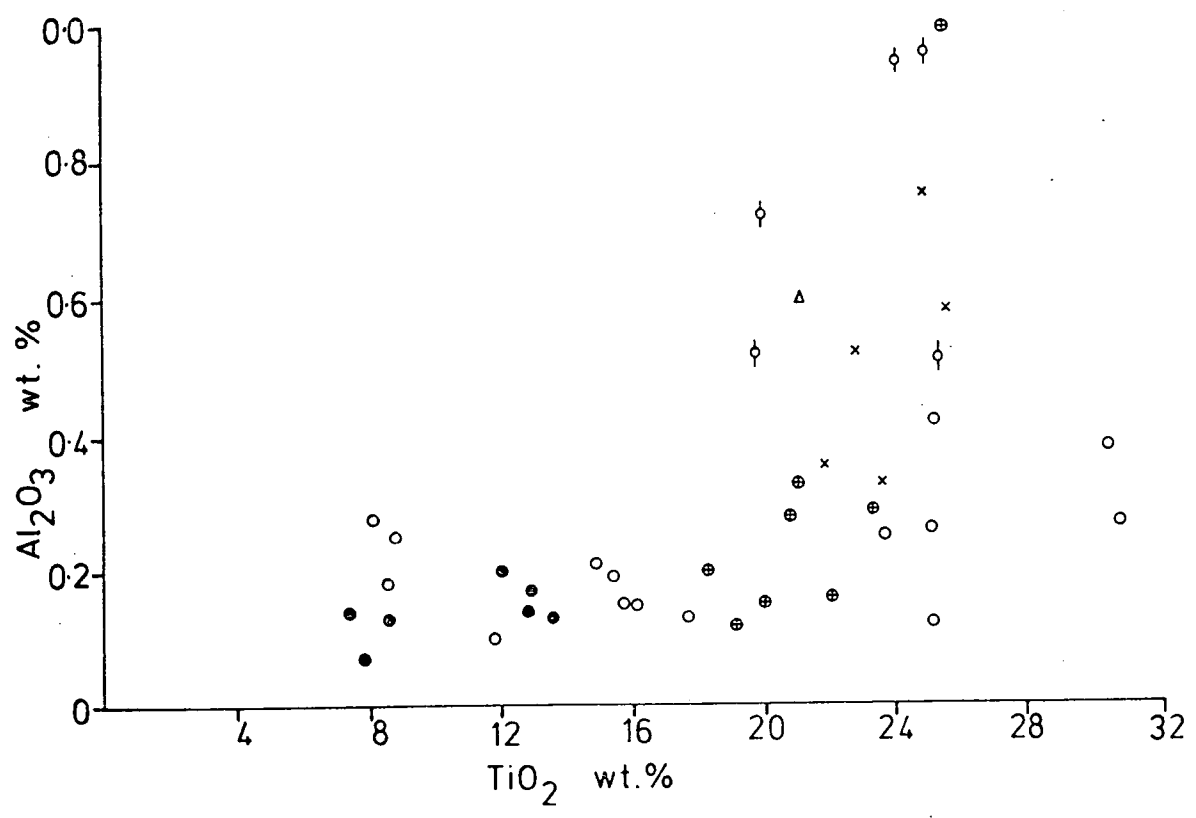
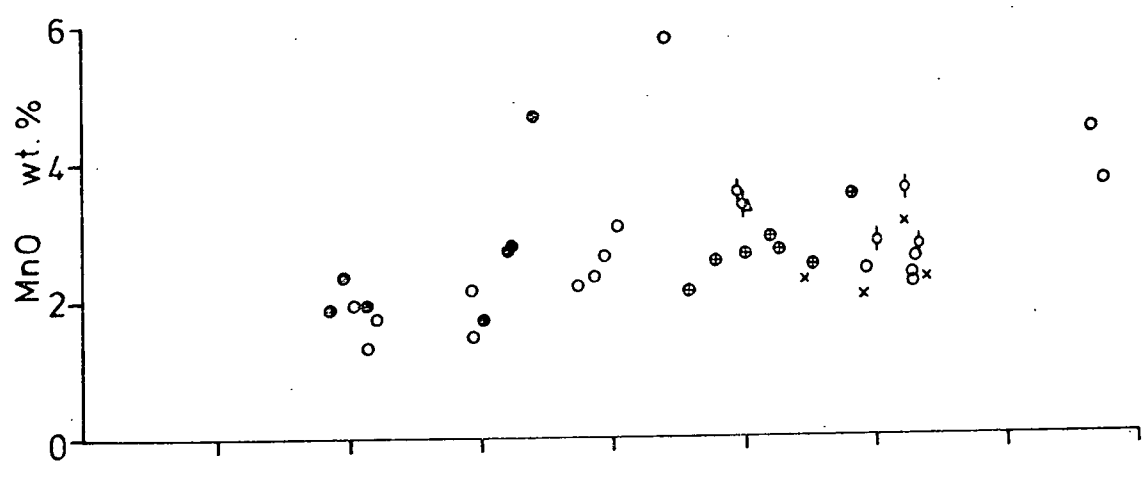
The major chemical variation shown is a decrease in the Ti content of the bulk oxides with fractionation, resulting in quite considerable differences both in and between units. The least evolved marginal rocks of SN.1A show up to 30 wt.%  $TiO_2$ . Oxides from SN.2, SN.4A and SN.4B show 18-25 wt.%  $TiO_2$ , and those from the highly fractionated interior of SN.1A and unit SN.5 8-14 wt.%  $TiO_2$ . This difference in the Ti content shows itself not only in the



Fig.4.15 Variation in the Mn and Al contents (plotted as wt.% oxides), with the decrease in the Ti content (wt.% oxide) that occurs with increased fractionation state of the host rock.

Symbols used:

- - Unit SN.1A
- ◊ - Unit SN.2
- △ - Unit ?SN.3
- × - Unit SN.4A
- ⊗ - Unit SN.4B
- - Unit SN.5



undersaturated rocks of North Qôroq, the observed decrease in Al in the oxides is the reverse of that expected.

Closer examination of Fig. 4.15 shows that many of the analyses showing higher Al are from units SN.2 and ?SN.3, which also showed high Al contents in their amphiboles and biotites. Perhaps these high Al values simply reflect a high Al content in the magmas which formed SN.2 and ?SN.3 (i.e. high activity of  $Al_2O_3$ ).

The elements Zn and Ni were analysed for by microprobe, but were not detected, a result consistent with the low 'whole rock' values for these elements. V may be present in small quantities, but difficulties in separating the V and Ti peaks during probe analysis make this uncertain.

#### 4.6. Feldspars

##### 4.6.1. Introduction

Alkali feldspar is the major mineral phase in all units of the North Qôroq Centre. In the least fractionated rocks it occurs as one of the later phases, crystallizing after olivine, pyroxene and Fe/Ti oxides. In more fractionated rocks it is early-formed, occurring together with nepheline. The effect of feldspar fractionation on the composition of residual liquids is discussed in Chapter 5.

The North Qôroq feldspars are perthitic and bulk analyses of these perthites have been obtained. The

technique employed was similar to that used for the exsolved Fe/Ti oxides. The electron beam was defocussed to approximately 50 $\mu$ m , and counts accumulated over a traverse, the traverse being repeated for all elements. For very finely exsolved material only a short traverse was necessary to ensure a reasonable value for the bulk feldspar composition. When coarser scale exsolution was encountered, e.g. SN.5 and inner parts of SN.1A, it was often necessary to perform several traverses per crystal, and to average the analyses from several crystals, to obtain a reasonable value for the feldspar composition prior to exsolution.

#### 4.6.2. Structural state and exsolution

The feldspars were treated from the point of view of the chemical variation they showed, and not that of variation in their structural state. No attempt was made to define structural state, either by X-ray diffraction methods, or by determination of the optic axial angle coupled with composition. Investigation of the structural state of feldspars from Gardar intrusions has proved informative, and those from North Qôroq may repay similar investigation. Stephenson (1973) used the plot of optic axial angle against composition for South Qôroq feldspars, and established that the bulk of them fell between the low

albite - orthoclase series, and the low albite-microcline series. Most North Qôroq feldspars are probably similar, but rapidly cooled, volatile-poor rocks, such as units SN.4A and SN.4B, may contain feldspars showing a higher structural state.

The degree of feldspar unmixing is very variable in the North Qôroq rocks. Feldspars from marginal SN.1A, SN.2, SN.4A and SN.4B are cryptoperthites and microperthites, with blebs of albite in which the albite twinning is just discernable. The extent of unmixing increases in an irregular fashion from core to rim and is more noticeable along fractures. In the interior of SN.1A, and in unit SN.5, perthitic exsolution is on an extremely coarse scale and irregular, interlocking patches of albite, up to 1 mm. long, show clearly discernible albite twinning. The potassic phase tends to be cloudy and microcline twinning is never observed. The coarse perthites show albite rims and 'swapped rims', both probably exsolution features. At times the Na-feldspar component is dominant, when the feldspar should strictly be termed antiperthites.

Exsolution in North Qôroq feldspars may be controlled by a number of factors. Feldspars from the rapidly cooled augite syenites and marginal rocks show fine scale exsolution, suggesting that rate of cooling may be a factor. Occasional point analyses were made of host and associated blebs in

the perthites. These show extreme compositions for fractionated rocks, which, when related to the feldspar solvus, suggest unmixing to a very low temperature. The augite syenite feldspars show less extreme compositions, compatible with unmixing to temperatures of 500-600°C. There is, however, with these microperthites the possibility of not having been able to analyse pure host or pure bleb, and the result can not be viewed with much confidence as that for the more fractionated feldspars.

Undoubtedly of importance with regard to the exsolution phenomenon is the Ca content of the feldspars. In many feldspars with optically homogeneous cores and microperthite rims, the cores show higher Ca-values. Ca, although raising the solvus and hence the temperature at which unmixing begins, inhibits the rate of unmixing. This is because diffusion of the divalent Ca ion into the sodic parts of the feldspar requires a restructuring of the alumino-silicate framework and hence a high energy input, whereas diffusion of Na and K ions does not.

A further important factor is the probable presence of a volatile phase. Smith (1974) suggests that interlocking perthites, a common feature of the more fractionated rocks of North Qôroq, are indicative of metasomatism. The concentration of coarser perthite along fractures and around crystal margins also suggests that exsolution is

being aided by a volatile phase. Emeleus and Smith (1959) stress the importance of volatiles in controlling structural state. This has been confirmed by Martin (1969), who demonstrated experimentally that the presence of sodium disilicate ( $\text{Na}_2\text{Si}_2\text{O}_5$ ) greatly aids the attainment of a low structural state by albite (at  $300^\circ\text{C}$  and  $10\text{Kb. P.H}_2\text{O}$ ). He claims that the widespread occurrence of ordered albite suggests the common presence of a per sodic fluid in certain igneous rocks. Highly fractionated members of the North Qôroq Centre are per sodic, containing acmite and occasionally sodium metasilicate ( $\text{Na}_2\text{SiO}_3$ ) in the norm. The general indication is that the dominant factor controlling degree of exsolution and probably structural state in North Qôroq feldspars is the presence of a per sodic liquid, either magmatic, or more probably a co-existing vapour phase (Chapter 6). Other factors, such as variable Ca contents and variable rates of cooling, may also contribute to the final state of the feldspars.

Mention must be made of the problematical feldspar types encountered in units SN.4A and SN.4B, and described in the petrography chapter. These feldspars usually have clear untwinned cores and microperthitic rims, the two being separated by a 'dusting' of tiny rounded pyroxene and/or amphibole crystals. Rare cores showing diffuse

cross-hatch twinning, reminiscent of anorthoclase, proved to be oligoclase on analysis. Smith and Muir (1958), describing oligoclase from their 'Sp.8 feldspar' from the Oslo larvikites, comment that these show both albite and pericline twinning, so resembling anorthoclase.

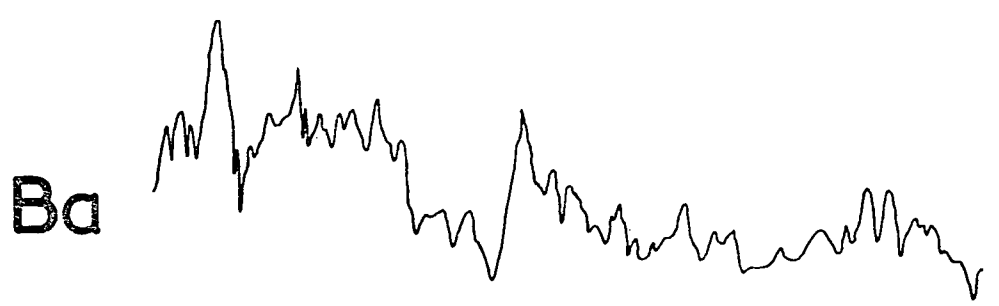
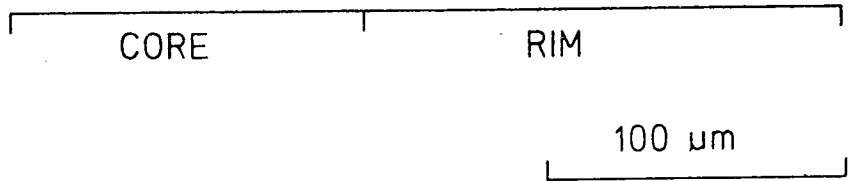
Plagioclase cores to perthitic alkali feldspar are frequently mentioned in the literature. Among Gardar workers Upton (1964a) gives a detailed description, with sketches, of similar problematical feldspars from the Tugtutôq central ring complex. Parsons (1972) describes plagioclase cores from granitic rocks of the Puklen intrusion, preferring to explain them as being xenocrysts assimilated from the neighbouring Juliãnehãb granite. Stephenson (1973) describes oligoclase cores for feldspars of unit SS.4B of South Qôroq and Anderson (1974) similar cores to feldspars from the Nunarssuit syenite and Biotite granite. Probably the best documented example is presented by the larvikites of the Oslo region (Muir and Smith, 1956; Smith and Muir, *opacit.*; Harnik, 1969).

The first problem presenting itself is whether these rocks are sub-solvus, two feldspar monzonites, or hyper-solvus, one feldspar syenites showing a simple fractionation sequence from plagioclase to alkali feldspar. Workers on the Oslo larvikites have expressed both views, but Smith

and Muir conclude that they are single feldspar rocks. Upton (op.cit.) encounters a similar problem for feldspars from the Tugtutôq central ring complex. Syenites of the North Qôroq Centre are definitely hyper-solvus, containing a single feldspar, and it seems unlikely that the SN.4 units, thought from their petrography to be relatively dry, would be sub-solvus. It is proposed therefore, that the plagioclase represents an early formed member of the feldspar series which, if equilibrium had been maintained, would have been resorbed to become a lime-rich alkali feldspar. Examination of Bowen's original work on the simple system Ab-An (1912), shows that oligoclase could precipitate from a liquid containing as little as 1 wt.% CaO.

Fig. 4.16 shows probe traces across a feldspar phenocryst from SN.4A. The core of oligoclase can be seen to contain occasional thin zones ( $\sim 20\mu\text{m}$ ) of Ba-rich K-feldspar, a feature noted in Oslo larvikite plagioclase cores (Harnik, op.cit.). The rim consists of typical microperthite. The characteristic sharp compositional break between core and rim is very noticeable in these traces. These large feldspar phenocrysts in a fine-grained groundmass appear to have formed at depth. It may be that the rise of the magma to the surface and consequent pressure drop removed sodic plagioclase from the liquidus surface, and that when

Fig.4.16 The results of a probe traverse for selected elements across a feldspar phenocryst from unit SN.4A.



feldspar returned to the liquidus at low pressure, i.e. when the magma was emplaced, its composition was that of an alkali feldspar. Jorgensen (1971) proposed a similar pressure control to account for compositional change in plagioclase feldspars. He demonstrated that a drop in pressure moves the plagioclase-pyroxene phase boundary in the system Ab-An-Di, and results in a liquid that was originally crystallizing plagioclase now crystallizing pyroxene. When plagioclase returns to the liquidus, after a period of pyroxene crystallization, it is much more sodic.

The dusting of fine pyroxene and amphibole crystals occurring between core and rim probably represent small crystals trapped when the feldspar resumed crystallization.

#### 4.6.3. Major element variation

The major element variation for the feldspars is given in Fig. 4.17, in terms of the end members Ab-An-Or. Units SN.2, SN.4A and SN.4B show the early formed plagioclase cores, plotting in the field of oligoclase. Fig. 4.16 demonstrated the presence of K in the cores, which from Fig. 4.17 can be seen to be usually low, but occasionally reaching almost 12 wt.% Or. The clear compositional break between these compositions and the perthitic alkali feldspars is apparent. A surprising feature of the alkali feldspars

Fig.4.17 The major element variation shown by the feldspars of North Qôroq, in terms of the end members Albite-Anorthite-Orthoclase. Each syenite unit is plotted separately.

Symbols used:

- - Feldspars from normal rocks
- - Feldspars from recrystallized rocks

An  
↑

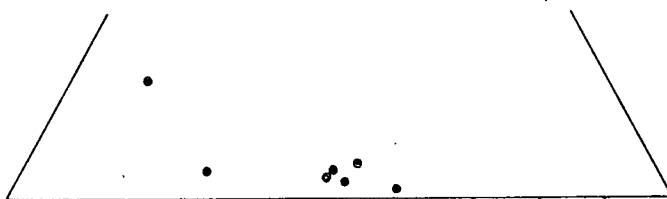
SN.1A



SN.1B



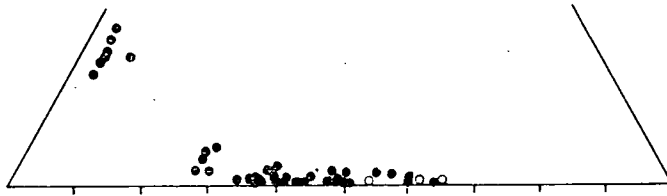
SN.2



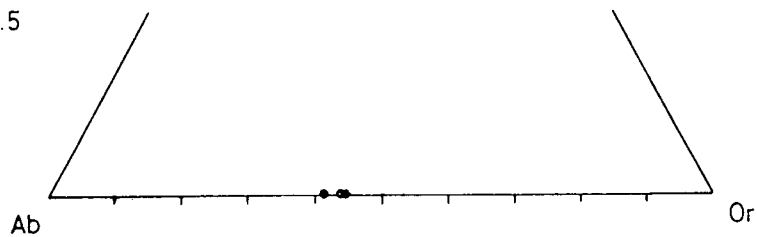
SN.4A



SN.4B



SN.5



Ab

Or

Mol. wt. %

is their extreme variability from Or-rich to Ab-rich members. This variability was carefully checked and reflects a true change in composition. For coarsely exsolved feldspars the points plotted represent the average of several grains, each grain being analysed over a considerable area. Zoning can be detected in individual crystals if they are not too perthitic. An-rich alkali feldspar cores tend to zone towards more An-poor, K-rich rims. In the low An feldspars zonation from core to rim proceeds either towards Na or K enrichment. The groundmass feldspars co-existing with nepheline are relatively orthoclase rich. An explanation must be provided, both for the extent of variability in the feldspar compositions, and the variable trends towards both Na and K-enrichment.

Consideration of the experimental system  $\text{NaAlSi}_3\text{O}_8 - \text{KAlSi}_3\text{O}_8 - \text{SiO}_2 - \text{H}_2\text{O}$  (Hamilton and MacKenzie, 1965) helps to elucidate this problem. A discussion on liquid lines of descent shown by North Qôroq rocks is reserved for Chapter 5, but it can be mentioned here that a liquid close to the feldspar boundary in the residua system, and on the potassic side of the unique fractionation curve (Hamilton and MacKenzie, op.cit. Fig.3), will initially precipitate an extremely potassic feldspar, which will be zoned to more sodic rims. When the liquid reaches the

nepheline-feldspar phase boundary, and nepheline crystallizes, a more potassic feldspar is again produced. The final feldspar to crystallize will have a composition around the  $Or_{50}Ab_{50}$  point, which is where many of the North Qôroq groundmass feldspars occur. The An-rich alkali feldspars, showing zonation towards K-rich Ca-poor rims, occur in rocks containing appreciable mafic minerals and can not be represented by the residua system. For the other feldspars the observable variation can be explained by consideration of the experimentally determined phase equilibria relations. Alternatively, complex fractionation curves, such as those suggested by Nash et al. (1969) to explain similar zonation in Mt. Suswa feldspars, would produce the required K and Na enrichment observed in North Qôroq feldspars.

It should be mentioned that a number of the K-rich feldspars occur in recrystallized rocks where K-metasomatism may be a factor.

Stephenson (1973, pp.107) maintains that it is necessary for feldspars from South Qôroq to cross the 5Kb. cotectic (Yoder et al., 1957). It is arguable that the cotectic at 5Kb. is hardly appropriate for either North or South Qôroq rocks, which must have formed at higher levels and much reduced pressures. Putting aside this factor, there is no

reason why feldspar compositions should not cross the cotectic, as it only represents a barrier for liquids of feldspar composition. Both North and South Qôroq liquids must have rapidly proceeded towards the undersaturated minimum in the residua system, and hence are not represented by the system Ab-An-Or. It is the liquid which must not arbitrarily cross phase boundaries. The feldspar compositions crystallizing from this liquid are not similarly restricted.

#### 4.6.4. Trace element variation

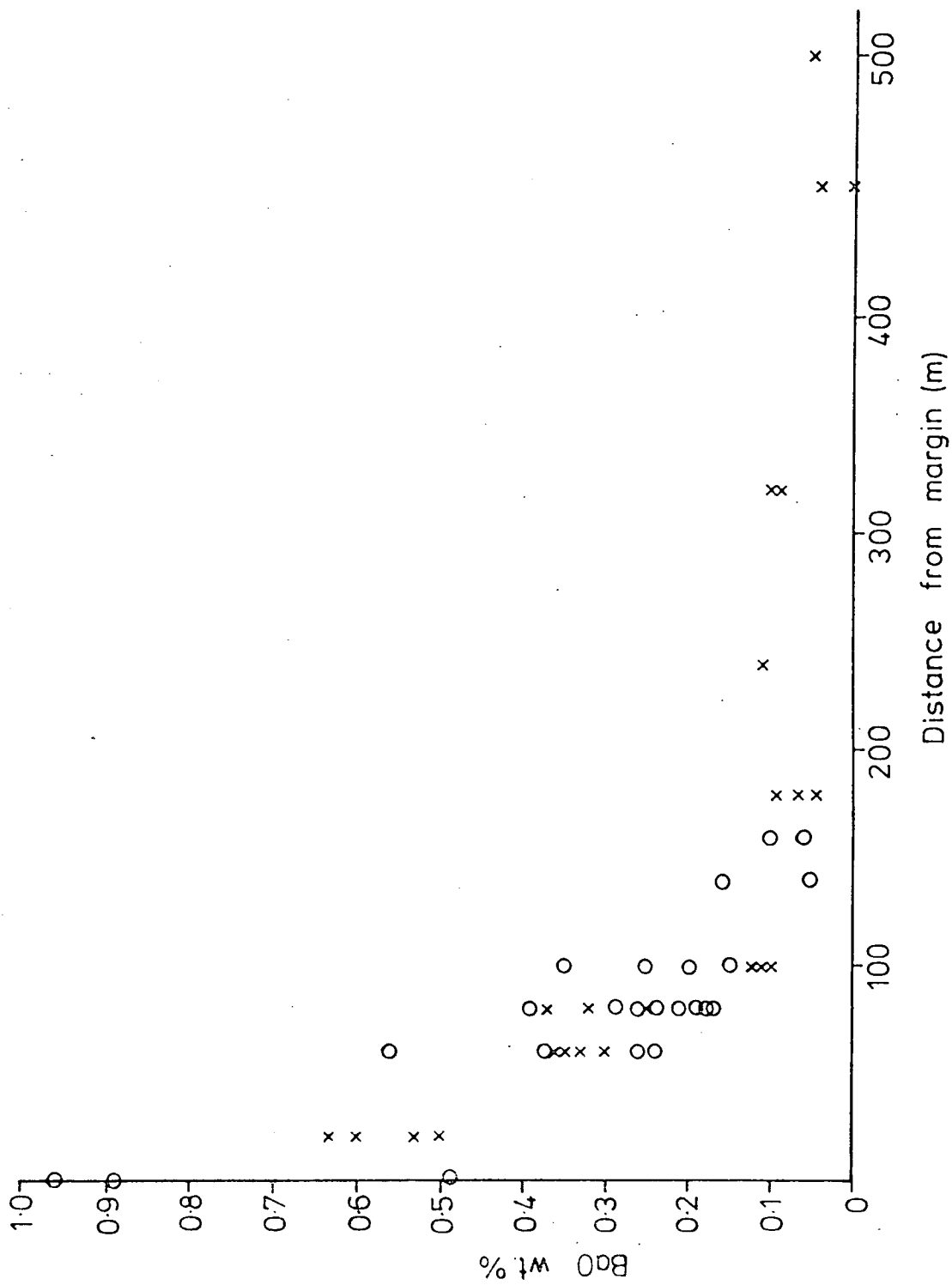
Among the trace elements analysed for Fe, Mg and Ti were present in small quantities. No systematic variation in these elements was observed. The only trace element present in significant amounts was Ba, which could reach values of 1 wt.% BaO. It was found concentrated in feldspars from the least fractionated rocks, and reached the highest values in the margins of unit SN.1A. Fig. 4.18 shows the concentration of BaO in the feldspar, against distance from a unit's margins for SN.1A and SN.4 (A and B). It can be seen that the Ba content decreases rapidly as the more highly fractionated interiors of units are approached. Unit SN.1A shows a more rapid increase in degree of fractionation from margin to core of the unit than either of the SN.4 units. This is paralleled by the more rapid decrease in the Ba content of the feldspars.

Fig.4.18 The variation in Ba contents of the feldspars with distance from the margins of a unit.

Symbols used:

O - Unit SN.1A

X - Units SN.4A and SN.4B



Many workers have stated that Ba readily substitutes for K in the feldspar structure (Flower, 1973; Smith, op.cit.). An inspection of Fig. 4.16 confirms the strong positive correlation of Ba and K. Indeed, by virtue of the divalent nature of Ba, it is taken preferentially into the feldspar structure. The massive concentrations of Ba in the margins of units, particularly SN.1A, suggests that here, one had the first opportunity for potassic feldspars to crystallize from the magma. Any previous crystallization at depth would rapidly have depleted the magma in Ba. The consistently low Ba values from unit SN.5 suggest that crystallization and fractionation of alkali feldspar took place at depth, and that a Ba-depleted magma was emplaced.

Sr and Rb never occurred in sufficient quantities in the feldspar to be detected by electron probe.

#### 4.6.5. The feldspar solvus, T and P.H<sub>2</sub>O

The hyper-solvus nature of North Qôroq feldspars sets limits on the temperature and P.H<sub>2</sub>O of their formation, as beyond these limits, i.e. at lower temperatures or higher P.H<sub>2</sub>O, the intersection of solvus and solidus would have resulted in the separation of 2 feldspars. Maximum P.H<sub>2</sub>O and minimum temperatures have been obtained for other intrusions by a consideration of experimental data and feldspar composition (Parsons, 1965; Morse, 1969; Parsons, 1972; Parsons and Smith, 1974).

The first problem is the choice of suitable solvus and liquidus (and hence solidus) data. The solvus used is that determined by Smith and Parsons (1974) at 1 Kb. P.H<sub>2</sub>O. This solvus is in close agreement with that determined by Orville (1963), when a suitable pressure correction (16°/Kb.) is applied, and also with that of Thompson and Wauldbaum (1969), using data of Orville, and Luth and Tuttle (1966). Liquidus data was obtained for the Ab-Or system under varying P.H<sub>2</sub>O from Bowen and Tuttle (1958). These data, however, are only applicable to rocks lying on the feldspar divide in the residua system. For under-saturated rocks, liquidus data was taken from Hamilton and MacKenzie (op.cit.) for 1 Kb. P.H<sub>2</sub>O, and Morse for 5 Kb. P.H<sub>2</sub>O. The change in liquidus temperatures between these values was assumed to parallel the Ab-Or liquidus. The effect of increased pressure on the solvus is to raise it by 16°/Kb. approximately. Anorthite in the feldspars dramatically raises the solvus; Backinski and Müller (1971), from data of Morse, state that the solvus is raised by 33° C/mol.%An.

Hence data are available on the solvus at 1 Kb. P.H<sub>2</sub>O, and on the effect of pressure and Ca content on this solvus. Liquidus data appropriate to North Qôroq magmas are also known, together with variation of liquidus temperatures with changing P.H<sub>2</sub>O. It is possible to take the bulk

feldspar analyses and obtain a maximum temperature, below which two feldspars would form instead of the one observed. Using this temperature, a maximum value for the water pressure can be calculated, above which two feldspars would again form. The results obtained for various units are given in Table 4.

TABLE 4

<u>UNIT</u>	<u>T<sub>min.</sub> °C</u> <u>(nearest 5 °C)</u>	<u>P.H<sub>2</sub>O max. bars</u> <u>(nearest 100 bars)</u>
SN.1A(marginal)	745	2700
SN.1A(interior)	665	2200
SN.1B	625	5000
SN.2	835	1300
?SN.3	685	3200
SN.4A	820	1500
SN.4B	865	1000
SN.5	675	2200

The limiting values obtained for certain units are not particularly informative but for units SN.2, SN.4A and SN.4B high crystallization temperatures are indicated and relatively low values for P.H<sub>2</sub>O. Thompson and MacKenzie (1967) demonstrated that in late stage peralkaline rocks acmite lowers the liquidus slightly and sodium metasilicate more markedly. Alkali chlorides also produce a marked drop in liquidus temperatures. The effect of these

components, present in North Qôroq syenites, is ignored in the calculations, but they will serve to further lower  $P.H_2O$  max. This suggests that SN.4A feldspars, for example, were crystallized at temperatures in excess of  $865^{\circ}C$  and at a  $P.H_2O$  well below 1000 bars. These results are discussed further in the thermodynamics section (4.16.).

#### 4.7. Nepheline

##### 4.7.1. Introduction

Nepheline only occurs as a major phase in the more fractionated of the North Qôroq syenites. In marginal SN.1A, SN.2, SN.4A and SN.4B the nepheline is restricted to small interstitial patches, and is one of the last phases to crystallize. Moving into more fractionated parts of SN.1A and in unit SN.5, nepheline rapidly begins to constitute a greater proportion of the rock. Together with feldspar, it tends to be an early formed phase and occurs as large euhedral crystals. In these fractionated syenites the nepheline may be rimmed and partly replaced by cancrinite. The variation in nepheline paragenesis, from the least fractionated augite syenites to the highly fractionated late stage syenites, is comparable to that described by Upton (1964b) for the Hviddal composite dyke, and by Stephenson (1973) for South Qôroq syenites.

An interesting mode of nepheline occurrence is as blebs in alkali feldspar phenocrysts. This only occurs in the augite syenites and a similar phenomenon has been described by Widenfalk (1972) for Oslo larvikites. He suggests that these blebs are an exsolution feature, and that larvikitic feldspars can contain 13-14 mol.% nepheline in solid solution. Certainly, when considering all the North Qôroq feldspar analyses, there is a tendency for them to show a slight silica deficiency, indicating nepheline in solid solution. According to Widenfalk the nepheline 'exsolution process' is encouraged by Ca in the feldspars and indeed, feldspars from North Qôroq showing this property have relatively high Ca contents (up to 8 mol.% An). The nepheline blebs in a single feldspar are in optical continuity, suggesting exsolution, and against co-precipitation with feldspar is the fact that nepheline in the remainder of the slide is markedly interstitial and obviously formed after the feldspar.

Alteration of nepheline is common. In SN.1B it frequently alters to analcite containing parallel peg-like crystals of cancrinite. Alternatively, nepheline may alter to analcite containing small mica crystals orientated in two mutually perpendicular directions. The most common type of alteration is to 'gieseckite', where the nepheline

is partly or completely altered to a very fine-grained micaceous aggregate.

Probe analyses were obtained using a defocussed beam to prevent specimen decay, and analyses are tabulated in Appendix III.4.

#### 4.7.2. Chemical variation

Most natural nephelines, in equilibrium with alkali feldspar, have a limited quantity of silica in solid solution. Previous workers have tended to refer to this as 'excess silica', and plotted nepheline analyses in terms of the three end members, nepheline, kalsilite and 'excess silica'. North Qôroq nephelines are plotted in a similar fashion in Fig. 4.19. Hamilton and MacKenzie (1960) and Hamilton (1961) determined the extent of the nepheline-silica solid solution at 500, 700 and 775°C (P.H<sub>2</sub>O = 1 Kb.). These limits, together with the approximate limit at 1068°C, are also given in Fig. 4.19.

The amount of excess silica in nepheline has been used as an indication of temperature of formation. Barth (1963) points out that, to use this geothermometer, extremely accurate analyses are required, not only for SiO<sub>2</sub>, but for all elements. A further complication arises from post-crystallization re-equilibration. Tilley (1954) stated that plutonic nephelines re-equilibrated at sub-solidus temperatures and their compositions approached what

Fig.4.19 The variation shown by North Qoroq nepheline analyses in terms of the three end members, nepheline (Ne), kalsilite (Ks) and 'excess silica' ( $\text{SiO}_2$ ). The analyses taken from the more fractionated rocks are outlined and labelled as field 'A', whereas those from the less fractionated units, SN.4A and SN.4B, are outlined and labelled as field 'B'. Also marked on the figure are the limits of nepheline-silica solid solution at various temperatures (Hamilton and MacKenzie, 1960; Hamilton, 1961). M-B refers to the 'Morozewicz Buerger convergence field' (Tilley, 1954; see text).

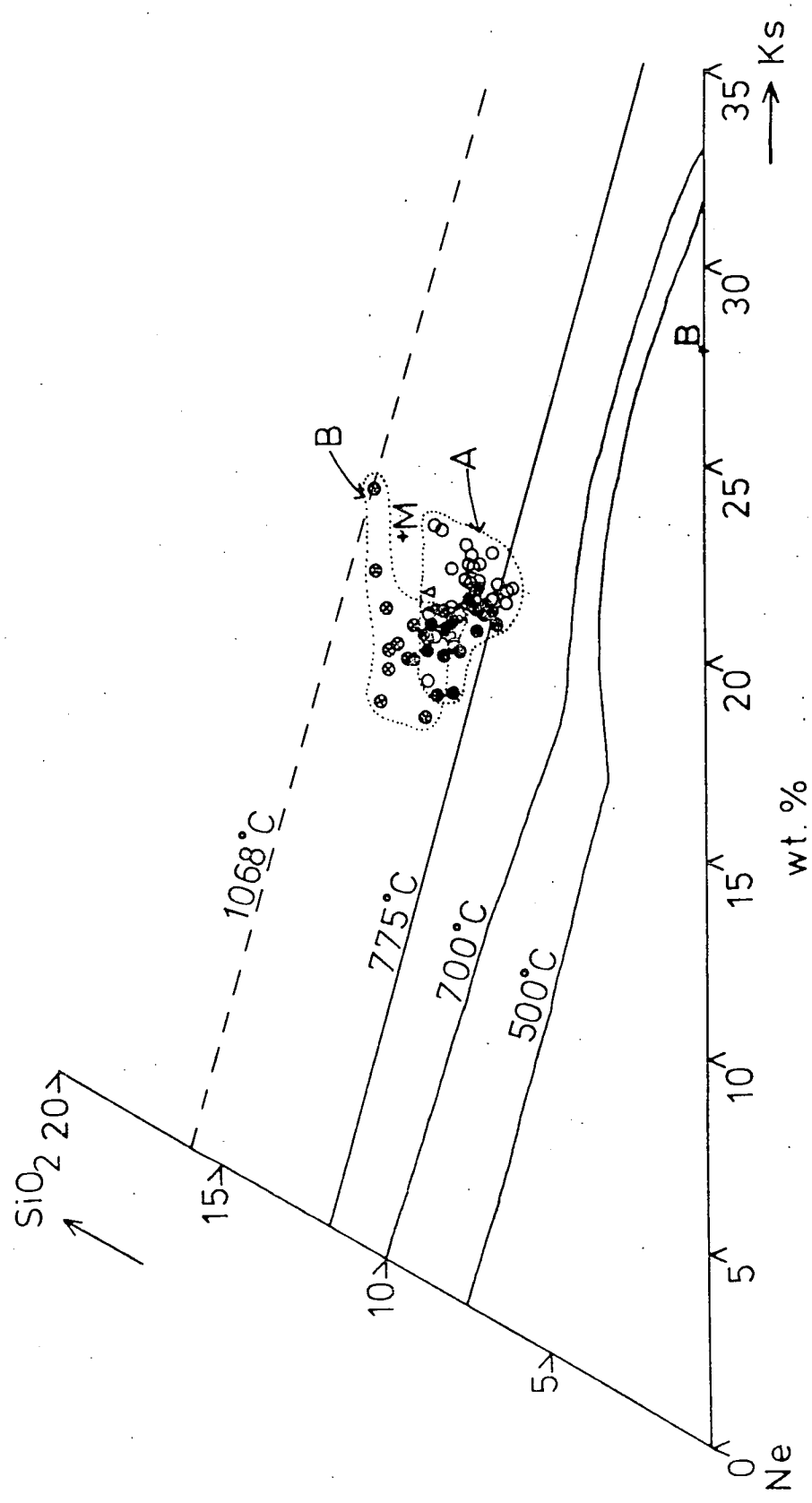
○ - SN. 1A

△ - SN. 1B

× - SN. 4A

⊗ - SN. 4B

● - SN. 5



he termed the 'Morozewicz-Buerger convergence field'. Tuttle and Smith (1958) suggested that at low temperatures the composition  $\text{Na}_3\text{KAl}_4\text{Si}_4\text{O}_{16}$  was a compound, and this was the ideal composition towards which nephelines re-equilibrated on cooling. Hamilton (op.cit.) proposed that nepheline might re-equilibrate with the magma by Al replacing Si and by alkali exchange, but that in the subsolidus condition the aluminosilicate framework could not be altered and re-equilibration was limited to Na/K exchange.

If Fig. 4.19 is examined with these factors in mind, a number of points emerge. Nephelines from the more fractionated rocks, outlined as field A, plot more towards the 'ideal composition' than those from units SN.4A and SN.4B, outlined as field B. This may indicate that nephelines in SN.4A and SN.4B did form at a higher temperature than those from the other units. Certainly, both these units give the appearance of being drier and hotter bodies of magma. Higher silica content, and the more sodic nature of SN.4A and SN.4B nephelines may, however, simply reflect more rapid cooling and less opportunity for re-equilibration. Much of the Na/K variation shown on the figure may be due to a degree of subsolidus exchange with feldspar. This is further indicated by rims of nepheline against feldspar, which tend to be more K-rich than either

nepheline cores, or rims against other minerals. The blebs of nepheline in the feldspars of SN.4A and SN.4B show little compositional variation from the normal groundmass nephelines.

The North Qôroq nephelines plot outside the Morozewicz-Buerger convergence field, as do those of South Qôroq and the Kangerdlugssuaq syenite (Kempe and Deer, 1970). This suggests minimal subsolidus re-equilibration particularly for SN.4A and SN.4B. If core analyses of nepheline are considered, this will minimise sub-solidus Na/K exchange with feldspar, and in the thermodynamics section compositions such as these have been used, together with those of co-existing feldspar, in a nepheline-feldspar geothermometer.

Nash et al. (1969) points out that sodalite co-precipitating with nepheline renders the nepheline geothermometer useless. Sodalite generally forms after nepheline in North Qôroq (although it may co-precipitate with groundmass nepheline and feldspar) and so this problem can be neglected. It is interesting to note that Stephenson (1973), analysing nephelines surrounded by sodalite from South Qôroq rocks, found them to have no 'excess silica', thus supporting the contention of Nash.

Two analyses were made of the patches of 'gieseckite' alteration occurring in many of the nephelines. These

reveal that K, Al and Si are virtually identical to that of the original nepheline, but that Na has been extensively removed, apparently being replaced by water.

Trace elements are virtually absent from the nephelines. Ca, as with most plutonic nephelines, is extremely low, averaging 0.12 wt.% CaO in the augite syenites and being effectively absent from the more fractionated rocks. The only other trace element occurring in any quantity is Fe which reaches 0.4-0.5 wt.% FeO in the augite syenites and 0.6-0.8 wt.% FeO in more fractionated rocks.

#### 4.8. Cancrinite

Cancrinite occurs only in the more fractionated rocks. It may rim and embay nepheline, or occur together with analcite in interstitial patches. In SN.1B it also occurs as peg-shaped lamellae in analcite, pseudomorphing original nepheline. It is a characteristic mineral of unit ?SN.3, where it occurs as a major phase, intensely embaying and replacing nepheline.

The presence of cancrinite suggests a late stage build up of CO<sub>2</sub> in the magma. This is further indicated by the presence of interstitial calcite, associated with cancrinite. Although nepheline is rimmed by cancrinite, no examples were found of the reaction sequence described by Saether (1957) of nepheline, rimmed by cancrinite,

which in turn is rimmed by calcite. Koster van Groos and Wyllie (1968) demonstrated the presence of a wide miscibility gap between silicate liquids and  $\text{Na}_2\text{CO}_3$  liquids. It is possible that cancrinite and calcite are indicative of the late stage formation of an immiscible carbonate liquid, due to steady build up of carbonate in the silicate magma. This separate carbonate liquid may have remained trapped, and crystallized in the interstices of the syenite.

Two analyses of cancrinite were made and are tabulated in Appendix III.4. Of the determined elements only Si, Al, Ca and Na were present in more than trace amounts. Although carbonate was not analysed for, the low concentration of S confirms that the mineral is close to end member cancrinite in the cancrinite-vishnevite solid solution series.

#### 4.9. Sodalite

Sodalite occurs interstitially in the vast majority of specimens. It is most easily recognised under ultraviolet light, where it fluoresces a vivid orange colour, probably due to the presence of small quantities of sulphide (Kirk, 1955). In the augite syenites it is a very minor phase, or even absent, whereas in more evolved

rocks, although still interstitial, it tends to form in large wedge shaped patches or, more rarely, to poikilitically enclose feldspar and nepheline.

The sodalite analyses, tabulated in Appendix III.4, are virtually identical to those obtained from South Qôroq. They correspond closely to the ideal formula  $\text{Na}_8 \text{Al}_6 \text{Si}_6 \text{O}_{24} \text{Cl}_2$ , and MgO, CaO, FeO and  $\text{K}_2\text{O}$  are present in only trace amounts. Cl reaches 7 wt.%, whereas S occurs in much smaller quantities, 0.15-0.35 wt.%. No differences in composition between units occur.

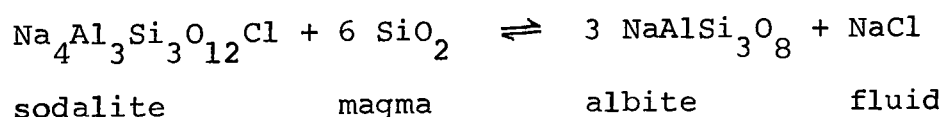
Wellman (1970) studied stability in the system Ab-Or-Ne-Ks-NaCl-KCl- $\text{H}_2\text{O}$ . This system, and his discussion of it, are applicable to North Qôroq rocks. He maintains that the abundance of Cl-rich fluid inclusions, and of sodalite, in syenites suggests that syenitic pore fluids are essentially alkali chlorides. All the late stage minerals in the North Qôroq syenites, with the exception of analcite (and natrolite - see later), are anhydrous, amphibole at this stage having been replaced by acmite. Wellman suggests that the crystallization of anhydrous phases from a hydrous melt must result in the evolution of an aqueous fluid. Even with analcite crystallizing, it would only be from very dry initial melts that an aqueous fluid would not evolve. The more fractionated of the North Qôroq syenites crystallized near the water

saturated minimum melting point in the undersaturated portion of residua system. The presence or absence of sodalite in this final assemblage, assuming for the moment vapour saturation, depends on the composition of the co-existing aqueous fluid, and hence the water and chloride content of the original magma. Wellman (op.cit.) shows that, if the fluid phase is sufficiently Cl-rich, sodalite may well crystallize together with nepheline and feldspar, as it appears to in the more fractionated North Qôroq rocks. Indeed, at  $P.H_2O \approx 1000$  bars the ratio  $H_2O/(H_2O + Cl)$  can be as high as 0.99 and sodalite will still crystallize.

Analcite occurs in many of the North Qôroq rocks. If sufficient water is incorporated to prevent the evolution of a separate aqueous fluid, there is a consequential build up of Cl in the melt, which again results in the formation of sodalite. If analcite merely delays the appearance of a co-existing aqueous fluid, this fluid when it evolves will be enriched in Cl relative to  $H_2O$ , because of the removal of  $H_2O$  by the analcite. This Cl-rich fluid will promote the crystallization of sodalite and may explain the occurrence of co-existing sodalite and analcite, as observed in North Qôroq rocks.

A significant effect of chloride phases is to depress the liquidus in the residua system (the value for the undersaturated minimum is  $660^{\circ}\text{C}$  at 2 Kb. P.H<sub>2</sub>O). As the feldspars of North Qôroq are hyper-solvus, this lowering of the liquidus further restricts the P.H<sub>2</sub>O at which the rocks evolved (see section 4.6.). For inner parts of SN.1A and unit SN.5, where this liquidus temperature is applicable, the maximum P.H<sub>2</sub>O permissible for hyper-solvus feldspars is lowered from around 2200 bars to 1600 bars.

Stormer and Carmichael (1971) determined the effect of the activity of silica ( $a.\text{SiO}_2$ ) on sodalite stability. From the reaction given below, it can be seen that low  $a.\text{SiO}_2$  favours the formation of sodalite, whereas high  $a.\text{SiO}_2$  favours the formation of albite, with Cl probably being expelled as part of a fluid phase:



Using this reaction, it was demonstrated that, in undersaturated liquids, sodalite may even precede nepheline in the crystallization sequence, depending on temperature and feldspar composition.

The presence of sodalite in North Qôroq rocks does not necessarily imply an unusually high Cl content in

the parent magma. Oversaturated magmas may have similar initial chloride contents, but, by virtue of the higher  $a_{\text{SiO}_2}$ , the Cl will be lost to the aqueous phase.

The possibilities of North Qôroq being an open system, with resultant escape of a Cl-rich aqueous fluid phase are discussed in Chapter 6.

#### 4.10. Analcite

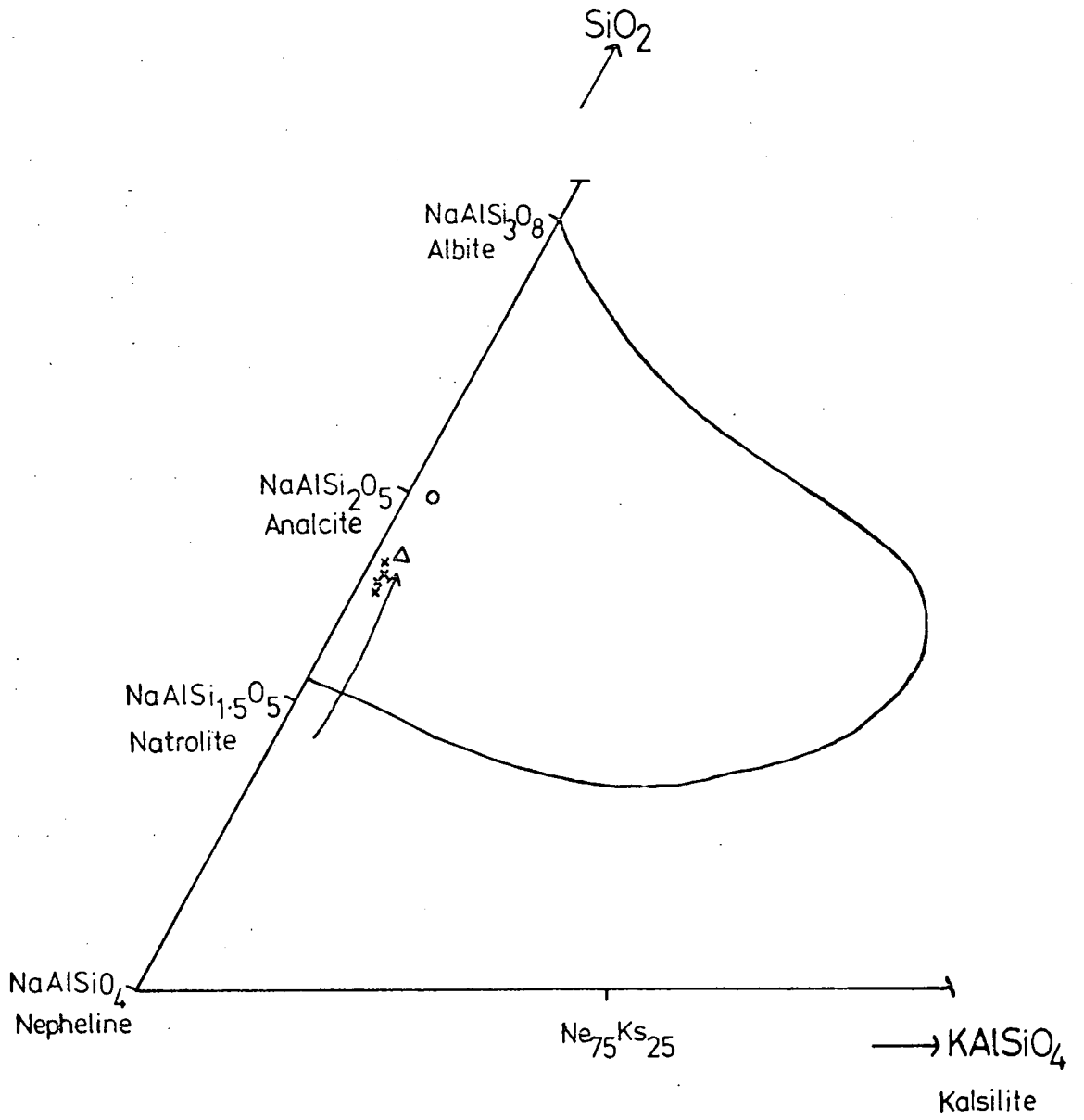
Analcite, like sodalite, is a common phase in the most highly fractionated syenites. It is interstitial and may be associated with cancrinite and sodalite. The analcite shows slight birefringence and irregular polysynthetic twinning. It resembles that described from the Hviddal composite dyke (Upton, 1964b) and from Ilímaussaq (Sørensen, 1962).

A small number of probe analyses were performed, and all show negligible quantities of minor elements. The analcites contain small quantities of K and are plotted in Fig. 4.20, the relevant portion of the residua system. Data from Ki-Tae Kim and Burley (1971) are also plotted, showing the thermal peak of the analcite stability field at an invariant pressure and temperature ( $\sim 5$  Kb. and  $635^{\circ}\text{C}$ ), and the thermal trough of the stability field ( $2-5$  Kb. and  $150^{\circ}-50^{\circ}\text{C}$ ). The compositional change for liquidus analcites during progressive fractionation is

Fig.4.20 North Qôroq analcite compositions plotted in the system nepheline-kalsilite-silica. Also shown are the limits of naturally occurring analcite compositions (curved line), the thermal peak and thermal trough of the analcite stability field according to Ki-Tae Kim and Burley (1971), and the compositional change for liquidus analcites (Wilkinson, 1965).

Symbols used:

- x - North Qôroq analcite analyses
- Δ - Thermal peak of analcite stability field
- o - Thermal trough of analcite stability field
- ↗ - Trend of Wilkinson



also shown (Wilkinson, 1965). It can be seen that the analcites analysed show a limited chemical variation and plot close to the quaternary invariant analcrite composition. As this is a thermal peak in the analcrite stability field, it suggests that little, if any, subsolidus adjustment in analcrite composition towards the thermal trough has taken place. Further analyses of analcites, from less fractionated North Qôroq syenites, may extend the analcrite compositions towards natrolite, so paralleling the trend of Wilkinson.

An extremely important point when considering analcrite is whether it is a primary magmatic phase, or of secondary origins. For analcites from North Qôroq the limited amount of K in solid solution is in keeping with that found from other supposedly primary analcites.

Experimental work by Peters et al. (1966) and Ki-Tae Kim and Burley (op.cit.), on analcrite stability in the system Ne-Ab-H<sub>2</sub>O, indicates that it only occurs on the liquidus over a very limited temperature range and at P.H<sub>2</sub>O > 5 Kb. Ki-Tae Kim and Burley state categorically that analcrite cannot crystallize directly from a melt below 5 Kb. North Qôroq rocks must have formed at pressures below 5 Kb. and yet analcrite does appear to be a primary phase. Wilkinson (1965), describing high level analcrite bearing rocks from New South Wales, comments that

'despite experimental studies, petrographic evidence suggests that the bulk of analcite is primary'. Peters et al. (op.cit.) also studied the effect of the addition of K to the system Ne-Ab-H<sub>2</sub>O, so bringing it closer to natural systems, and found that analcite and liquid could co-exist at much lower pressures (2.3 Kb. P.H<sub>2</sub>O). Platt and Rose-Hansen (1976), studying Ussingite stability in the peralcaline portions of the system Na<sub>2</sub>O-Al<sub>2</sub>O<sub>3</sub>-SiO<sub>2</sub>-H<sub>2</sub>O at 1 Kb. P.H<sub>2</sub>O, found that liquidus analcite could exist at this pressure over a wide temperature range. Certainly the highly fractionated North Qôroq syenites containing analcite are acmite, and occasionally sodium metasilicate (NaSiO<sub>3</sub>), normative, indicating a tendency towards peralkaline liquids with a high Na content. It is suggested that this tendency, and possibly the small K content of the magma, is responsible for lowering dramatically the minimum pressure at which analcite can exist as a liquidus phase. Hence, North Qôroq analcites, and those from many other high level undersaturated peralkaline plutons, are of primary magmatic origins.

#### 4.11. Natrolite

As described in the petrography section, natrolite tends to show an antipathetic relationship to analcite, and to vein the syenites in a diffuse fashion. Natrolite

is only stable at relatively low temperatures and the pervasive nature of the mineral in North Qôroq syenites suggests a secondary origin. The natrolite may result from a breakdown of nepheline and/or analcite, possibly aided by a late stage aqueous fluid. An X.R.D. investigation on the common, irregular, brick-red areas in the more fractionated syenites, showed them to be composed of a mixture of natrolite and nepheline-hydrate, again suggesting patchy breakdown of pre-existing aluminosilicates. No probe analyses were performed on the natrolite, but its presence was confirmed, both optically and by X.R.D. techniques.

#### 4.12. Aenigmatite

Aenigmatite is not common in North Qôroq rocks, but it is a significant mineral in two types of environment. Almost opaque aenigmatite occurs in the most highly fractionated rocks of SN.1A and SN.5, where Fe/Ti oxides are rare or absent. The second paragenesis is where aenigmatite, showing deep red to black pleochroism, occurs, together with sodic pyroxene and sodic amphibole, as the mafic phase in recrystallized rocks. Again, Fe/Ti oxides are usually absent, but occasionally aenigmatite can be found rimming Fe/Ti oxides and replacing them, particularly

the ilmenite lamellae. The textures and mineralogical changes in these rocks are discussed in the petrography chapter.

Probe analyses reveal that the aenigmatites from both types of environment are Ti-rich, but show small degrees of substitution of  $\text{Fe}^{3+}$  for Ti. They correspond chemically to those reported from Mt. Suswa (Nash et al. op.cit.). Approximately 1 wt.%  $\text{Al}_2\text{O}_3$  was present in all analyses together with trace amounts of Mg, Ca and K. Mn is the principle minor element and shows significant variation between the two parageneses. MnO content is low in the highly fractionated rocks (0.25 wt.% approx.), whereas in aenigmatites from the recrystallized rocks it forms 1.65-2.00 wt.%. This high Mn value is almost certainly a function of the recrystallized aenigmatites being formed from pre-existing Fe/Ti oxides rich in Mn, whereas primary aenigmatite formed from a Mn-depleted melt.

Much discussion has ensued over recent years as to what magmatic conditions favour the formation of aenigmatite. Ernst (1962), working on amphibole stability fields, encountered Ti-free aenigmatite only at very low oxygen fugacities ( $f.\text{O}_2$ ). Kelsey and McKie (1964) and Abbot (1967) concluded from this that aenigmatite in

general was stable only under conditions of low  $f.O_2$ . Lindsley (1971), however, synthesised Ti-bearing aenigmatite at an  $f.O_2$  appropriate to the quartz-fayalite-magnetite buffer (F.M.Q.), where it was apparently stable, but concluded that it was probably metastable at an  $f.O_2$  appropriate to the Ni-NiO buffer, with respect to the more oxidized assemblage acmite and Fe/Ti oxides.

Nicholls and Carmichael (1969) calculated that aenigmatite may be stable at an  $f.O_2$  well above Ni-NiO, but they admit that the calculated stability field is subject to considerable error. It appears that, although aenigmatite will not crystallize under conditions of high  $f.O_2$ , other factors are more crucial to its formation. In both North Qôroq rocks and elsewhere, aenigmatite is characteristically accompanied by sodic pyroxene and/or sodic amphibole.

Nicholls and Carmichael (op.cit.) and Hodges and Barker (1974) both suggest that aenigmatite forms in response to the peralkaline condition which the former two workers equate with the activity of sodium disilicate ( $Na_2Si_2O_5$ ) in the liquid. The implications of this are discussed in the thermodynamics section.

The absence or rarity of Fe/Ti oxides occurring with aenigmatite supports the existence of a 'no-oxide field', proposed for oversaturated rocks by Nicholls and Carmichael

(op.cit.), and extended to undersaturated rocks by Marsh (1975). The former two authors suggest termination of the no-oxide field by the stability field of riebeckite-arfvedsonite solid solutions (Ernst, op.cit.). The association aenigmatite  $\pm$  acmite  $\pm$  alkali amphibole in the recrystallized rocks of North Qôroq suggests that  $f.O_2$  and temperature conditions were close to those appropriate to the boundary between the amphibole stability field and that of aenigmatite-acmite.

#### 4.13. Rinkite

The occurrence of this rare mineral was discussed at the end of the petrography chapter. It was noted that only in recrystallized rocks was rinkite found as distinct, identifiable crystals, but that in normal syenites probe traverses across grain boundaries suggested the presence of submicroscopic rinkite grains. These grains look to have been mobilised by later intrusions and to have formed a band of identifiable rinkite a short distance from the margins of the new intrusion.

Rinkite from North Qôroq corresponds in optical properties to the description given by Wenschell (1951) and to that given by Sørensen (1962). Partial probe analyses confirmed that the mineral is a member of the rinkite family. Trace elements were not analysed for

quantitatively, but qualitative inspection showed appreciable quantities of Nb, Y and La. The rinkite differed from that found in the naujaite pegmatites of Qeqertaussaq (Ilímaussaq) in having lower concentrations of Ti, but higher concentrations of Zr, probably substituting for Ti.

#### 4.14. Other mineral phases

Of the major phases constituting the North Qôroq Centre, only apatite was not analysed. This mineral may repay investigation, as it could help to determine the behaviour of F and Cl in the magma (Ebström, 1973). The only analysed minor phase not so far mentioned, is a secondary zeolite found in association with natrolite. It proved to be thompsonite, a mineral thought to be a late stage phase in the Hviddal composite dyke (Upton, 1964b).

#### 4.15. Conclusions from the mineralogy

Analyses of the major mineral phases occurring in the North Qôroq rocks clearly support the conclusions, recorded in the petrography chapter, that there is a considerable mineralogical variation both in and between the major units. Pyroxenes and amphiboles in particular show an extensive amount of chemical variation. The Al

content of the amphiboles, biotites and Fe/Ti oxides of units SN.2 and ?SN.3 clearly differentiate them from the other major units.

The considerable intra-unit variation suggests a degree of in situ crystal fractionation, particularly noticeable in SN.1A. Here, there must have been a considerable temperature interval between initial crystallization and final crystallization of the most highly fractionated parts of the unit. Rocks showing early crystallization of olivine, pyroxene, and Fe/Ti oxides followed by biotite, amphibole, alkali feldspar and then nepheline are common in alkali provinces. The last formed, highly fractionated rocks of North Qôroq, composed of considerable quantities of cancrinite, sodalite, analcite, natrolite and acmite are, however, much more rare. The phase relations appropriate to such rocks are hard to predict, although the effects of  $\text{Na}_2\text{CO}_3$  and NaCl on the residua system have been investigated and are discussed in the text. The presence of large numbers of these constituents must result in complex relationships which would, perhaps, repay further experimental investigation. Certainly the solidus temperatures in such rocks must be extremely low, and the distinction between primary mineralogical features and secondary ones becomes a blurred one,

especially with regard to the aluminosilicates.

At times during the mineralogical descriptions a thermodynamic approach has been employed, mainly in a qualitative sense. In the following section an attempt is made to quantify the conditions and parameters affecting formation of North Qôroq rocks, using thermodynamic principles established by previous workers.

#### 4.16. Thermodynamic treatment of mineral data

##### 4.16.1. Introduction

Increasingly in recent years, thermodynamic techniques have been applied to geological data. This has enabled values to be obtained for the pressure and temperature of various geological environments, and an evaluation of the behaviour of important magma components, particularly volatile ones. At the present stage many more basic thermodynamic data need to be obtained, relevant to mineral species, and many existing data require updating. As this work proceeds, a thermodynamic approach will become increasingly important in geology.

The technique employed in the present account is to apply established thermodynamically-based methods to North Qôroq mineral assemblages and to establish something of the conditions of formation and evolution of

the nepheline syenites. Reactions used in the following account involve components of the observed phases, a component being defined as 'a chemical unit which can be added to, or subtracted from, a phase without destroying that phase'. These reactions should not be confused with reactions, such as those given in Chapter III, which attempt to reproduce mineralogical changes due to processes such as metamorphism.

A basic assumption is that the mineral assemblages considered were in a state of stable or metastable equilibrium at the time of formation and that little or no re-equilibration has taken place. Petrographic evidence has been widely used in establishing probable equilibrium assemblages.

The first stage in the thermodynamic treatment of mineral data is to write a balanced equation involving components of phases thought to reflect an equilibrium assemblage. To illustrate this consider the reaction



For this reaction

$$K = \frac{(a_C)^2}{(a_A)(a_B)}$$

where  $K$  is the equilibrium constant for the reaction and  $a$  is the activity of the component in its host phase. The activity of a component can be expressed as a function of the mole fraction  $X$  of that component and the activity coefficient  $\gamma$  such that

$$a_A = X_A \cdot \gamma_A$$

Hence, for the above reaction

$$K = \frac{(X_C)^2}{(X_A)(X_B)} \cdot \frac{(\gamma_C)^2}{(\gamma_A)(\gamma_B)}$$

Considering also the relationship

$$\Delta G = \Delta G_r^{\circ} + RT \ln K$$

where  $\Delta G_r^{\circ}$  is the standard Gibbs free energy change of the reaction,  $T$  is the temperature in  $^{\circ}\text{K}$  and  $R$  the gas constant. At equilibrium  $\Delta G = 0$ , hence

$$-\Delta G_r^{\circ} = RT \ln K = RT \ln \frac{(a_C)^2}{(a_A)(a_B)}$$

This relationship is the basis for the majority of thermodynamic calculations.

At fixed  $P, T$  it is possible to solve for chemical parameters, e.g. activity of silica in the liquid ( $a_{\text{SiO}_2}$ ),

if  $\Delta G_r^{\circ}$  and  $K$  are known. If the necessary chemical parameters are known, it is possible to solve for  $P$  or  $T$ . Many of the basic thermodata can be found tabulated (Robie and Wauldbaum, 1968; Kelley, 1960) and  $\Delta G_r^{\circ}$  values can be obtained. It remains for the equilibrium constants, i.e. activity coefficients and mole fractions of the relevant components, to be calculated. In this account the example of previous workers has been followed and an ideal solution model has been employed, unless more suitable models are available. For an ideal solution, the activity coefficient,  $\gamma$ , equals 1 and activity is thus equal to the mole fraction. In reality few solid solutions are ideal except at extreme dilution. The presence of a solvus, such as is found in the alkali feldspar, pyroxene and Fe/Ti oxide solid solution series, or of intermediate compounds at low temperature are a clear indication of non-ideality. To obtain the mole fractions of various components from chemical analyses, it is necessary to make assumptions regarding site occupancies. For the mineral phases used in this section, a reasonable estimate of the site occupancy of individual elements can be arrived at.

In the following sections pressure and temperature of formation are the first parameters to be obtained. Using these values, the behaviour of the other components

during fractionation is discussed in terms of their activities and fugacities.

#### 4.16.2. Lithostatic pressure ( $\approx P_T$ )

The North Qôroq Centre syenites are high level intrusive bodies. This can be stated with confidence because the centre cuts the Eriksfjord formation basalts and sandstones, which have a maximum recorded thickness in the area of 3000 m. If it is assumed that the centre was capped by an equivalent thickness of sediments and basalts at the time of intrusion, this suggests a lithostatic pressure of approximately 1000 bars.

From feldspar solvus-solidus relationships, it was seen that, for the highly fractionated one-feldspar syenites, water pressure ( $P_{H_2O}$ ) could not exceed 1600 bars. If  $P_{H_2O}$  equalled total pressure ( $P_T$ ) at a late stage in the evolution of the syenites, the hypersolvus nature of the feldspars suggests an upper limit for  $P_T$  of 1600 bars.

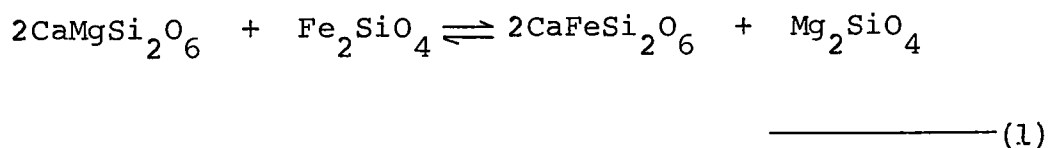
The presence of analcite in these rocks, as has previously been indicated (section 4.10) in no way restricts the total pressure.

Both field relations and feldspar considerations suggest that use of a value for  $P$  of 1000 bars would not result in any gross errors in subsequent calculations.

#### 4.16.3. Temperature (T.).

The absence of ilmenite as a separate distinct phase in North Qôroq syenites means that the Fe/Ti oxide geothermometer of Buddington and Lindsley (1964) cannot be directly applied. The minerals present do, however, allow the application of alternative geothermometers.

The first phases to crystallize in the least fractionated syenites were augitic pyroxene, olivine, and titanomagnetite. Powell and Powell (1974) used the Fe-Mg exchange reaction between olivine and Ca-rich clinopyroxene to formulate a geothermometer. The relevant reaction is



In the absence of more definite data, olivine mixing properties were assumed to be ideal. Pyroxene cations were allocated to sites, following a scheme that is independent of the unreliable silica analysis. The mixing properties of Ca-rich clinopyroxene were shown to be non-ideal, and a regular solution model implemented. The mixing parameters were calculated for a set of groundmass olivine/clinopyroxene pairs, from lavas with groundmass Fe/Ti oxide temperatures. The pressure dependence of the geothermometer is approximately  $5^\circ/\text{Kb}$ . The geothermometer can be

expressed as

$$T = \frac{-2X_{Al} (920000 + 3.6P) - 0.0435 (P-1) + 10100}{8 + 2R \ln \frac{X_{Mg,Ol}}{X_{Fe,Ol}} \frac{X_{Fe,Ml}}{X_{Mg,Ml}} - 714.3 (2X_{Al})} \quad \text{—————(1B)}$$

where T = temperature ( $^{\circ}$ K)    P = pressure (bars)

$X_{A,B}$  = mole fraction of A in B

$X_{Al}^A = X_{Al} + X_{Ti} + X_{Cr} + X_{Fe^{3+}}$  (all on Ml site)

The geothermometer has only been used, and is only applicable, where the Na content of the pyroxenes is low (< 0.8wt.%Na<sub>2</sub>O). A number of probe analyses of co-existing olivines and pyroxenes, from marginal SN.1A, SN.4A and SN.4B, have been used to determine temperatures and these results are given in Table 3. Where data allow, each result represents the average of several olivine/clino-pyroxene pairs.

A second geothermometer used, is based on the composition of co-existing feldspar and nepheline, a paragenesis common in North Qôroq rocks. Perchuk and Ryabchikov (1968) considered the exchange reaction



—————(2)

They derived isotherms for the distribution of Na components between nepheline and alkali feldspar. Both 'excess silica' in the nepheline, and anorthite in the nepheline and feldspar, were assumed not to affect the calculated equilibrium temperature. Powell and Powell (in press) produced a refinement of the geothermometer and it is this refined version that is used in the present account. They considered an exchange reaction involving only the Na-site in the nepheline and adopted regular solution models for the alkali sites. They included the effect of 'excess silica' and, for different values of 'excess silica', produced graphs of mole fraction kalsilite in the nepheline against mole fraction albite in the feldspar, contoured in temperature. This geothermometer is effectively independent of pressure. Using core analyses of co-existing feldspars and nepheline for inner SN.1A, SN.1B, SN.4A, SN.4B and SN.5 temperatures were calculated and the results are given in Table 3, alongside those of the olivine/clinopyroxene geothermometer.

Also, in this table are included minimum temperature values obtained both from the feldspar solvus-solidus relationships (see section 4.6.) and from the bulk Fe/Ti

oxide analyses. Buddington and Lindsley's work (op.cit.) on Fe/Ti oxides sets a minimum temperature, below which a given titanomagnetite would have ilmenite co-existing with it (Simmons, Lindsley and Papike, 1974). A separate estimate of oxygen fugacity ( $f.O_2$ ) must be available, and the values used are justified in a following section.

A number of conclusions can be drawn from the temperature values given in Table 3.

It can be seen that frequently temperatures from olivine/clinopyroxene and feldspar/nepheline geothermometers are not available from the same sample. This is merely because only the least fractionated rocks contain olivine and clinopyroxene, and in these rocks nepheline is either absent or interstitial. In more fractionated rocks, where feldspar and nepheline are abundant, olivine is absent.

One of the most obvious points of interest is the large temperature interval between the value obtained from the olivine/clinopyroxene geothermometer ( $\sim 900^\circ\text{C}$ ) and that obtained from the feldspar/nepheline geothermometer ( $\sim 730^\circ\text{C}$ ). The difference is an expected one, in that the olivine/clinopyroxene equilibrium assemblage is the first to crystallize from the least fractionated augite syenites, whereas the feldspar/nepheline equilibrium

assemblage is the last to crystallize from these rocks, and only occurs as an early-forming assemblage in more fractionated, lower temperature rocks. Hence, the olivine/clinopyroxene assemblage could be interpreted as giving a near liquidus temperature and the feldspar/nepheline assemblage a near solidus temperature for the augite syenites. Comparison with melting experiments on undersaturated alkaline rocks (Sood and Edgar, 1970; Piotrowski and Edgar, 1970) reveals that the olivine/clinopyroxene temperatures are typical of liquidus temperatures for these rocks, at P.H<sub>2</sub>O in excess of 300 bars, and feldspar/nepheline temperatures are just below solidus temperatures. The temperature difference is perhaps a reflection of the large crystallization interval (solidus-liquidus) of these syenitic rocks. Both geothermometer assemblages may well have suffered some re-equilibration and this may account for the low, possibly subsolidus temperatures indicated by feldspar/nepheline.

Recrystallized rocks show slightly lower olivine/clinopyroxene temperatures, indicating subsolidus readjustment during the metamorphic event.

Ignoring recrystallized rocks and temperatures obtained from nepheline blebs in feldspar, a slight temperature difference can be seen, for both geothermometer

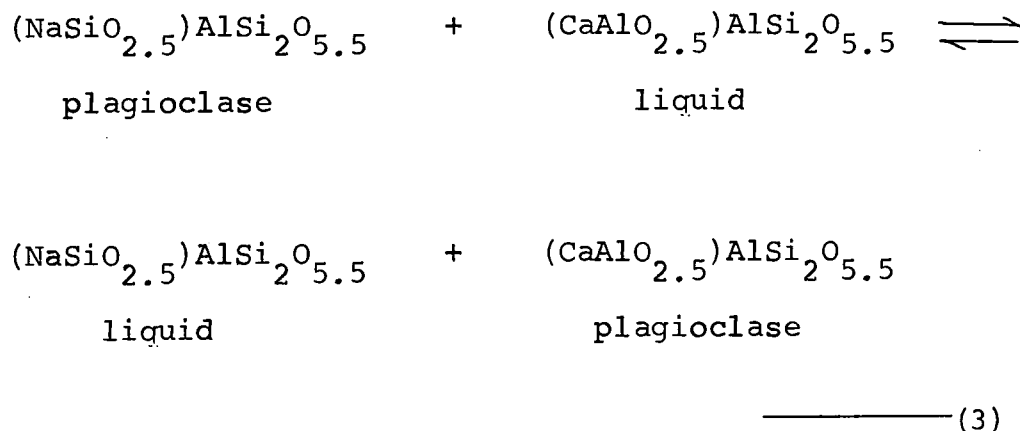
values, between the higher temperatures of the SN.4 units and the lower ones of SN.1A and SN.5. This is in keeping with petrographic observations, that both SN.4 units are the result of drier and slightly hotter magma influxes.

Fe/Ti oxides crystallize as an early phase, but also occur in more fractionated rocks. A range in minimum temperature values, using the Buddington and Lindsley geothermometer, is to be expected, the highest temperatures occurring in the least fractionated rocks and approximating to the olivine/clinopyroxene temperatures. The minimum temperature values tabulated do not contradict this.

It is noticeable that feldspar temperatures, based on the interval between solvus and solidus, are often much higher than those obtained from the feldspar/nepheline geothermometer. This is reasonable, as the higher temperature feldspars are Ca-rich, forming, petrographic evidence indicates, well before nepheline.

At this point it is worthwhile considering the partially resorbed plagioclase phenocrysts found in units SN.2, SN.4A and SN.4B and discussed in section 4.6. It is possible to apply the Kudo-Weill plagioclase geothermometer (Kudo and Weill, 1970) to these feldspars, providing a good indication of the composition of the co-existing liquid can be obtained. Sample 155152 is

taken from the chilled margins of unit SN.4A. It contains sporadic plagioclase phenocrysts in a very fine grained groundmass that should approximate to a liquid. The geothermometer is based on the reaction



Regular solution models were assumed for the activities of species in the liquid and ideal mixing models for high temperature plagioclase. Kudo and Weill give a series of equations relating T at a given P.H<sub>2</sub>O to composition of plagioclase and co-existing liquid.

$$2.303 \log \lambda/\sigma + 1.29 \times 10^{-4} \phi'/T = 10.34 \times 10^{-3} T - 17.24 \quad (\text{Dry})$$

$$2.303 \log \lambda/\sigma + 1.29 \times 10^{-4} \phi'/T = 11.05 \times 10^{-3} T - 17.86 \quad (\text{P.H}_2\text{O} = 0.5\text{Kb})$$

$$2.303 \log \lambda/\sigma + 1.29 \times 10^{-4} \phi'/T = 11.14 \times 10^{-3} T - 17.67 \quad (\text{P.H}_2\text{O} = 1.0\text{Kb})$$

$$\text{where } \lambda = (\text{XNa}_2\text{O} \cdot \text{XSiO}_2) / (\text{XCaO} \cdot \text{XAl}_2\text{O}_3)$$

(i.e. mole fraction oxide components in the liquid)

Unit	p.No.	Olivine/ clinopyroxene		Feldspar/ nepheline		Feldspar/ solvus/solidus		Fe/Ti oxides	
		Sp. T. C-30	Average for unit	Sp. T. C-35	Average for unit	Sp. T. C-30	Average for unit	Sp. T. C-35	Average for unit
SN.1A	46297	907	-	-	724	745	-	880	-
marginal	52218	920	891	-	724	745	-	880	-
	52221	879	-	-	724	745	-	880	-
	155088	859	724	724	724	745	-	880	-
SN.1A	52246	-	714	714	723	665	-	-	-
interior	59751	-	725	725	723	665	-	-	-
	155005	-	724	724	723	665	-	-	-
	155095	-	727	727	723	625	-	-	-
SN.1B	155108	-	723	723	723	625	-	-	-
SN.2	-	-	-	-	-	835	-	-	-
?SN.3	-	-	-	-	-	685	-	-	-
SN.4A	59795	917	920	-	-	820	-	860	-
	59800	922	920	719*	-	820	-	860	-
	54193	-	-	714*	-	820	-	860	-
	59758	883	-	-	-	820	-	860	-
	59787	-	764	764	-	820	-	860	-
	59788 <sup>R</sup>	856	738	738	739	865	870	870	870
	59794 <sup>R</sup>	858	716	716	739	865	870	870	870
SN.4B	155075 <sup>R</sup>	887	906	-	-	865	870	870	870
	155114	904	-	722*	-	865	870	870	870
	155150	-	-	726*	-	865	870	870	870
	155152	931	-	-	-	865	870	870	870
	54187	-	708	708	-	865	870	870	870
	54226	-	728	728	722	675	-	-	-
SN.5	155069	-	724	724	722	675	-	-	-
	155159	-	726	726	722	675	-	-	-

TABLE 3

R=recrystallized rocks  
 \*=nepheline blebs in  
 feldspar (?exsolution)

$\sigma = X_{Ab}/X_{An}$  (i.e. mole fraction Albite and Anorthite in the feldspar)

$\phi' = (X_{CaO} + X_{Al_2O_3} - X_{Na_2O} - X_{SiO_2})$

and  $T =$  temperature ( $^{\circ}K$ )

The temperatures obtained for the plagioclase/liquid equilibrium of sample 155152 are

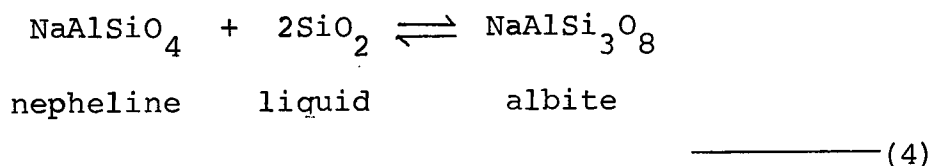
$P.H_2O = 0$ Kb (Dry)	—————	$949^{\circ}C$
$P.H_2O = 0.5$ Kb	—————	$909^{\circ}C$
$P.H_2O = 1.0$ Kb	—————	$860^{\circ}C$

These values, particularly those for  $P.H_2O = 0$  Kb and  $P.H_2O = 0.5$  Kb are in good agreement with that obtained from olivine/clinopyroxene in this sample ( $931^{\circ}C$ ), assuming total pressure has a negligible affect (neither geothermometer is sensitive to  $P.T$ ). Further discussion of these values is deferred until the section on  $P.H_2O$ .

#### 4.16.4. Activity of silica in the magma ( $a.SiO_2$ )

Silica activity can be thought of as the effective concentration of silica in the liquid. Carmichael *et al.* (1970) demonstrated that  $a.SiO_2$  can be buffered, or fixed, by various equilibrium mineral assemblages. A knowledge of  $a.SiO_2$  in North Qôroq rocks, apart from its intrinsic interest, enables oxygen fugacities to be calculated.

The vast majority of North Qôroq syenites contain nepheline and alkali feldspar. Crystallization of this assemblage resulted in  $a_{\text{SiO}_2}$  being fixed. Any addition of silica to the magma would merely have resulted in the formation of more feldspar, at the expense of nepheline, and vice versa. The reaction is



For this reaction, applied to the natural assemblage

$$2\log a_{\text{SiO}_2} = \frac{\Delta G_r^\circ}{2.303RT} + \log a_{\text{NaAlSi}_3\text{O}_8}^{\text{feldspar}} - \log a_{\text{NaAlSiO}_4}^{\text{nepheline}}$$

----- (4B)

where  $a_{\text{NaAlSi}_3\text{O}_8}^{\text{feldspar}}$  refers to the activity of the albite component in the feldspar, and  $a_{\text{NaAlSiO}_4}^{\text{nepheline}}$  the activity of  $\text{NaAlSiO}_4$  in the nepheline. Other symbols are as previously defined. From Nicholls et al. (1971)

$$\frac{\Delta G_r^\circ}{2.303RT} = \frac{-1742}{T} + 0.062 - \frac{0.0216(P-1)}{T}$$

Activities for the albite component were obtained from Carmichael et al. (1974). For nepheline a simple Na-K mixing model was employed, ignoring 'excess silica'.

The  $a.\text{SiO}_2$  values obtained, at 1000 bars pressure, are plotted in Fig. 4.21, against temperatures obtained from the feldspar/nepheline geothermometer. The values can be seen to lie fractionally above those defined by the pure albite/nepheline buffer, apart from two recrystallized rocks of SN.1A which plot distinctly below the buffer. This indicates that during the recrystallization process  $a.\text{SiO}_2$  was not defined in the same fashion as for magmatic processes and that the metasomatising fluid had a lower  $a.\text{SiO}_2$  than the magma.

Although nepheline and feldspar are present in the vast majority of syenites,  $a.\text{SiO}_2$  in the early stages of crystallization, when nepheline and albite were merely components in the liquid, can not easily be established. Reactions between fayalite and clinopyroxene are not suitable, because of the small or non-existent ferrosilite component in the Ca-rich clinopyroxene. Stormer (1973) suggested that the Ca-olivine component in the olivine is a function of  $a.\text{SiO}_2$  and considered the following two reactions

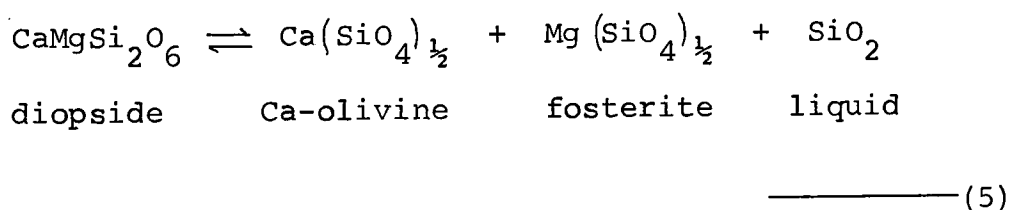
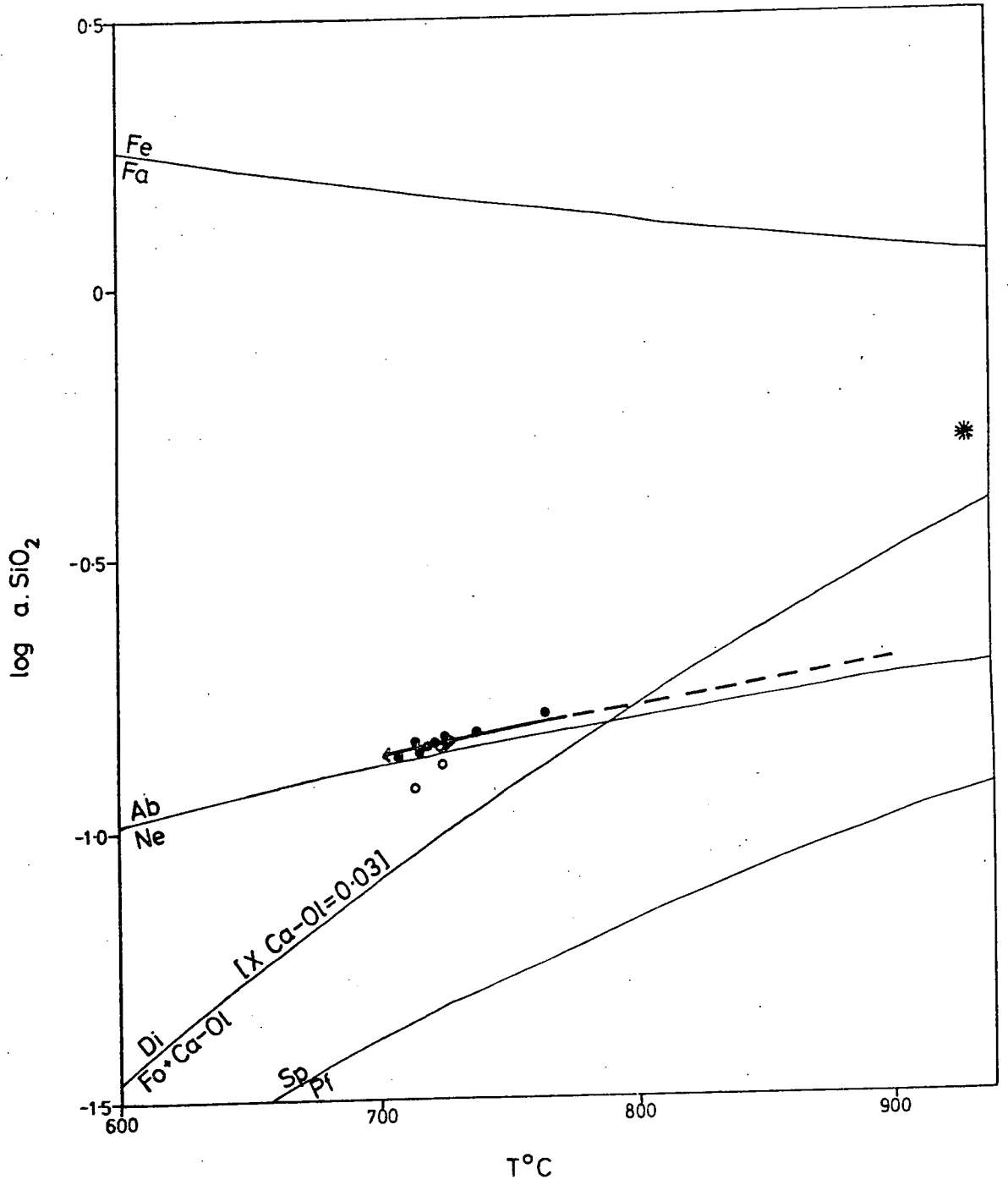
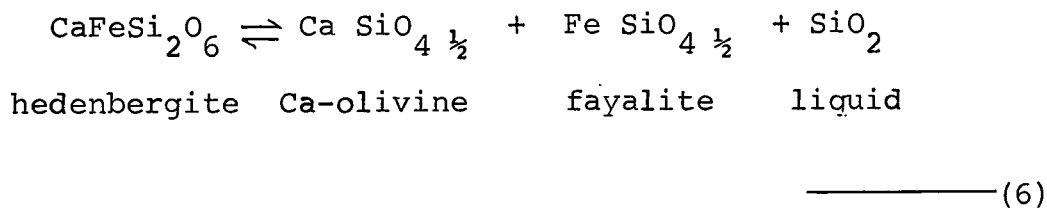


Fig.4.21 The variation of silica activity ( $a_{\text{SiO}_2}$ ) with temperature for North Qôroq rocks.<sup>2</sup> The solid arrowed line represents the  $a_{\text{SiO}_2}$  variation defined by the assemblage nepheline + feldspar and the dashed portion of this line, the probable  $a_{\text{SiO}_2}$  variation at higher temperatures, prior to the crystallization of this assemblage (see text). The ferrosilite/fayalite, albite/nepheline and sphene/perovskite buffer curves are also marked on the diagram, together with the buffer curve for the diopside/fosterite/Ca-olivine reaction (Stormer, 1973). For this line, a value for the mole fraction Ca-olivine in the olivine of 0.03 was chosen, a suitable value for North Qôroq olivines. A maximum value for  $a_{\text{SiO}_2}$  at higher temperatures is indicated by a star (see text).

Symbols used:

- -  $a_{\text{SiO}_2}$  values for normal North Qoroq syenites, calculated from the assemblage nepheline + feldspar.
- -  $a_{\text{SiO}_2}$  values for metasomatised syenites.
- \* - A maximum value for  $a_{\text{SiO}_2}$  at high temperatures.

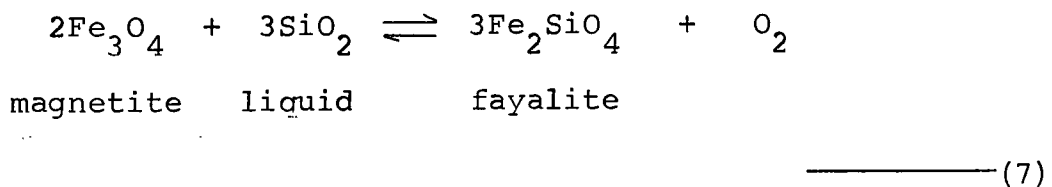




These two reactions may be of use in defining  $a.\text{SiO}_2$ . The most appropriate for the Fe-rich North Qôroq syenites is reaction (6), but unfortunately no reliable thermodata exist for hedenbergite. Thermodata do exist for all phases in reaction (5). Stormer (op.cit.) suggests that, when solving for  $a.\text{SiO}_2$ , at a particular temperature, activity terms for fosterite and diopside cancel and  $a.\text{SiO}_2$  is essentially a function of  $a.\text{Ca-olivine}$  in the olivine. Adopting this suggestion, the silica activity line appropriate to 0.03 mole fraction Ca-olivine, a suitable value for North Qôroq olivines, is reproduced in Fig.4.21. At an appropriate temperature for the early formed syenites, the  $a.\text{SiO}_2$  can be seen to lie just above albite/nepheline. Unfortunately, in North Qôroq syenites, the activity of diopside in the pyroxene exceeds the activity of fosterite in the olivine, and the mole fraction of all three of the crystalline components is small. The reaction, therefore, can not be used to define  $a.\text{SiO}_2$  with any accuracy. Also, as indicated in section 4.1, the Ca content of the olivine may be strongly pressure dependent, and compositions of ground-mass olivines and pyroxenes would need to be used.

The presence of almost pure fayalite, with ferrosilite being a component in the liquid, requires  $a.\text{SiO}_2$  to lie below the fayalite/ferrosilite silica buffer. Likewise, the occasional presence of sphene, with perovskite being a component in the liquid, requires  $a.\text{SiO}_2$  to lie above the sphene/perovskite silica buffer. Both these buffers are given in Fig. 4.21.

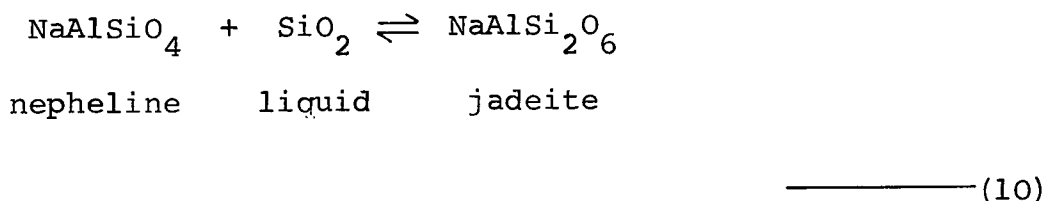
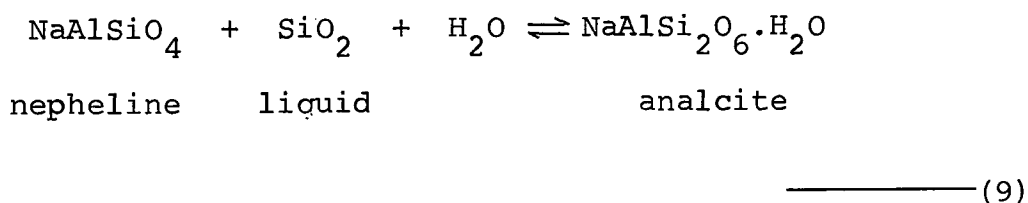
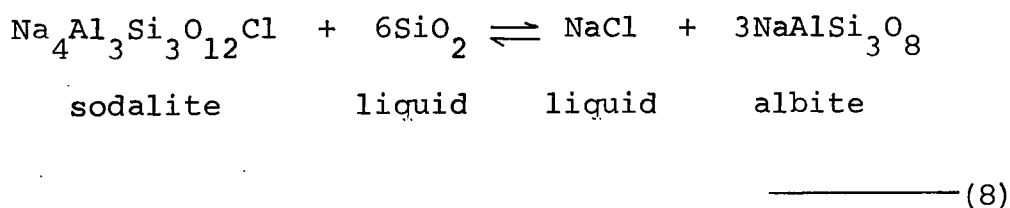
If the fugacity of oxygen were known,  $a.\text{SiO}_2$  could be calculated using the FMQ buffer reaction



The mole fraction ulvöspinel in one bulk Fe/Ti oxide, coupled with an olivine/clinopyroxene temperature, suggests a maximum value for  $\log f.\text{O}_2$  of -13.5. Applying this value in reaction (7) gives a maximum value for  $\log a.\text{SiO}_2$  of -0.29 at  $930^\circ\text{C}$ . This value is indicated by a star in Fig. 4.21, and further restricts the possible range of  $\log a.\text{SiO}_2$  in these rocks. It seems reasonable that, even before feldspar and nepheline crystallized,  $a.\text{SiO}_2$  was in the region of the albite/nepheline buffer. Parsons (personal communication) has determined the probable value for  $a.\text{SiO}_2$  in an alkali gabbro, by obtaining  $\log f.\text{O}_2$  and temperature from the co-existing magnetite-ilmenite pairs, and

substituting them in reaction (7). He reports that for this rock, more basic and at higher temperature than any from North Qôroq,  $a.\text{SiO}_2$  again lies slightly above albite/nepheline. From this evidence, it seems justifiable to use a value just above the albite/nepheline buffer, for  $a.\text{SiO}_2$ , when calculating  $f.\text{O}_2$  using reaction (7) (see next section).

Turning now to the late stage assemblage of nepheline, sodalite, analcite and acmite. In the highly fractionated syenites it may be possible to define  $a.\text{SiO}_2$  using one of the following reactions



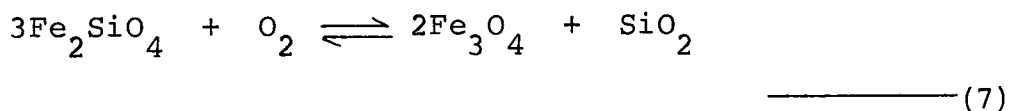
Thermodata are available for sodalite (Stormer and Carmichael, 1971) and for analcite, jadeite and nepheline (Thompson, 1974).

Reaction (8) requires a knowledge of the activity of NaCl in the magma and (9) a knowledge of the fugacity of water. Reaction (9) may be of use if  $P_{H_2O}$  is assumed to equal total pressure, as may well occur in these highly fractionated rocks. Reaction (10) is of doubtful application because, as pointed out in section 4.2, the mole fraction of jadeite in the acmitic pyroxenes is extremely variable, even in single crystals, and its use in calculation would result in unrealistically variable  $a_{SiO_2}$  values.

#### 4.16.5. The fugacity of oxygen ( $f_{O_2}$ )

Fugacity, like activity, is a way of expressing the chemical potential of a component. The  $f_{O_2}$  in a magma can be thought of as a measure of the tendency for oxygen to escape from the magma. Past workers have demonstrated conclusively that the crystallization of certain mineral phases is dependent on  $f_{O_2}$ . The stability fields of acmite (Bailey, 1969), calcic and alkali amphiboles (Gilbert, 1966; Ernst, 1962), biotites (Eugster and Wones, 1962; Wones and Eugster, 1965) and aenigmatite (Lindsley, 1971) have all been shown to be highly dependent on  $f_{O_2}$ . Hence, a knowledge of variation in  $f_{O_2}$  during the evolution of North Qôroq syenites is an invaluable aid in interpreting petrographic changes.

In the augite syenites, among the first phases to crystallize are olivine and Fe/Ti oxides, suggesting that  $f.O_2$  is initially defined by the FMQ buffer reaction



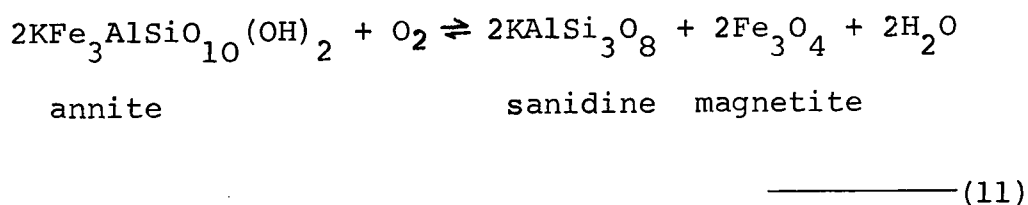
$$\log f.O_2 = \frac{\Delta G^{\circ}_r}{2.303RT} + 2\log a_{Fe_3O_4}^{oxide} + 3\log a_{SiO_2}^{liquid} - 3\log a_{Fe_2SiO_4}^{olivine} \quad \text{-----} (7B)$$

$$\frac{\Delta G^{\circ}_r}{2.303RT} = \frac{-24810}{T} + 8.47 \quad (\text{at } P = 1000 \text{ bars; Nicholls et al., 1971})$$

If the activities of fayalite in the olivines and magnetite in the Fe/Ti oxides can be obtained from probe analyses, and if  $a.SiO_2$  can be estimated, the variation of  $f.O_2$  with temperature at  $P = 1000$  bars can be calculated. The activity of fayalite is taken as being equal to the mole fraction of fayalite squared and the activity of magnetite as being equal to the mole fraction. This procedure is argued and adopted by Lindsley and Haggerty (1971). In the previous section, it was demonstrated that in the early formed augite syenites, where  $f.O_2$  is being controlled by the FMQ reaction, the  $a.SiO_2$  is probably just greater than the albite/nepheline buffer. Using this value,

variation in  $f.O_2$  is plotted in Fig. 4.22 against temperature obtained from the olivine/clinopyroxene geothermometer. The variation is the line A-B, which can be seen to be at an appreciably lower  $f.O_2$  than the synthetic buffer FMQ, also shown in the diagram. This is in agreement with observations from other under-saturated rocks (Nash et al., 1969; Nash and Wilkinson, 1970).

In the augite syenites the next evolutionary stage is the rimming of olivine by Fe/Ti oxides and the crystallization of biotite and alkali feldspar. Removal of olivine as a participating phase, means that  $f.O_2$  is no longer defined by the FMQ reaction. A reaction, appropriate to the observed assemblage at this stage, which defines  $f.O_2$  is that involving feldspar, biotite and Fe/Ti oxide.



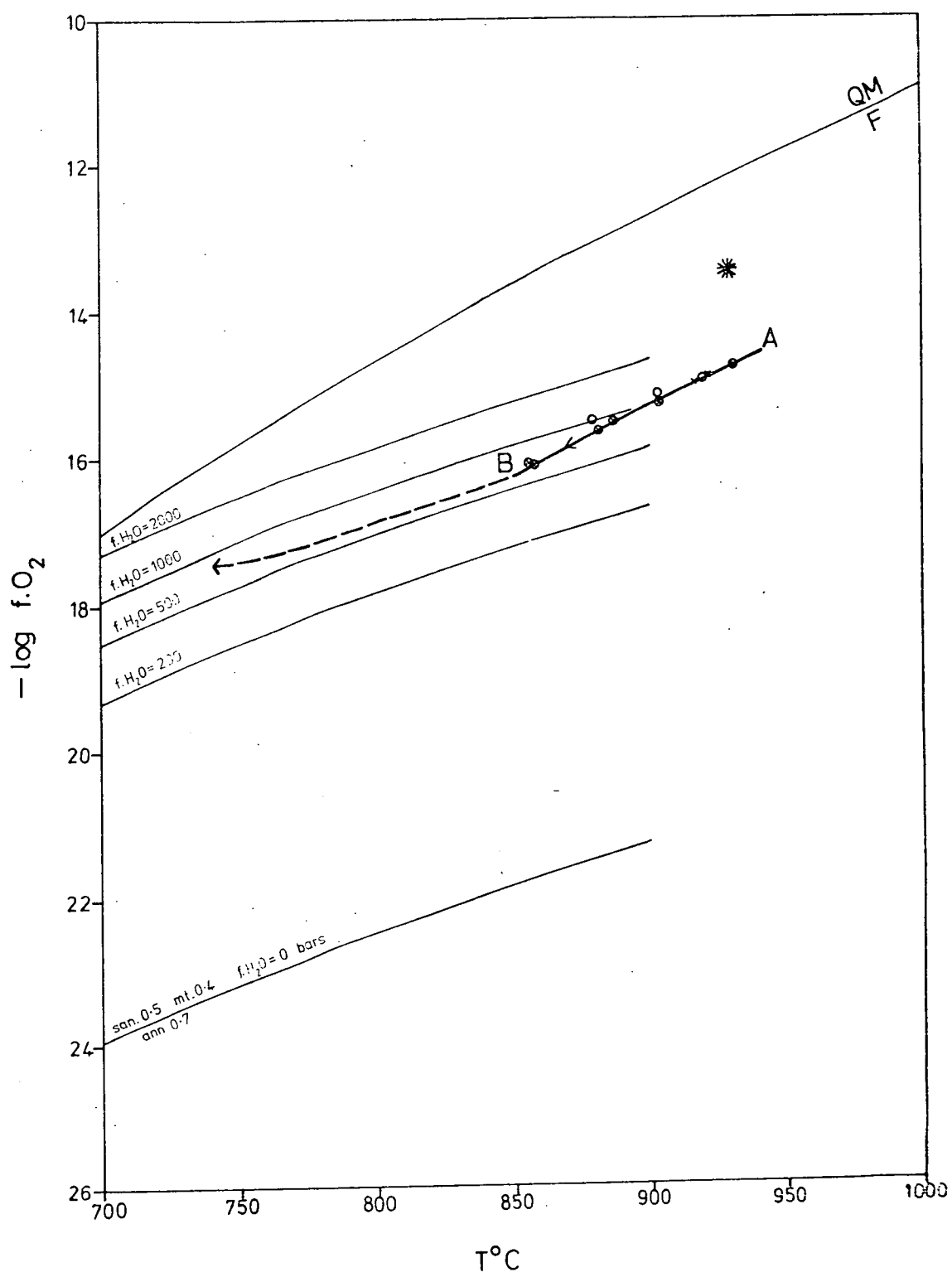
$$\begin{aligned}
 \log f.O_2 = & \frac{\Delta G^{\circ}_r}{2.303RT} + 2 \log a_{\text{feldspar}}^{KAlSi_3O_8} + 2 \log a_{\text{oxide}}^{Fe_3O_4} \\
 & + 2 \log f.H_2O - 6 \log x
 \end{aligned}
 \text{-----} (11B)$$

where  $x$  equals mole fraction  $Fe^{2+}$  in octahedral layer.

Fig.4.22 The variation of oxygen fugacity ( $f.O_2$ ) with temperature for North Qôroq syenites. The solid arrowed line, A-B, represents the  $f.O_2$  variation early in the evolution of the magmas, as defined by the assemblage olivine + Fe/Ti oxides, with silica being a component in the liquid. The dashed continuation of this line is the possible variation of  $f.O_2$  at lower temperatures, when defined by the new assemblage alkali feldspar + Fe/Ti oxides + biotite. Also marked on the figure is the fayalite/magnetite/quartz buffer curve (F.M.Q.) and various buffer curves for the assemblage sanidine + magnetite + annite, at different values of the fugacity of water (see text). The star represents a maximum value for  $f.O_2$  (Buddington and Lindsley, 1964), above which separate ilmenite and magnetite would crystallize.

Symbols used:

- -  $f.O_2$  values for unit SN.1A
- × -  $f.O_2$  values for unit SN.4A
- ⊙ -  $f.O_2$  values for unit SN.4B



For this reaction

$$\frac{\Delta G^{\circ}_r}{2.303RT} = \frac{-14818}{T} - 8.51 \quad (\text{at } P = 1000 \text{ bars;} \\ \text{Wones, 1972}).$$

Both activity of magnetite in the Fe/Ti oxide and activity of sanidine in the feldspar are obtained as outlined previously. The activity of annite is taken as being equal to the mole fraction Fe in the octahedral layer cubed, both  $\text{Fe}^{3+}$  and F being assumed to be negligible (Czamanske and Wones, 1973). The activities of sanidine and annite vary little with the state of fractionation of the host rock, and the activity of magnetite only increases slightly with increased degree of fractionation. Taking average values for these three variables, curves have been produced of  $\log f.\text{O}_2$  against temperature, contoured in varying fugacities of water (approximately equal to  $P.\text{H}_2\text{O}$  for these rocks). The resulting curves are given in Fig. 4.22. The lowest temperature obtained from the olivine/clinopyroxene geothermometer is  $850^{\circ}\text{C}$ , corresponding to the extreme rim of an olivine grain. It is proposed that around this temperature reaction (11) beings to define  $f.\text{O}_2$ . Wones and Eugster (op.cit.) have demonstrated that biotites of the composition of North Qôroq biotites are stable at

temperatures in excess of  $850^{\circ}\text{C}$ , under suitable  $\text{P.H}_2\text{O}$  conditions. The termination of the FMQ defined  $f.\text{O}_2$  line at  $850^{\circ}\text{C}$ , coincides with the magnetite/sanidine/annite line appropriate to a  $f.\text{H}_2\text{O}$  of approximately 600 bars (see section on  $\text{P.H}_2\text{O}$ ). If  $f.\text{O}_2$  was defined by FMQ to lower temperatures than  $850^{\circ}\text{C}$ , as it appears to be in the Shonkin Sag laccolith (Nash and Wilkinson, *op.cit.*), this would necessitate the magma being drier than would appear reasonable, on the basis of evidence presented in the later section on  $\text{P.H}_2\text{O}$ . If FMQ defined  $f.\text{O}_2$  down to Shonkin Sag temperatures,  $f.\text{H}_2\text{O}$  would have to be much lower than 200 bars, indicating an improbably dry magma.

The dashed line in Fig. 4.22 indicates the possible change in  $f.\text{O}_2$  with temperature, if defined by the assemblage Fe/Ti oxide-feldspar-biotite. It curves towards the horizontal with decreasing temperature, because of the presumed increase in  $f.\text{H}_2\text{O}$  with magma fractionation, and because the activity of magnetite in the Fe/Ti oxides also increases slightly. It must be emphasised that this curve merely gives an indication of the likely  $f.\text{O}_2$  variation.

Ferro-pargasite is a common phase in the less fractionated North Qôroq syenites (section 4.3). In Fig. 4.23a the stability field of ferro-pargasite, at  $\text{P.H}_2\text{O} = 1000$  bars

(Gilbert op.cit.), can be seen to almost intersect the proposed  $f.O_2$ -temperature trend for North Qôroq. As pargasite has a greater stability range than ferro-pargasite, and as these amphiboles contain a pargasite component, the amphibole stability field would intersect the proposed  $f.O_2$ -temperature trend. The observed rimming of pyroxene by pargasite/ferro-pargasite may not only be a function of increasing  $P.H_2O$ , but may also be associated with the predicted fall in  $f.O_2$  with temperatures, at uniform  $P.H_2O$ , until the pargasite/ferro-pargasite stability field is intersected.

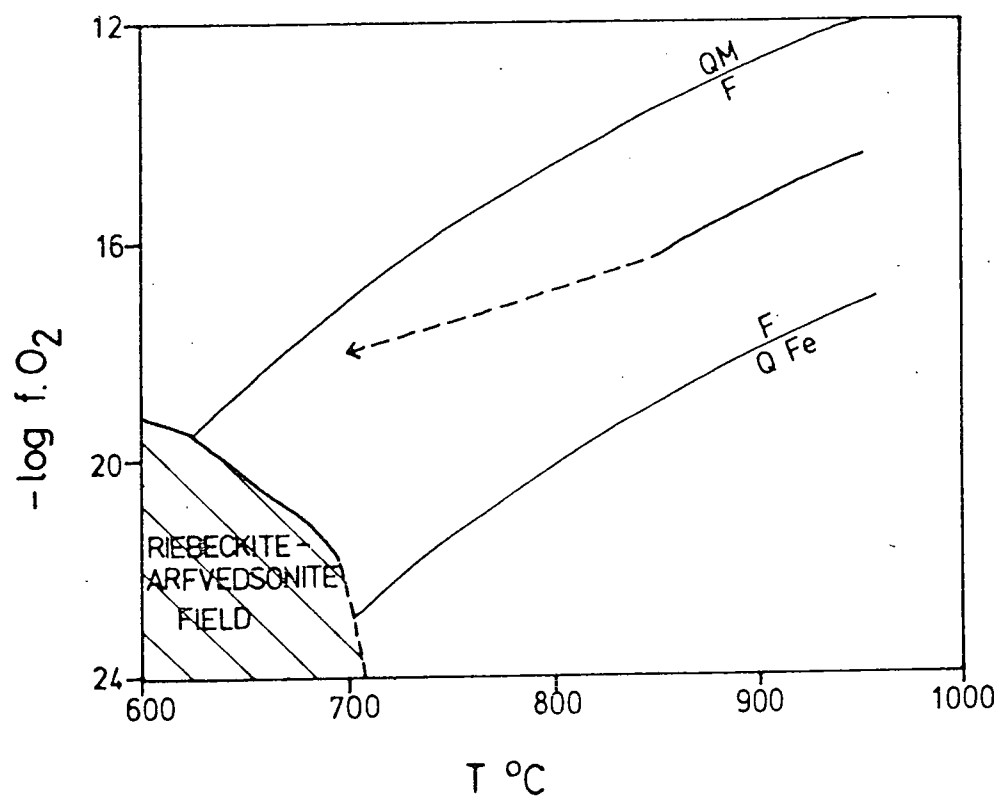
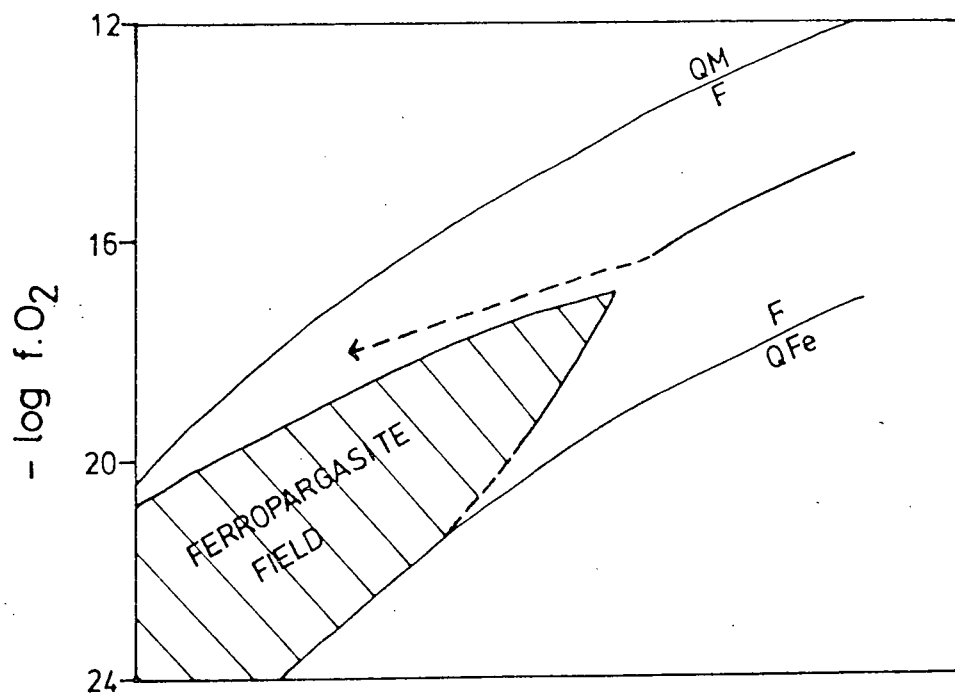
In the more fractionated nepheline syenites of North Qôroq, blue arfvedsonitic amphibole is a common phase. Fig. 4.23b shows the stability field of riebeckite-arfvedsonite solid solution, at  $P.H_2O = 1000$  bars, in terms of  $f.O_2$  and temperature (Ernst, op.cit.). This field can be seen to lie at lower  $f.O_2$  than the proposed  $f.O_2$ -temperature trend for North Qôroq syenites. These amphiboles, however, contain appreciable quantities of F. Ernst (1968) points out that F, substituting for OH, greatly increases amphibole stability and would expand the amphibole stability field in Fig. 4.23b.

Acmite is frequently found rimming blue arfvedsonite, or as the only mafic phase in more fractionated rocks.

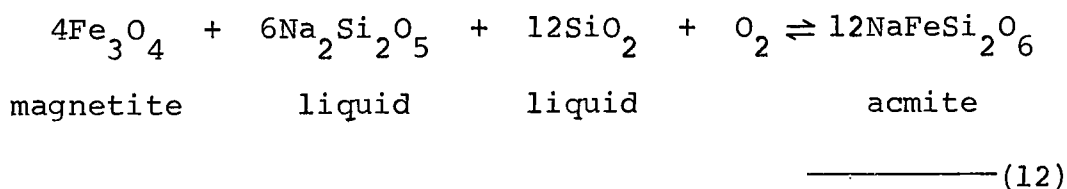
Fig.4.23

(a) The proposed  $f.O_2$  - temperature trend for North Qôroq syenites, relative to the stability field of ferropargasite at  $P.H_2O = 1000$  bars (Gilbert, 1966). Also shown on the figure are the fayalite/magnetite/quartz and quartz/Fe/fayalite buffer curves.

(b) The proposed  $f.O_2$  - temperature trend for North Qôroq syenites, relative to the stability field of riebeckite arfvedsonite solid solution at  $P.H_2O = 1000$  bars (Ernst, 1962). The two buffer curves mentioned for the previous figure are also given.



Biotite is usually absent from these rocks and this suggests that at low temperatures, in highly fractionated rocks,  $f.O_2$  is defined by a new reaction. The occurrence of granular Fe/Ti oxides with acmite suggests that  $f.O_2$  may be defined by the reaction



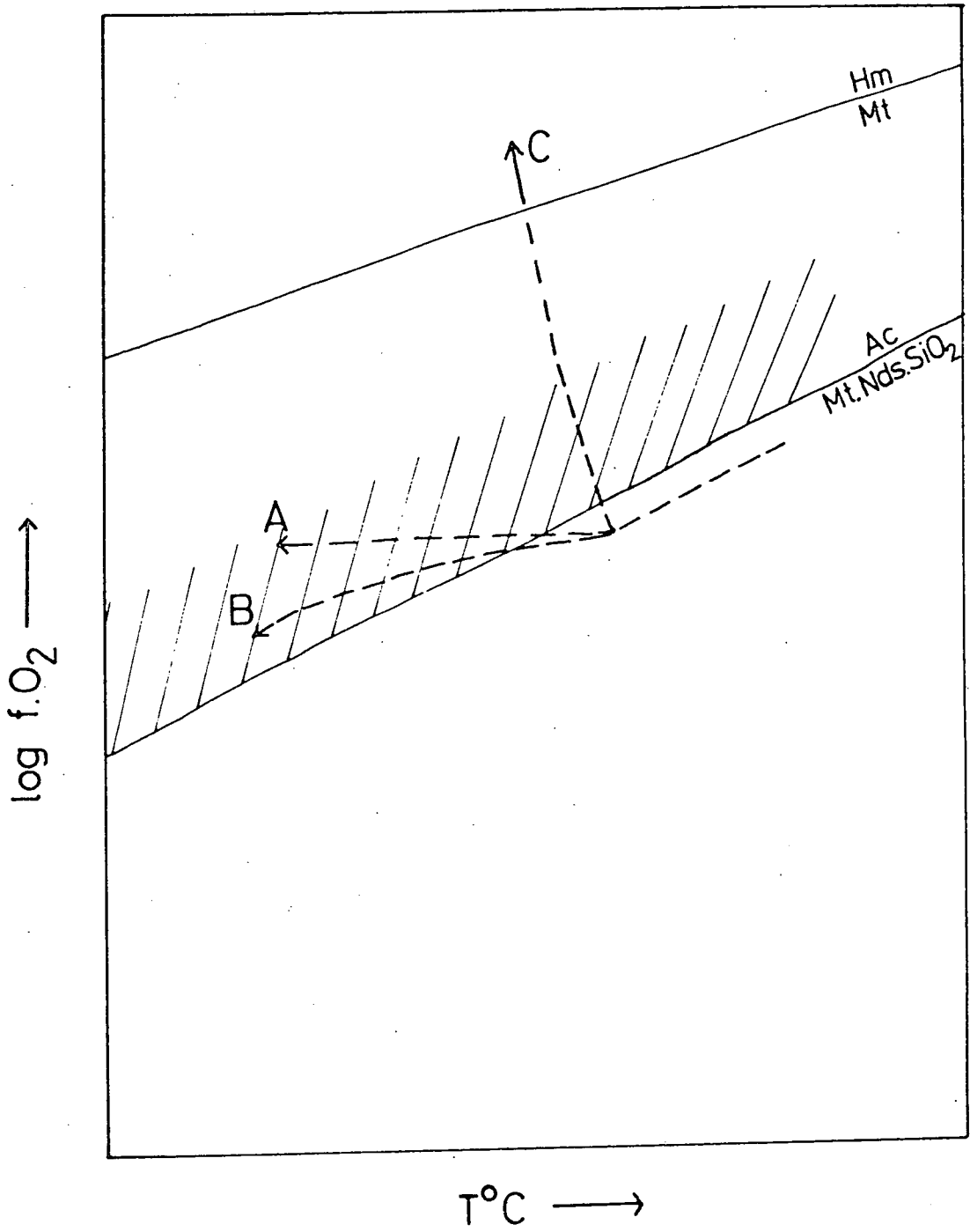
$$\begin{array}{l}
 \log f.O_2 = \frac{\Delta G^{\circ}_r}{2.303RT} + 12 \log a_{\text{pyroxene}}^{NaFeSi_2O_6} - 4 \log a_{\text{oxide}}^{Fe_3O_4} \\
 \quad \quad \quad - 6 \log a_{\text{liquid}}^{Na_2Si_2O_5} - 12 \log a_{\text{liquid}}^{SiO_2} \\
 \text{-----} \\
 (12B)
 \end{array}$$

This is the reaction used by Nicholls and Carmichael (1969) to define the lower boundary of their 'no-oxide field'. The reaction poses a significant problem. Numerous workers have suggested that the trend towards acmite in alkali pyroxenes is controlled by  $f.O_2$ . However, it may well be, as suggested by Anderson (1974) and proposed here, that reaction (12) defines  $f.O_2$  and that other factors affect the pyroxene trend. This will be discussed in the next section.

In the most highly fractionated rocks of North Qôroq the assemblage acmite and aenigmatite, with magnetite

absent, can be observed. This would suggest that  $f.O_2$  has departed from the acmite-magnetite defined trend and entered a field comparable with the 'no-oxide field', proposed by Nicholls and Carmichael (op.cit.) for over-saturated rocks. Marsh (1975) has shown it to be difficult to define a similar field for undersaturated rocks, but nevertheless favours the existence of one on the basis of the observed petrography. Fig. 4.24 shows in a qualitative fashion the possible behaviour of  $f.O_2$  at low temperatures. It may leave the acmite-magnetite defined line when magnetite ceases to crystallize and remain relatively constant and unbuffered with temperature fall, as indicated by line A. Alternatively, it may decline systematically with temperature, the variation being defined by a new buffer involving the last-fractionating magma components, as indicated by line B. The third possibility is that a dramatic increase in oxygen fugacity may occur, due to dissociation of magmatic water and diffusion of  $H_2$  out of the system at a greater rate than  $O_2$ . An increase of this type was noted by Sato and Wright (1966), when measuring  $f.O_2$  directly in a cooling Hawaiian lava lake, and attributed to rapid diffusion of  $H_2$  and slow or non-existent diffusion of  $O_2$ . This possible trend is indicated by line C. If this trend represents the true

Fig.4.24 Schematic diagram illustrating the possible behaviour, at low temperature, of the  $f.O_2$ . After being defined by a reaction<sup>2</sup> involving acmitic pyroxene, magnetite and species in the liquid, the  $f.O_2$  may vary in one of three ways (see text). Shown on the figure are the haematite/magnetite buffer curve and the magnetite/silica/sodium disilicate/acmite buffer curve. The exact position of the latter curve is uncertain. The shaded area represents the possible stability field of aenigmatite.



behaviour of  $f.O_2$ , at a late stage in the syenites evolution, it may be that rims of haematite around magnetite grains reflect an increase in  $f.O_2$  above the haematite-magnetite oxygen buffer, as indicated in Fig. 4.24.

No accurate positioning of the acmite-magnetite-sodium disilicate-silica buffer is possible, as free energy data for acmite are unreliable as well as values for the activities of silica and sodium disilicate in the magma.

4.16.6. The activity of sodium disilicate ( $a.Na_2Si_2O_5$ ) and its mineralogical effects

Highly fractionated syenites from North Qôroq, have acmite and occasionally sodium metasilicate in the norm, indicating that the syenites were evolving towards a highly sodic residual liquid. In this liquid, the activity of sodium disilicate ( $a.Na_2Si_2O_5$ ) must have been high and this must have affected the observed mineralogy

Considering reaction (12) and re-writing it gives

$$12 \log a_{NaFeSi_2O_6}^{pyroxene} = \frac{\Delta G^{\circ}_r}{2.303RT} + \log f.O_2 + 4 \log a_{Fe_3O_4}^{oxide} + 6 \log a_{Na_2Si_2O_5}^{liquid} + 12 \log a_{SiO_2}^{liquid}$$

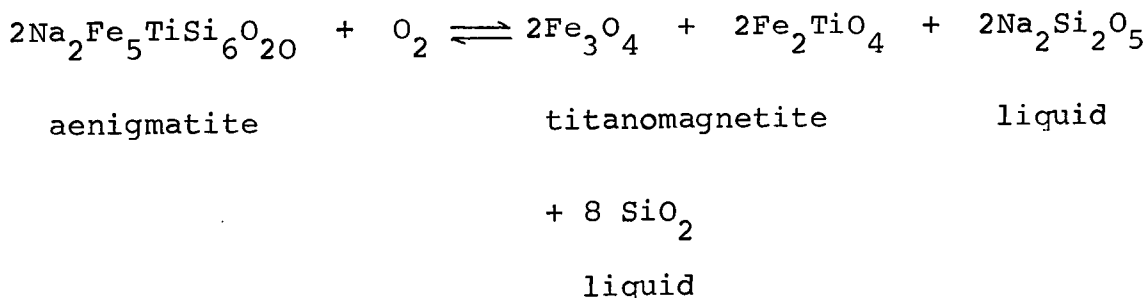
—————(12C)

This reaction can in fact be observed in recrystallized dyke rocks of the area, where Fe/Ti oxides are rimmed by a host of fine acmite needles. For the reaction the activity of the acmite component in the pyroxene, at a particular temperature and pressure, is dependent on  $f.O_2$ , activity of magnetite in the Fe/Ti oxide and the activities of  $Na_2Si_2O_5$  and  $SiO_2$  in the magma. An important feature of the reaction is that its stoichiometry means that the activity of acmite is much more dependent on variations in  $a.SiO_2$ ,  $a.Na_2Si_2O_5$  and  $a.Fe_3O_4$  than on  $f.O_2$ . In fractionated rocks the Fe/Ti oxide is magnetite-rich and varies only slightly. The two most important factors in controlling the point at which the pyroxene trend turns towards acmite are, therefore,  $a.SiO_2$  and  $a.Na_2Si_2O_5$  in the magma. As both these factors and  $f.O_2$  may affect the pyroxene trend, it is unrealistic to look for differences in pyroxene trends between oversaturated and undersaturated syenites. Indeed, pyroxenes from the oversaturated syenites from Gardar centres tend to trend towards acmite at a later stage than those from the majority of undersaturated syenites, the reverse of what would be expected if  $a.SiO_2$  was the controlling factor. In all the undersaturated rocks  $a.SiO_2$  probably lies close to the albite/nepheline silica buffer curve.

Perhaps, in these rocks, it is a high  $a.\text{Na}_2\text{Si}_2\text{O}_5$  in the magma causing an early increase in acmite, whereas, in magmas with lower values of  $a.\text{Na}_2\text{Si}_2\text{O}_5$ , the pyroxenes proceed further towards hedenbergite prior to Na enrichment. If this is so, why do the pyroxenes of the strongly perthitic Ilímaussaq intrusion only trend towards acmite after becoming strongly enriched in hedenbergite? Perhaps, in Ilímaussaq, low  $f.\text{O}_2$  and low  $a.\text{SiO}_2$  are dominant over the  $a.\text{Na}_2\text{Si}_2\text{O}_5$  effect.

On the topic of relating pyroxene trends to  $a.\text{Na}_2\text{Si}_2\text{O}_5$  in the magma, it is interesting to note that Bailey (1969) states that 'acmite only forms from liquids containing excess sodium silicate'.

The presence of aenigmatite and the absence of Fe/Ti oxides may also be a reflection of  $a.\text{Na}_2\text{Si}_2\text{O}_5$ . A reaction proposed by Marsh (1975), when trying to define a 'no-oxide field' for undersaturated rocks, is given below

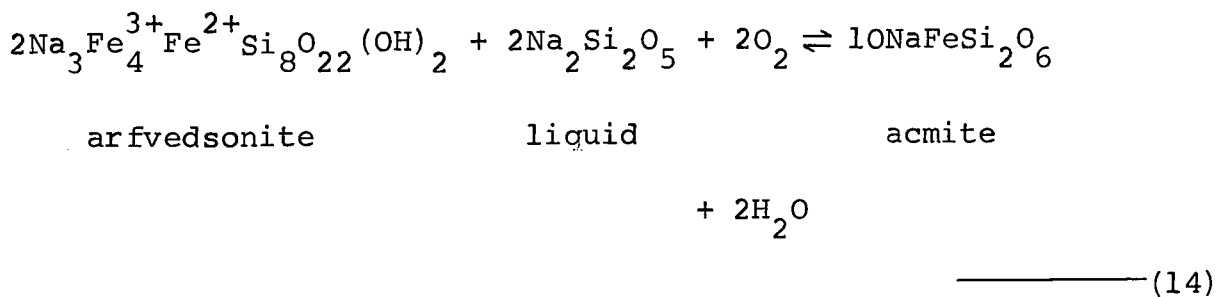


—————(13)

Here it can be seen that aenigmatite is favoured over the

Fe/Ti oxide by low  $f.O_2$ , high  $a.SiO_2$  and high  $a.Na_2Si_2O_5$ . As  $a.SiO_2$  lies close to, and may be defined by, the albite/nepheline buffer, it is the other two variables which will tend to control the presence or absence of aenigmatite, again indicating that  $a.Na_2Si_2O_5$  is important in controlling the phases present in the last fractionating liquids.

Consideration of the reaction rims of acmite around blue arfvedsonitic amphibole has implications with regard to  $a.Na_2Si_2O_5$ . The reaction can be expressed as



As  $f.H_2O$  in the magma would be expected to increase with fractionation, and acmite rims amphibole, other variables must be used to explain the reaction relationship. Either an increase in  $f.O_2$  or in  $a.Na_2Si_2O_5$  would result in acmite forming at the expense of arfvedsonite. At this stage  $f.O_2$  is probably defined by a buffer reaction and decreasing with falling temperature. It is proposed, therefore, that the acmite rims reflect increasing  $a.Na_2Si_2O_5$  in the residual, highly fractionated, syenitic magma.

Finally, mention must be made of the recrystallized syenites, where aenigmatite, acmite and arfvedsonitic amphibole are frequently the only mafic phases. This assemblage suggests high  $a.\text{Na}_2\text{Si}_2\text{O}_5$ , which would be consistent with a Na-metasomatising fluid. The patchy and mutually exclusive occurrence of arfvedsonite and acmite in these rocks may be due to variations in  $a.\text{Na}_2\text{Si}_2\text{O}_5$ , again a feature that would be in keeping with irregular invasion by a metasomatic fluid.

Stephenson (1972) suggested increasing  $f.\text{O}_2$  as being the key factor in producing an early trend towards acmite in recrystallized rocks. However, the presence of aenigmatite rather than Fe/Ti oxides in these rocks suggests (considering reaction (13)) a relatively low  $f.\text{O}_2$ . The sharply defined and early acmite enrichment in pyroxenes of recrystallized rocks can again be ascribed to the effect of metasomatic fluids with a high  $a.\text{Na}_2\text{Si}_2\text{O}_5$ .

#### 4.16.7 Water vapour pressure ( $P.\text{H}_2\text{O}$ )

From the feldspar solvus-solidus relationships (section 4.6) it was seen that, for the least fractionated rocks,  $P.\text{H}_2\text{O}$  must have been less than 1000 bars and, for the highly fractionated interiors of SN.1A and SN.5, less than 1600 bars.  $P.\text{H}_2\text{O}$  was, in fact, probably well below these values and it would be useful to obtain a better

idea of  $P.H_2O$  behaviour as fractionation took place.

In the early formed augite syenites the first phases to crystallize were anhydrous and of no value for directly determining  $P.H_2O$ . In SN.4A and SN.4B, early formed plagioclases are present, together with phenocrysts of olivine, pyroxene and Fe/Ti oxides. The Kudo-Weill plagioclase geothermometer, used in the section on temperature determination, is sensitive to changes in  $P.H_2O$ . For the chilled marginal sample 155152, the nearest approximation to a liquid in the centre, the olivine/clinopyroxene geothermometer gives a temperature of  $931^{\circ}C$ . Assuming all the phenocrysts were in equilibrium, and that total pressure effects were negligible or at least equivalent, the plagioclase geothermometer gives this temperature when  $P.H_2O$  is set at approximately 300 bars. This value, although approximate, is a reasonable one, as both SN.4 units, as previously mentioned, give the appearance of having intruded as hotter, drier bodies of magma than the other units.

The crystallization of the early formed anhydrous phases must result in the build up of water in the magma and an increase in  $P.H_2O$ . The first hydrous phase to crystallize is biotite, common in marginal SN.1A and present in many other units. Using reaction (11) the

following relationship applies:

$$\log f.H_2O = \frac{\Delta G^{\circ}_r}{2.303RT} + \frac{1}{2}\log f.O_2 + 3\log x - \log a_{\text{feldspar}}^{KAlSi_3O_8} - \log a_{\text{oxide}}^{Fe_3O_4} \quad (11C)$$

with, as before,  $x$  equalling the mole fraction  $Fe^{2+}$  (= total Fe) in the octahedral layer.

Using the lowest value of  $f.O_2$  determined along the FMQ reaction line, ie. at  $850^{\circ}C$ , and substituting the appropriate activity values in equation (11C) gives a value for  $f.H_2O$  of 630 bars. Fugacity is related to pressure of water

$$f = P.Y$$

where  $Y$  is the fugacity coefficient. At low total pressure  $f.H_2O \approx P.H_2O$ . From the above value for  $f.H_2O$ , and using data from Burnham et al. (1969), the pressure of water at the stage when biotite started to crystallize was of the order of 700 bars.

With continued fractionation the crystallization of hydrous phases, biotite, amphibole and later analcite, would have resulted in a less rapid increase in  $P.H_2O$ . At a late stage in the evolution of the more fractionated

syenites it may be possible to determine  $P.H_2O$  using reaction (9), providing a value for  $a.SiO_2$  is known. At this stage it is possible that  $P.H_2O$  approached 1000 bars, the postulated value for  $P$ . total, and resulted in the 'boiling off' of an aqueous fluid (see Chapter 6).

#### 4.16.8. Other volatile phases

Other volatile phases may be significant in the evolution of North Qôroq syenites, particularly  $CO_2$  and the halogens. By writing reactions involving analysed phases containing carbonate (e.g. cancrinite) or halides (e.g. sodalite) it would be possible, providing adequate thermodata were available, to determine the behaviour of these volatile phases with fractionation. Stormer and Carmichael (1971), for example, have determined the variation in the fugacity of HCl with temperature for a sodalite trachyte, using the equilibrium assemblage acmite-nepheline-sodalite-magnetite.

#### 4.16.9. Conclusions from the thermodynamic treatment of North Qôroq mineral data

A thermodynamic approach has enabled a quantitative assessment to be made of the behaviour of such important magmatic controls as temperature, pressure,  $P.H_2O$ ,  $f.O_2$  and  $a.SiO_2$ . It is admitted that some of the assumptions made, particularly with regard to obtaining activities of

components, will have resulted in small errors. The values obtained, however, seem reasonable and compare well with observations from field relations, petrography and experimental work on similar rocks. Even when inadequate thermodata prevent quantitative values being obtained, a qualitative approach, using constructed reactions, has given an insight into the powerful effect of certain of the variables. This is particularly true of  $a.\text{Na}_2\text{Si}_2\text{O}_5$  in late stage highly fractionated syenites.

## CHAPTER FIVE: GEOCHEMISTRY

### 5.1. Introduction

Samples from North Qôroq were analysed for 10 major elements (Si, Ti, Al, Fe, Mn, Mg, Ca, Na, K, P) and a selected number of trace elements (Ba, Sr, Rb, V, Ni, Cr, Cu, Sn, Zn, Nb, Y, La, Pb, Th, U). Analyses were performed using X-ray fluorescence techniques and details of sample preparation and analytical methods are given in Appendix IV. In a selected number of fresh syenites, H<sub>2</sub>O, CO<sub>2</sub> and the Fe<sup>3+</sup>/Fe<sup>2+</sup> oxidation ratio were determined wet-chemically. The methods employed are also given in Appendix IV. The analyses are listed, and followed by a listing of C.I.P.W. norms.

The geochemical variation found in North Qôroq syenites is demonstrated by use of a number of 2-component and 3-component plots. Although, at times, a degree of explanation is necessary, use of these diagrams in general removes the need for lengthy description. Where one analysis overlaps another on a particular plot, it is omitted. Only those rocks appearing fresh and unaltered in thin section are included in the plots given in this chapter. Any rocks containing normative corundum are the products of nepheline breakdown (Na loss), and the analyses of these rocks have been discarded. Because of the coarse nature of many of the rocks, a considerable quantity of crushed material was

used in sample preparation to minimize sample size errors.

In North Qôroq syenites mafic banding is rare and feldspar lamination relatively uncommon. Few features that would be typical of strongly cumulate rocks can be seen. Upton (1964b), when considering the Hviddal dyke as a possible layered nepheline syenite intrusion, suggests that 'the syenites should be regarded as 'loosely packed' orthocumulates, in which the ratio of intercumulus to cumulus material was relatively high'. This statement can be well applied to many of the North Qôroq syenites. Units SN.2, SN.4A and SN.4B are relatively fine-grained and show no cumulate features. They probably approximate to liquid compositions, as do the marginal rocks of the other more variable units, SN.1A, SN.1B and SN.5. The smooth trends shown by analyses of the more variable units, and the fact that they parallel those shown by SN.2, SN.4A and SN.4B, suggest that they can be used to demonstrate liquid lines of descent.

With the exception of certain rocks in marginal SN.1A, which are saturated or just oversaturated with respect to silica, the North Qôroq syenites are under-saturated, some markedly so. The peralkalinity index,  $(Na+K)/Al$ , is below unity in the less fractionated syenites (0.85-1.00), but the rocks become peralkaline with fractionation, the index reaching a maximum value of 1.30.

## 5.2. Major element variation

Fig. 5.1 (a-1) gives the major element, peralkalinity and normative nepheline variation with fractionation. The degree of fractionation is defined by the Fractionation Index of Macdonald (1969). This index is the sum of normative albite, orthoclase, nepheline, acmite and sodium silicate. It has been used by Stephenson (1973) and Anderson (1974) to describe chemical variation in other Gardar centres. The Differentiation Index of Thornton and Tuttle (1960) is not used, as peralkaline rocks are not adequately represented by it. Likewise, a mineralogical measure of fractionation, e.g. Na-Mg in the pyroxenes, is inadequate because of the extreme zonation shown by the pyroxenes, even within single crystals.

Examination of Fig. 5.1 shows that all major elements display a smooth continuous variation with fractionation.

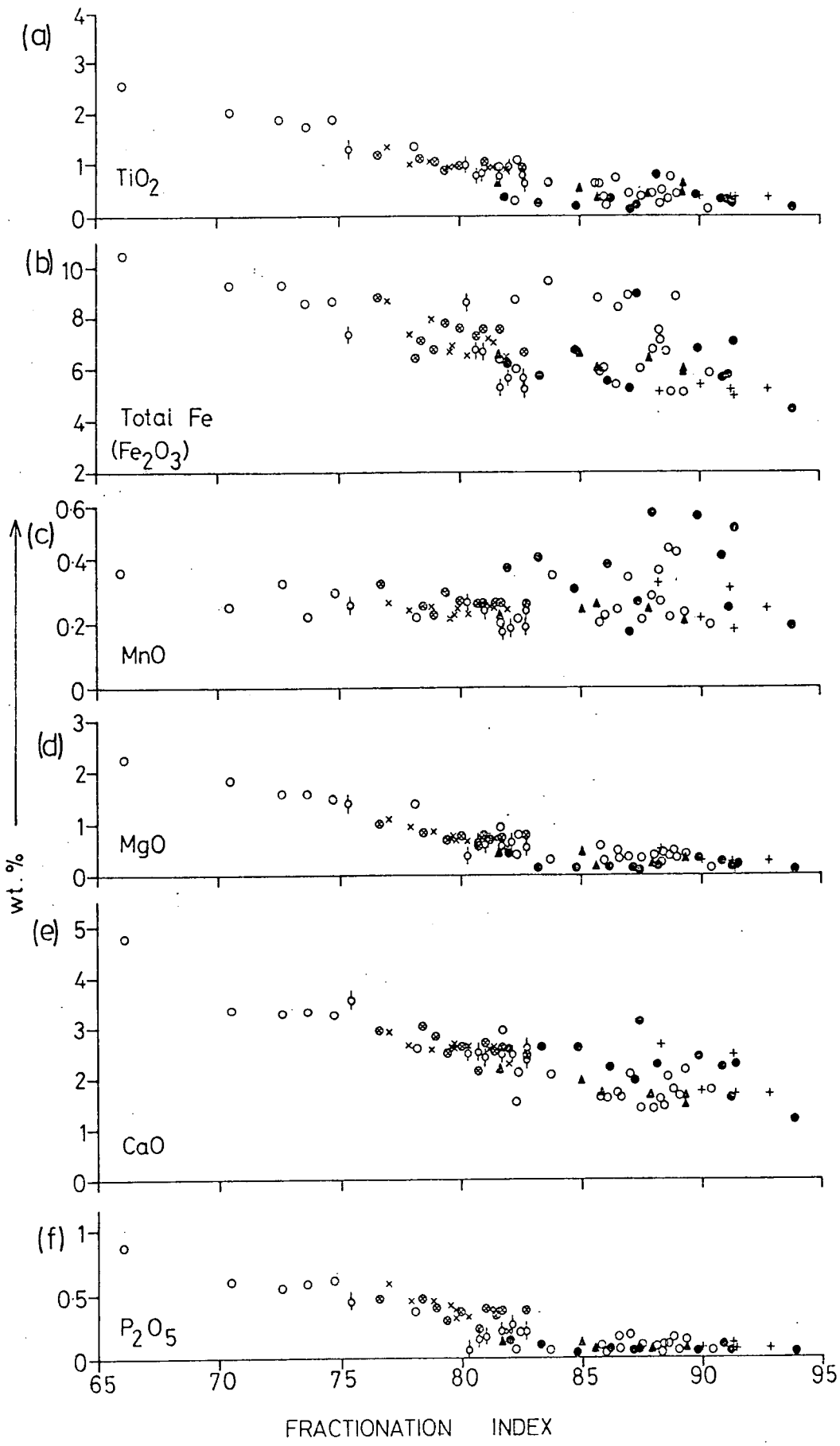
$\text{SiO}_2$  values increase in the augite syenites, due to the increasing proportion of felsic phases to mafic phases and oxides, and decrease in the more fractionated rocks, a reflection of the higher proportion of nepheline, sodalite and analcite to feldspar.

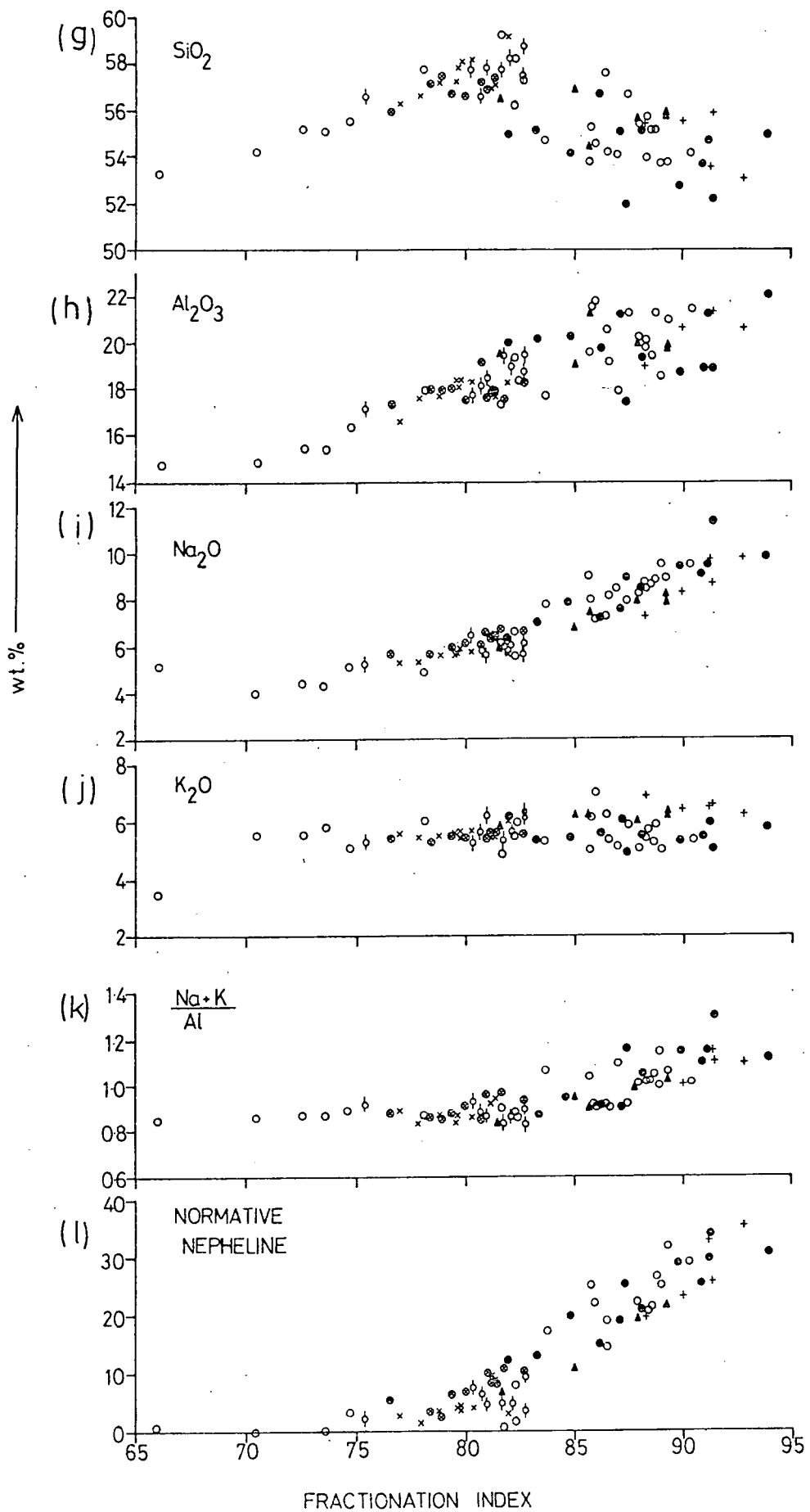
Both  $\text{Al}_2\text{O}_3$  and  $\text{Na}_2\text{O}$  increase steadily with fractionation, whereas  $\text{K}_2\text{O}$  remains approximately constant. The increase in  $\text{Na}_2\text{O}$  is a true increase, reflected in the occurrence of Na-rich alumino-silicates and sodic pyroxene

Fig.5.1 (two pages) The major element, peralkalinity and normative nepheline variation of North Qôroq syenites, plotted against the 'Fractionation Index' of Macdonald (1969). This index is the 'Differentiation Index' of Thornton and Tuttle (1960), i.e. normative orthoclase, albite and nepheline, plus normative acmite (and, where present, normative sodium disilicate).

Symbols used:

- - Unit SN.1A
- ▲ - Unit SN.1B
- ⊖ - Unit SN.2
- † - Unit ?SN.3
- × - Unit SN.4A
- ⊗ - Unit SN.4B
- - Unit SN.5





and amphibole. The increase in  $\text{Al}_2\text{O}_3$  may be due, at least in part, to the fact that with fractionation the average atomic weight of the magma decreased and hence  $\text{Al}_2\text{O}_3$ , in terms of weight, constituted a greater proportion of the magma.

$\text{TiO}_2$ , Total Fe,  $\text{MgO}$ ,  $\text{CaO}$  and  $\text{P}_2\text{O}_5$  all decreased steadily as the magmas evolved. This is reflected in the decrease and eventual absence of olivine (Fe), augitic-pyroxene (Ca, Ti, Mg), Ti-rich oxides, Ca-rich feldspar and apatite (Ca, P) during the early stages of fractionation. In more fractionated rocks, there is a change in amphibole compositions from Ca, Mg, Ti-rich pargasites to Na-rich arfvedsonites.

$\text{MnO}$  remains approximately constant, the content being distinctly variable in the highly fractionated rocks.

Although not plotted, the  $\text{Fe}^{3+}/\text{Fe}^{2+}$  ratio increases markedly with fractionation. In the augite syenites most of the Fe is  $\text{Fe}^{2+}$  occurring in augite, fayalite, and Fe/Ti oxides. In more fractionated rocks Fe occurs as  $\text{Fe}^{3+}$  in acmitic pyroxene,  $\text{Fe}^{2+}$  in aenigmatite and  $\text{Fe}^{2+}$  and  $\text{Fe}^{3+}$  in alkali amphibole.

$\text{H}_2\text{O}$  contents of the rocks are irregular, a reflection of the irregular concentrations of amphibole and biotite. The content increases in highly fractionated rocks, presumably due to the presence of water-rich analcite and

natrolite. In these rocks, the presence of cancrinite and calcite results in high  $\text{CO}_2$  values.

All syenites of North Qôroq, even the least fractionated, are Na-rich and Mg-poor and plot, on an AFM diagram, towards the more fractionated end of the general Gardar trend (Watt, 1966).

Recrystallized rocks are similar to normal syenites in major element terms, with the exception of the alkalis. In these rocks  $\text{Na}_2\text{O}$  tends to be higher and  $\text{K}_2\text{O}$  lower than in the normal syenites.  $\text{K}_2\text{O}$  enrichment has already been mentioned (section 4.6) as affecting the alkali feldspar in recrystallized syenites and  $\text{Na}_2\text{O}$  enrichment as affecting the mafic phases. This suggests alkali exchange with a metasomatising fluid phase (see Chapter 6).

### 5.3. Minor element variation

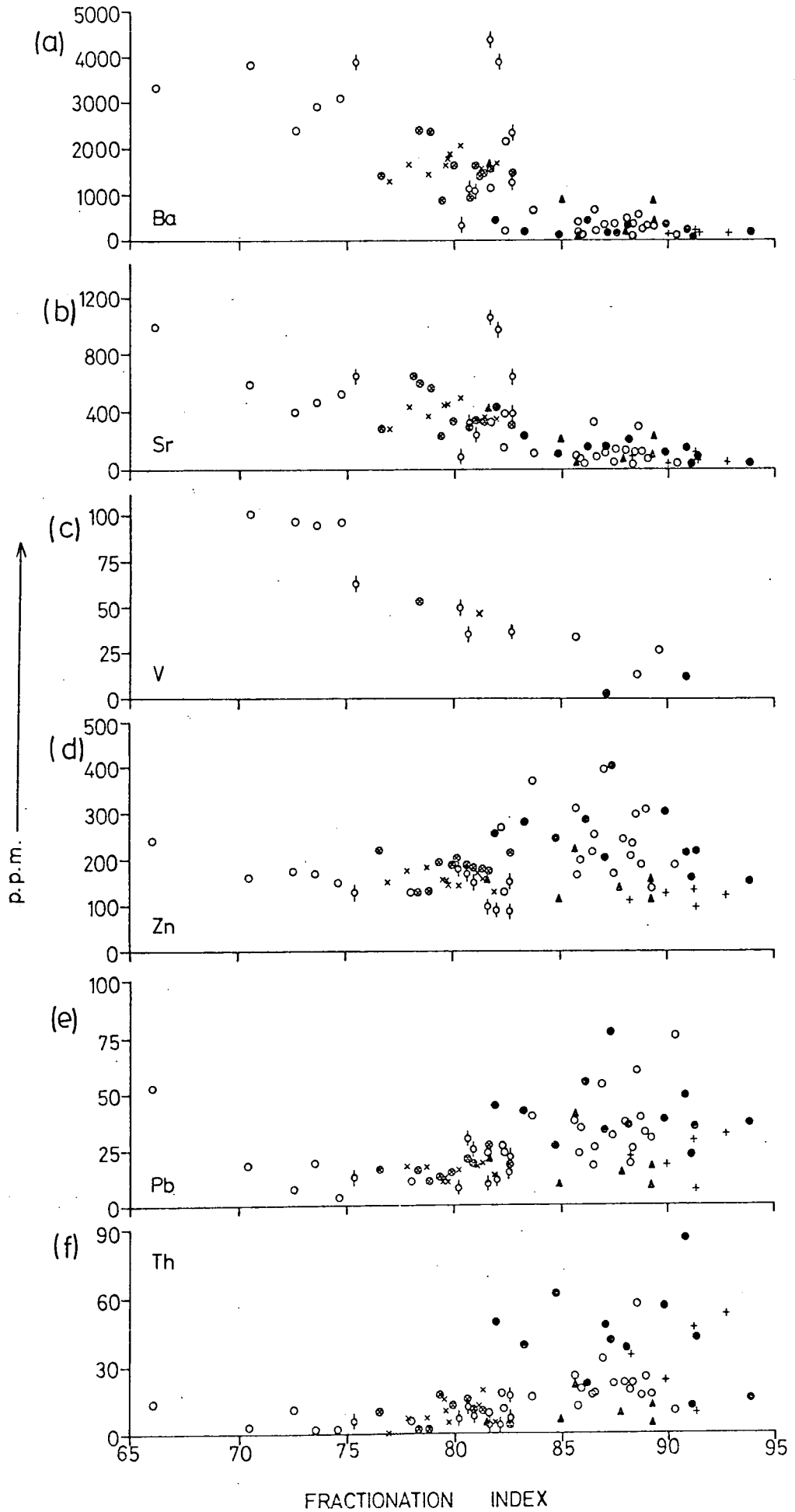
In Fig. 5.2 (a-1) all analysed minor elements that are present in any significant quantities, and the K/Rb ratio, are plotted against the Fractionation Index.

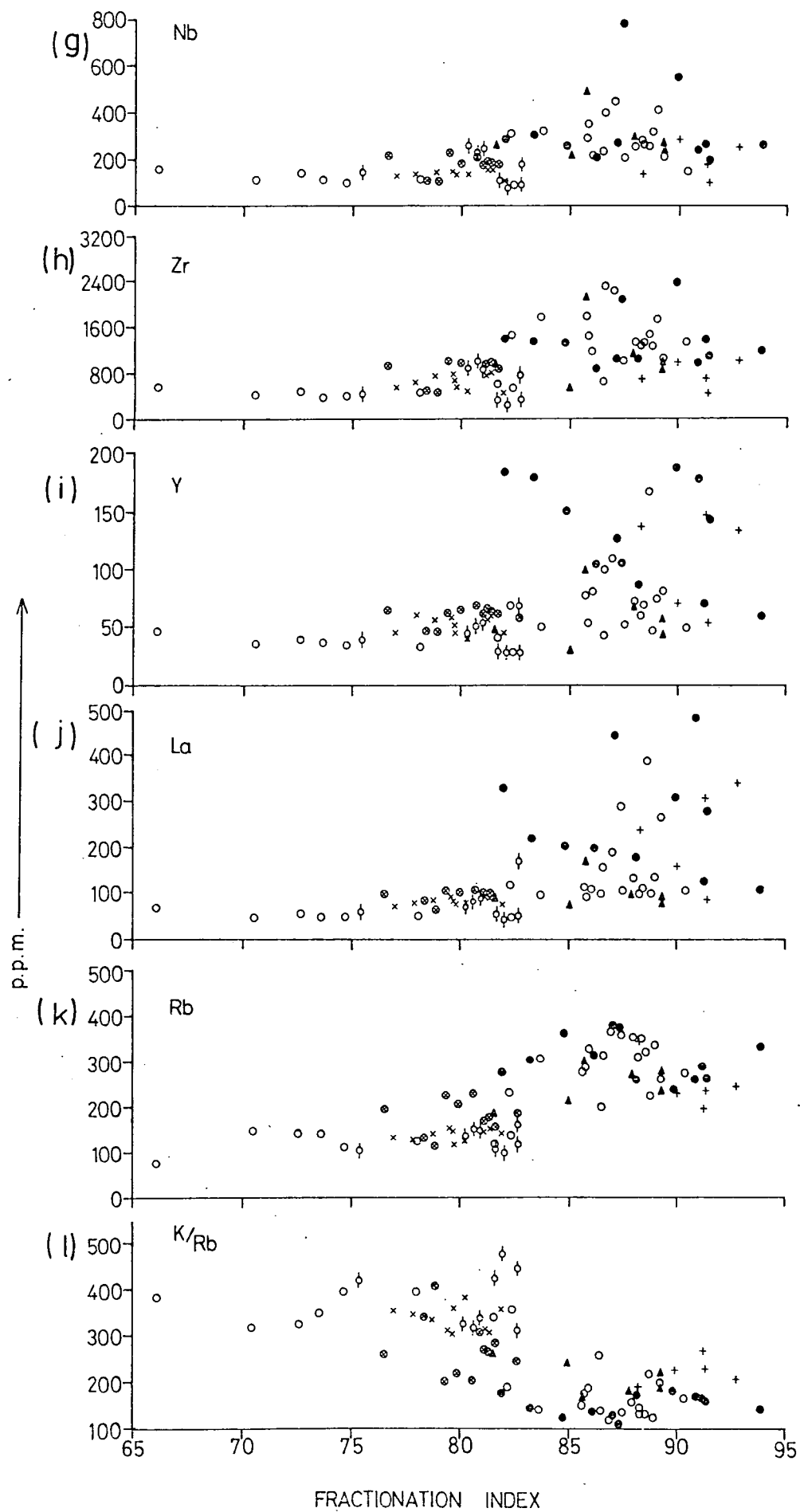
Cr and Ni never occur in any quantity in the syenites (<10p.p.m.). They are strongly stabilised by entering octahedral sites in minerals and are preferentially incorporated into early formed phases. Presumably North Qôroq magmas were depleted in Cr and Ni by crystallization prior to emplacement.

Fig.5.2 (two pages) The variation of trace element abundances and K/Rb ratio in North Qôroq syenites, plotted against the 'Fractionation Index' of Macdonald (see Fig.5.1).

Symbols used:

- - Unit SN.1A
- ▲ - Unit SN.1B
- ⊖ - Unit SN.2
- † - Unit ?SN.3
- × - Unit SN.4A
- ⊗ - Unit SN.4B
- - Unit SN.5





V (Fig. 5.2(c)) is also concentrated in the less fractionated rocks. It varies from 100 p.p.m. in the augite syenites to almost zero in the foyaites. V probably resides in the early formed Fe/Ti oxides, although not detected by microprobe analysis. As mentioned in section 4.5.3., V is particularly hard to analyse for as its peak overlaps that of Ti.

Ba and Sr (Fig. 5.2 (a and b)) are two elements that occur in high concentrations in the early formed augite syenites, but are rapidly depleted in the magma and are insignificant in more evolved rocks. The rapid depletion in Ba and Sr suggests feldspar fractionation. As indicated in section 4.6.4., Ba is preferentially taken into the feldspar structure and is thus concentrated in the first formed alkali feldspar. Sr can concentrate in sodic plagioclase and Sr depletion may have been initiated, prior to high level fractionation, by plagioclase crystallizing at depth. This may be indicated in units SN.2, SN.4A and SN.4B, where resorbed oligoclase phenocrysts are present.

The Zn content of the rocks increases with the Fractionation Index, although the concentration appears to drop again in the most highly evolved syenites. In section 4.3.4., Zn was seen to be concentrated in alkali

amphiboles, particularly the more evolved ones found in pegmatites. The most fractionated syenites contain acmitic pyroxene rather than alkali amphibole and are correspondingly low in Zn. In the magma at this stage Zn may have been preferentially partitioned into an aqueous phase and the moderate Zn contents of the fenitized Julianehåb Granite supports this proposal.

Nb, Zr, Y and La (Fig. 5.2 (g,h,i and j)) are all concentrated in the late stage, residual magma. Their high charge results in their being stabilised as complexes in the liquid and charge, combined with their large size, means that they are not accepted into the lattices of the common silicates. Zr was detected in alkali pyroxene and amphibole, but its high concentration in the foyaitic rocks suggests that it occurs elsewhere as well. As suggested in section 4.13., the mineral rinkite is a likely reservoir for these elements.

Fig. 5.2 (e and f) shows that Pb and Th also tend to be concentrated in the highly fractionated residual liquids. As with the previous group of elements, Pb and Th, both large ions with high charge, are stabilised as complexes in the magma. It is possible that monazite, a mineral noticed in several of the thin sections, is the chief reservoir for these elements and also for some of the La and Y.

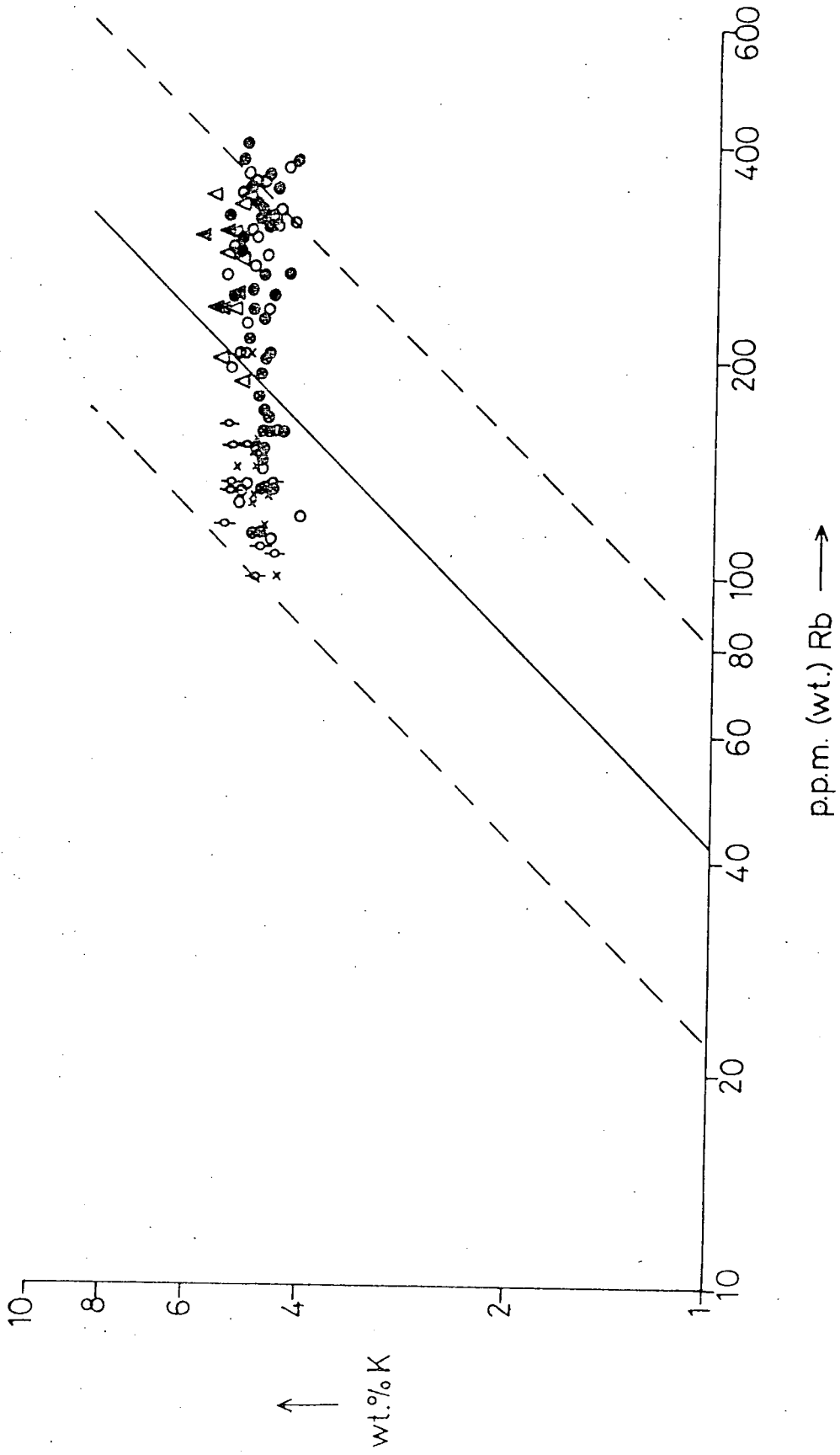
Examination of Fig. 5.2 shows that several elements, particularly Pb, Th, Zr, Nb, Y and La, show very variable concentrations in more evolved rocks. In part this is due to mobilization of these elements, giving depleted and enriched areas, by the action of later intrusions. It may, however, also be a reflection of the sporadic and patchy occurrence of these minerals. Hence, although samples were sufficiently large to contain representative proportions of the major minerals, they contain variable amounts of the sporadic minor minerals in which these elements are concentrated.

Rb (Fig. 5.2 (k)) shows a steadily increasing concentration with fractionation and the K/Rb ratio (Fig. 5.2 (l)), a steady fall. This can be more clearly seen in Fig. 5.3 where wt.%K is plotted against wt. p.p.m. Rb on a log. scale. Also on the diagram is the K/Rb curve of Ahrens et al. (1952), and broken lines indicating the normal limits of scattering. On this plot, the variation shown by the North Qôroq syenites is similar to that found in Kûngnât rocks (Upton, 1960) and South Qôroq rocks (Stephenson, op.cit.). The trend cuts across the curve of Ahrens, due to the abundant crystallization of K-rich alkali feldspar. Rb is preferentially concentrated in the liquid if alkali feldspar is fractionating.

Fig.5.3 K(wt.%) plotted against Rb(wt. p.p.m.) on a log. scale. The solid line on the diagram is the K/Rb curve of Ahrens et al. (1952) and the dashed lines represent the normal limits of scattering.

Symbols used:

- - Unit SN.1A
- ▲ - Unit SN.1B
- ⊖ - Unit SN.2
- △ - Unit ?SN.3
- × - Unit SN.4A
- ⊗ - Unit SN.4B
- - Unit SN.5



#### 5.4. Geographical variation in trace element abundances

Previous workers have attempted, with varying degrees of success, to demonstrate a geographical variation in the concentrations of certain chemical elements, for Gardar alkaline centres. Upton (1964b, Fig.2) successfully showed there to be a distinct variation along the Hviddal composite dyke. Anderson (1974), however, attempted to examine the F content of the Helene Granite by trend surface analysis, without any meaningful pattern emerging. Stephenson (op.cit.) attempted to identify chemical variation in units of the South Qôroq Centre, both with distance from the margins of a unit and height in the unit. No systematic variation in a vertical sense was found and only very limited systematic variation in a horizontal sense. It is likely that Upton was successful in demonstrating chemical variation along the dyke because he was dealing with a linear feature. Intrusions, such as the units of South and North Qôroq, which are essentially circular bodies would perhaps be more fruitfully studied by examining the chemical variation over the total area of their outcrop. With this in mind unit SN.1A was chosen, as it presented the largest outcrop area of any unit and was accessible over most of that outcrop. Also, work on samples collected by Harry and Emeleus had demonstrated

that the unit showed extensive chemical variation. In the summer of 1972, SN.1A was sampled, as far as possible on a grid basis. Certain grid points could not be collected from, either because of lack of exposure, or inaccessibility. Suitable collection sites were chosen, as close as possible to these points. Large representative samples of 'typical syenite' were collected from each specified location. It should be noted that collecting 'typical syenite' involves a subjective decision as to what is typical. The rare mafic bands, xenoliths and pegmatitic patches were avoided. Recrystallized rocks, close to later units were collected and included in later analysis. Including samples collected by Emeleus and Harry, 81 samples of SN.1A were analysed and used to determine geographical variation.

The way in which to determine and present this variation posed a problem. The variation could be subjected to trend surface analysis, which may reveal an overlying broad pattern. Alternatively, simple contouring of the analysed values may be used, either by hand or computer, and may be particularly useful in revealing significant local variations. Both methods were tried. Trend surface analysis involves fitting polynomial surfaces, by computer, to the mapped data; these surfaces

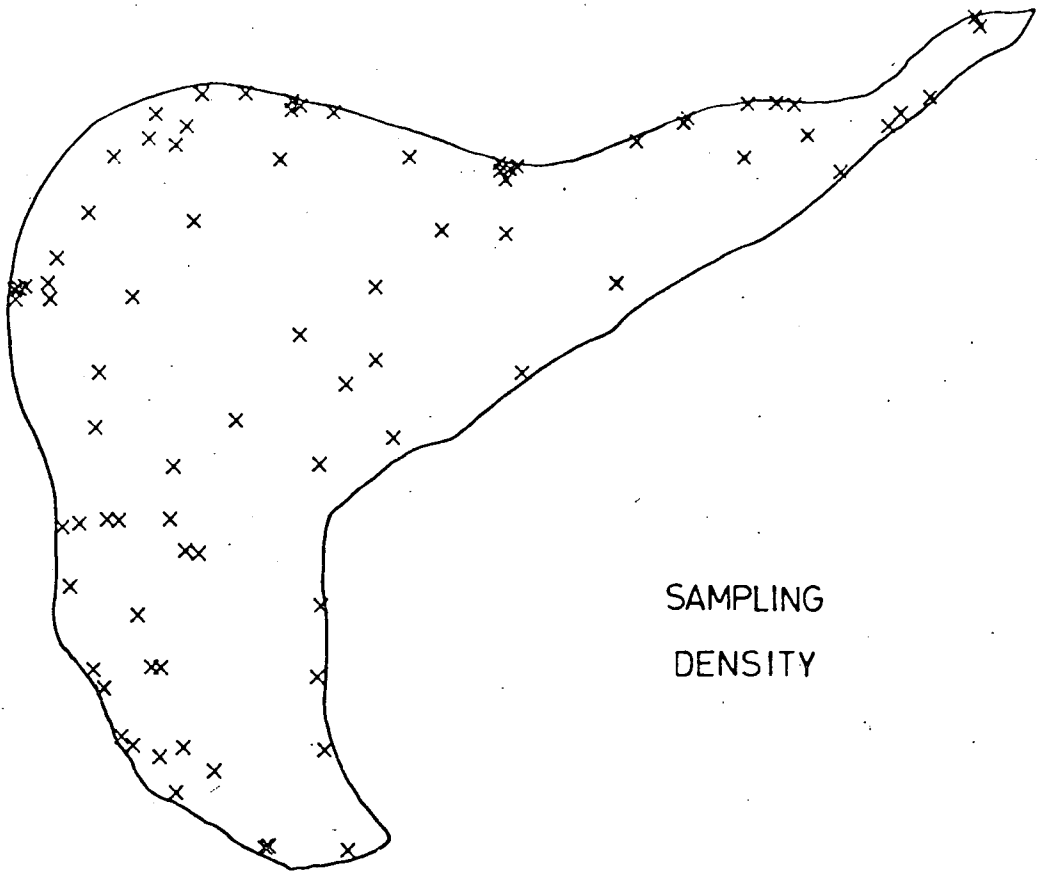
possibly being useful in developing models related to the known geological conditions and processes. The resulting contoured trend surfaces were found to be less useful than the rolling-mean contour maps described below. Trend surface maps for two elements, Nb and Ba, are however, included in Appendix IV.7. The maps show the 2nd-degree surfaces (quadratic), 3rd-degree surfaces (cubic) and 4th-degree surfaces (quartic). The higher degree surfaces account for larger proportions of the total variability and begin to resemble the contoured maps presented below.

Contoured maps are given of a number of trace elements and the K/Rb ratio for unit SN.1A. The contoured maps are based on those obtained from a computer program written by G.K. Westbrook (University of Durham). The basis of the method is given in Appendix IV.7. The computer maps have been modified by hand to take account of areas where sampling was not possible, and to correct for the 6:4, N-S geographical distortion produced by the computer line-printer.

Fig. 5.4(a) shows the sampling density for unit SN.1A and Fig. 5.4(b) the contours for the K/Rb ratio. Fig. 5.4 (c) - 5.4(h) show the contour maps for Ba, Sr, Zr, Nb, Y and La respectively. On all the diagrams the range of values is indicated. Fig. 5.2 showed that Ba and Sr

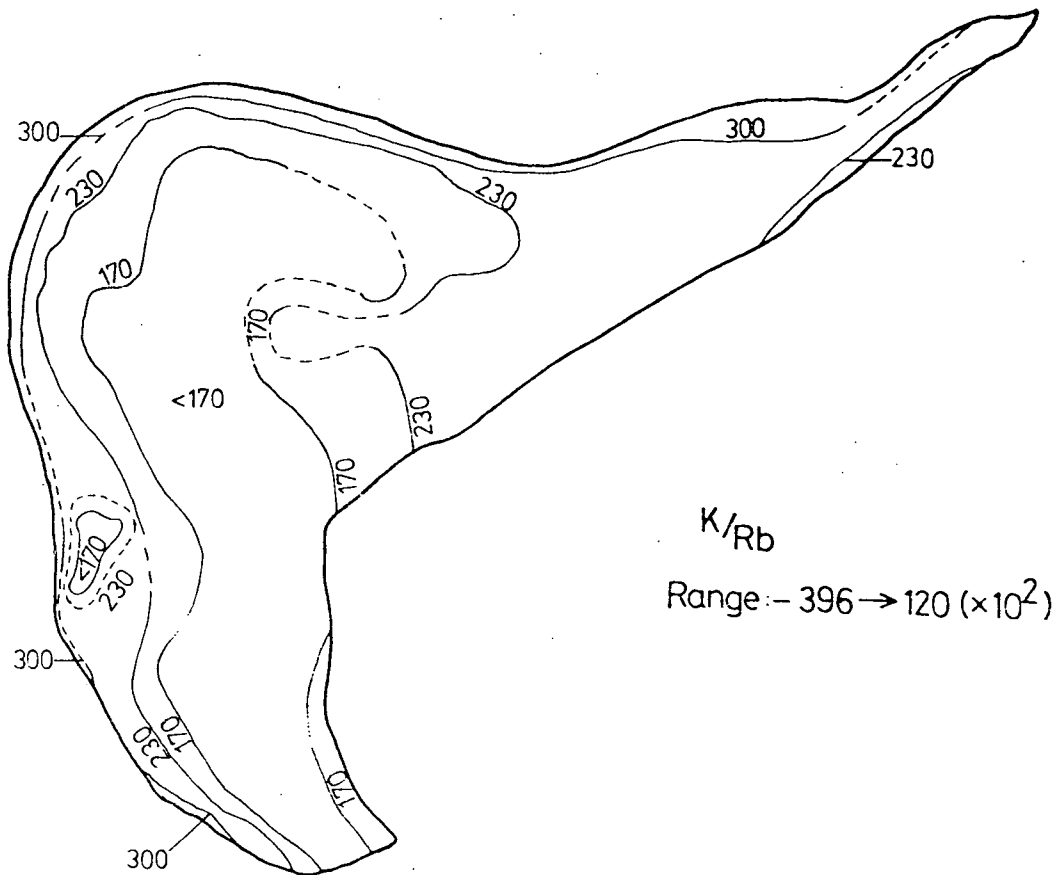
Fig.5.4 (four pages) Contoured maps showing the variation in trace element abundances and the K/Rb ratio over the present outcrop area of unit SN.1A. On each map the contour values and range in values are indicated. Fig.5.4(a) shows the sampling density over the unit.

(a)



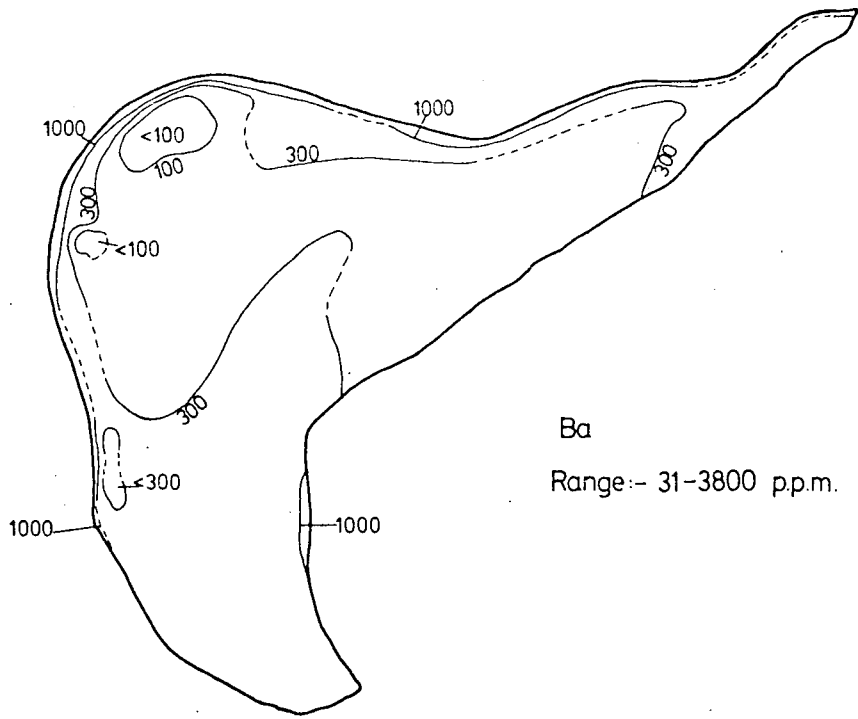
SAMPLING  
DENSITY

(b)



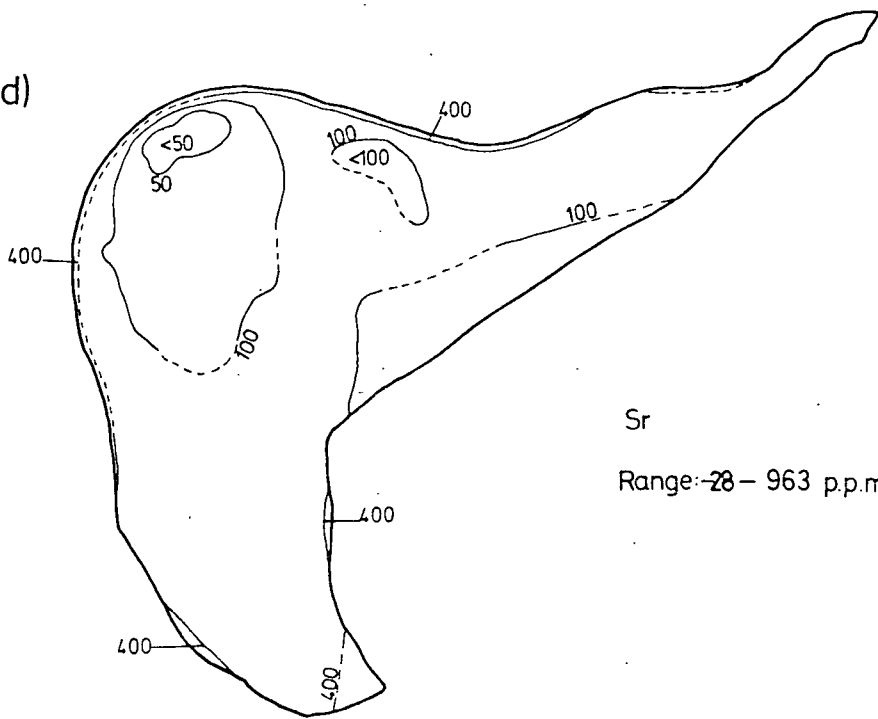
K/Rb  
Range: - 396 → 120 ( $\times 10^2$ )

(c)



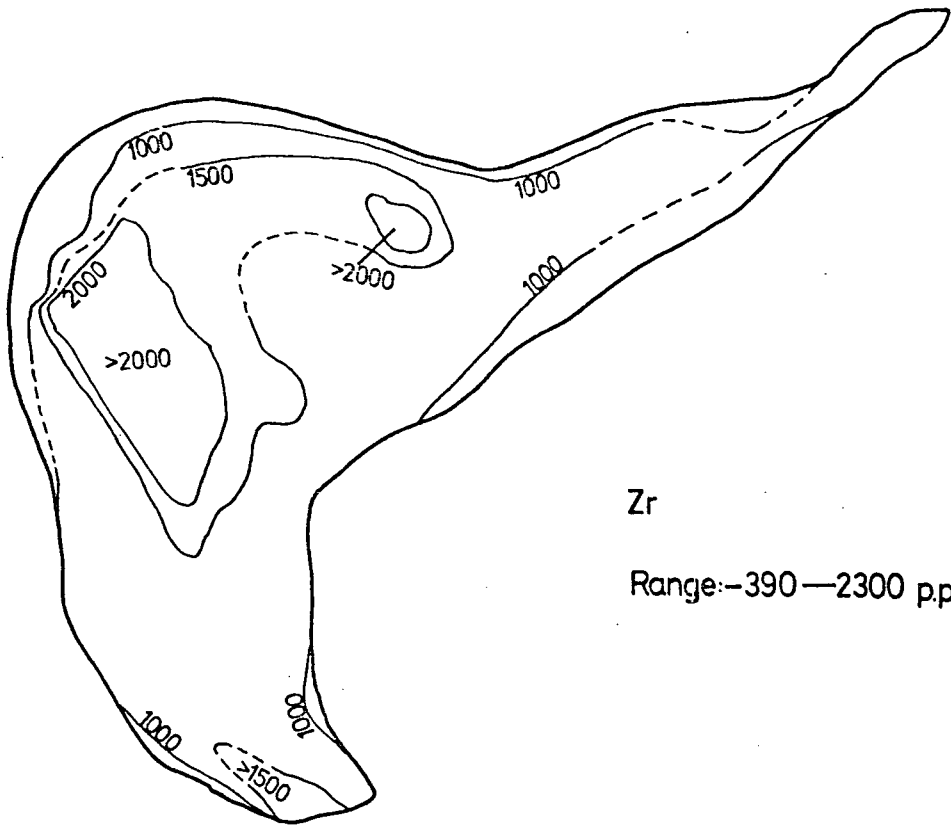
Ba  
Range:- 31-3800 p.p.m.

(d)



Sr  
Range:- 28 - 963 p.p.m.

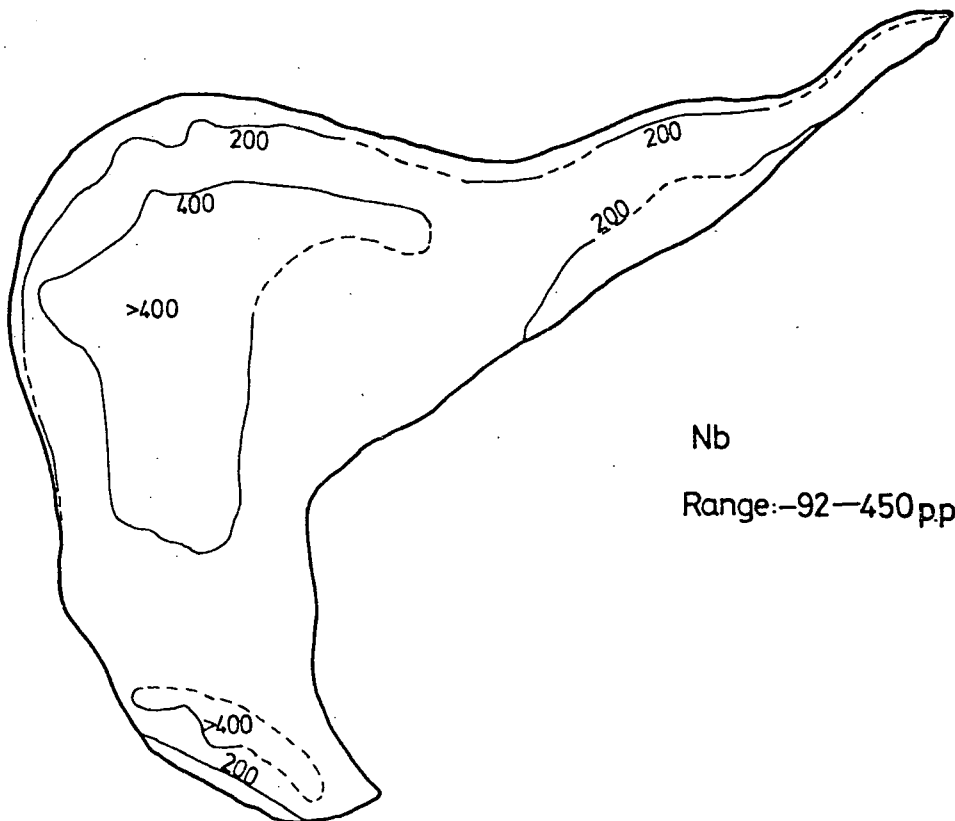
(e)



Zr

Range: -390—2300 p.p.m.

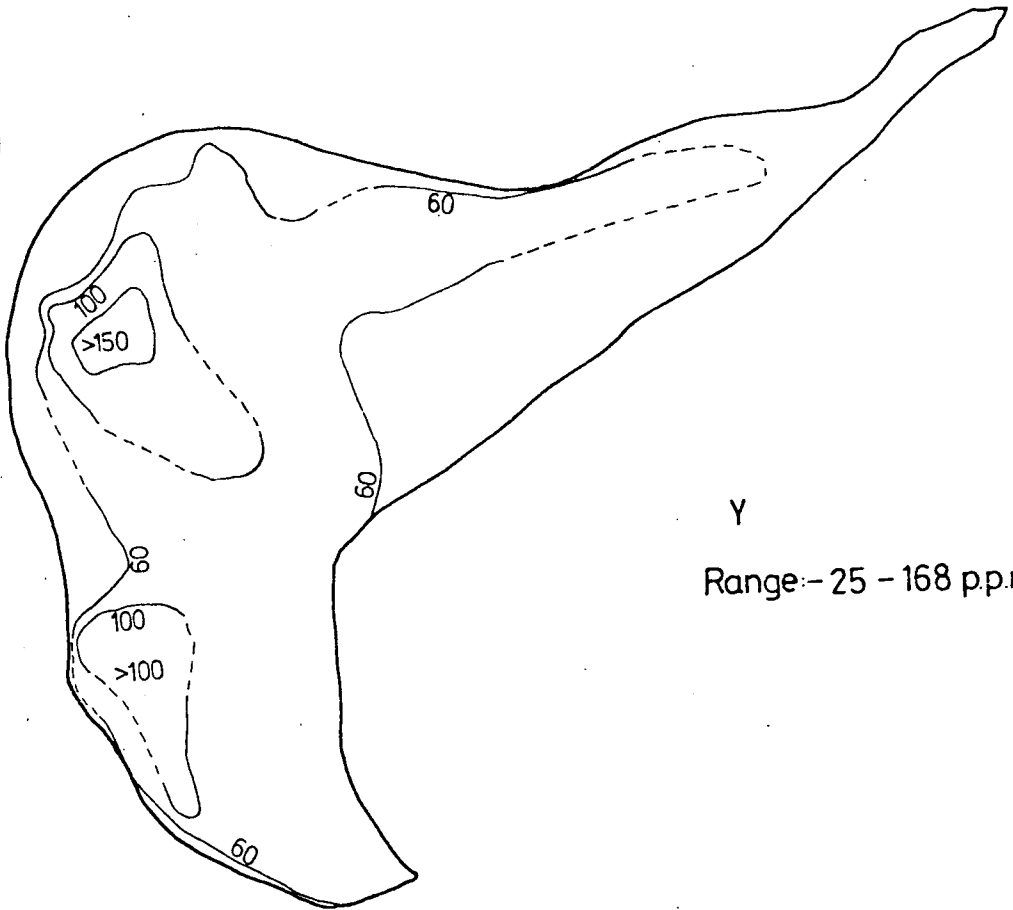
(f)



Nb

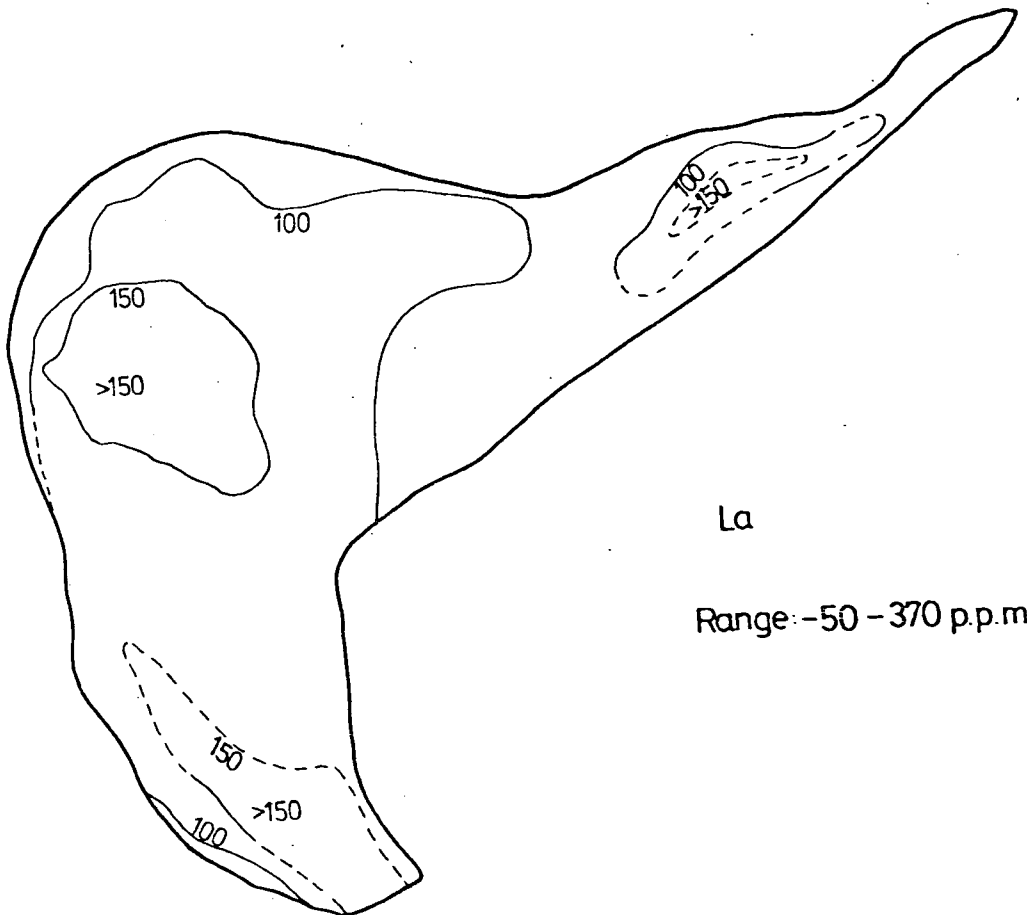
Range: -92—450 p.p.m.

(g)



Y  
Range: -25 - 168 p.p.m.

(h)



La  
Range: -50 - 370 p.p.m.

contents decrease with fractionation, as does the K/Rb ratio, and that Zr, Nb, Y and La contents all increase. Examination of Fig. 5.4, with these facts in mind, reveals several significant features. It should be remembered that the present aerial extent of SN.1A, and that indicated on the maps, is only a proportion of the original extent.

Considering the occurrence of Ba and Sr (Fig. 5.4 (c and d)), both residing in alkali feldspar, the first point to notice is the thin, but persistent outer zone of SN.1A, which is strongly enriched in both these elements. This zone corresponds to the least fractionated augite syenite 'facies' of SN.1A. Moving into the unit, the content of both elements in the samples drops. Of particular interest is the very marked depletion of Ba and Sr in the north-west part of the unit, not far from the margins. This suggests a limited area of highly fractionated syenites, where the feldspars are strongly depleted in both Ba and Sr.

Turning to Fig. 5.4(b), the K/Rb ratio variation, the Rb-depleted, least fractionated rocks are again clearly defined all around the original margins of the intrusion. The Rb-enriched, highly fractionated area coincides approximately to the area of Ba and Sr

depletion, but is extended in a southerly direction.

(Obviously the exact contour pattern depends on the contour values chosen.)

Considering Fig. 5.4(e) - 5.4(h) further points of interest emerge. All these elements are concentrated in the more fractionated rocks. The outer zone of depletion can be seen in every case, as can a zone of strong enrichment in these residual elements in the north-western portion of the unit, coinciding approximately with the zone showing low K/Rb ratios and Ba and Sr depletion. However, further areas of enrichment and depletion can be seen for these four elements. Depleted zones occur close to younger intrusive units, especially SN.1B, and SS.2 of the South Qôroq Centre. A short distance into SN.1A from the contact with SS.2 is a distinct zone where these elements are enriched. This demonstrates conclusively that, as suggested previously, these elements are mobilised by the metamorphic effects of a later intrusive unit and concentrated a short distance into the older unit. The zone where these elements, particularly Zr, La and Nb, are concentrated is rich in identifiable rinkite crystals.

Although zones of enrichment and depletion of Zr, Nb, Y and La close to younger intrusive units have been

explained, what explanation can be given for the very obvious zone, strongly enriched in these elements and depleted in Ba and Sr? It seems peculiar that this area of highly fractionated rocks should occur in the north-west quadrant of SN.1A, until account is taken of the topographic effects. In this area, the level of erosion is much deeper than elsewhere in the unit. Whereas, over the bulk of the unit erosion is only thought to have proceeded to just below the roof-zone, in this area deeper levels are exposed. Hence, the geographical distribution in Fig. 5.4 can be explained by postulating an inner, more highly fractionated 'core' to unit SN.1A, only exposed in the north-west part of the unit, where erosion has been sufficiently deep. This is demonstrated schematically in Fig. 5.5, on which the outer augite syenite zone and the inner highly fractionated zone are marked. In this diagram the boundaries of the various zones have been extrapolated to give a simplified structure. Such a regular structure has implications with regard to the mechanisms of formation of these syenite variants. These implications are discussed in Chapter 7.

It can be seen that examination of the geographical variation shown by various elements has confirmed the

Fig.5.5 Schematic section through the North Qôroq Centre, showing the effect of depth of erosion in exposing the proposed, highly fractionated core of unit SN.1A.

Abbreviations used:

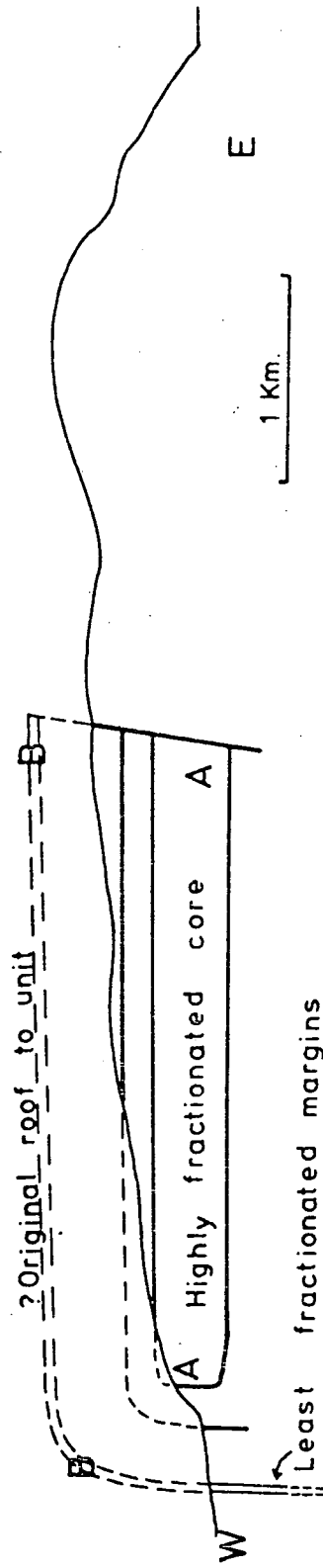
A - Highly fractionated core  
of unit SN.1A

B - Less fractionated margins  
of unit SN.1A, of augite  
syenite composition.

SN.1A

YOUNGER UNITS

Height  
(m)  
1000  
750  
500  
250  
0



Least fractionated margins

1 Km.

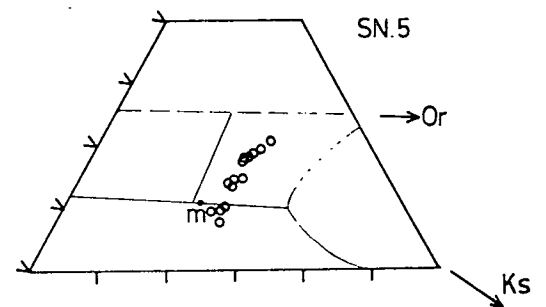
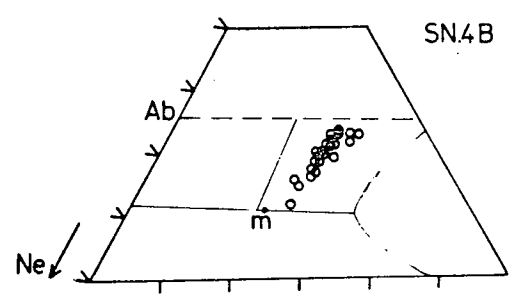
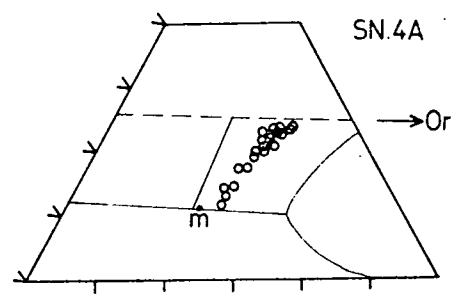
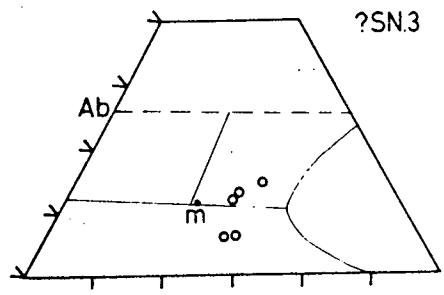
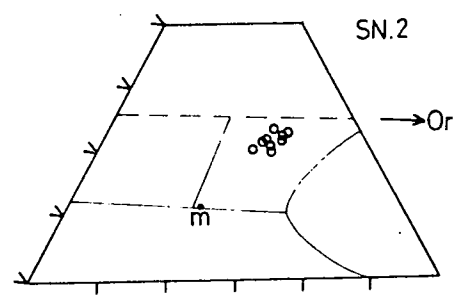
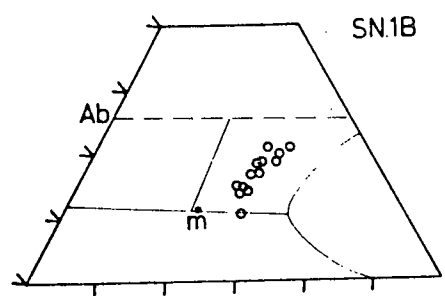
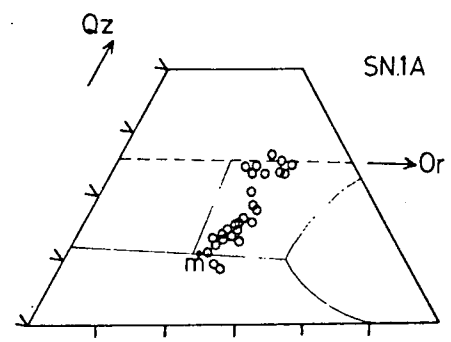
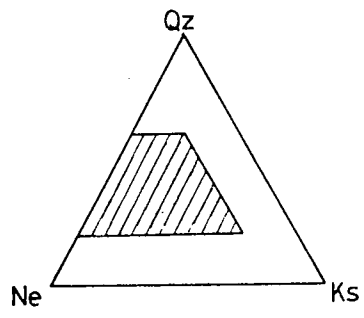
mobilizing effect of later intrusive units and suggested a model for the evolution of SN.1A (see Chapter 7), which may be applied to other units.

#### 5.5. Normative mineralogy and the residua system

The vast majority of North Qôroq syenites have normative albite, orthoclase and nepheline exceeding 80%, and can reasonably be plotted in the 'residua system', Qz-Ne-Ks (Bowen, 1937). Augite syenites, particularly from marginal SN.1A, containing relatively high concentrations of MgO, FeO and CaO, can not be adequately represented in this system. Highly fractionated syenites of SN.1A, SN.1B, ?SN.3 and SN.5 tend to be peralkaline ( $(Na+K) > Al$ ). They are plotted on the residua system diagram in this account, but in reality lie off the plane of the diagram, in the Al-poor section of the larger system  $Al_2O_3 - Na_2O - K_2O - SiO_2$ .

Fig. 5.6 shows a number of syenites from each of the North Qôroq units, plotted in the appropriate under-saturated portion of the residua system. Also given in the figure are the phase boundaries at 1Kb.P.H<sub>2</sub>O (Hamilton and MacKenzie, 1965). As indicated in section 4.16.7., this is considered to be an appropriate water pressure for syenites of North Qôroq, particularly in their later stages of evolution.

Fig.5.6 Normative variation shown by the various units of North Qôroq, in terms of the end-members quartz-nepheline-kalsilite (the 'residua system' of Bowen, 1937). The feldspar join is indicated by a dashed line. Solid lines indicate the phase boundaries at 1Kb. P.H<sub>2</sub>O and the 'unique fractionation curve' (Hamilton and MacKenzie, 1965). The undersaturated minimum in the system is indicated by the letter 'm'.



wt. %

Examination of Fig. 5.6 shows that all of the syenites follow a relatively smooth trend. Analyses from SN.1A range from around the albite-orthoclase join to just inside the nepheline field at 1Kb.P.H<sub>2</sub>O. Certain augite syenites of SN.1A are just oversaturated. This may be due to assimilation of country rock by these marginal syenites, a factor discussed in Chapter 7. SN.1B would probably show a similar trend to SN.1A, but insufficient analyses were obtained. Units SN.2, SN.4A and SN.4B commenced crystallization just to the undersaturated side of the feldspar join. SN.2 shows no extensive range in compositions, but both SN.4A and SN.4B show smooth trends to the region of the nepheline-feldspar phase boundary. SN.3, despite there being fewer analyses, can be seen to be highly undersaturated, two analyses plotting well into the field of nepheline. Analyses of even the least fractionated rocks of SN.5 plot well below the feldspar divide, and the most fractionated rocks again plot within the nepheline field. Highly evolved syenites from the Grønødal-Ika intrusion (Gill, 1972) also plot in the nepheline field, as do certain of the South Qôroq syenites (Stephenson, 1973), and the Kangerdlugssuaq syenites (Kempe, Deer and Wager, 1970). It should be remembered that many of these analyses, plotting within the nepheline field, are peralkaline and in reality lie off the plane of the

diagram. Nevertheless, the position of these analyses may indicate that the nepheline-feldspar phase boundary has been displaced towards the nepheline-kalsilite join by either higher  $P.H_2O$ , as demonstrated by Hamilton and Mackenzie (op.cit), or by additional magma components. Kogarko (1974) showed that an increase in the acid volatile component in a magma tends to depress strongly the feldspar-nepheline phase boundary towards the nepheline-kalsilite join. Hence, concentrations of HF and particularly HCl, both of which were present in North Qôroq syenites, may have displayed this effect.

As the syenite analyses follow a well-defined, generally straight trend towards the undersaturated minimum, the magmas were probably changing composition along a 'thermal trough', analogous to the unique fractionation curve of Hamilton and MacKenzie. The analyses, however, tend to lie on the K-rich side of this unique fractionation curve. This is a common feature of undersaturated alkaline rocks and Hamilton and MacKenzie note that analyses of naturally occurring phonolites and nepheline syenites plot on the potassic side of the isobasic minimum at 1Kb. $P.H_2O$  (n. in Fig. 5.6). This displacement is probably due to additional components present in natural liquids. The peralkaline condition displaces the thermal trough in the residua system, but

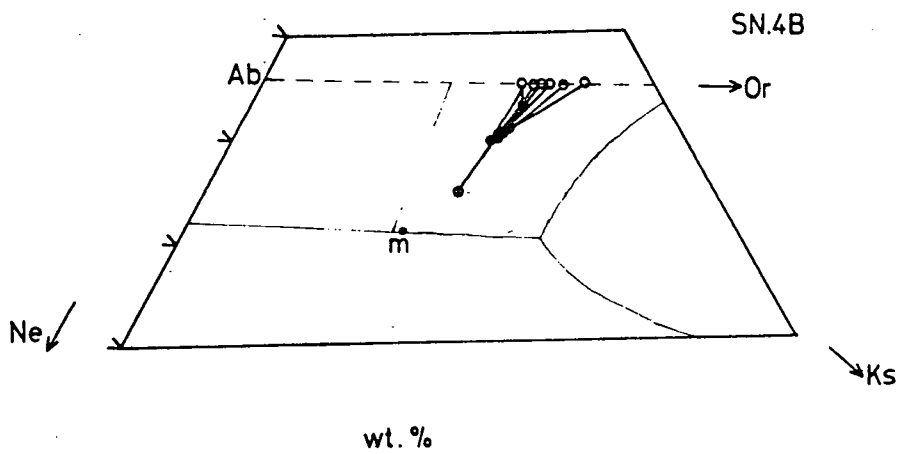
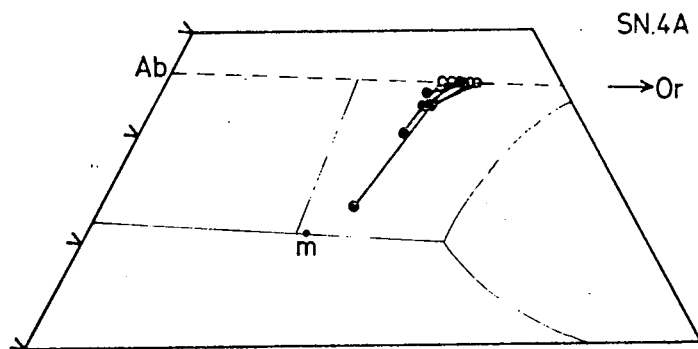
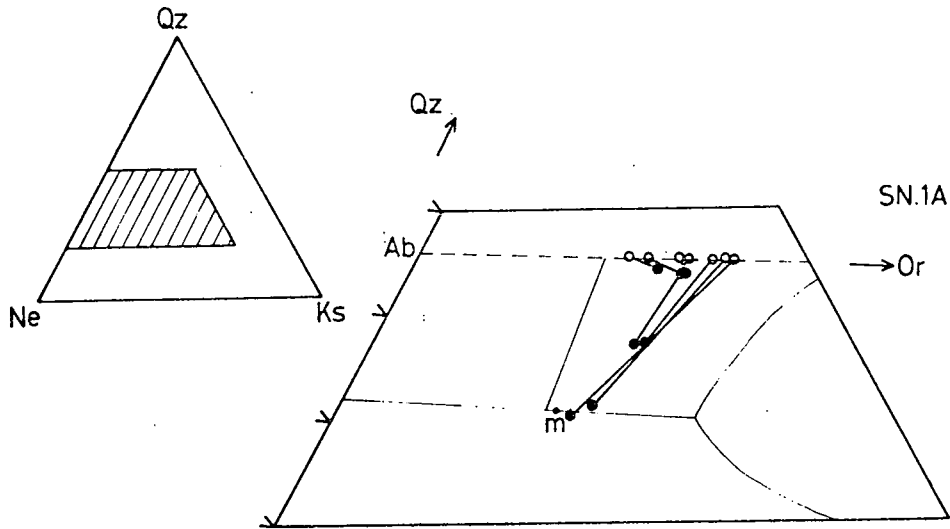
the displacement is towards the sodic portion of the system in undersaturated rocks. This may explain why the trend shown by North Qôroq syenites becomes noticeably more sodic with the increased degree of fractionation and increased peralkalinity. The much more potassic nature of the proposed thermal trough in less fractionated rocks may be caused by the presence of Ca, which James and Hamilton (1969) have shown to have a marked effect on the position of the trough, at least in the oversaturated portion of the residua system. Further displacement of the thermal trough towards the potassic side of the diagram may be caused by acid-volatile components. Kogarko (op.cit.) indicated that, as well as displacing the nepheline-feldspar phase boundary, increased acid volatile content also displaces the thermal trough towards the potassic side of the residua system.

Close examination of Fig. 5.6 shows that, for unit SN.1A, the trend towards undersaturation is concave towards albite. This suggests that the initial magma was on the sodic side of the thermal trough, and probably proceeded rapidly towards the thermal trough by crystallization and separation of a feldspar more sodic than the magma. Similar, concave 'fractionation curves' are found in the Hviddal dyke nepheline syenites (Upton, op.cit.)

and in unit SS.4B, an augite syenite, of South Qôroq (Stephenson, op.cit.). The remaining units of North Qôroq, however, show either a straight trend towards undersaturation, or one which is slightly convex towards albite. This suggests that these liquids commenced crystallization on the potassic side of the thermal trough and approached the trough by separation of a still more potassic feldspar. This explanation can be critically examined by plotting compositions of early formed alkali feldspars (core compositions) on the residual system diagram and connecting them to the host rock analysis, which presumably approximates to the magma from which these feldspars crystallized. This is done in Fig. 5.7 for units SN.1A, SN.4A and SN.4B. It can be seen that most of the feldspar analyses plot close to where the postulated thermal trough intersects the albite-orthoclase join. Nevertheless, feldspars from the least fractionated rocks of SN.1A tend to be more Na-rich than either the host rock or feldspars from more fractionated rocks. In units SN.4A and SN.4B the reverse can be seen to be true. Here, feldspars from the least fractionated rocks are more potassic than both the host rock and feldspars from more fractionated rocks. This adds strong weight to the theory that SN.1A magma originally lay on the sodic side of the thermal trough and SN.4A and SN.4B

Fig.5.7 Selected rock compositions for units SN.1A, SN.4A and SN.4B, plotted in terms of their normative quartz, nepheline and kalsilite contents, and joined by tie-lines to co-existing feldspar core compositions (ignoring plagioclase cores in units SN.4A and SN.4B). The phase boundaries and the isobaric minimum, 'm', are the same as those given in Fig. 5.6.

- — rock compositions
- — Feldspar core compositions.



magmas on the potassic side. It also suggests that feldspar fractionation is the dominant process causing the syenite magmas to change composition, from the region of the feldspar thermal divide to the nepheline-feldspar boundary. Postulated crystallization trends are given in Fig. 5.8 and can be compared with fractionation curves obtained by Hamilton and MacKenzie.

Fig. 5.9 shows rock analyses for SN.1A and SN.4 (A and B) plotted in the residua system. Tie-lines join the rock compositions to co-existing nepheline and feldspar, the feldspars being rim or groundmass analyses. These feldspars are much more K-rich than the alkali feldspar core analyses shown in Fig. 5.7. This is a reflection on the fact that, when these feldspars crystallized, a Na-rich nepheline co-precipitated with them. Consideration of the crystallization path of SN.4 magma reveals the reason for zoning, both towards K-rich and Na-rich rims in the feldspars of these rocks. As for the majority of units, the magma lies on the potassic side of the thermal trough, the first feldspar to crystallize is more K-rich than the magma and its crystallization and separation results in the residual magma composition moving towards the thermal trough. As the magma approaches the trough, the feldspar becomes more Na-rich, i.e. it zones towards

Fig.5.8 A comparison of proposed fractionation trends shown by North Qôroq syenites with fractionation curves obtained by Hamilton and MacKenzie (1965). Phase boundaries are as given in Fig. 5.6.

Top-Hamilton & Mackenzie.

Bottom- This account.

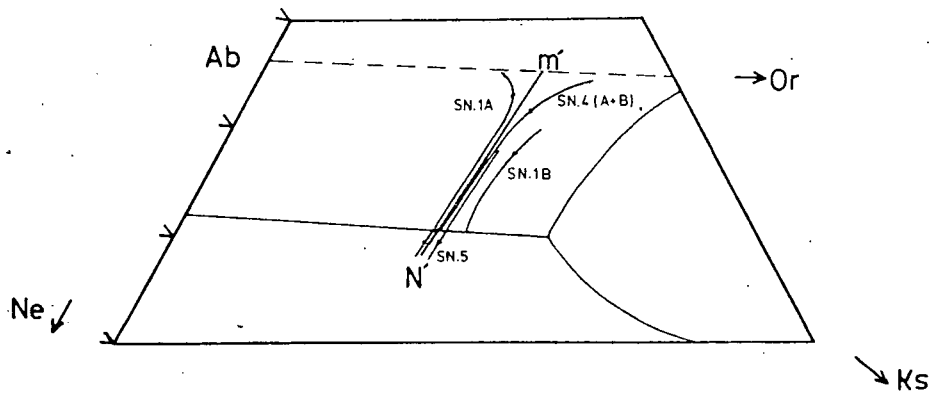
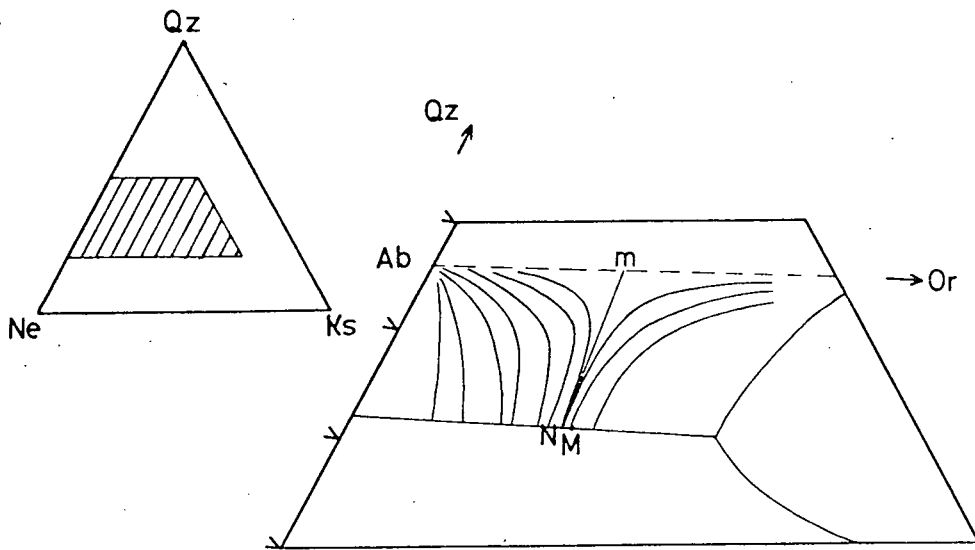
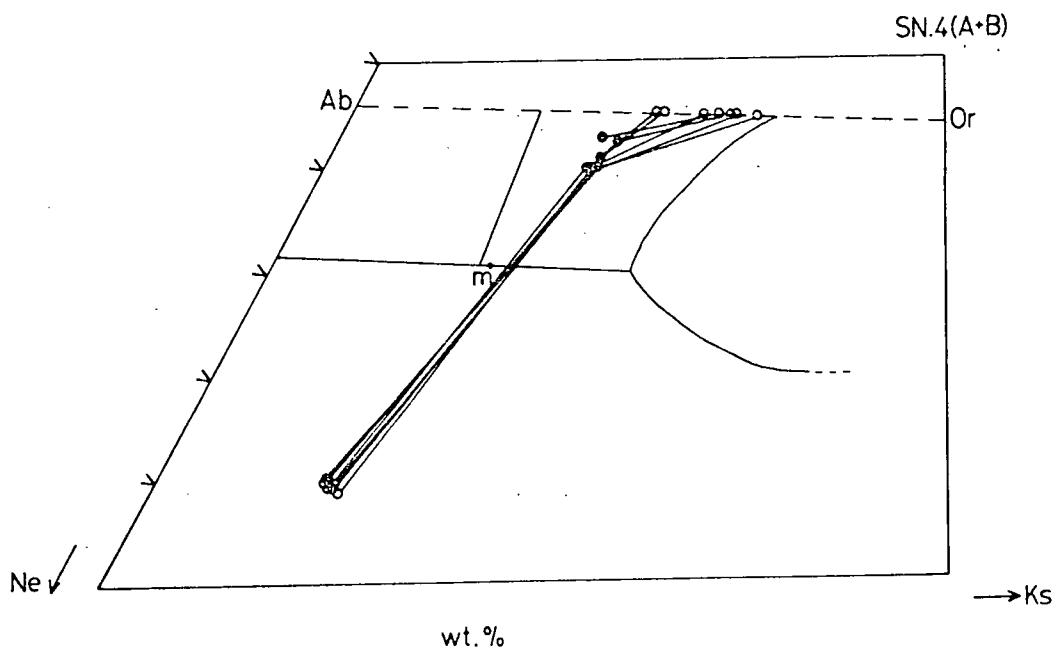
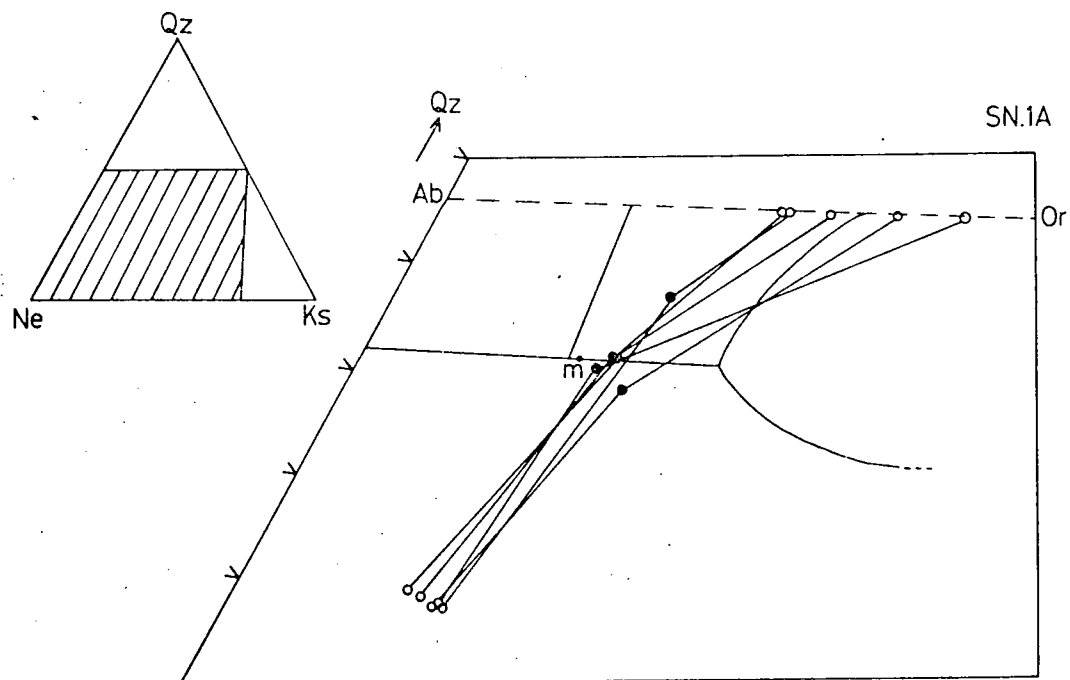


Fig.5.9 The normative compositions of selected rocks of units SN.1A, SN.4A and SN.4B plotted in the 'residua system' and joined by tie-lines to co-existing nepheline and alkali feldspar compositions. Nepheline compositions are generally from groundmass nephelines and feldspar compositions from either the groundmass or from feldspar rims. Phase boundaries etc. are as given in Fig. 5.6.

- — Rock compositions
- — Nepheline and Feldspar compositions.



sodic rims. As the magma composition proceeds down the thermal trough, towards the nepheline-feldspar phase boundary, its progress is controlled by separation of a feldspar of constant composition ( $Ab_{54}Or_{46}$  approx.), assuming the thermal trough is linear. When the phase boundary is reached, nepheline crystallizes and, alongside it, a much more K-rich feldspar, which results in zonation of the feldspar to give K-rich rims. The liquid then proceeds to the undersaturated minimum, crystallizing nepheline and alkali feldspar.

Further examination of Fig. 5.9 reveals that the nepheline-rock-feldspar tie-lines tend to kink rather than form a straight line. For South Qôroq the tie lines are usually straight and Stephenson (1973) interprets this as meaning that the trends shown for syenitic rocks in the residua system reflect liquid lines of descent. Do the North Qôroq trends shown in Fig. 5.6, therefore not reflect changes in liquid composition? The answer is that they probably do and that the kink is due to the contemporaneous crystallization of sodalite and possibly analcite, together with groundmass nepheline and feldspar. Also, as mentioned in section 4.6.3., some of the feldspars may have undergone K-metasomatism. Small groundmass feldspars would have been more susceptible to

this process and it may be a further reason for the kink in the nepheline-rock-feldspar tie-line.

#### 5.6. The peralkaline condition

North Qôroq syenites become peralkaline with fractionation. This is indicated by the presence of acmite and occasionally sodium metasilicate in the rock norms. The highest value attained by the peralkalinity index,  $(Na+K)/Al$ , is 1.30.

In Fig. 5.10 syenites are plotted in the system  $Al_2O_3 \cdot 3SiO_2 - K_2O \cdot 3SiO_2 - Na_2O \cdot 3SiO_2$ . This is a plane almost at right angles to that of the residua system and was used by Gill (1972) to demonstrate the peralkaline nature of Grønnedal-Ika phonolites. The system has also been used by Thompson and MacKenzie (1967) and Nash et al. (1969), but was referred to incorrectly as  $Al_2O_3 \cdot 6SiO_2 - Na_2O \cdot 6SiO_2 - K_2O \cdot 6SiO_2$  (see Gill, 1972, p.96). Two diagrams are used in Fig. 5.10; one for the units which fractionate to give peralkaline foyaites, i.e. SN.1A, SN.1B and SN.5; and one for those which only fractionate to give weakly peralkaline or non-peralkaline syenites, i.e. SN.2, SN.4A and SN.4B. Also shown in the diagrams are tie-lines to co-existing feldspar core compositions. The starred points A, B,  $A_1$  and  $A_2$  refer to the average compositions of the first amphibole to

Fig.5.10

(a) Syenite compositions of units SN.1A, SN.1B and SN.5 plotted in the system  $Al_2O_3 \cdot 3SiO_2 - K_2O \cdot 3SiO_2 - Na_2O \cdot 3SiO_2$  (see text). Certain of the syenite compositions are joined, by tie lines, to co-existing feldspar compositions. The compositions of early-formed amphibole and biotite are also indicated.

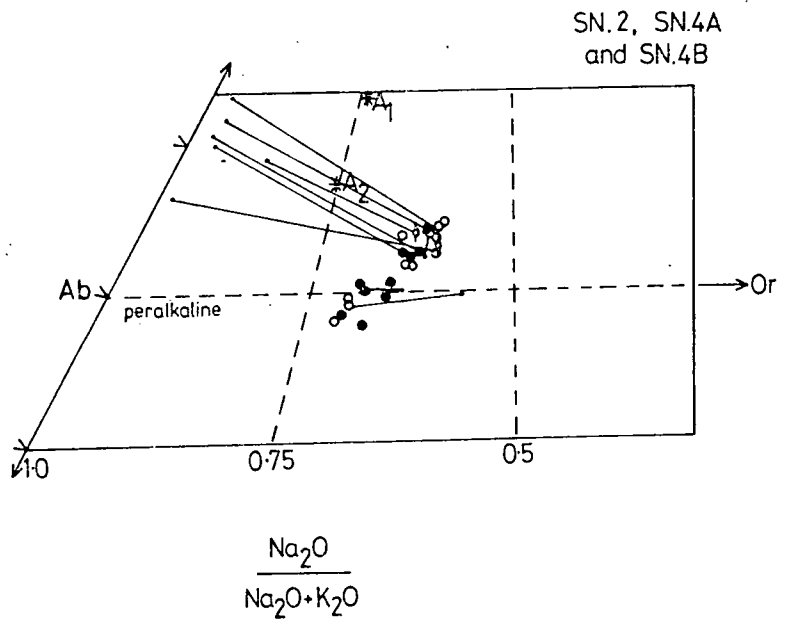
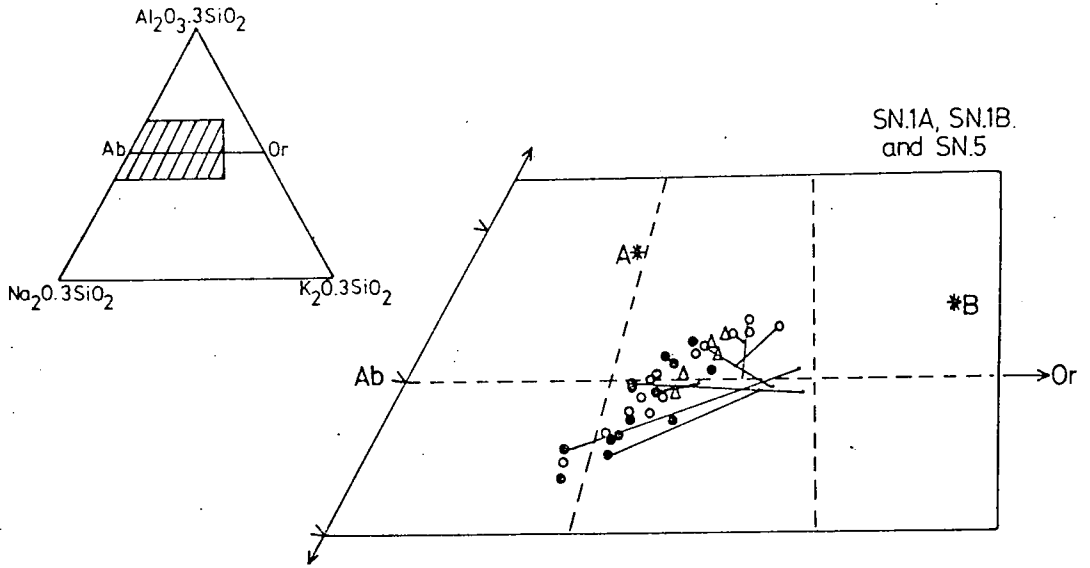
Symbols used:

- - Unit SN.1A
- △ - Unit SN.1B
- - Unit SN.5
- A \* - First formed amphibole in unit SN.1A
- B \* - First formed biotite in unit SN.1A
- - Feldspar core compositions

(b) Syenite compositions of units SN.2, SN.4A and SN.4B, plotted as for Fig.5.10(a). Syenite compositions are again joined to co-existing feldspar compositions. The compositions of the first formed amphiboles in units SN.2 and SN.4(A+B) are indicated.

Symbols used:

- ⊙ - Unit SN.2
- - Unit SN.4A
- - Unit SN.4B
- A<sub>1</sub> \* - First formed amphibole in unit SN.2
- A<sub>2</sub> \* - First formed amphibole in units SN.4(A+B)
- - Feldspar core compositions



crystallize in SN.1A, the first biotite in SN.1A, the first amphibole in SN.2 and the first amphibole in SN.4 (A and B), respectively.

Considering firstly Fig. 5.10(a), it can be seen that rock analyses trend from the peraluminous (Ca content negligible) to the peralkaline field in a distinctly linear fashion. This is because the magma is changing composition along a thermal trough, which is the thermal trough of the residua system extended into the volume of the tetrahedron  $\text{SiO}_2 - \text{Al}_2\text{O}_3 - \text{Na}_2\text{O} - \text{K}_2\text{O}$ . Normally, fractionation of a Ca-bearing feldspar is invoked as the cause of the peralkaline condition. This is referred to as 'the plagioclase effect' (Bowen, 1945). However, examination of Fig. 5.10 shows that in the least fractionated, peraluminous rocks the feldspar cores are always more peralkaline than the host rock. Separation of these feldspars would tend to produce a more peraluminous residual magma. Even in relatively rapidly cooled marginal rocks of SN.1A, where there would be little chance of feldspar settling, the feldspar cores, although calcic, are not sufficiently calcic to promote the peralkaline condition. It is only when the liquid has become peralkaline that fractionation of alkali feldspar, 'the orthoclase effect' of Bowen and Schairer (1964), increases the peralkalinity (and sodicity)

of the residual liquid. SN.1A, SN.1B and SN.5 contain early-formed amphibole and in the case of SN.1A early-formed biotite. The compositions of early-formed amphibole (A) and early-formed biotite (B) are indicated on Fig. 10(a), and it can be seen that both these minerals are strongly metaluminous or peraluminous. It is proposed, therefore, that in these units the peralkaline trend was initiated by the fractionation of amphibole and biotite and that, once a deficiency in alumina had been achieved, feldspar fractionation accentuated the tendency towards peralkalinity. It is also possible that Al-rich augitic pyroxene and opaques assisted the trend towards peralkalinity.

In Fig. 5.10(b) a different picture emerges. Here, all the units have feldspar phenocrysts with resorbed oligoclase cores. These core compositions are plotted in Fig. 5.10(b) and joined to their host rock composition by tie-lines. It can be seen that fractionation of feldspars of this composition would have promoted the peralkaline conditions.  $A_1$  is a typical amphibole composition of SN.2 and  $A_2$  of SN.4A and SN.4B. Hence, fractionation of amphibole would also assist the trend towards peralkalinity. Biotite present in these rocks, and Al-rich opaques and pyroxenes, may also have played a part.

Once again, when the residual liquid had become peralkaline, continued fractionation of alkali feldspar would have further increased the peralkalinity.

Engell (1975) related rocks of Ilimaussaq to the 'peralkaline residua system',  $\text{Na}_2\text{O} - \text{Fe}_2\text{O}_3 - \text{Al}_2\text{O}_3 - \text{SiO}_2$  (Bailey and Schairer, 1966). He stated that Ilimaussaq magma was fractionating towards a eutectic where acmite, albite, nepheline, sodium disilicate and liquid co-existed. However, the effect of  $f.\text{O}_2$ ,  $P.\text{H}_2\text{O}$ , and particularly the activity of a diopside component in the pyroxene, is to displace considerably the phase boundaries. Consequently, the plots given by Engell do not convincingly prove his hypothesis; the eutectic in the experimentally determined system and Engell's endpoint for the Ilimaussaq liquid trend being extensively displaced relative to each other (Engell, 1973, Fig.3). Stephenson, plotting South Qôroq syenites in the same system notes an even greater displacement relative to the experimentally determined phase boundaries. North Qôroq syenites, when plotted in this system, occur in much the same position as those of South Qôroq (Stephenson, 1973, Fig. 5.8). It is very probable that the residual liquids of North Qôroq are approaching a eutectic involving acmite, albite, nepheline, sodium disilicate and liquid,

but, because other components greatly affect the position of phase boundaries, this cannot be convincingly shown on a phase diagram.

From the data presented it can be seen that North Qôroq magmas fractionated towards a strongly undersaturated, peralkaline liquid, rich in Na and 'residual elements'.

## CHAPTER SIX: FENITIZATION AND THE AQUEOUS PHASE

### 6.1. Introduction

Fenitization, as the term is used in this account, refers to the metasomatic alteration of pre-existing country rocks. These include basement granite-gneisses (Julianehåb Granite), amphibolite in the Julianehåb Granite, and quartzites and basalts of the Eriksfjord Formation (see Section 2.2.). A degree of metasomatic alteration, described in section 3.4., has also affected pre-existing syenites. Fenitization is ill-defined and have been used in the past to describe metasomatism associated with carbonatite bodies. Woolley et al. (1972) has suggested it should be used simply to imply metasomatism of a strongly alkaline nature. In this account fenitization refers to the action of aqueous fluids originating from, and possibly co-existing with, a residual peralkaline magma, typified by the more evolved North Qôroq syenites.

Limited fenitization has been described from around other Gardar plutons. Macdonald et al. (1973) give information on the metasomatism of troctolitic gabbros of the Kûngnât Fjeld Syenite Complex and Upton (1960) describes metasomatism of gneisses around the Western Lower Layered Series (W.L.L.S.) of the same complex. Ferguson (1964)

mentions fenitization of the Julianehåb Granite for a distance of up to 40 m. from the margins of the Ilímaussaq intrusion, further along shear zones. Sodic pyroxene and sodic amphibole are both developed. In the Igaliko Complex itself, Emeleus and Harry (1970) have shown there to be strong evidence of metasomatism in the Motzfeldt Centre, where xenoliths of country rocks are again rich in sodic pyroxene and amphibole. Stephenson (1973) indicates that quartzites of the Eriksfjord Formation in the close vicinity of South Qôroq show the development of acmitic pyroxene.

The present account is an attempt to look, in detail, at the metasomatic changes, both geochemical and mineralogical, around the North Qôroq Centre. Prior to recent years, little mineralogical data on fenites has been available due to the small grain size of the sodic pyroxene and amphibole formed. Sutherland (1969) attempted, with limited success, to separate fenitic amphibole and pyroxene from East African rocks, but she admits a degree of mutual contamination. The advent of the electron microprobe facilitated analysis of fenitic phases. The present account is based on 52 probe analyses of fenitic amphiboles, 17 of pyroxenes, 6 of micas (Appendix III.4) and 27 X.R.F. 'whole rock' analyses for major and trace

elements (Appendix IV.6). A later section of this chapter deals with the behaviour of water in the North Qoroq magmas and the effects produced, either by a co-existing aqueous phase, or an extremely hydrous late stage melt.

## 6.2. Fenitization of the country rocks around the North

### Qôroq Centre

#### 6.2.1. Field relations

Fenitization can be seen in the country rocks around the North Qôroq Centre, particularly the Julianehâb Granite, and in Julianehâb Granite and quartzite xenoliths found in the centre. The fenitization is thought to be related to the intrusion and evolution of the outer units of North Qôroq, namely SN.1A and SN.1B. Development of alkali amphibole and pyroxene is restricted to rocks within 60m. of the centre, perhaps slightly further along fracture zones. The hydrothermal fluids, however, appear to have caused a low grade of fenitization for a distance of 200m. or more from the margins of the centre.

#### 6.2.2. Petrography

In the Julianehâb Granite both the metamorphic and metasomatic effects of the intrusion of the syenites can be seen in thin section. Metamorphic effects are evident perhaps 60m. from the intrusion where the Julianehâb Granite shows a tendency to display granoblastic textures.

Within 10m. of the intrusion the rims of alkali feldspar crystals are embayed and replaced by a granophyric intergrowth of quartz and alkali feldspar (Plate 40). This texture, not seen in the normal granite of the area, is strongly suggestive of partial melting. Upton (op.cit.) indicates that a relatively large amount of partial melting of gneiss was caused by the intrusion of the W.L.L.S. of the Kûngnât Complex. The partial melting and metamorphism affecting the Julianehåb Granite around North Qôroq presumably occurred at the time of intrusion of units SN.1A and SN.1B. The metasomatism, however, may not have occurred until some short interval later, when these units had had a chance to evolve an aqueous phase.

The fenitization affecting the Julianehåb Granite can be divided, in a somewhat arbitrary fashion, into 3 zones. Increasing grade of these zones corresponds very roughly to decreasing distance from the margins of the intrusions.

The typical petrographic features of the outer zone, the least fenitized, may occur as close as 30m. to the margins of the North Qôroq Centre. This zone certainly occurs 200m. from the centre, and may well occur at even greater distances. In this zone the feldspars, both sodic plagioclase and K-feldspar, are extremely cloudy and altered in appearance, and any biotite is completely

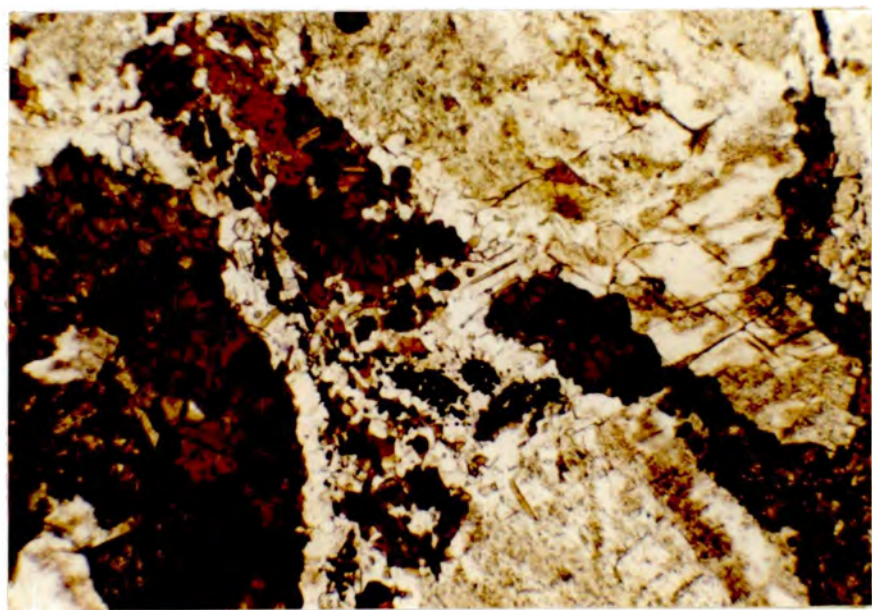
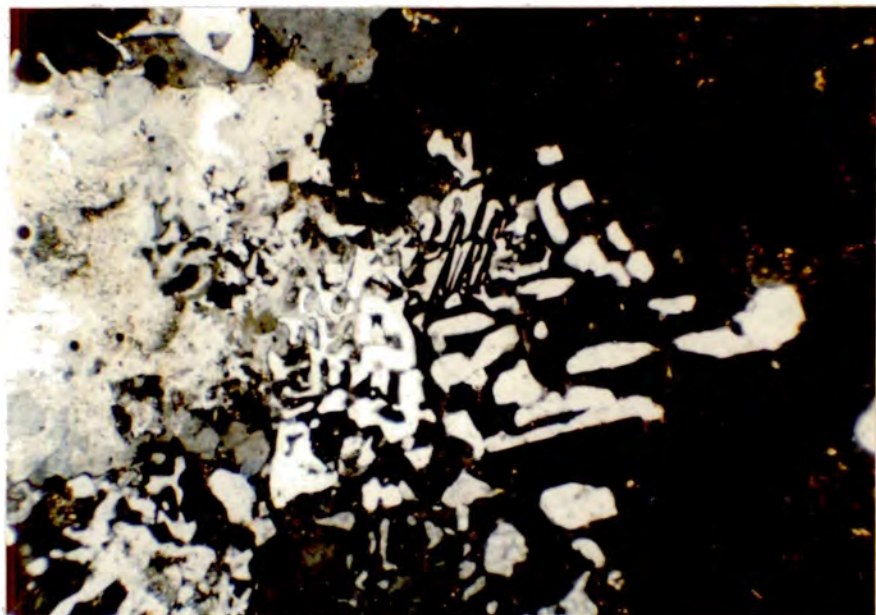
chloritised. Microfractures in the granite contain haematite and larger fractures contain fluorite, carbonate and epidote.

The middle zone of fenitization occurs up to 60m. out from the margins of the intrusion, and as close as 10m. to the intrusion. Here, the feldspars, although still altered, contain small but discernable mica flakes, probably resulting from recrystallization of sericite. The most characteristic features of this zone are the occurrence, in veins and patches, of red-brown mica and amphibole of 'muddy' brown or green-brown hue. A typical development of these two minerals is shown in Plate 41. The minerals are associated with small amounts of opaque material, apatite, fluorite and carbonate, and there is a noticeable decrease in the quantity of quartz in the granite. Those parts of the middle zone which have suffered more extensive fenitization occur either closer to the intrusion contacts or along fracture zones and joints, where the fenitizing fluids would be expected to flow with ease. Here, the red-brown mica may be absent and the amphibole is less 'muddy' in appearance and pleochroic in shades of green and yellow.

The inner zone of fenitization which has undergone the most dramatic alteration, is restricted to the immediate vicinity of units SN.1A and SN.1B, and to xenoliths enclosed

Plate 40. Granophyric intergrowth of quartz and alkali feldspar, seen in the Julianehåb Granite close to its contact with unit SN.1A of the North Qôroq Centre. The texture is suggestive of partial melting. (Julianehåb Granite, Sp.No. 52223, crossed polars, X30).

Plate 41. Fenitized Julianehåb Granite, showing the patchy development of red brown mica and green brown amphibole. Taken from the middle zone of fenitization. (Fenitized Julianehåb Granite, Sp.No. 155041, X30).



in these syenites. The feldspars of these rocks are fresh, but original K-feldspar has been replaced by a mosaic of numerous crystals of sodic plagioclase (Plate 42). This mosaic of albite was described by Ferguson (op.cit.) as occurring in the Julianehåb Granite close to the borders of the Ilímaussaq intrusion, and indicates strong Na-metasomatism. Quartz is relatively rare in the inner zone and has been replaced by numerous small crystals of sodic amphibole and pyroxene. The amphibole is either pleochroic from deep indigo-blue to grey-blue, or in shades of pale lilac and pale blue-green. The outer part of the inner zone may show only the growth of indigo-blue amphibole, whereas in xenoliths of granite in the syenites and in the inner parts of the inner zone a green sodic pyroxene is developed, either as the only mafic phase, or co-existing with the indigo-blue or lilac to blue-green amphibole. In fenite veins pyroxene often forms the inner parts and amphibole the outer. Mica is absent from the inner zone, and the only other phases present are occasional opaques, carbonate and fluorite.

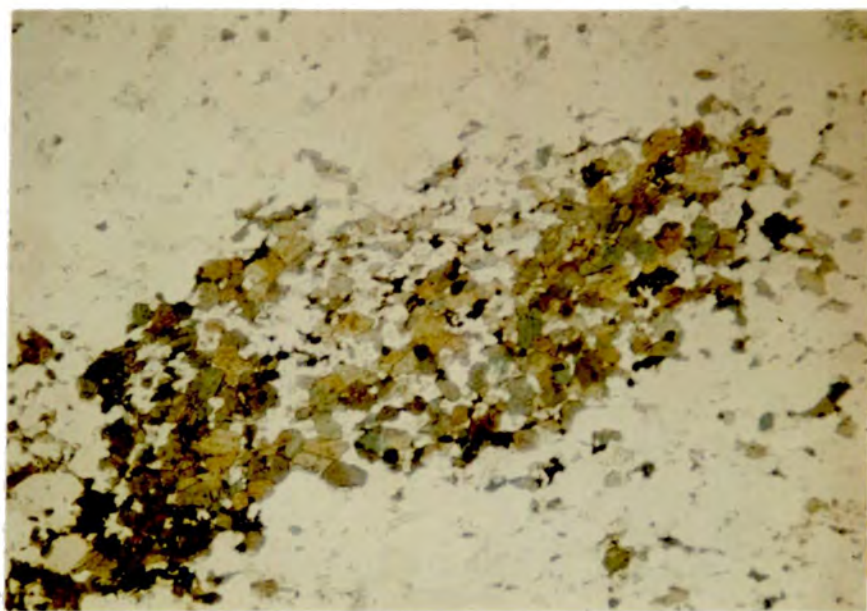
With the exception of the 'albitization' the general sequence to progressively higher grades of fenitization is similar to that recorded by Currie and Ferguson (1971) around the carbonatite complex at Callander Bay, Ontario.

Eriksfjord Formation sandstones (quartzites) show extensive fenitization where large xenoliths are enclosed in syenite of SN.1B. The mineralogical development is similar to that of the inner zone of the Julianehåb Granite fenites, with quartz being replaced by patches of pale lilac to pale blue-green amphibole and green sodic pyroxene. A typical development of these two minerals in quartzite is shown in Plate 43. The amphibole and pyroxene resemble those described by Woolley et al. (1972) from fenitized quartzite around the Loch Borralan Complex.

An interesting 'dyke' rock (52243) occurs in the Julianehåb Granite close to the contact with SN.1A. It is very irregular in outcrop and is presumably a pre-Gardar 'amphibolite dyke' but it was described by Harry (1961) as an 'Fe-rich band' due to its rusty colour in hand specimen. Thin section examination shows the dyke in the vicinity of North Qôroq to be composed dominantly of a bright orange mica (X=yellow, Y=Z=orange-red) and smaller quantities of apatite. Veins running through the micaceous rock show an interesting paragenesis. They are composed of calcic minerals and show a distinct zonation. An inner zone is composed of fluorite, carbonate and an isotropic mineral which probe analysis showed to be hydro-grossular garnet. This zone is surrounded by a zone rich in diopsidic pyroxene and epidote, and this

Plate 42. Mosaic of sodic plagioclase replacing original K-feldspar in the inner zone of fenitization. (Fenitized Julianehåb Granite, Sp.No. 52224, crossed polars, X30).

Plate 43. Typical fenitic development of pale lilac to pale blue-green amphibole and green sodic pyroxene in a quartzite xenolith from unit SN.1B. (Fenitized Eriksfjord Formation quartzite, Sp.No. 155104, X30).



in turn by a zone rich in pale green amphibole, zoning outwards to pale brown amphibole and then to the orange mica. These veins suggest late stage calcic metasomatism.

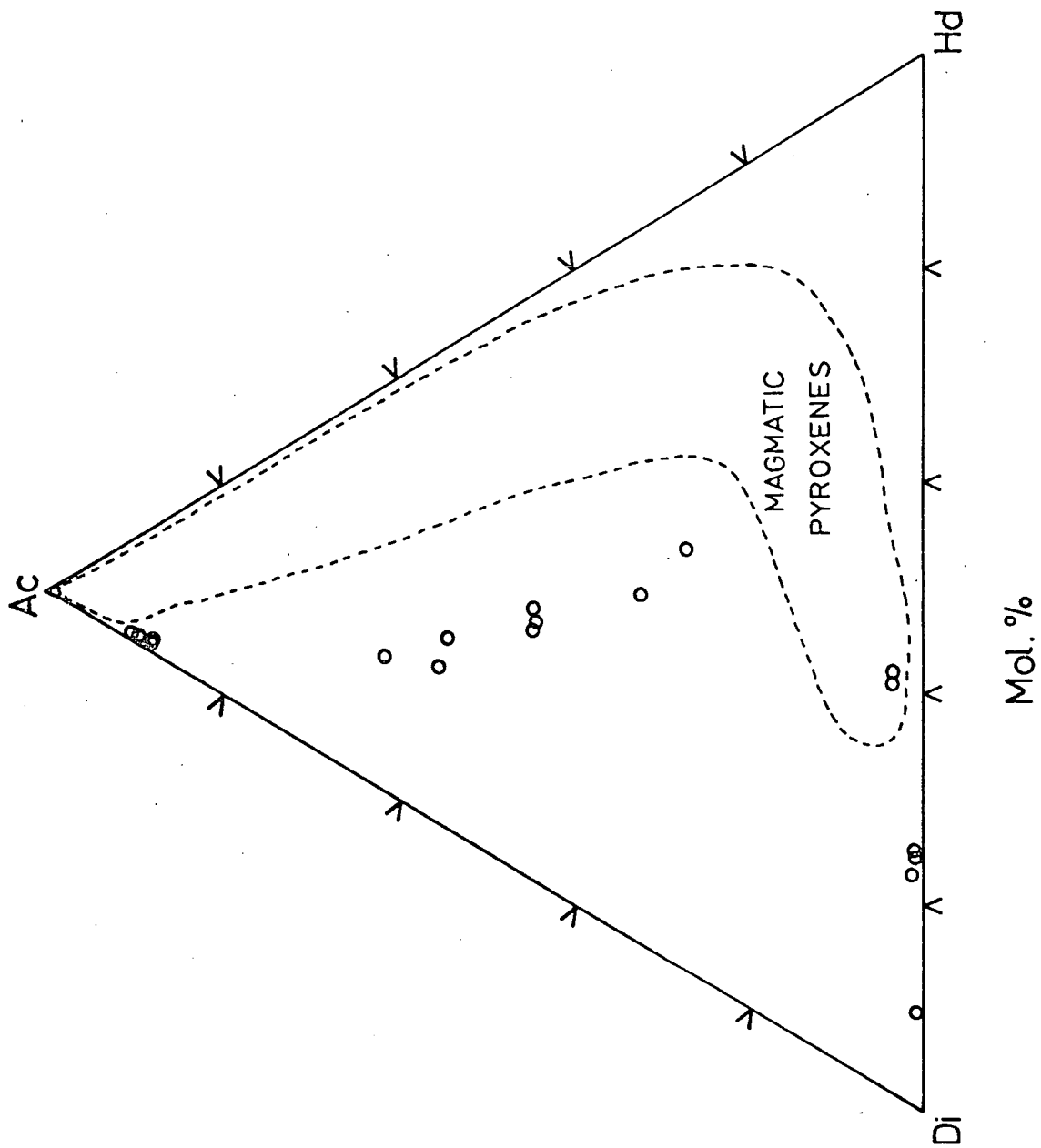
The Eriksfjord Formation basalts show little evidence of any fenitization. The only metasomatic feature of these rocks, where they abut against SN.1A, is a thin and imper-sistent development of apatite, biotite and opaques.

### 6.2.3. Mineralogy

Fenitic pyroxenes, amphiboles and biotites were analysed by electron microprobe.

The pyroxene analyses are plotted, as were the magmatic pyroxenes, in the system Ac.-Di.-Hd. (Fig. 6.1). The field of North Qôroq magmatic pyroxenes, indicated by a dashed line, is given for comparison. The four most diopsidic pyroxenes are from the fenitized 'dyke' rock mentioned above (52243) and the remainder from the Julianehåb Granite. It can be seen that the fenitic pyroxenes are generally Na-rich. It is interesting to note that they parallel the pyroxenes of the recrystallized rocks in so much as they trend towards acmite before getting appreciably hedenbergite-rich. Similar, relatively Mg-rich, sodic pyroxenes are described by Woolley et al. (op.cit.) occurring around the Borralan Complex. Of the pyroxene trace elements, Zr is only present in very low concentrations and Mn is in moderate amounts (0.1-0.9 wt.%)

Fig.6.1 Fenitic pyroxene compositions plotted in terms of the end-members Diopside-Hedenbergite-Acmite. The field of magmatic pyroxene compositions is indicated on the figure.



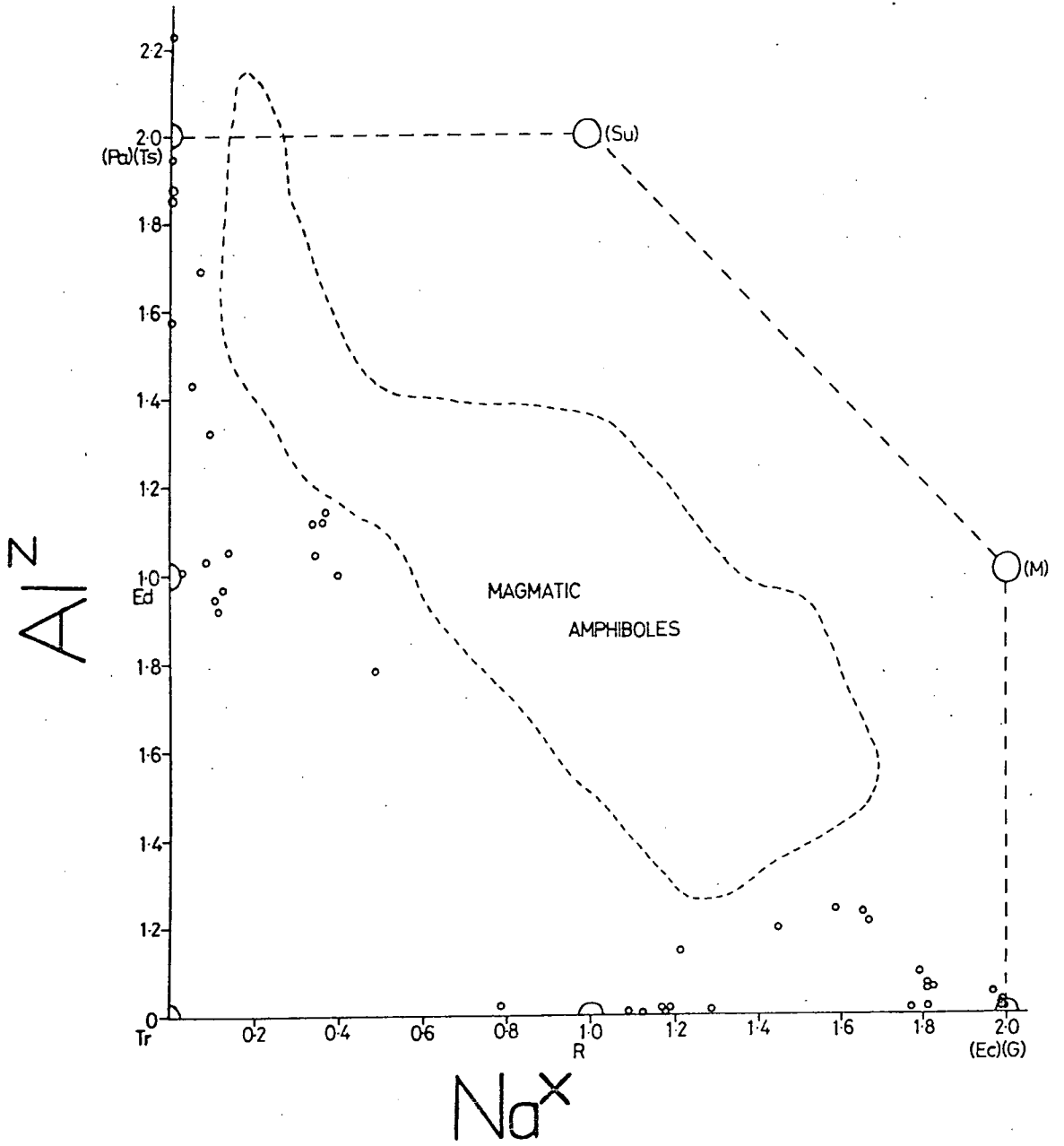
MnO). Al occurs in the less sodic pyroxenes in concentrations of up to 3.8 wt.%  $\text{Al}_2\text{O}_3$ , but is virtually absent from the more acmitic pyroxenes, in contrast to the magmatic acmites where Al can be an important constituent (section 4.2.3.). The Ti contents resemble those of the magmatic pyroxenes, the fenitic acmites containing up to 2.2 wt.%  $\text{TiO}_2$ .

Numerous complete analyses of fenitic amphiboles were obtained (Appendix III.4) and they show as much variation as those from the syenites. The fenitic amphiboles range in composition from pargasite-magnesiohastingsite-edenite compositions, through richterite-ferrorichterite, to compositions intermediate between eckermannite and arfvedsonite. These latter compositions can be termed magnesioarfvedsonites and are similar to amphiboles described from East African fenites (Sutherland, *op.cit.*). A similar, but less extensive range in amphibole composition was found by Woolley *et al.* (*op.cit.*).

Fig. 6.2 shows the amphiboles plotted on a diagram of  $\text{Na}^x$  against  $\text{Al}^z$ , with the field of magmatic amphibole compositions indicated by a dashed line. Examination of this diagram reveals a number of points of interest. The most obvious is that the fenitic amphiboles plot outside the magmatic field and exhibit a greater chemical variation.

Fig.6.2 Fenitic amphibole compositions, plotted, as were the magmatic amphiboles on a diagram of the Na content of the X site against the Al content of the Z site. The field of magmatic amphibole compositions is indicated on the figure.

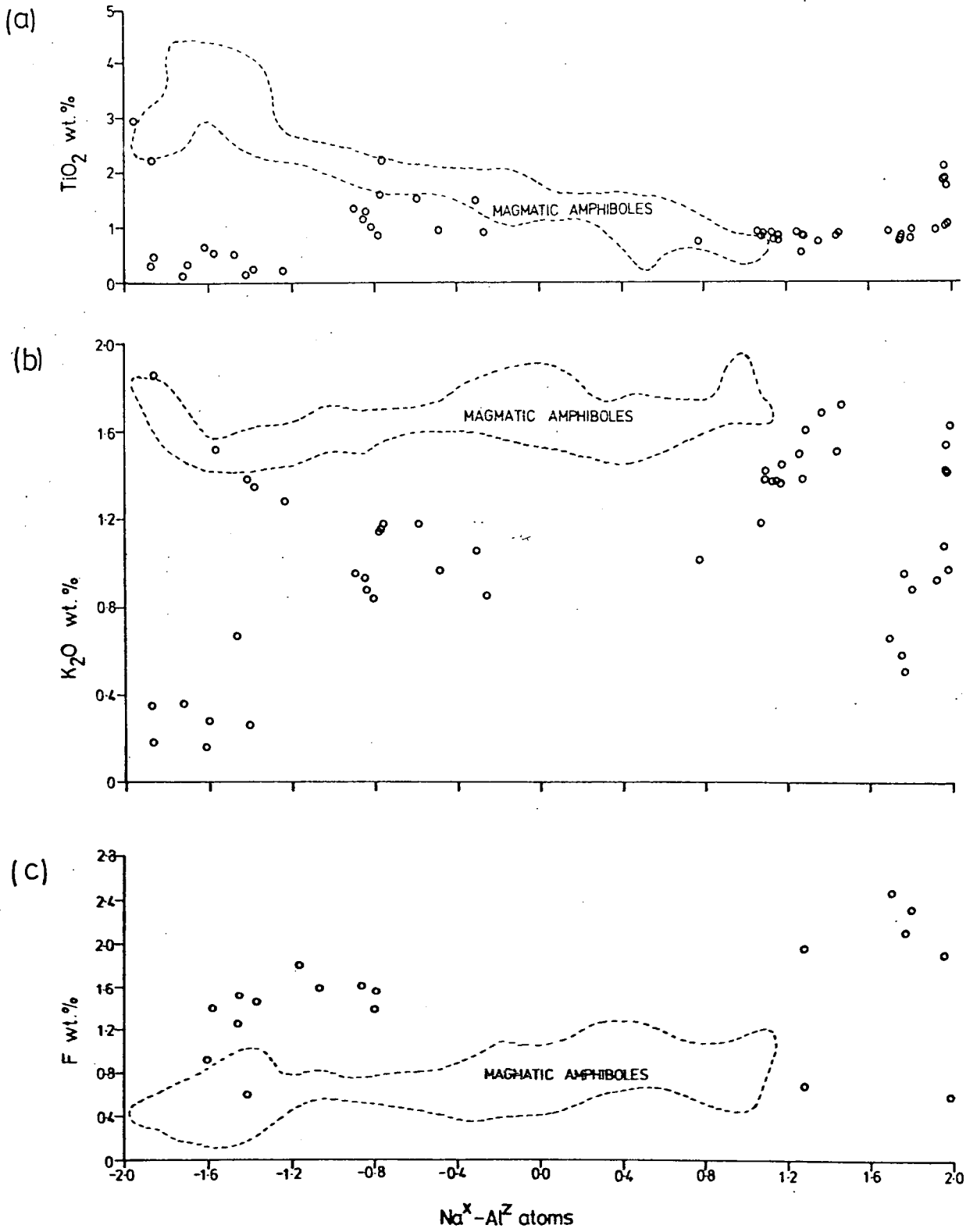
End-member compositions in the Phillips classification scheme are indicated by their first letters (see text).

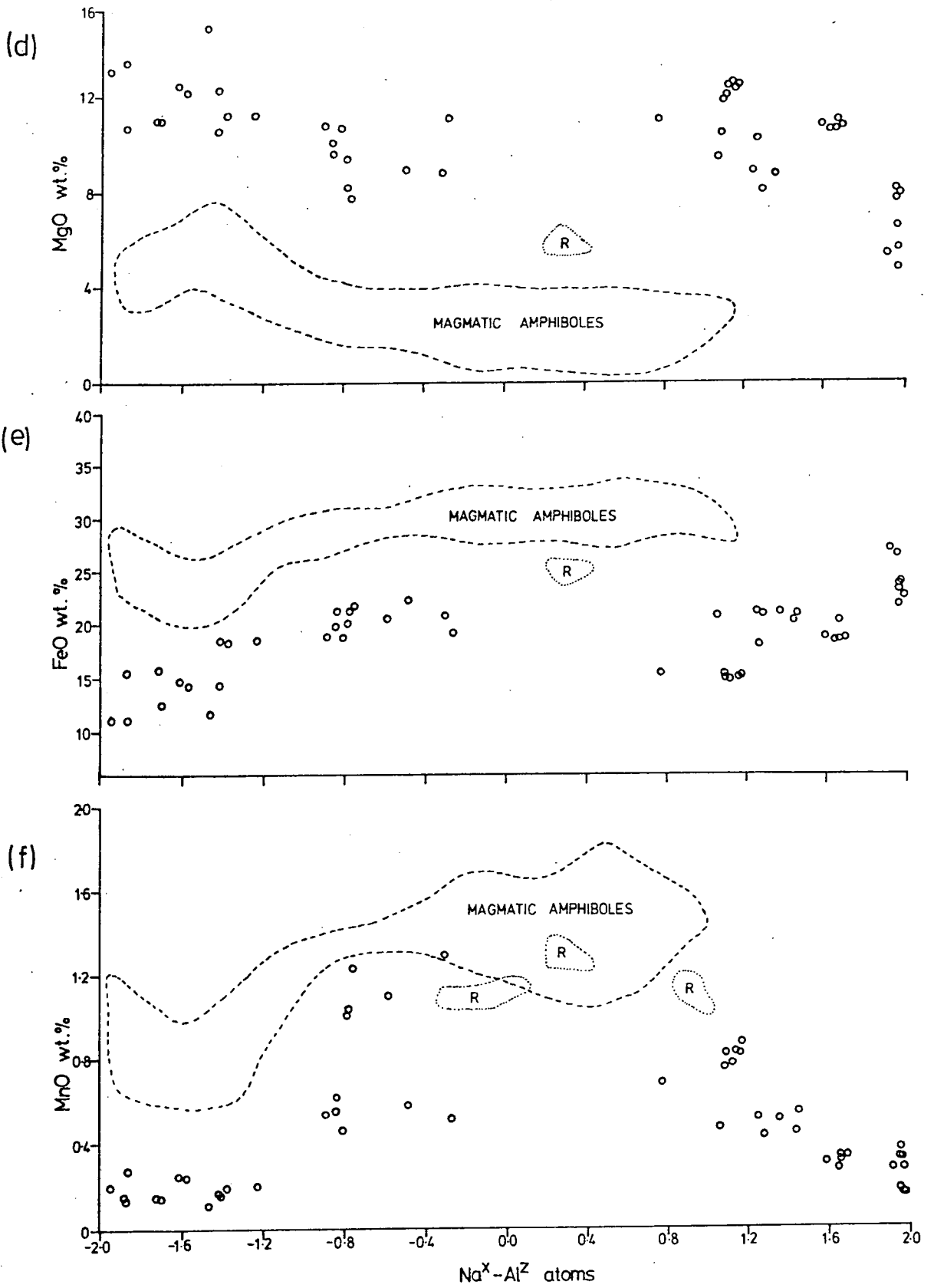


In general, a fenitic amphibole with a particular content of Na assigned to the X site has a smaller quantity of Al in the tetrahedral (Z) site than a magmatic amphibole with the same  $\text{Na}^{\text{X}}$  content.

Fig. 6.3 (a-f) shows selected trace element concentrations in the amphiboles plotted against the fractionation index of  $\text{Na}^{\text{X}}\text{-Al}^{\text{Z}}$  used in section 4.3. The field of magmatic amphibole compositions is again indicated by a dashed line, and there is remarkably little overlap, on all the diagrams, between this field and the fenitic amphibole compositions. The fenitic amphiboles are low in  $\text{TiO}_2$ , apart from the most sodic members, where  $\text{TiO}_2$  reaches 2 wt.%, mirroring the high  $\text{TiO}_2$  contents of the fenitic acmites.  $\text{K}_2\text{O}$  contents are generally lower than in the magmatic amphiboles, although there is a considerable spread on  $\text{K}_2\text{O}$  values. Fig. 6.3(c) shows clearly that the F contents of the fenitic amphiboles are usually higher than those of the magmatic amphiboles reaching 2.6 wt.%. Recrystallized magmatic amphiboles, however, show higher F contents, approaching those of the amphiboles from the fenites.  $\text{MgO}$  contents decrease systematically with increase in  $\text{Na}^{\text{X}}$ . Although this mirrors the trend shown by magmatic amphiboles, the  $\text{MgO}$  contents for a particular value of the fractionation index are always considerably higher. In contrast, both  $\text{FeO}$ (total Fe) and  $\text{MnO}$  contents are markedly lower in the fenitic amphiboles,

Fig.6.3 (two pages) Minor element concentrations of the fenitic amphiboles plotted against a Fractionation Index of  $\text{Na}^{\text{X}}\text{-Al}^{\text{Z}}$  (see text, section 4.3.3.). The field of magmatic amphibole compositions is outlined with a dashed line and amphibole compositions from recrystallized rocks with dotted lines.





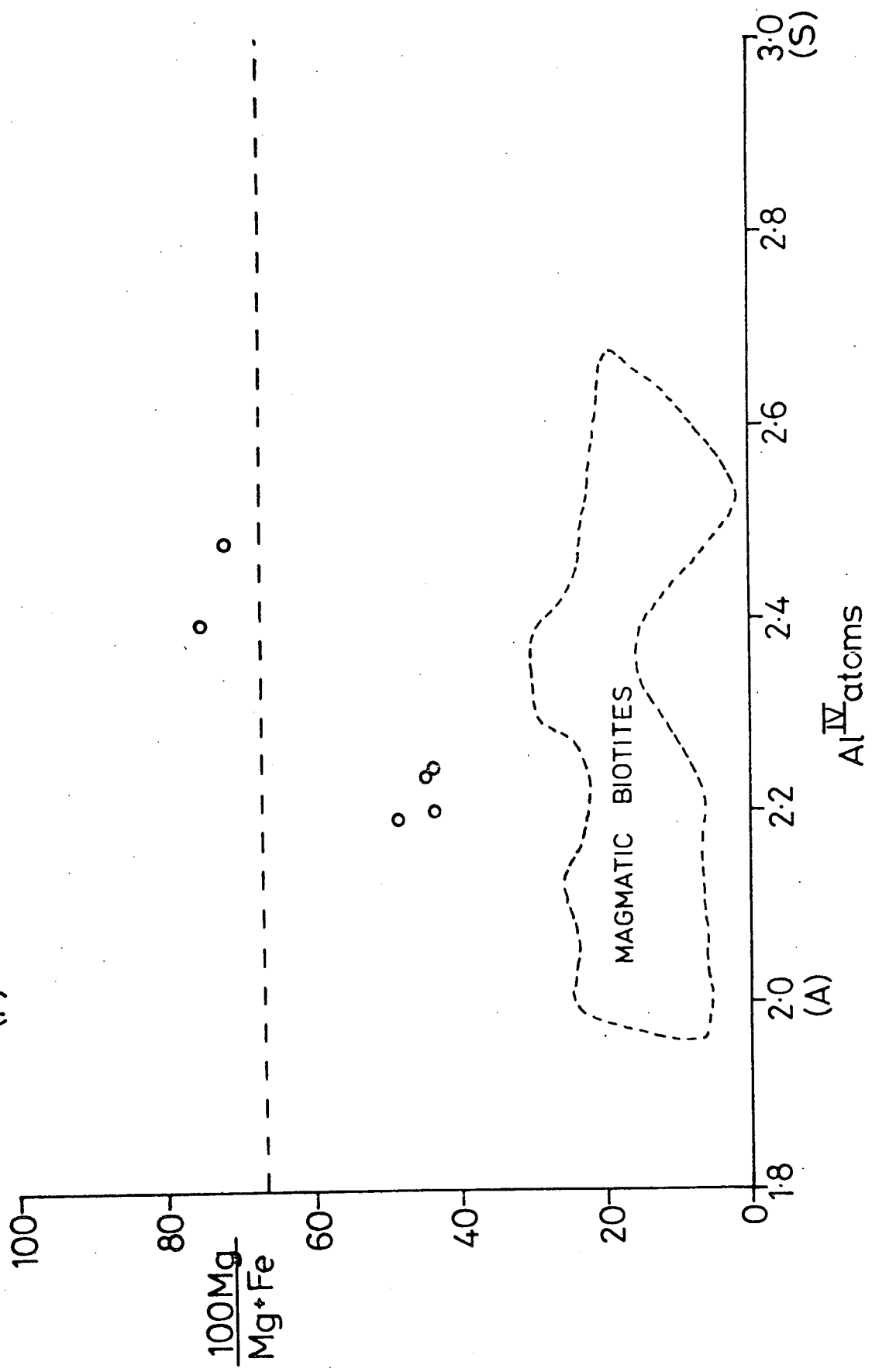
although the general trends from both types of environment are similar. It is significant that recrystallized amphiboles from the syenites, outlined by a dotted line and marked by a letter R, are often chemically closer to the fenitic rather than the magmatic amphiboles.

Fig. 6.4 shows fenitic biotites plotted in the same manner as the magmatic ones. It is noticeable that, as with other fenitic phases, the biotites are more Mg-rich than those from the syenites. Two of the biotites could, in fact, be termed phlogopites. Fig. 6.5 shows the F content of the fenitic biotites to be considerably higher than the very low contents found in their magmatic counterparts, with biotites from recrystallized syenites (R) plotting in an intermediate position. This perhaps indicates that the magmatic biotites did not lose considerable quantities of F to circulating ground-water as suggested in section 4.4. If ground-water leached the bulk of the F from the magmatic biotites, why did it not similarly affect the fine-grained fenitic biotites, which, occurring as they do in sheared and jointed Julianehåb Granite, would have been more accessible to ground-water? It suggests that either F was never present in the magmatic biotites to any extent, or was removed prior to the formation of the fenitic biotites. The first possibility is the one

Fig.6.4 Fenitic biotite compositions plotted in the same fashion as the magmatic ones (see Fig.4.13). The field of magmatic amphibole compositions is indicated by a dashed line.

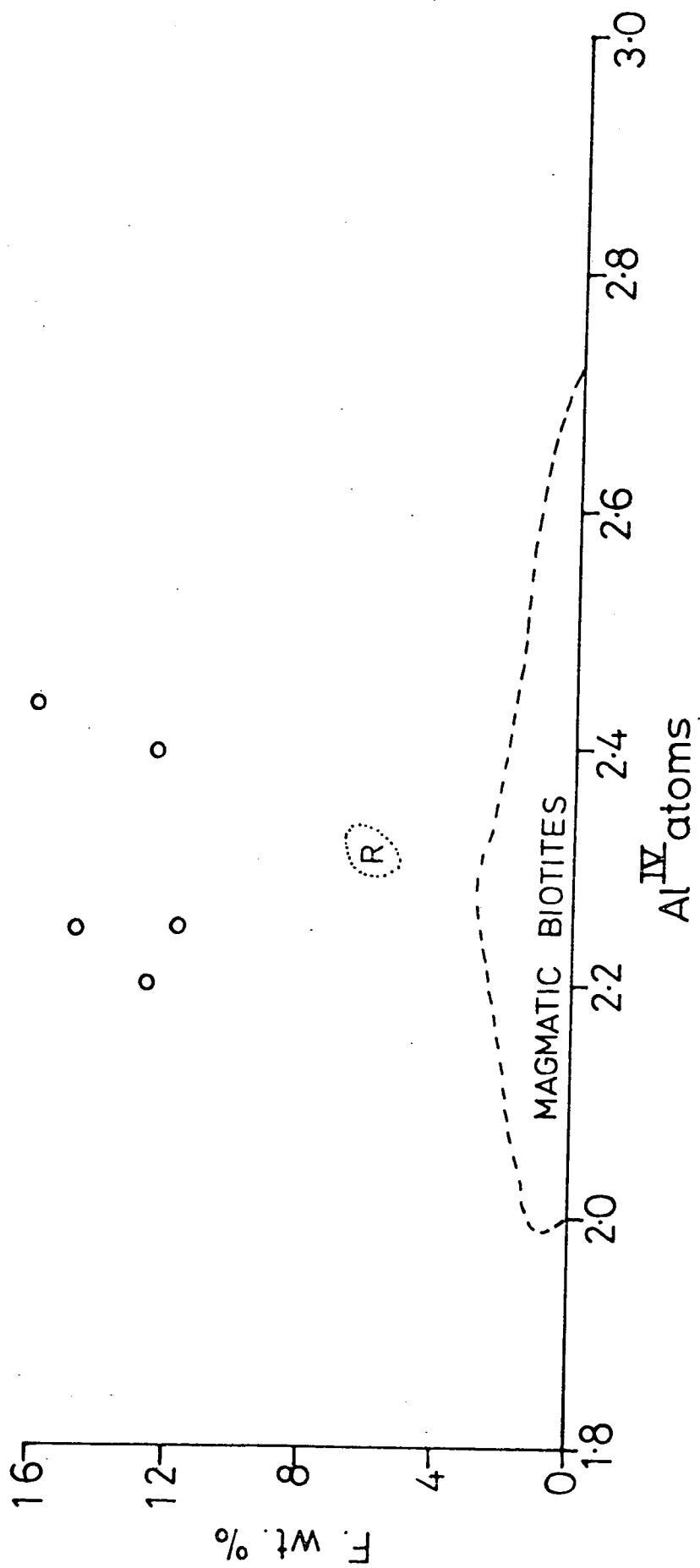
(E)

(P)



(S)

Fig.6.5 A comparison of the F contents of the magmatic biotites, outlined by a dashed line, a recrystallized biotite, outlined by a dotted line, and the fenitic biotites.



favoured, and a low F content for the magmatic biotites sets the application of the magnetite/sanidine/annite buffer reaction (section 4.16.5.) on a firmer foundation. In the contents of the other elements, the fenitic biotites resemble those from the syenites. The exception is MnO, which is only present in trace amounts in biotites from the fenites.

The only other fenitic phases analysed are a hydro-grossular garnet for identification purposes, and fluorite. Two fluorites in the fenitic zone were analysed by X.R.F. techniques for trace elements. The high rare earth contents they showed (Smith, 1974) are typical of fluorites with a high temperature igneous origin. It is by no means certain, however, that the fluorite veins can be related to the intrusion of North Qôroq, as they were noticed in the country rock some distance (400m.) from the syenite's outer contacts.

#### 6.2.4. Geochemistry

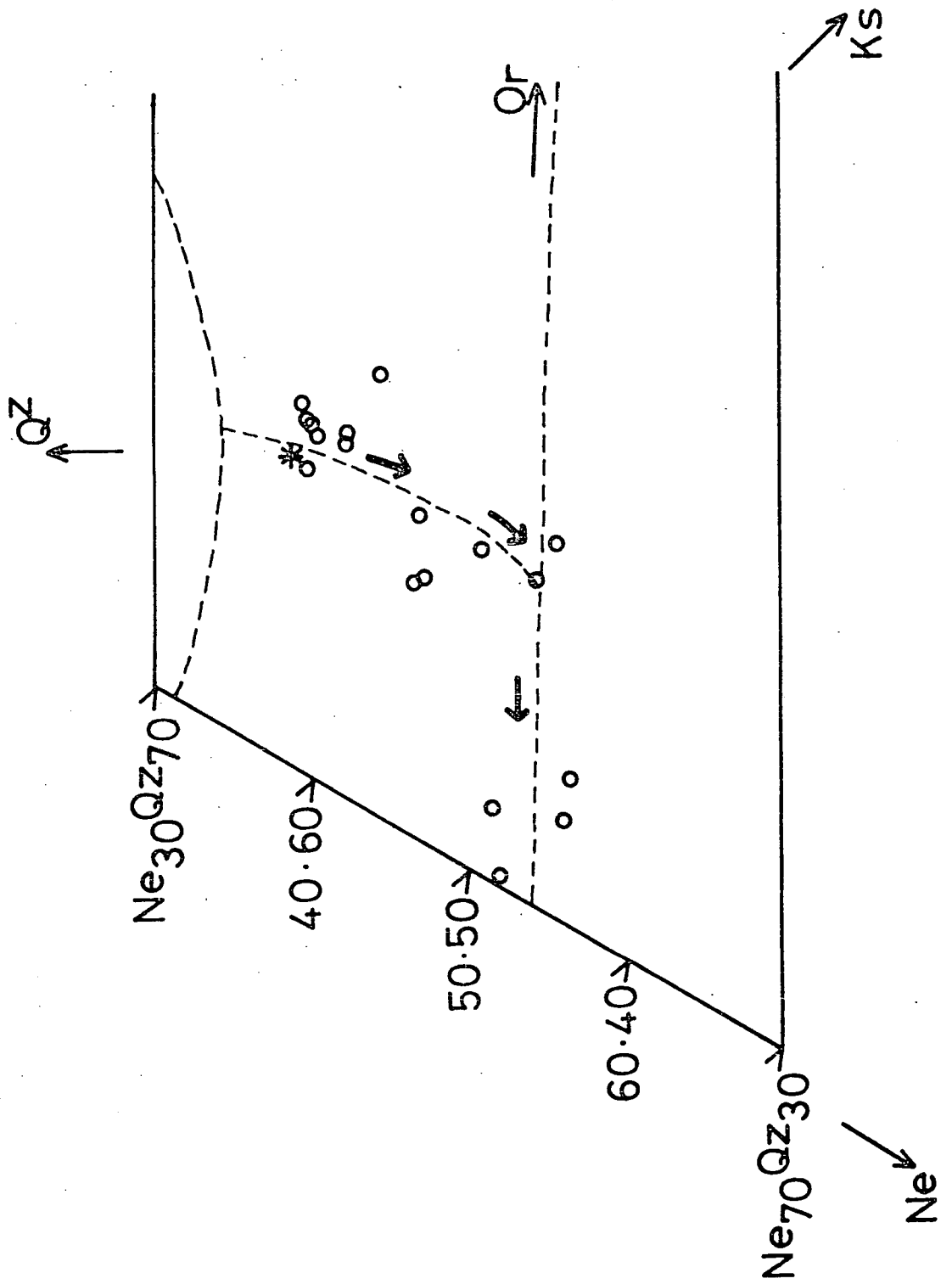
All collected samples of fenitized Julianehåb Granite and the fenitized 'dyke' rock (52243) were analysed by X.R.F. analysis for major and selected trace elements. Also analysed was a typical non-fenitized specimen of the Julianehåb Granite (155001).

On Fig. 6.6, the residua system diagram, the fenitized

Fig.6.6 The composition of fenitized Julianehåb Granite samples, plotted in terms of their normative quartz, nepheline and kalsilite contents. The dashed lines indicate the feldspar join, the quartz feldspar phase boundary and the thermal trough, determined at 1Kb. P.H<sub>2</sub>O by Bowen and Tuttle (1950). The thick arrowed line indicates the trend followed with increasing grade of fenitization.

Symbols used:

- \* - Unaltered Julianehåb Granite
- o - Fenitized Julianehåb Granite



Julianehåb Granite specimens are plotted. Both analyses of those rocks showing marked fenitization, and those where the fenitization is only slight, are included. Also marked, by dashed lines, are the albite-orthoclase join, the quartz-feldspar phase boundary and the thermal trough, determined at 1Kb.P.H<sub>2</sub>O by Bowen and Tuttle (1950). The starred point represents unaltered Julianehåb Granite. Despite some spread in the analysed points, a general trend can be seen from the region of the quartz-feldspar phase boundary, where the unaltered Julianehåb Granite plots, to the albite-orthoclase join and then towards albite. This trend of increasing fenitization is indicated by thick arrows. The trend suggests that two processes are affecting the felsic mineralogy. Initially, in low to medium grades of fenitization, the quartz reacts with the fenitizing fluid to form fenitic amphiboles and pyroxenes, as previously indicated, and possibly feldspar. The second process only affects the granite within a few metres of the outer margins of SN.1A and SN.1B, i.e. at high grades of fenitization. This is a replacement of K-feldspar by a mosaic of albite as shown in Plate 42. Woolley (1969), describing fenitization processes in general, notes 2 stages during the alteration of country rock. The first is the loss of quartz with the analyses plotting towards the feldspar join,

similar to that described in this account. Woolley's second process, however, is an increase in the  $K_2O/Na_2O$  ratio with the fenites becoming more orthoclase-rich, the reverse of that observed around North Qôroq. He suggests that the K-metasomatism is due to highly potassic liquids associated with carbonatites. A closer look at the K/Na ratios in the fenitized rocks reveals a slight, but definite, increase in the ratio, relative to unaltered granite, in rocks that have suffered low to medium grade fenitization. It appears, therefore, that pronounced Na-metasomatism occurred at the very margins of the syenite intrusions, and that less pronounced K-metasomatism occurred over a more extensive area further out from the margins of the intrusions. This observation agrees well with the theoretical predictions and experimental results of Orville (1963). He showed that with two feldspars present, as there are in the Julianehåb Granite, and a co-existing vapour phase, there is a net diffusive movement of K ions towards a lower temperature environment and Na ions towards a higher temperature one. Hence, rocks at a higher temperature suffer Na-metasomatism and those at a lower temperature K-metasomatism, exactly the situation observed at North Qôroq.

The restriction of the zone of Na-metasomatism to

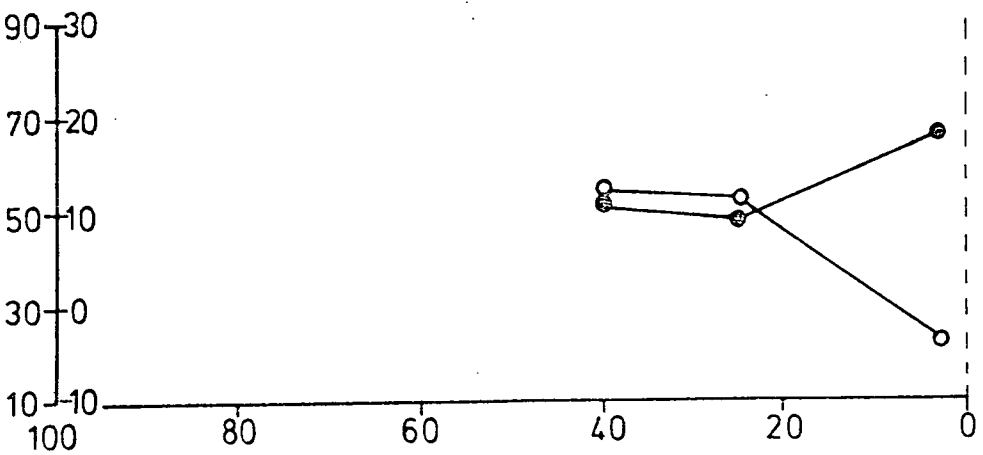
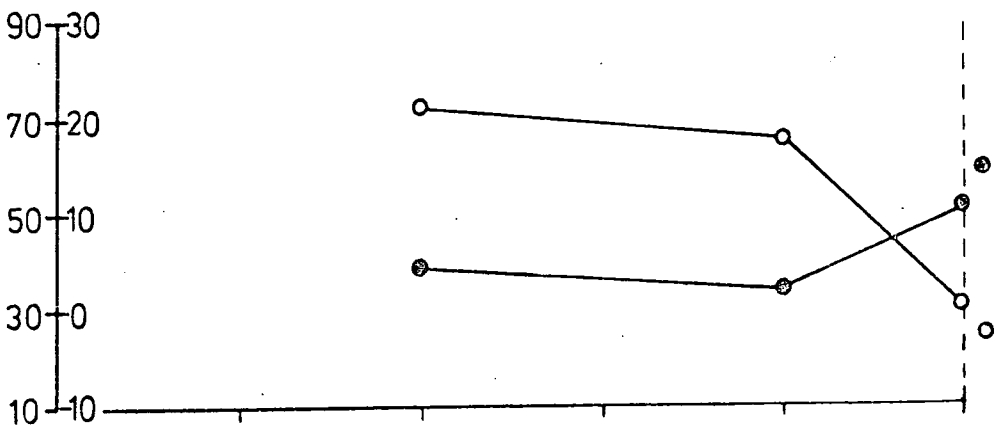
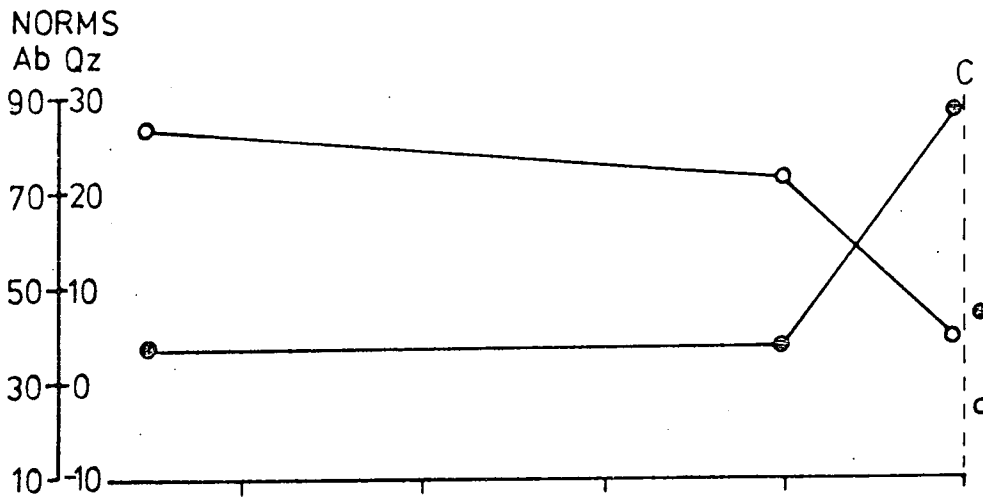
the contact zone of the intrusion is indicated in Fig. 6.7. Here, normative albite in a sample is plotted against distance from the point of collection of that sample to the granite/syenite contact, represented by a vertical dashed line. It can be seen that there is a marked increase in normative albite only within a few metres of the contact. The diagram also shows normative quartz to decrease markedly as the contact is approached.

McKie (1966) points out that molecular variation diagrams are not an ideal method of representing chemical change during fenitization, because they imply that the number of oxide molecules is constant, which is not so. He suggests that a better assumption is that the anion content (O, OH, F) of the rock is constant. Following McKie's principles the cation (atom) contents of the fenites were recalculated to a standard cell of 100 oxygens. As Si decreases with fenitization other elements are plotted against it. Fig. 6.8 shows the variation of Na and K (atoms) with decrease in Si (atoms). The solid arrowed line represents the general trend of the low to medium grades of fenitization. The dashed lines show the high grade fenitization process with a marked increase in Na and decrease in K. These dashed lines represent the variation along a number of short traverses taken from the granite/syenite contact a

Fig.6.7 The normative quartz and albite contents of fenitized Julianehåb Granite specimens, plotted against distance to the granite/syenite contact, indicated by a vertical dashed line.

Symbols used:

- - Normative quartz
- - Normative albite

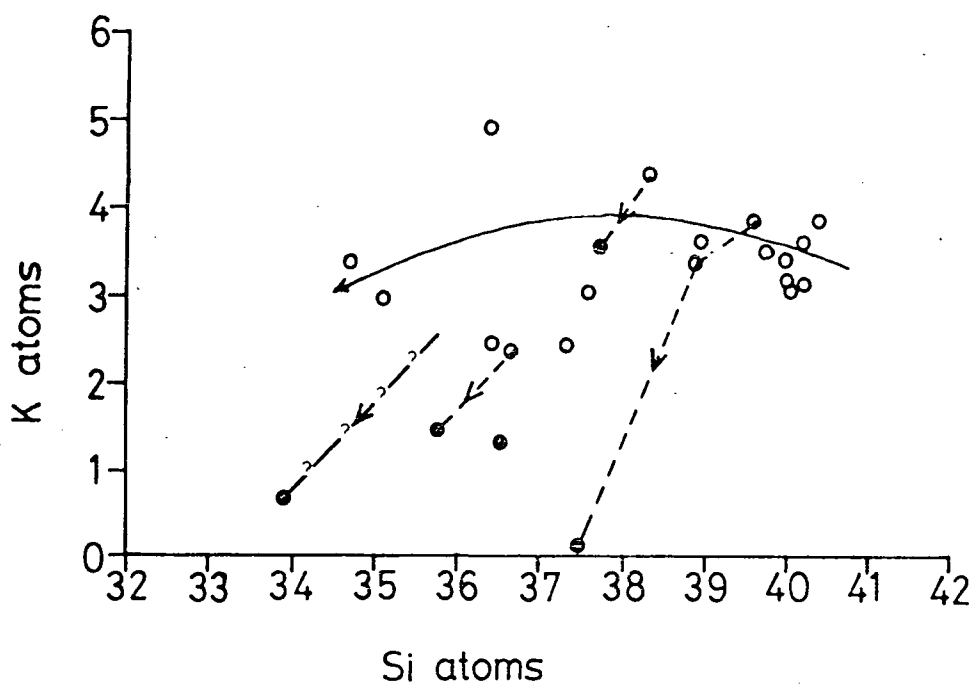
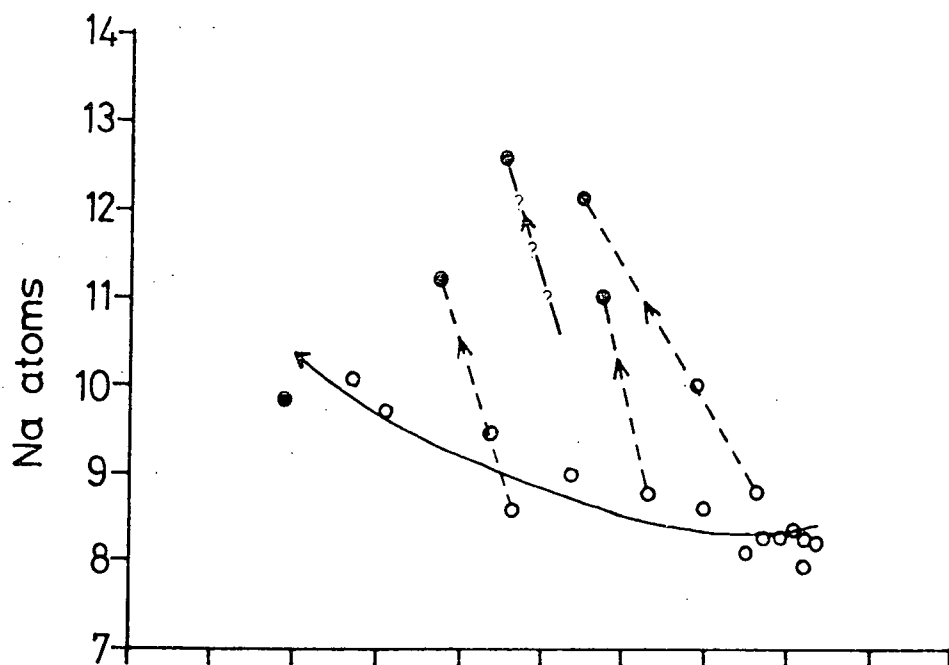


DISTANCE TO GRANITE/SYENITE CONTACT (M)

Fig.6.8 Variation diagram of alkalis plotted against silica for the fenitized rocks. The atomic proportions are plotted to a standard cell of 100 oxygens (McKie, 1966). The solid arrowed lines represents the trends found in low to medium grades of fenitization, and the dashed arrowed lines those found in high grades of fenitization.

Symbols used:

- - Highly fenitized granite
- - Moderately or slightly fenitized granite



short distance into the country rock. It can be seen that there is relatively poor correlation between either of the alkalis and Si. This is to be expected with the representation of fenitic processes, occurring as they do in a patchy and irregular manner within the country rock.

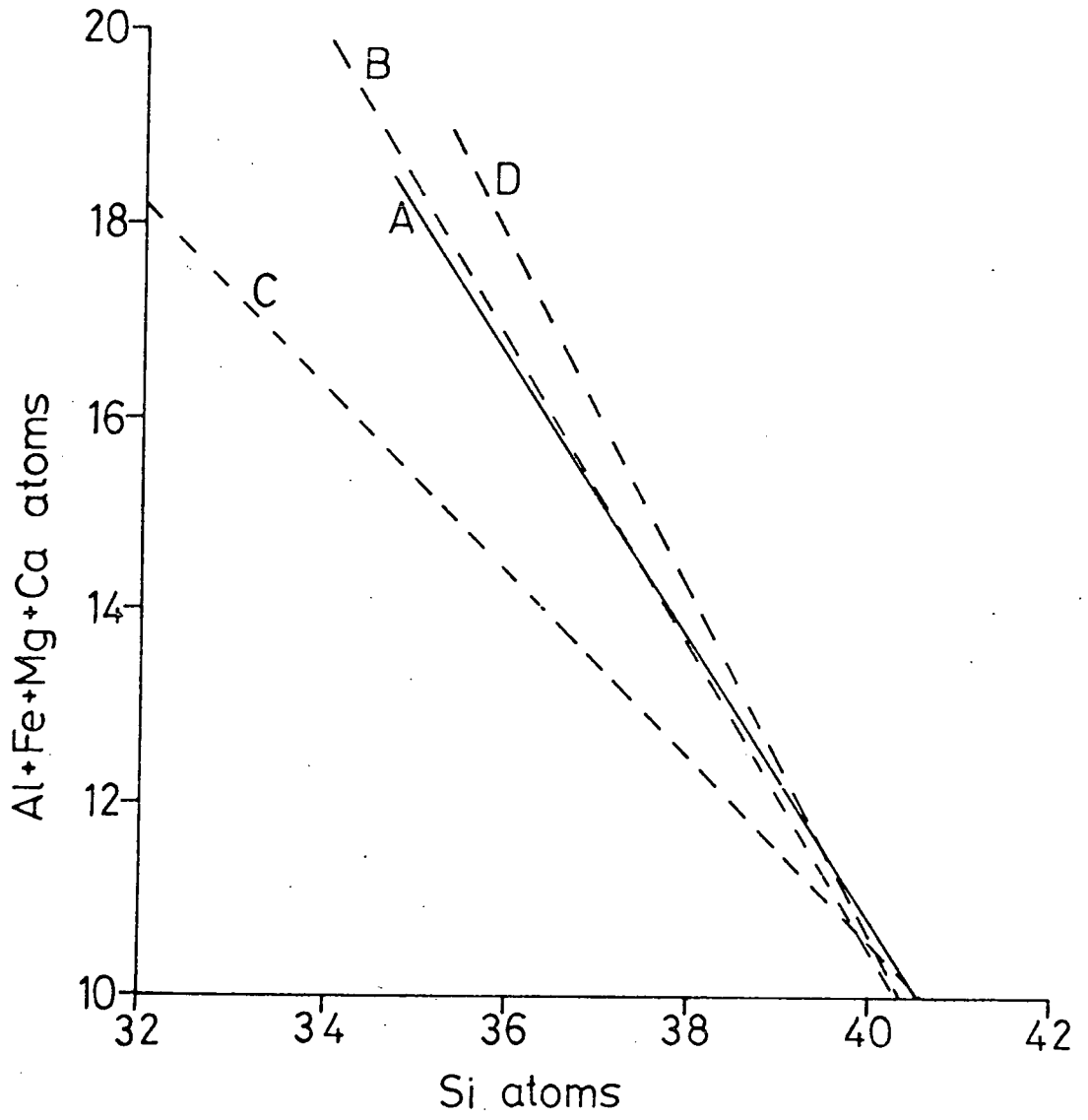
Fig. 6.9 shows the marked increase in the total of Ca, Mg, Fe and Al atoms with fenitization, (i.e. decrease in Si). The North Qôroq trend (A) is compared with similar trends for fenites from Callander Bay ((B) Currie and Ferguson, 1971), Spitskop and Oldonyo Dili ((C) McKie, 1966) and Alnø Island ((D) von Eckermann, 1948). All, particularly Callander Bay, show a similar increase in these elements with increased grade of fenitization. Considering these elements individually in the North Qôroq fenites, total Fe and Mg show a marked increase, Ca a slight increase and Al little or no variation.

Also worthy of consideration are the major element effects seen in the fenitized 'dyke' (52243) and to a lesser extent in the Eriksfjord Formation basalts. In marked contrast to adjacent granite these basic rocks show K, P and F-metasomatism and no increase in Na. The samples were taken right at the syenite contact, a position where the granite shows intense Na-metasomatism.

Fig.6.9 The marked increase in 'cafemic' atoms with increasing fenitization, i.e. decrease in Si atoms, compared to similar increases found in other areas of fenitization.

Abbreviations used:

- A - North Qôroq
- B - Callander Bay
- C - Oldonyo Dili
- D - Alno Island



Macdonald et al. (1973) describe similar K and F-metasomatism affecting gabbros of the Kûngnât Complex, and caused by fluids derived from peralkaline granite sheets. They propose that this fenitization is caused by a K and F-rich fluid phase. In North Qôroq, however, the close proximity of the K, F-metasomatism to the intense Na-metasomatism affecting the Julíanehab Granite suggests that it is the initial composition of the material being fenitized that determines which elements are 'fixed' in the fenite, and which pass through unaffected, either to cause fenitization further out into the country rock, or to continue circulating through the rocks as components in hot brines. Fenitization of basic material by the North Qôroq fluids appears principally to result in the formation of biotite and apatite, so resulting in the extraction of K, F and P from the vapour phase. No mineral is formed which can accommodate Na in any quantity, and hence this element passes through the basic material without being extracted. Acid material, however, rich in alkali feldspar can, at high temperatures, readily exchange K in the feldspar for Na from the vapour phase, a relatively K-rich vapour phase passing through to cause K-metasomatism at lower temperatures in rocks further removed from the syenite body. Na, along with other elements, is also fixed in the acid rocks

by reaction with quartz to form alkali amphibole and pyroxene.

The minor element variation shown by the fenitized Julianehåb Granite is variable. Elements showing the most marked increases, particularly in the inner zone of high grade fenitization, are Zr and Zn. Rb, following K, is rapidly depleted in this inner zone. There is a slight tendency for Ba, Sr, Nb, Y and La to have increased concentration in the fenites; the increase being most marked in the vicinity of the contact.

#### 6.2.5. The nature of the fenitizing fluid

From the chemical and mineralogical changes observed in the fenitized rocks around North Qôroq, and from observations made elsewhere, tentative conclusions can be made about the nature of the fenitizing fluid.

The fenitized Julianehåb Granite mineralogy and chemistry indicate that the fluids have introduced appreciable quantities of Na and lesser quantities of K, Fe, Mg, Ca, F and CO<sub>2</sub>. Fenitization of the basic rocks suggests introduction of appreciable quantities of K and lesser quantities of P and F. Many of the pyroxenes and amphiboles formed during fenitization are low in Al, the tetrahedral sites often being filled exclusively by Si. In section 4.16.3., on the activity of silica, it

was suggested that the fluid causing metasomatism of the syenites had a low a.SiO<sub>2</sub>. Much of the Si in the fenitic minerals was derived from quartz in the Julianehåb Granite, and it may well be that the fenitizing solutions were poor in both Al and Si.

One of the best guides to the nature of late stage aqueous fluids, probably responsible for fenitization, is the composition of fluid inclusions. Sobolev et al. (1974) report on analysis of fluid inclusions in nepheline, clinopyroxene and alkali feldspar, all the minerals occurring in various nepheline syenites. They note that the aqueous phase in the fluid inclusions contains between 12 and 27 wt.% solute. The dominant ionic species in the solute are Na (4.0-13.0 wt.%) and Cl (2.6-6.4 wt.%). Typically present in smaller quantities are the anions SO<sub>4</sub>, F and HCO<sub>3</sub>, and the cations K, Ca, Fe, Mg, Ti, Al and Si. Of the cations, only K is always present and Al and Si are frequently absent.

Burnham (1967) has studied experimentally the systems granite-water, and granite-water-other volatiles. He shows that in a simple granite-water system the total solute content of the aqueous solution is low, and that the anhydrous composition of the solute is similar to, but slightly more potassic than, the co-existing granite.

This type of aqueous solution does not correspond to the Si and Al-poor one thought to be responsible for fenitization around the North Qôroq Centre. Burnham showed, however, that Cl was partitioned strongly in favour of the aqueous phase, that it markedly enhanced the solubilities of alkalis and Ca in the aqueous phase and, at the same time, depressed those of Si and Al. Cl-rich solutions can also transport relatively high concentrations of Fe, Mg, Ba and Sr. It must be remembered that Burnham's arguments apply to the system granite-water, and that differences may occur when the system being studied is nepheline syenite-water. An important difference is the greater solubility of water in a nepheline syenite melt when compared to a granite melt, a feature discussed more fully later. Also, as mentioned in section 4.9., Cl is less likely to be partitioned strongly into a fluid phase, because the low  $a_{\text{SiO}_2}$  favours the formation of sodalite, stabilising Cl in the magma.

Consideration of the chemical and mineralogical changes seen around North Qôroq, of fluid inclusion studies on minerals from other nepheline syenites, and of experimental work on silicate-water systems, suggests a number of points relevant to the North Qôroq fenitizing fluid.

1. The fenitization was probably caused by a hydrous phase rich in Na and K.

2. Strong Na-metasomatism occurred in the hotter parts of the Julianehåb Granite and K-metasomatism in somewhat cooler parts. This resulted from Na and K diffusing through a vapour phase.

3. This diffusion process requires high concentrations of the alkali ions (Orville, 1962), such as could only occur in a Cl-rich fluid.

4. In nearby basic rocks only K was fixed, the Na moving through to cause metasomatism elsewhere, or circulating through the rocks as a hot NaCl 'brine'.

5. Because of the high Cl contents, moderate amounts of Ca, Mg, Fe, Mn, Ti, F and P were carried in the aqueous phase and deposited in the fenitized rocks forming alkali amphibole, pyroxene, mica, fluorite and apatite.

6. Carbonate material deposited during fenitization, and the CO<sub>2</sub> content of the fluid inclusions from other nepheline syenites suggests that the fenitizing fluid contained quantities of CO<sub>2</sub>. The late stage veins rich in fluorite, calcite, hydro-grossular garnet, diopside and epidote, cutting the fenitized 'dyke' rock (52243) suggest that later liquids evolving from North Qôroq were Ca and CO<sub>2</sub>-rich and perhaps Cl-poor. Koster van Groos and Wyllie (1966, 1969) show that the first aqueous fluid forming from an albite melt can be more NaCl-rich than later ones, which are more CO<sub>2</sub>-rich, so supporting this contention.

### 6.3. The aqueous phase in the North Qôroq Centre

#### 6.3.1. Metasomatism of the syenites

As indicated in section 3.4., many of the North Qôroq syenites show evidence of metasomatic alteration where they are adjacent to younger intrusive units. This is particularly true of rocks close to units SN.1B, SN.5, and unit SS.2 of the South Qôroq Centre. In the proximity of the contact the metasomatism has been extensive, with the formation of aenigmatite, sodic amphibole and sodic pyroxene, at the expense of pre-existing mafics. This alteration suggests strong Na-metasomatism and a high  $a_{\text{Na}_2\text{Si}_2\text{O}_5}$  in the metasomatising fluid (see section 4.16.6.). It is interesting to note that around the margins of units SN.4A and SN.4B, despite extensive recrystallization, there is no evidence of metasomatism. This is a further indication that the magma forming these two units contained less water than that forming the other units, and, partly because of this dry character, did not give rise to any metasomatism.

In addition to metasomatic alteration by later intrusive units, there is evidence, particularly in the margins of SN.1A, of what may well be termed auto-metasomatism. Along fractures in the marginal augite syenite, augitic pyroxenes are patchily replaced by green aegirine augite, and brown amphibole by blue arfvedsonite.

Where fractures cut through microperthite, the exsolution is on a much coarser scale and small distinct grains of albite may occur. The evidence again suggests action of Na-rich metasomatising fluids in these marginal rocks of SN.1A, probably the same fluid causing fenitization in the Julianehåb Granite, and originating from highly evolved residual syenites in the interior of SN.1A.

It was mentioned in section 4.6. that the feldspars from strongly recrystallized rocks may show a degree of K-enrichment. This enrichment, however, is more than compensated for by Na-enrichment in the mafic phases and the net result for the whole rock tends to be an increase in Na.

#### 6.3.2. Co-existing vapour phase: presence or absence?

From the present study of the alteration of various rock types adjacent to the syenites, it is apparent that they have been affected by a metasomatising fluid associated with these syenites. One obvious possibility is that this fluid phase results from a build up of volatiles, principally  $H_2O$ , in the magma, and the eventual 'boiling off' of a separate aqueous vapour phase which co-exists with the residual magma. An alternative process, however, is the fractionation of a syenitic magma, becoming more water-rich, until it evolves, through a hydrous silicate melt,

to a siliceous aqueous phase. This process also could have caused the observed metasomatism, but requires mutual solubility between the silicate melt and the aqueous phase. The feasibility of this second process has been indicated by a number of experimental studies.

Koster van Groos and Wyllie (1968, 1969) examined the effect of adding NaF and NaCl to the system  $\text{NaAlSi}_3\text{O}_8\text{-H}_2\text{O}$ . Both additives markedly increase the solubility of water in the silicate melt, even if only present in small quantities. They suggest that it is possible to get continuous solubility although this only seems probable at relatively high pressures ( $>10\text{Kb.}$ ). In referring to the possibility of continuous solubility they state that 'residual magmas of this kind, transitional in composition and physical state between silicate melts and hydrothermal solutions, would be potent agents for alkali metasomatism'. At the relatively low pressures at which the North Qôroq magmas evolved, NaF and NaCl alone are probably unable to promote continuous solubility, although they may markedly increase the capacity of the melts to dissolve water. Both Koster van Groos and Wyllie (1968) and Luth and Tuttle (1966) show the presence of sodium silicates greatly to increase the solubility of water in silicate melts. As demonstrated in Chapter 5, the residual magmas of North

Qôroq tend to be rich in Na relative to Al, due to early separation of peraluminous (or metaluminous) phases.

Kogarko (1974) states that high mole fractions of alkalis result in high water solubilities, and that it may be possible to get a magmatic melt gradually changing into a hydrothermal solution. This would take place, even at low pressures, without the separation of an aqueous vapour phase.

What evidence can be presented, either from North Qôroq itself, or from similar Gardar plutons, for or against the existence of a co-existing aqueous phase? The presence of drusy pegmatites would suggest gas cavities formed by a vapour phase co-existing with the melt. Drusy cavities have been described from pegmatites of the Puklen Complex (Parsons, 1972) and the Kûngnât Complex (Upton, 1960), but neither of these intrusions approaches the strongly undersaturated peralkaline residual melts of North Qôroq. In the North Qôroq Centre, pegmatites are a common feature in the margins of syenites and are discussed in the next section. Pegmatites in the interior of the intrusion are rarer, but do occasionally show drusy cavities.

The presence of fluid inclusions in minerals can be a good indication of the existence of a separate vapour phase. Fluid inclusions, occurring in nephelines from the naujaïtes

and tujavrites of the Ilímaussaq intrusion, have been studied by Sobolev et al. (1972). The authors suggest that certain of these inclusions are primary, i.e. forming during the crystallization of these minerals from the magma, and this suggests an aqueous phase co-existing with the magma. Certainly, homogenization temperatures obtained from these inclusions (850-1040°C) are indicative of a primary origin.

Also in favour of a co-existing aqueous phase in Ilímaussaq magmas are observations by Larsen and Steenfelt (1974) who describe loss of Na, F, H<sub>2</sub>O and probably Cl from a peralkaline dyke. This dyke is similar in composition to nearby kakortokites (layered eudialyte-nepheline syenites) of the Ilímaussaq intrusion. Separation of a co-existing vapour phase seems a reasonable explanation for the loss, as these magma components might be expected to concentrate in a vapour phase.

The evidence tends to suggest that the highly sodic, Cl-rich Ilímaussaq magma evolved a co-existing aqueous phase. If so, it is probable that the North Qôroq magmas, less sodic and consequently with less potential to dissolve water, behaved similarly. It may be that the North Qôroq magmas evolved a separate aqueous phase, but that as the residual magma became more fractionated, the solubility gap closed, resulting in one homogenous water-rich melt.

In section 4.16.2., on the  $P.H_2O$  of North Qôroq magmas, a build-up of this parameter with fractionation was suggested, possibly culminating in the 'boiling-off' of an aqueous fluid from the highly fractionated residual syenite magma. In conclusion, it is probable that the North Qôroq syenites, at least the more evolved ones, SN.1A, SN.1B and SN.5, evolved a co-existing aqueous phase, but that the evolution of this phase occurred at a much later stage than would be the case in similar, but over-saturated, magma bodies.

Three mechanisms may have contributed to the process of movement of the aqueous phase into the country rocks. Diffusion along pressure and temperature gradients, prior to the formation of a separate aqueous phase, may have helped to concentrate volatiles in the margins of North Qôroq. This mechanism was suggested by Kennedy (1955), although Burnham (1967) demonstrated that the mechanism was unable to account for movement of volatiles any significant distance in the time available. The low viscosity of the syenite magmas, however, may have aided diffusion and resulted in it being a process of at least local importance. Probably of greater significance was the process of 'filter-pressing' whereby the residual hydrous pore fluids were forcibly 'squeezed out' of the interior of the intrusion

by movements of the wall rocks. The very low viscosity of these residual fluids will have aided their movement. The third possible mechanism involves movement of a separate vapour phase by the process of gas bubbles rising towards the roof of the intrusion, by Stokes' Law, through the co-existing magma, a process again aided by the low viscosity of the magma. As the outer contacts of the individual syenite units are outward sloping, this process would also result in a concentration of the vapour phase towards the margins of the intrusion.

### 6.3.3. Marginal pegmatites

Marginal pegmatites are a common feature of many Gardar plutons and, indeed, plutons from elsewhere. Ferguson (1964) describes pegmatites from the margins of the Ilímaussaq augite syenite, and Upton (1960) pegmatites from the margins of the western and eastern Kûngnât syenite intrusions. Emeleus and Harry (1970) comment on the presence of marginal pegmatites or coarsely crystalline syenites, and note that they are often a useful aid in identifying the margins of the syenite units. Upton describes Kûngnât marginal pegmatites as being drusy and occurring in veinlets, often cutting across the margins of the intrusion. He suggests that the pegmatites are a late stage feature, caused by the migration of volatiles towards the margins of

the intrusion, and that the drusy nature of the pegmatites suggests that the vapour pressure exceeded total pressure ( $P.H_2O > P.T.$ ) and a separate aqueous phase 'boiled-off'. This explanation seems reasonable for the Kûngnât syenites, from which an aqueous phase would have evolved quite readily and perhaps at a relatively early stage in their evolution. In North Qôroq, however, the marginal pegmatites are not drusy and are intimately associated with relatively fine grained syenites. Petrographic examination reveals that they tend to have the same mineralogy as these syenites, with the exception of more coarsely exsolved feldspars and a greater proportion of biotite. This petrographic similarity between the marginal pegmatites and the normal marginal rocks was also noted by Stephenson (1973) for syenites of South Qôroq. The clearly cross-cutting pegmatite veins of the Kûngnât syenites are not seen, the North Qôroq pegmatites occurring in irregular patches, restricted to the margins of the syenite units. They are particularly noticeable in the margins of the outer syenites, SN.1A and SN.1B.

Assuming that these marginal pegmatites are related to an increased volatile content, it appears that, for North Qôroq, this increase occurred at an early stage, probably at the time of consolidation of the marginal rocks. It has been shown (section 4.16.7.) that, on intrusion, the

syenitic magmas might have had a relatively low  $P.H_2O$ .

It is suggested that the water pressure in the surrounding rocks exceeded that of the magma at the time of intrusion, resulting in an influx of water from the country rock. Shaw (1974) has postulated that this process will occur when the country rocks are wet.

Supporting evidence for this type of mechanism comes from a study of the Kangerdlugssuaq alkaline intrusion by Pankhurst et al. (1976). They noticed that, as the outer margins of the intrusion were approached, there was an increase, both in the initial  $Sr^{87}/Sr^{86}$  ratio and in  $O^{18}$ . They attribute these increases to the admittance of meteoric water to the high level magma chamber at an early stage in the evolution of the syenites, this water containing basement Sr isotope proportions in solution. A similar process may well have operated in North Qôroq. Indeed, initial Sr isotope ratios for the North Qôroq Centre may be high ( $0.7052 \pm 0.0030$ ) when compared to typical mantle values, and to values from the majority of the other Gardar centres. However, when samples taken from the margins of SN.1A are ignored the initial ratio gives a value consistent with a mantle origin ( $\sim 0.703$ ). Although this increase in the initial ratio may well be due to assimilation of basement material, it may also be caused by interaction

with meteoric ground-water enriched in  $\text{Sr}^{87}$ .

A further indication of an influx of meteoric water and consequent increase in  $f.\text{H}_2\text{O}$  is suggested by the occurrence of large quantities of biotite in the marginal rocks of SN.1A and SN.1B, and of Fe/Ti oxides rimming olivine. As explained in section 4.16.5., an influx of meteoric <sup>water</sup> would have resulted in an increase in  $f.\text{O}_2$ , because the water would dissociate and  $\text{H}_2$  would diffuse out of the system much more rapidly than  $\text{O}_2$  (in silica glass  $\text{H}_2$  has been shown to diffuse approximately a million times faster than  $\text{O}_2$ ). This increase in  $f.\text{O}_2$  would have resulted in the rimming of olivine by Fe/Ti oxides and the fixing of  $f.\text{O}_2$  by the new assemblage alkali feldspar - Fe/Ti oxides-biotite.

Hence, it is proposed that meteoric ground water entered the North Qôroq magmas, dissociated, and lowered the magma viscosity, resulting in the formation of pegmatites. The relatively short distances the ionic species could travel through the magma during the period before solidification, and the irregular entrance of ground-water, along joints and fractures in the country rocks, resulted in the patchy nature of the pegmatites. They also caused the pegmatites to be restricted to the margins of the intrusion. Solidification of the marginal rocks closed the system to further influxes

of ground-water, although circulation of ground-water through the solid syenites may subsequently have taken place after cooling joints had provided suitable pathways. The marginal pegmatites are most extensive in the outer units of the North Qôroq Centre, SN.1A and SN.1B, because the heavily jointed basement rocks supported a strong system of ground-water circulation. Inner syenite units, SN.2 and SN.5, show less extensive pegmatite development, because of the weak ground-water influx through the pre-existing syenites. It is interesting that both SN.4A and SN.4B apparently show no development of marginal pegmatites. Perhaps these two fine-grained, rapidly cooled units produced an impermeable chill before ground-water could enter.

## CHAPTER SEVEN: CONCLUSIONS

### 7.1. Introduction

In the preceding chapters a number of conclusions have been reached regarding the characteristics of the North Qôroq magmas, their mode of evolution and their effect on pre-existing rocks. In the present chapter these conclusions are drawn together and summarized. Possible modes of evolution of the syenitic parent magma at depth are also considered, although it must be borne in mind that this requires considerable extrapolation from the features observed in the North Qôroq Centre. Hence, certain of the proposals can only be regarded as tentative and require further investigation to be confirmed. The Gardar Province as a whole is considered, by briefly comparing it to other, apparently similar provinces. An attempt is made to place the province into its correct position with regard to global tectonics.

### 7.2. High level evolution and the state of North Qôroq magmas

#### 7.2.1. Fractional crystallization

The major units of the North Qôroq Centre are thought to have been intruded by a process of ring fracture and cauldron subsidence (Emeleus and Harry, 1970), combined

with a degree of stoping.

Petrographic, mineralogical and geochemical evidence suggests that, after intrusion, evolution of the syenites occurred in situ. In Chapter 3 it was noted that the syenites became more evolved with increased distance from the margins (and roof) of a unit. In section 5.4 it was seen that the geochemical pattern over the outcrop of unit SN.1A was consistent with the presence of an inner, highly fractionated core to that unit. A reasonable mechanism to explain the observed variation within the unit is one of crystal fractionation. Confirmation of the importance of this mechanism comes from observations on the phenocryst content of unit SN.4B. It was seen that the phenocryst content decreased from margin to centre of the unit, and that the effect was most noticeable for the denser phases, opaques, olivine and augite, and less noticeable for the less dense feldspar. This observation is consistent with a model of gravitational settling. Hence, it is proposed that the bulk of the chemical and mineralogical variation seen in the North Qôroq syenites is due to in situ crystal fractionation. In the relatively quickly chilled units SN.4A and SN.4B the amount of fractionation was small resulting in limited chemical variation. In the large, more slowly cooled units, particularly SN.1A, a considerable

degree of crystal fractionation is thought to have taken place, resulting in the extensive chemical and mineralogical variation shown by these units. This is particularly well demonstrated, for SN.1A by the dense, early-formed phases, olivine and augitic pyroxene, which are only found in the very margins of this unit.

At this point the variation shown by other Gardar centres can be considered and related to that seen in North Qôroq. Feldspar lamination and mafic banding are common throughout the major Gardar centres, but cryptic variation is less common. The best example of cryptic variation is seen in the western stock of the Kûngnât fjeld Complex (Upton, 1960). The similar Tugtutôq Central Complex (Upton, 1964a), however, shows only slight variation. Among the undersaturated rocks the nepheline syenites of the Hviddal dyke (Upton, 1964b) show the best development of cryptic variation, although there is a marked absence of mineral lamination or mafic banding and other processes apart from crystal settling could have been involved. In the Igaliko Complex, unit SI.4 of the Igdlérfigssalik Centre is reported as showing cryptic variation (Emeleus and Upton, 1976), but Stephenson (1973) suggests that in South Qôroq the in situ crystal fractionation is negligible.

What factors cause one intrusion to show apparently

marked cryptic variation, suggesting considerable in situ fractionation, whereas other similar intrusions show little or no variation? One factor must be the rate of cooling. Small, relatively rapidly cooled bodies will solidify before there has been any large degree of crystal settling. These bodies will show only limited cryptic variation compared to larger, more slowly cooled bodies.

Another extremely important factor is the level at which the intrusion is exposed at the present time (Upton et al., 1971; Upton, 1974), and the vertical thickness of rock that can be seen in the intrusion. Considering unit SN.1A of North Qôroq, it can be stated that if it were not for the deeper level of erosion at the north-west edge of the unit, that exposes the highly fractionated core, the variation would apparently be much less dramatic, suggesting a much smaller degree of in situ fractionation than actually took place. Considering Fig. 5.5 it can be seen that, if the level of erosion was below the highly fractionated core, again a lesser degree of cryptic variation would be seen. It should be mentioned that the highly fractionated core is itself thought to lie in the upper part of the original magma body, hence erosion to below the level of this core does not imply that the base, or even the lower levels, of the original magma body are

exposed. It is likely that both the North Qôroq and Motzfeldt Centres are exposed close to their roof zones and that erosion below the roof zone level has exposed the inner core, whereas the Igdlerfigssalik and South Qôroq Centres are exposed to deeper levels, below the core, and consequently do not tend to show the same highly fractionated rock types rich in analcite, cancrinite, sodalite and acmite. If crystal fractionation can account for the bulk of the variation seen in the syenites this implies that below the present level of erosion are layered sequences of cumulate rocks similar to those seen in the more deeply eroded Kûngnât Complex.

The common occurrence of layered structures in the Gardar central complexes suggests that convection was a common process. Both the convection process and the gravitational settling of crystals would be aided by low viscosity (Upton, 1974). This low viscosity may be a result of a high volatile content particularly with regard to the elements F and Cl. Shaw (1972) indicates that these extremely electronegative elements act as 'network modifiers' and may markedly reduce the viscosity of magmas. Both elements are thought to have been in high concentrations, particularly in the more fractionated of the North Qôroq magmas. Shaw (op. cit.) and Bottinga and Weill (1972) give

simple methods for calculating the viscosity from the chemical composition of a rock and its magmatic temperature. Application of Shaw's method to the marginal augite syenite of SN.1A, using a temperature of 900°C gives an approximate value for the viscosity of  $5 \times 10^4$  poises. This is higher than typical basalt magma ( $\sim 10^2$  poises) but much lower than typical granite magma ( $\sim 10^8$  poises) (values from Bottinga and Weill, op.cit.). The presence of network modifiers, not accounted for in the calculation, will lower the viscosity still further.

Another aid to crystal fractionation is the large crystallization interval demonstrated by melting experiments on undersaturated plutonic rocks. Edgar and Parker (1974) show a correlation between the melting interval (solidus-liquidus) and alkaicity (alkalic index =  $(\text{Na}_2\text{O} + \text{K}_2\text{O})/\text{Al}_2\text{O}_3$ ). This, they suggest, may be due to the highly alkaline nature of the magmas, coupled with the high volatile contents. The large melting interval typical of nepheline syenites, often several hundred °C, greatly aids the crystal fractionation process.

Assuming that crystal fractionation is the major process controlling the evolution of North Qôroq magmas, the first phases fractionating will be olivine, augitic pyroxene, Fe/Ti oxides and apatite (and in unit SN.4A and SN.4B

oligoclase), causing residual magmas to be depleted in Mg, Ca, Fe, Ti and P. These phases are followed by biotite, amphibole and alkali feldspar. In section 5.6. it was shown that early crystallization of biotite, amphibole and aluminous clinopyroxenes and oxides result in the residual liquid becoming peralkaline. Once the magma is peralkaline and undersaturated, fractionation of stoichiometric alkali feldspar will enhance both conditions. Feldspar fractionation was probably the dominant process over much of the crystallization interval of the North Qôroq magmas.

#### 7.2.2. Other processes affecting North Qôroq rocks

Stephenson (1973) considers that the major process giving variation in the South Qôroq syenites is the diffusion of alkalis and volatiles outwards towards the margins of the intrusions. There is no evidence for such diffusion in the North Qôroq Centre where the marginal rocks are the least fractionated. Considering Burnham's (1967) conclusion that diffusion is much too slow a process to account for significant transfer of material, it seems unlikely to have played an important role in high level Gardar plutons. These presumably cooled relatively quickly and would have been solid before any appreciable transfer of material could have been brought

about by a diffusion process, despite the low viscosity.

A process which has been shown to have considerable effect on the character of the North Qôroq rocks is the metasomatic alteration of pre-existing syenite units by aqueous fluids, rich in alkalis, associated with later units, or with more evolved fractions of the same unit. These effects are discussed in section 6.3. It is emphasised that it is necessary to take into account the later metasomatic alteration before the geochemical and mineralogical patterns of the crystal fractionation model can be fully appreciated.

### 7.2.3. Physical and chemical conditions of the evolving North Qôroq magmas

Thermodynamic treatment of the mineral data (section 4.16.) enabled values to be placed on many of the physical and chemical conditions as the North Qôroq magmas evolved.

It is thought that units SN.1A, SN.1B, SN.2, SN.4A, and SN.4B were intruded as magmas of augite syenite composition. The temperature of the magma on intrusion is thought to have been between 900<sup>o</sup> and 950<sup>o</sup>C. Units SN.4A and SN.4B give the impression of being drier, hotter bodies of magma. It is possible, however, that they have merely suffered less re-equilibration than the other, more slowly cooled units. Also, certain temperatures for these

two units, obtained from the phenocryst assemblage, reflect temperatures prior to emplacement at the present level. SN.2, SN.4A and SN.4B suffered only limited crystal fractionation and may have been virtually solid at temperatures given by the feldspar/nepheline geothermometer of around  $700^{\circ}\text{C}$ . Units SN.1A and SN.1B suffered more extensive crystal fractionation, and the residual liquids may not have solidified until much lower temperatures. As mentioned previously, it is possible that the syenitic magmas evolved through to a hydrothermal liquid making solidus temperatures difficult to define. Unit SN.5, emplaced as a more highly fractionated syenite magma, was at a lower temperature than the other magmas, and again produced highly fractionated, low temperature, residual liquids.

On intrusion, all the syenitic magmas of North Qôroq were probably relatively dry. It has been suggested that SN.4A and SN.4B were the driest, a value for  $\text{P.H}_2\text{O}$  of around 300 bars being obtained from the  $\text{P.H}_2\text{O}$  sensitive plagioclase geothermometer (section 4.16.7.). The other units may, however, have been equally dry, the more hydrous nature of their early-formed mafic assemblages being produced by the introduction of meteoric water into the marginal rocks immediately after emplacement. This

contention is supported by the presence of marginal pegmatites in all units except SN.4A and SN.4B. Crystallization of early-formed anhydrous phases would have resulted in an increase in  $P.H_2O$ . It is likely that for SN.1A, SN.1B and SN.5 the units showing the most fractionated syenites,  $P.H_2O$  exceeded  $P. Total$  and a co-existing aqueous phase 'boiled off'.

Other volatile constituents will also have become concentrated with evolution of the syenites, and this is indicated by the occurrence of sodalite (Cl), cancrinite ( $CO_2$ ), calcite ( $CO_2$ ), fluorite (F) and rinkite (F) in more fractionated syenites. If a separate aqueous phase did 'boil off' at a late stage, Cl and  $CO_2$  may well have been preferentially partitioned into it and contributed to the fenitization process.

The extremely important parameter  $f.O_2$  is thought to have been defined by various buffer assemblages during the syenite's evolution (section 4.16.5). Its importance lies in the fact that the value of  $f.O_2$  is a controlling factor in the crystallization of mafic phases containing elements showing variable oxidation states (valency). Early in the evolution of the less fractionated units,  $f.O_2$  was defined by the fayalite-magnetite-quartz buffer reaction (F.M.Q.). Later, possibly due to the influx of meteoric water  $f.O_2$

was defined by a new buffer assemblage, biotite-feldspar-Fe/Ti oxides. Later still, it has been proposed that  $f.O_2$  was defined by a reaction involving magnetite and acmite, meaning that the pyroxene composition was instrumental in controlling  $f.O_2$  rather than the other way around. When magnetite ceased to be a crystallizing phase  $f.O_2$  may have been defined by a new buffer involving the last-fractionating magma components. If an aqueous phase 'boiled off' as seems probable, the rapid diffusion of  $H_2$  relative to  $O_2$  may have resulted in a marked increase in  $f.O_2$ , above the haematite/magnetite buffer curve (Fig. 4.24).

The activity of silica ( $a.SiO_2$ ) was defined during the bulk of the evolution of the North Qôroq syenites by the reaction involving nepheline and alkali feldspar.  $a.SiO_2$  was always low and, although no definite values can be obtained, it is likely that, prior to the crystallization of these phases, at higher temperatures,  $a.SiO_2$  was also in the region of the albite/nepheline buffer curve. In the most highly fractionated late stage liquids it has been proposed that one of a number of reactions may control  $a.SiO_2$  (see section 4.16.4.).

The Na content of the magmas, or more specifically  $a.Na_2Si_2O_5$ , increased with fractionation. The high values of this parameter were probably instrumental in controlling

the pyroxene trend towards acmite, the crystallization of aenigmatite instead Fe/Ti oxides and the rimming of arfvedsonitic amphibole by acmite. In highly metasomatised rocks the very high  $a.\text{Na}_2\text{Si}_2\text{O}_5$  in the fenitizing fluid controlled the formation of the total mafic assemblage (aenigmatite + acmite + arfvedsonite).

### 7.3. Oversaturated or undersaturated nature of Gardar magmas

In the Gardar province all syenites of a particular centre tend to be either oversaturated or undersaturated, with the exception of Ilímaussaq. In both environments augite syenite is common and has often been invoked as the immediate parent magma (Ferguson, 1964; Stephenson, 1973; Emeleus and Upton, 1975).

The question arises as to whether the trend towards oversaturation or undersaturation is controlled by conditions at depth, i.e. the augite syenite is predisposed towards one or the other, or whether it is controlled by processes occurring as the magma ascends or after it has been emplaced? Obviously, a small initial difference in the augite syenite composition could be accentuated by feldspar fractionation, and in the case of the oversaturated syenites by early loss of an aqueous phase removing alkalis. A great number of previous workers have discussed the trend towards over-

saturation and undersaturation and proposed methods for crossing the feldspar thermal divide (Tilley, 1958; Morse, 1968; Macdonald, 1974; Kempe and Deer, 1976).

Upton (1974) notes that small quantities of nepheline may appear in the norms of some of the more basic syenites from the saturated or oversaturated complexes. This may indicate that, for the oversaturated complexes, some process or processes drive the residual magmas towards the oversaturated minimum whereas normally the trend would be towards the undersaturated minimum. It is proposed here that two processes may be of significance.

The first and most obvious is the assimilation of crustal material, occurring either at the present level of emplacement, at depth, or as the magma ascended. The second possible process is the interaction of the magma with meteoric water. As previously explained (section 6.3.3.) the influx of water would result in a tendency for  $f.O_2$  to rise. This tendency would be resisted by the crystallization of oxides in preference to olivine (see section 4.16.5., reaction 7), resulting in the residual magma being enriched in silica and moving the composition of this residual magma towards the oversaturated minimum. This mechanism has been suggested by Morse (op.cit.). A further effect of the influx of meteoric water would be to promote the crystal-

lization of biotite and amphibole. Both these phases are relatively undersaturated (Macdonald, op.cit.) and their separation would again promote the formation of an oversaturated residual magma. A third effect of the influx would be to lower the temperature of the feldspar thermal divide (Morse, op.cit.) resulting in the undersaturated to oversaturated transformation occurring more readily.

Evidence in favour of one or both of these processes comes from the outer unit, SN.1A, of the North Qôroq Centre. Values from the marginal rocks of this unit cause the  $Sr^{87}/Sr^{86}$  initial ratio for the centre to be high, probably indicating either crustal contamination or an influx of  $Sr^{87}$ -enriched meteoric water. The marginal pegmatites, the common occurrence of biotite (and amphibole), and the extensive rimming of olivine by Fe/Ti oxides in these marginal rocks are consistent with there having been an influx of meteoric water. It is thought to be significant that certain of these marginal rocks are just oversaturated suggesting operation of the effect outlined above. The Kangerdlugssuaq syenite (Kempe and Deer, 1970; Kempe et al., 1970) shows an even more marked gradational variation from marginal nordmarkitic syenites with modal quartz 10-15% to a central, thoroughly undersaturated foyaite. Pankhurst et al. (1976) have demonstrated

convincingly, on the basis of isotopic studies, that this syenitic magma suffered a strong influx of ground water at an early stage in its evolution. It is proposed, therefore, that the Kangerdlugssuaq intrusion represents a more advanced stage of the process for 'silica enrichment' outlined for the marginal rocks of SN.1A. Oversaturated Gardar centres may be caused by even more complete operation of the same process.

The question remains as to why certain centres should show this effect so markedly and others (e.g. North Qôroq) less markedly or not at all? In North Qôroq, the marginal rocks showing the effect have an extensive development of patchy marginal pegmatite. The occurrence of this early-formed, patchy pegmatite requires there to have been an absence of magmatic convection currents at this stage, otherwise the influx of water would have been more equally distributed throughout the intrusion. In Kûngnât, marginal pegmatites are drusy, cross-cutting and demonstrably late stage features (Upton, 1960). The absence of early formed marginal pegmatites suggests that convection in the western and eastern syenitic bodies was initiated at an early stage. There is abundant field evidence for the operation of strong convection currents in the Kûngnât syenites with common 'wash-outs', 'trough-bands' and other sedimentary features.

The strong and early convection would have resulted in any influx of meteoric water being carried to the interior of the intrusion allowing more meteoric water to enter the then depleted margins. If this were so the 'silica enrichment' process outlined above may well have operated.

Harry and Pulvertaft (1963) and Stephenson (1976) note that the strongly undersaturated central complexes in the Gardar province are associated with strongly faulted areas, particularly the intersection of the E.S.E. trending sinistral wrench faults with the E.N.E. regional dyke swarm. The saturated and oversaturated complexes are either determined by faulting to a lesser extent, or not at all. It may be that the wrench fault/dyke (tension) intersection provided a point of weakness in the crust along which the augite syenite and related magmas could ascend rapidly whereas, in non-faulted areas, ascent of magma to the surface was a much slower process, involving stoping and gradual upward movement. The slower process would allow greater time for either assimilation of crustal material and/or an influx of meteoric water and could have been the cause of the oversaturated trend.

The two possible evolutionary sequences outlined above can be summarized as follows:

- (a) Process leading to undersaturated trend. The magma ascended rapidly in a weakened crustal area, so allowing little time for contamination either by acid basement material or meteoric water. The 'silica enrichment' effect only occurred at the level of emplacement and hence was restricted by the rapid cooling at this crustal level. Lack of early convection cells restricted the effect even further to the margins of the intrusion.
- (b) Process leading to oversaturated trend. Magma ascended slowly in an area where the crust was not appreciably weakened. There was opportunity for assimilation and the influx of meteoric water, both at depth and as the magma ascended. The stoping process would have made available considerable quantities of material which may have been assimilated and have contained considerable quantities of meteoric ground-water. Both assimilated material and the increased  $f.O_2$  and  $f.H_2O$  caused by the water could have resulted in the magma following a trend towards silica oversaturation.

Initial  $\text{Sr}^{87}/\text{Sr}^{86}$  ratios (Blaxland et al., in press) could be expected to give confirmation of the processes mentioned above. Unfortunately they do not provide unequivocal confirmation. Certainly, some of the oversaturated centres, particularly the Nunarssuit Biotite Granite and the Ivigtut Granite do show enrichment in radiogenic Sr. The Kûngnât syenites, Helene Granite and Nunarssuit Syenite show a possible slight enrichment, but the Klokken intrusion (Blaxland and Parsons, 1975) shows a typical 'mantle value' suggesting no assimilation and no reaction with  $\text{Sr}^{87}$  enriched water. It may be, however, that the amount of either assimilation, or water influx need only be small to 'push' the magma along an oversaturated trend, and would not affect the initial Sr ratio to any extent. The one really anomalous value comes from the Ilímaussaq intrusion, which is thoroughly undersaturated while showing a  $\text{Sr}^{87}/\text{Sr}^{86}$  ratio of 0.7096 for its agpaitic rocks. Blaxland et al. (1976) discount bulk contamination by the crust on chemical grounds and attribute the value to selective radiogenic  $\text{Sr}^{87}$  enrichment. The augite syenite of the Ilímaussaq Complex has an initial ratio with a normal low mantle value (0.703) suggesting that, if the high ratio for the agpaitic rocks was due to crustal contamination, it occurred at depth, when the magma may

already have been thoroughly committed to an undersaturated trend.

If the crustal contamination/meteoric water process can generally be applied to central complex syenites it should also be applicable to dyke rocks. Emeleus and Upton (1975) state that the oversaturated dykes concentrate to a degree near to the oversaturated central complexes and the undersaturated dykes near to undersaturated ones. This suggests that the 'silica enrichment' process occurred at depth or as the magma ascended and that this magma was parental to both the dykes and central complex units.

Although the petrographic scheme outlined has drawbacks, it does explain many of the observed features of Gardar central complexes. Other factors almost certainly play parts in controlling trends towards undersaturation and oversaturation, but the mechanism presented here may well be of major significance in this context.

#### 7.4. Evolution of the syenites at depth

##### 7.4.1. Partial melting

Partial melting of the upper mantle and particularly the lower crust has been advocated by Bailey (1964, 1970, 1974) as the mechanism for generating phonolitic and trachytic magmas in continental regions. He suggests that partial melting of a gabbroic lower crust is promoted by

relief of pressure at depth, in areas of continental uplift, leading to an influx of volatiles and 'mobile elements'. He particularly favours this mechanism as that generating the alkali volcanics of the East African Rift System.

Operation of this mechanism in the Gardar would explain a number of the observed features. The common occurrence of rocks of augite syenite and more fractionated compositions could be explained by saying that temperatures imposed by the geothermal gradient rarely exceeded the augite syenite liquidus resulting in extensive evolution of augite syenite magma and only rarely more basic magma. The Kûngnât Complex (Upton, 1960) and the South Qôroq Centre of the Igaliko Complex (Stephenson, 1973) both appear to have successive intrusive units of more basic material. Progressive partial melting could explain this feature. The mechanism of volatile fluxing, proposed by Bailey, would also account for the high volatile and alkali contents of the rocks.

Several features of the Gardar province, however, argue against partial melting. Although not common at the present erosional level, basic material is found in several of the central complexes, in dyke rocks, and in the early-formed lavas. It is also very likely that large quantities of

basic material lie at depth beneath the Gardar, a speculation awaiting confirmation by geophysical work at present being carried out by Lancaster University. Igneous centres such as North Qôroq, Tugtutôq Central Complex and Ilímaussaq show the intrusion of more evolved magmas with time, more in keeping with a crystal fractionation model than partial melting. The Sr isotope studies of Blaxland et al. (op.cit.) suggest that, with few exceptions, the initial  $\text{Sr}^{87}/\text{Sr}^{86}$  ratios are consistent with a mantle origin. Partial melting of mantle material to produce augite syenite poses problems with regard to segregation and collection of a partial melt that would only represent a tiny fraction of the source material. Chemical trends shown by the North Qôroq syenites are consistent with crystal fractionation models. Macdonald (1974) states that 'where the volumes of basic and salic magmas are of the right order, and where the chemical trends are explicable by fractional crystallization of the observed phenocryst assemblages, there is no strong case for doubting the derivation of the salic liquids by fractionation of a basic magma'. He quotes the Gardar province as an example of this situation where fractional crystallization is thought to be the dominant mechanism operating.

#### 7.4.2. Fractionation of basalt parent

Upton (1971), from melting experiments on basic Gardar material, has indicated that, in a high pressure environment (i.e. 15-60km. depth), clinopyroxene fractionation may have been a significant process affecting primary basic Gardar magmas. This would have produced high alumina alkali basalts. At lower pressures Upton suggests that expansion of the plagioclase field would have resulted in anorthosite formation and the enrichment of the residual liquid in alkalis. Eventually, this process could well yield trachytic (augite syenite) magma, thought to be the immediate parental type in many Gardar centres.

Bridgwater (1967) and Bridgwater in Bridgwater and Harry (1968) suggests a complex history to account for many of the geological features noted in the Gardar province. He suggests that a primary Gardar magma suffered liquid fractionation in a magma chamber, in response to pressure and temperature gradients, resulting in an alkali basalt composition at the top of the chamber and a more calcic magma at lower levels. This compositionally zoned liquid would explain the occurrence of dyke rocks with cores more basic than their margins, formed by tapping successively deeper levels in the magma chamber. Bridgwater proposes that crystallization took place, labradorite crystallizing

from the alkali basalt and floating to form an anorthosite capping, and bytownite from the more calcic basalt and sinking, together with the mafic minerals to form a layered sequence at the bottom of the chamber. A combination of crystal fractionation and upward movement of volatiles and associated alkalis eventually resulted in the formation of syenitic magmas, which were then intruded to form the central complexes.

Whatever the exact method of formation of the syenite, it appears that alkali basalt played a crucial role. Indeed, analyses of basalt lavas of the Eriksfjord Formation show them to be alkali olivine basalts and hawaiites (Emeleus and Upton, op.cit.). The large quantity of anorthosite inclusions and plagioclase megacrysts concentrated in the upper parts of exposed basic intrusives in the Gardar confirms the importance of plagioclase fractionation and adds credence to the 'anorthosite flotation cumulate' hypothesis of Bridgwater and Harry.

One problem arising in the interpretation of Gardar petrogenesis is the relative scarcity of rocks compositionally intermediate between gabbro and augite syenite. Upton (1974) has suggested that this may be due to these 'intermediate' rocks having a higher viscosity than the hotter less silicious basalts on the one hand and the volatile rich

trachytic magmas on the other. The abundance of augite syenite and more fractionated rocks may have been due to the effect of the geothermal gradient, which was probably high in the Gardar province at this time. Taking a typical value of  $45^{\circ}\text{C}/\text{Km}$  for a continental region of high heat flow (Bailey, 1970), the crustal rocks surrounding the magma chamber, if it lay at a depth of about 20-30Km., would be at a temperature in excess of  $900^{\circ}\text{C}$ . This is thought to be a reasonable liquidus temperature for augite syenite magma. Hence, although more basic material would suffer crystallization, the residual augite syenite would remain in a liquid state, available for intrusion at higher levels until either depleted by ascent to higher levels and consequential crystallization, or by solidification occurring in situ as a result of the geothermal gradient returning to a normal continental value. If this mechanism operated the occurrence of later basic intrusions would have to be related to a repetition of the mantle partial melting and basalt genesis process.

#### 7.4.3. Origin of North Qôroq magmas

A relatively simple model can be presented, consistent with the observed geological features, to explain the sequence and types of syenitic magma in the North Qôroq Centre and their evolution from an immediate parent of

augite syenite.

Units SN.1A, SN.1B, SN.2, SN.4A and SN.4B all intruded as magmas not far removed from augite syenite in composition. In contrast to the earlier units, SN.4A and SN.4B contained a moderately high proportion of phenocrysts on intrusion. The final unit, SN.5, was emplaced as an altogether more fractionated magma. The sequence is consistent with an augite syenite magma source, cooling and fractionating at depth, and intruding more fractionated material with time. This simple type of model with more fractionated rocks following less fractionated ones can also be invoked to explain the sequence of rock types observed in other Gardar centres (e.g. Ilímaussaq, Tugtutôq Central Complex).

In the Kûngnât and South Qôroq centres, however, the trend is for later intrusive units to be less fractionated than earlier ones, a feature not consistent with the simple mechanism outlined above. Stephenson (1973) has suggested that this phenomenon of decreasing fractionation state with time could be explained by the presence of a magma chamber at depth in which the liquid was zoned from more highly fractionated upper regions to less fractionated lower regions. Tapping this magma source for high level emplacement would result in successive magma batches being less fractionated. This fractionated syenite body at depth could

have arisen through the process of volatile and alkali diffusion along pressure and temperature gradients (Kennedy, 1955). Stephenson (1973) favours this process as occurring after emplacement, at high level, and is dubious that a fractionated magma column of this type could be maintained at depth. It has been mentioned earlier that such diffusion is a slow process. It seems much more likely that the process operated at depth, as proposed by Bridgwater and Harry (op.cit.), where the slow cooling of the magma would allow compositional zoning, than after emplacement where the relatively rapid cooling would restrict such a process. Indeed, it may be that the process is only feasible in deep magma chambers under conditions of high heat flow where the magma is maintained in a liquid state over considerable periods of time.

#### 7.5. Global setting of the Gardar province

The Gardar province resembles the East African rift in many of its tectonic, sedimentary, volcanic and plutonic features. Typical continental-type sediments are developed, together with a wide range of alkali rock types, many of which have counterparts in East Africa. Kempe and Deer (1970) state that the Kangerdlugssuaq Syenite shows many similarities to Gardar syenites. Burke and Dewey (1973a) and Brooks (1973) state that the general geology of the

Kangerdlugssuaq area is very similar to that of the Gardar province. Kangerdlugssuaq, according to these authors, is one of three arms of a plume-generated triple junction. Where ocean floor spreading and tholeiitic magmatism took place in the other two arms, the Kangerdlugssuaq fjord represents a 'failed arm' characterised by extensive alkali magmatism. The concept of 'failed arms' of rift systems seems a reasonable one. Certainly, Burke and Dewey (op. cit.) quote numerous examples of triple junction development, many of which include a 'failed arm', and the simple angular relationship ( $\sim 120^\circ$ ) between the Greenland coast and the Kangerdlugssuaq fjord strongly supports their contention that Kangerdlugssuaq is a recent example.

If, as is suggested, the Gardar province represents a similar 'failed arm', then it is likely that it was one branch of a much larger rift system analogous to the East African rift of the present day. Burke and Dewey (op.cit.) state that 1300-1100 m. years ago, exactly the period of Gardar igneous activity, widespread rifting affected a large continental mass, part of which now forms North America and Greenland. Emeleus and Upton (op.cit) also comment on this North American rift system and suggest that a branch of this rift extended across South Greenland and that the Gardar province is merely 'a localised tectonic-

volcanic province within the extended system'.

Assuming the Gardar to be part of a rift system, probably a 'failed arm', something of its formation and evolution can be tentatively mentioned.

Burke and Dewey (1973b) and Sutton (1973) suggest that lithosphere plates had developed by about 2000 m. years B.P., well before the Gardar period. At present, and presumably in Gardar times, these plates would appear to be driven by some kind of mantle convection, the scale of which remains a point of contention. The proposed scale varies from involving the whole mantle to only the asthenosphere. The plume model, favoured by Burke and Dewey, and developed by Morgan (1971) involves a limited number of mantle plumes, each of only a few hundred kilometres diameter, originating at the core/mantle boundary. On reaching the lithosphere these plumes cause a 'hot spot' (e.g. Iceland) and the motion becomes horizontal.

Whatever the mechanism for upward movement of mantle material in Gardar times there were two probable effects. The adiabatic rise of the material resulted in partial melting in the region of the lithosphere/ asthenosphere boundary. The second effect was one of uplift caused by the hot, low density upper mantle. Oxburgh and Turcott (1968) considering a type of plume model show that the zone

of partial melting should be about 400km. in width. It may be more than coincidence that the observed uplift in East Africa, thought to be caused by rising plumes is typically over an area 80km. wide and 200-300km. long (Burke and Whiteman, 1973). This is very similar to Oxburgh and Turcott's predicted dimensions and to the extent of the Gardar province observed at the present time (80km. x 180km., Upton, 1974).

The partial melting of mantle material beneath the Gardar will have resulted in magma generation, which may, by the processes already outlined have given rise to the spectrum of igneous rock types observed at the present time. Basic lavas and dykes of various types would have been emplaced in the zone of tension caused by the uplift, and considerable volumes of magma may have fractionated at depth and periodically been 'tapped off' to form both central complexes and dykes.

In response to the uplift produced by the upwelling of mantle material, rifting occurred, probably along three arms (the rrr triple junction of Burke and Dewey). It is possible that separation occurred along two of the rifts with the formation of new oceanic crust and tholeiitic magmatism, whereas the Gardar rift remained as a 'failed arm' typified by deeper seated alkali magmatism. The situation is analogous to that proposed for the

Kangerdlugssuaq 'failed arm'.

One final point worthy of mention is that the age dating of Gardar rocks suggests that the central complexes at least tended to form at two restricted periods of magmatism falling around 1300 and 1160 m. years B.P. Burke and Whiteman (op.cit.) show that uplift affecting the East African rift occurred 180-130m. years B.P. and again within the last 25m. years. An explanation for these two observations may be found in the statement by Burke and Dewey that 'there has been a tendency to infer, because an area suffered uplift say 100m. years B.P. and is being rifted now, that the area has remained in an environment favourable to uplift throughout the intervening period. If rifting is a product of plume generated uplift, this is improbable, because plates are generally in motion over the world plume population and rifting is a response to the episodic probing of passing plumes under slowly moving or stationary plates.' Hence, the time gap of 100m. years separating similar major units of the Igaliko Complex may simply reflect two separate periods in which a mantle plume was centered under the area of the Gardar province, generating magmas which intruded the area of presumed crustal weakness at Igaliko. This reactivation of a 'failed arm' would be due to the initial rifting, which Burke and Dewey

think would extend through the thickness of the continental lithosphere presenting zones of weakness where plumes may probe.

#### 7.6. Summary

In this chapter the important mechanism of in situ crystal fractionation has been presented as being the principal cause of variation seen within units of the North Qôroq Centre. The effects of fenitization and water influx have also been mentioned. The latter mechanism, and the process of assimilation, even if limited in extent may have important implications in deciding the ultimate fate of an augite syenite magma, i.e. whether it fractionates towards an undersaturated or oversaturated minimum.

More speculative conclusions have been drawn about the evolution of North Qôroq magmas, and Gardar magmas generally, at depth in the upper mantle and lower crust. Possible mechanisms for evolution have been briefly examined.

Finally, an attempt has been made to present the Gardar province in its possible global tectonic and magmatic setting, discussing the likely causes of the formation of the province in the light of plate tectonics theory.

REFERENCES

- ABBOTT, M.J., 1967. Aenigmatite from the groundmass of a peralkaline trachyte. *Am. Miner.* 52, 1895-1901.
- AHRENS, L.H., PINSON, W.H. and KEARNS, M., 1952. Association of rubidium and potassium and their abundance in common igneous rocks and meteorites. *Geochim. Cosmochim. Acta*, 2, 229-242.
- ALLAART, J.H., 1964. Review of the work on the Precambrian Basement (Pre-Gardar) between Kobberrminebugt and Frederiksdal, South Greenland. *Rapp. Grønlands geol. Unders.* 1.
- ANDERSON, J.G., 1974. The geology of Alángorssuaq, Northern Nunarssuit Complex, South Greenland. Unpubl. Ph.D. Thesis, University of Aberdeen.
- AOKI, K., 1964. Clinopyroxenes from alkaline rocks of Japan. *Am. Miner.* 49, 1199-1223.
- BACKINSKI, S.W. and MULLER, G., 1971. Experimental determinations of the microcline - low albite solvus. *J. Petrology*, 12, 329-356.
- BAILEY, D.K., 1964. Crustal warping - a possible tectonic control of alkaline magmatism. *J. Geophys. Res.* 69, 1103-1111.
- BAILEY, D.K., 1969. The stability of acmite in the presence of H<sub>2</sub>O. *Am. J. Sci.*, 267A, 1-16.
- BAILEY, D.K., 1970. Volatile flux, heat focussing and the generation of magma. *Geol. J. Spec. Iss.* 2, 177-186.
- BAILEY, D.K., 1974. Origin of alkaline magmas as a result of anatexis - crustal anatexis. In Sørensen, H. (Ed.), *The alkaline rocks*, 436-442. John Wiley and Sons, London.
- BAILEY, D.K. and SCHAIRER, J.F., 1964. Feldspar-liquid equilibria in peralkaline liquids - the orthoclase effect. *Am. J. Sci.*, 262, 1198-1206.
- BAILEY, D.K. and SCHAIRER, J.F., 1966. The system Na<sub>2</sub>O-Al<sub>2</sub>O<sub>3</sub>-Fe<sub>2</sub>O<sub>3</sub>-SiO<sub>2</sub> at 1 atmosphere, and the petrogenesis of alkaline rocks. *J. Petrology*, 7, 114-170.

- BARTH, T.F.W., 1963. The composition of nepheline. Schweiz. Min. Petr. Mitt. 43, 153-161.
- BLAXLAND, A.B. and PARSONS, I., 1975. Age and origin of the Klokken gabbro-syenite intrusion, South Greenland: Rb-Sr study. Bull. geol. Soc. Denmark, 24, 27-32.
- BLAXLAND, A.B., van BREEMEN, O., EMELEUS, C.H. and ANDERSON, J.G., in press. Age and origin of the major syenite centres in the Gardar Province of South Greenland: Rb-Sr study.
- BLAXLAND, A.B., van BREEMEN, O. and STEENFELT, A., 1976. Age and origin of agpaitic magmatism at Ilímaussaq, South Greenland: Rb-Sr study. Lithos, 9, 31-38.
- BOTTINGA, Y. and WEILL, D.F., 1972. The viscosity of magmatic silicate liquids: a model for calculations. Am. J. Sci., 272, 438-475.
- BOWEN, N.L., 1913. The melting phenomena of the plagioclase feldspars. Am. J. Sci., 35, 577-599.
- BOWEN, N.L., 1937. Recent high temperature research on silicates and its significance in igneous geology. Am. J. Sci., 33, 1-21.
- BOWEN, N.L., 1945. Phase equilibria bearing on the origin and differentiation of alkaline rocks. Am. J. Sci. 243A, 75-89.
- BOWEN, N.L. and TUTTLE, O.F., 1950. The system  $\text{NaAlSi}_3\text{O}_8$ - $\text{KAlSi}_3\text{O}_8$ - $\text{H}_2\text{O}$ . J. Geol. 58, 489-511.
- BOYD, F.R. and ENGLAND, J.L., 1962. Melting of silicates at high pressure. Ann. Rept. Geophys. Lab. Yearbook, 60, 113-125.
- BRIDGWATER, D., 1967. Feldspathic inclusions in the Gardar igneous rocks of South Greenland and their relevance to the formation of major anorthosites in the Canadian Shield. Can. J. Earth Sci. 4, 995-1014.
- BRIDGWATER, D. and HARRY, W.T., 1968. Anorthosite xenoliths and plagioclase megacrysts in Precambrian intrusions of South Greenland. Bull. Grønlands geol. Unders., 77, also Meddr. Grønland, 185,2.

- BROCK, P.W.G., GELLATLY, D.C. and von KNORRING, O., 1964. Mboziite, a new sodic amphibole end-member. *Mineral. Mag.*, 33, 1057-1065.
- BROOKS, C.K., 1973. Rifting and doming in southern East Greenland. *Nature Phys. Sci.*, 244, 23-25.
- BUDDINGTON, A.F. and LINDSLEY, D.H., 1964. Iron-titanium oxide minerals and synthetic equivalents. *J. Petrology*, 5, 310-357.
- BURKE, K. and DEWEY, J.F., 1973a. Plume generated triple junctions: key indicators in applying plate tectonics to old rocks. *J. Geol.*, 81, 406-433.
- BURKE, K. and DEWEY, J.F., 1973b. An outline of Precambrian plate development. In Tarling, D.H. and Runcorn, S.K. (Eds.), *Implications of Continental Drift to the earth sciences*, 1035-1045. Academic Press, London and New York.
- BURKE, K. and WHITEMAN, A.J., 1973. Uplift, rifting and the break up of Africa. In Tarling, D.H. and Runcorn, S.K. (Eds.), *Implications of Continental Drift to the earth sciences*, 735-755. Academic Press, London and New York.
- BURNHAM, C.W., 1967. Hydrothermal fluids at the magmatic stage. In Barnes, H.L. (Ed.), *Geochemistry of hydrothermal ore deposits*, 34-76. Holt, New York.
- BURNHAM, C.W., HOLLOWAY, J.R. and DAVIS, N.F., 1969. Thermodynamic properties of water to 1000°C and 10,000 bars. *Geol. Soc. Am. Spec. Paper*, 132, 1-96.
- BURNS, R.G., 1970. Mineralogical applications of crystal field theory. Cambridge, London.
- CARMICHAEL, D.M., 1969. On the mechanism of prograde metamorphic reactions in quartz bearing pelitic rocks. *Contr. Mineral. Petrol.*, 20, 244-267.
- CARMICHAEL, I.S.E., NICHOLLS, J. and SMITH, A.L., 1970. Silica activity in igneous rocks. *Am. Miner.* 55, 246-263.
- CARMICHAEL, I.S.E., TURNER, F.J. and VERHOOGEN, J., 1974. *Igneous Petrology*. McGraw-Hill.

- CURRIE, K.L. and FERGUSON, J., 1971. A study of fenitization around the alkaline carbonatite complex at Callander Bay, Ontario, Canada. *Can. J. Earth Sci.*, 8, 498-517.
- CZAMANSKE, G.K. and WONES, O.R., 1973. Oxidation during magmatic differentiation, Finnmarka complex, Oslo area, Norway: Pt.2, the mafic silicates. *J. Petrology*, 14, 349-380.
- DEER, W.A., HOWIE, R.A. and ZUSSMAN, J., 1963. Rock forming minerals, Vol.2 (Chain Silicates). Longmans, London.
- DUCHESNE, J.C., 1972. Iron-titanium oxide minerals in the Bjerkren-Sogndal Massif, South-western Norway. *J. Petrology*, 13, 57-81.
- ERSTROM, T.K., 1973. Synthetic and natural chlorine-bearing apatite. *Contr. Mineral. Petrol.* 38, 329-338.
- EDGAR, A.D. and PARKER, L.M., 1974. Comparison of melting relationships of some plutonic and volcanic peralkaline undersaturated rocks. *Lithos*, 7, 263-273.
- ELSDON, R., 1972. Iron-titanium oxide minerals in the Upper Layered Series, Kap Edvard Holm, East Greenland. *Mineral. Mag.*, 38, 946-956.
- EMELEUS, C.H. and HARRY, W.T., 1970. The Igaliko Nepheline Syenite Complex. General description. *Bull. Grønlands geol. Unders.*, 85, also *Meddr. Grønland*, 196, 3.
- EMELEUS, C.H. and SMITH, J.V., 1959. The alkali feldspars VI. Sanidine and orthoclase perthites from the Slieve Gullion area, Northern Ireland. *Am. Miner.*, 44, 1187-1209.
- EMELEUS, C.H. and UPTON, B.G.J., 1976. The Gardar period in Southern Greenland. In Watt, W.S. and Escher, A. (Eds.), *Geology of Greenland*, 153-181.
- ENGELL, J., 1973. A closed system crystal fractionation model for the agpaitic Ilímaussaq intrusion, South Greenland, with special reference to the Lujavrites. *Bull. Geol. Soc. Denmark*, 22, 334-62.

- ERNST, W.G., 1962. Synthesis, stability relations and occurrence of riebeckite and riebeckite-arfvedsonite solid solutions. *J. Geol.* 70, 689-736.
- ERNST, W.G., 1968. Amphiboles. Minerals, rocks and inorganic materials, sub-series: experimental mineralogy, vol.1. Springer Verlag, Berlin, Heidelberg, New York.
- EUGSTER, H.P. and WONES, D.R., 1962. Stability relations of the ferruginous biotite, annite. *J. Petrology*, 3, 82-125.
- FERGUSON, J., 1964. Geology of the Ilímaussaq intrusion, South Greenland. Description of map and structure. *Bull. Grønlands geol. Unders.* 39, also *Meddr. Grønland*, 172, 4.
- FLINK, G., 1898. Berättelse om en Mineralogisk Resa i Syd-Grønland sommaren 1897. *Meddr. Grønland*, 14, 2.
- FLOWER, M.F.J., 1973. Evolution of basaltic and differentiated lavas from Anjouan, Comores archipelago. *Contr. Mineral. Petrol.*, 38, 237-260.
- FLOWER, M.F.J., 1974. Phase relations of titan-acmite in the system  $\text{Na}_2\text{O}-\text{Fe}_2\text{O}_3-\text{Al}_2\text{O}_3-\text{TiO}_2-\text{SiO}_2$  at 1000 bars total water pressure. *Am. Miner.*, 59, 536-548.
- GILBERT, M.C., 1966. Synthesis and stability relationships of ferropargasite. *Am. J. Sci.*, 264, 698-742.
- GILL, R.C.O., 1972. Geochemistry of peralkaline phonolite dykes from the Grønnedal-Ika area, South Greenland. *Contr. Mineral. Petrol.*, 34, 87-100.
- GILLBERG, M., 1964. Halogens and hydroxyl contents of micas and amphiboles in Swedish granitic rocks. *Geochim. Cosmochim. Acta*, 28, 495-516.
- HAMILTON, D.L., 1961. Nephelines as crystallization temperature indicators. *J. Geol.* 69, 321-329.
- HAMILTON, D.L. and MACKENZIE, W.S., 1960. Nepheline solid solution in the system  $\text{NaAlSi}_4\text{O}_{12}-\text{KAlSi}_4\text{O}_{12}-\text{SiO}_2$ . *J. Petrology*, 1, 56-72.
- HAMILTON, D.L. and MACKENZIE, W.S., 1965. Phase equilibria studies in the system  $\text{NaAlSi}_4\text{O}_{12}$  (nepheline)- $\text{KAlSi}_4\text{O}_{12}$  (Kalsilite)- $\text{SiO}_2$ - $\text{H}_2\text{O}$ . *Mineral. Mag.*, 34, 214-231.

- HARNIK, A.B., 1969. Strukturelle zustände in den anorthoklasen der Rhombenporphyre des Oslogebietes. Inaug. Diss. Universität Zürich. SMPM 49, 509-567.
- HARRY, W.T., 1961, 1962, 1963. G.G.U. field diaries.
- HARRY, W.T. and PULVERTAFT, T.C.R., 1963. The Nunarssuit intrusive complex, South Greenland, Part 1. Bull. Grønlands geol. Unders, 36, also Meddr. Grønland, 169, 1.
- HODGES, F.N. and BARKER, D.S., 1973. Solid solution in aenigmatite. Ann. Rept. Geophys. Lab. Yearbook, 71, 578-581.
- JAMES, R.S. and HAMILTON, D.L., 1969. Phase relations in the system  $\text{NaAlSi}_3\text{O}_8$ - $\text{KAlSi}_3\text{O}_8$ - $\text{CaAl}_2\text{Si}_2\text{O}_8$ - $\text{SiO}_2$  at 1 kilobar water vapour pressure. Contr. Mineral. Petrol., 21, 111-141.
- JORGENSEN, D.B., 1971. Origin of patchy zoning in plagioclase from gabbroic rocks of southwestern Oregon. Bull. Geol. Soc. Am., 82, 2667-2670.
- KELLEY, K.K., 1960. Contributions to the data on theoretical metallurgy: pt.13, high temperature heat content, heat capacity and entropy data for the elements and inorganic compounds. U.S. Bur. Mines Bull., 584.
- KELSEY, C.H. and MCKIE, D., 1964. The unit cell of aenigmatite. Mineral. Mag., 33, 986-1001.
- KEMPE, D.R.C. and DEER, W.A., 1970. The mineralogy of the Kangerdlugssuaq alkaline intrusion, E. Greenland. Meddr. Grønland, 190, 3.
- KEMPE, D.R.C. and DEER, W.A., 1976. The petrogenesis of the Kangerdlugssuaq alkaline intrusion, East Greenland. Lithos, 9, 111-123.
- KEMPE, D.R.C., DEER, W.A. and WAGER, L.R., 1970. The petrology of the Kangerdlugssuaq alkaline intrusion, East Greenland. Meddr. Grønland, 190, 2.
- KENNEDY, G.C., 1955. Some aspects of the role of water in rock melts. Geol. Soc. Am. Spec. Paper, 62, 489-504.
- KIRK, R.D., 1955. The luminescence and tenebrescence of natural and synthetic sodalite. Am. Miner., 40, 22-31.

- KI-TAE KIM and BURLEY, B.J., 1971. Phase equilibria in the system  $\text{NaAlSi}_3\text{O}_8$ - $\text{NaAlSiO}_4$ - $\text{H}_2\text{O}$  with special emphasis on the stability of analcite. *Can. J. Earth Sci.*, 8, 311-337.
- KOGARKO, L.N., 1974. Role of volatiles. In Sørensen, H. (Ed.), *The alkaline rocks*, 474-487. John Wiley and Sons, London.
- KOMAR, P.D., 1972. Flow differentiation in igneous dikes and sills: profiles of velocity and phenocryst concentration. *Bull. Geol. Soc. Am.*, 83, 3443-3448.
- KOSTER VAN GROOS, A.F. and WYLLIE, P.J., 1966. Liquid immiscibility in the system  $\text{Na}_2\text{O}$ - $\text{Al}_2\text{O}_3$ - $\text{SiO}_2$ - $\text{CO}_2$  at pressures to 1 Kilobar. *Am. J. Sci.* 264, 234-255.
- KOSTER VAN GROOS, A.F. and WYLLIE, P.J., 1968. Liquid immiscibility in the join  $\text{NaAlSi}_3\text{O}_8$ - $\text{Na}_2\text{CO}_3$ - $\text{H}_2\text{O}$ , and its bearing on the origin of carbonatites. *Am. J. Sci.*, 266, 932-967.
- KOSTER VAN GROOS, A.F. and WYLLIE, P.J., 1969. Melting relationships in the system  $\text{NaAlSi}_3\text{O}_8$ - $\text{NaCl}$ - $\text{H}_2\text{O}$  at one kilobar pressure with petrological applications. *J. Geol.*, 77, 581-605.
- KUDO, A.M. and WEILL, D.F., 1970. An igneous plagioclase geothermometer. *Contr. Mineral. Petrol.*, 25, 52-65.
- LARSEN, L.M. and STEENFELT, A., 1974. Alkali loss and retention in an iron-rich peralkaline phonolite dyke from the Gardar province, South Greenland. *Lithos*, 7, 81-90.
- LEAKE, B.E., 1962. On the non-existence of a vacant area in the Hallimond calciferous amphibole diagram. *Jap. J. Geol. Geog.*, 33, 1-13.
- LEUNG, I.S., 1974. Sector zoned titanogites; morphology, crystal chemistry and growth. *Am. Miner.*, 59, 127-138.
- LINDH, A., 1972. A hydrothermal investigation of the system  $\text{FeO}$ ,  $\text{Fe}_2\text{O}_3$ ,  $\text{TiO}_2$ . *Lithos*, 5, 325-343.
- LINDH, A., 1973. Element distribution among silicate and oxide minerals in a titanomagnetite ore body. *Contr. Mineral. Petrol.*, 39, 219-230.

- LINDSLEY, D.H., 1971. Synthesis and preliminary results on the stability of aenigmatite ( $\text{Na}_2\text{Fe}_5\text{TiSi}_6\text{O}_{20}$ ). Ann. Rept. Geophys. Lab. Yearbook, 69, 188-190.
- LINDSLEY, D.H. and HAGGERTY, S.E., 1971. Phase relations of Fe-Ti oxides and aenigmatite; oxygen fugacity of the pegmatoid zones. Ann. Rept. Geophys. Lab. Yearbook, 69, 278-284.
- LUTH, W.C. and TUTTLE, O.F., 1966. The alkali feldspar solvus in the system  $\text{Na}_2\text{O}-\text{K}_2\text{O}-\text{Al}_2\text{O}_3-\text{SiO}_2-\text{H}_2\text{O}$ . Am. Miner., 51, 1359-1373.
- MACDONALD, R., 1969. The petrology of alkaline dykes from the Tugtutôq region, South Greenland. Bull. Geol. Soc. Denmark, 19, 257-282.
- MACDONALD, R., 1974. The role of fractional crystallization in the formation of the alkaline rocks. In Sørensen, H. (Ed.), The alkaline rocks, 442-459. John Wiley and Sons, London.
- MACDONALD, R., UPTON, B.G.J. and THOMAS, J.E., 1973. Potassium and fluorine-rich hydrous phase coexisting with peralkaline granite in South Greenland. Earth and Planet. Sci. Letts., 18, 217-222.
- MARSH, J.S., 1975. Aenigmatite stability in silica-undersaturated rocks. Contr. Mineral. Petrol., 50, 135-144.
- MARTIN, R.E., 1969. The hydrothermal synthesis of low albite. Contr. Mineral. Petrol., 23, 323-339.
- McKIE, D., 1966. Fenitization. In Tuttle, O.F. and Gittins, J. (Eds.), Carbonatites, 261-294. Interscience, New York.
- MORGAN, W.J., 1971. Convection plumes in the lower mantle. Nature Phys. Sci., 230, 42-43.
- MORSE, S.A., 1969. Syenites. Ann. Rept. Geophys. Lab. Yearbook, 67, 112-120.
- MUIR, I.D. and SMITH, J.V., 1956. Crystallization of feldspars in larvikites. Zeit. Krist., 107, 182-195.
- NASH, W.P., CARMICHAEL, I.S.E. and JOHNSON, R.W., 1969. The mineralogy and petrology of Mount Suswa, Kenya. J. Petrology, 10, 409-439.

- NASH, W.P. and WILKINSON, J.F.G., 1970. Shonkin Sag laccolith, Montana: pt.I, mafic minerals and estimates of temperature, pressure, oxygen fugacity and silica activity. *Contr. Mineral. Petrol.*, 25, 241-269.
- NICHOLLS, J. and CARMICHAEL, I.S.E., 1969. Peralkaline acid liquids: a petrological study. *Contr. Mineral. Petrol.*, 20, 268-294.
- NICHOLLS, J., CARMICHAEL, I.S.E. and STORMER, J.C., 1971. Silica activity and P<sub>total</sub> in igneous rocks. *Contr. Mineral. Petrol.*, 33, 1-20.
- ORVILLE, P.M., 1963. Alkali ion exchange between vapour and feldspar phases. *Am. J. Sci.*, 261, 201-237.
- OXBURGH, E.R. and TURCOTTE, D.L., 1968. Mid-ocean ridges and geotherm distribution during mantle convection. *J. Geophys. Res.*, 73, 2643-2661.
- PANKHURST, R.J., BECKINSALE, R.D. and BROOKS, C.K., 1976. Strontium and oxygen isotope evidence relating to the petrogenesis of the Kangerdlugssuaq alkaline intrusion, East Greenland. *Contr. Mineral. Petrol.*, 54, 17-42.
- PARSONS, I., 1965. The feldspathic syenites of the Loch Ailsh intrusion, Assynt, Scotland. *J. Petrology*, 6, 365-394.
- PARSONS, I., 1972. Petrology of the Puklen syenite-alkali granite complex, Nunnarssuit, South Greenland. *Meddr. Grønland*, 195, 3.
- PARSONS, I. and SMITH, P., 1974. Experimental studies of sodic microperthites from the Loch Ailsh syenite.
- PERCHUK, L.L. and RYABCHIKOV, I.D., 1968. Mineral equilibria in the system nepheline-alkali feldspar-plagioclase and their petrological significance. *J. Petrology*, 9, 123-167.
- PETERS, T.J., LUTH, W.C. and TUTTLE, O.F., 1966. The melting of analcite solid solutions in the system  $\text{NaAlSi}_4\text{O}_{10} - \text{NaAlSi}_3\text{O}_8 - \text{H}_2\text{O}$ . *Am. Miner.*, 51, 736-753.
- PHILLIPS, R., 1966. Amphibole compositional space. *Mineral. Mag.*, 35, 945-952.

- PHILLIPS, R. and LAYTON, W., 1964. The calciferous and alkali amphiboles. *Mineral. Mag.*, 33, 1097-1109.
- PIOTROWSKI, J.M. and EDGAR, A.D., 1970. Melting relations of undersaturated alkaline rocks from South Greenland. *Meddr. Grønland*, 181, 9.
- PLATT, R.G. and ROSE-HANSEN, J., 1976. The system ussingite-water and its bearing on crystallization of per sodic portions of the system  $\text{Na}_2\text{O}-\text{Al}_2\text{O}_3-\text{SiO}_2-\text{H}_2\text{O}$  at 1 kb. total pressure. *J. Geol.*, 83, 763-772.
- POPP, R.K. and GILBERT, M.C., 1972. Stability of acmite-jadeite pyroxenes at low pressure. *Am. Miner.*, 57, 1210-1231.
- POWELL, M. and POWELL, R., 1974. An olivine-clinopyroxene geothermometer. *Contr. Mineral. Petrol.*, 48, 249-263.
- POWELL, M. and POWELL, R., in press. A nepheline-alkali feldspar geothermometer.
- RAMDOHR, P., 1969. The ore minerals and their intergrowths. Pergamon Press.
- ROBIE, R.A. and WAULDBAUM, D.R., 1968. Thermodynamic properties of minerals and related substances at  $298.15^\circ\text{K}$  ( $25.0^\circ\text{C}$ ) and one atmosphere (1.013 Bars) pressure and at higher temperatures. *U.S.G.S. Bull.* 1259.
- ROWBOTHAM, G., 1973. Hydrothermal synthesis and mineralogy of the alkali amphiboles. Unpubl. Ph.D. thesis, University of Durham.
- SAETHER, E., 1957. The alkaline rock province of the Fen area in southern Norway. *Det. Kgl. Norske Vidensk. Selskabs Skrifter*, 1.
- SATO, M. and WRIGHT, T.L., 1966. Oxygen fugacities directly measured in volcanic glasses. *Science*, 153, 1103-1105.
- SHAW, H.R., 1972. Viscosities of magmatic silicate liquids: an empirical method of prediction. *Am. J. Sci.*, 272, 870-893.

- SHAW, H.R., 1974. Diffusion of H<sub>2</sub>O in granitic liquids: pt.I experimental data; pt.II mass transfer in magma chambers. In Hofmann, A.W., Giletti, B.J., Yoder, H.S. and Yund, R.A. (Eds.), *Geochemical transport and kinetics*, 139-170. Carnegie Institute of Washington, publication 634.
- SIMKIN, T. and SMITH, J.V., 1970. Minor element distribution in olivine. *J. Geol.*, 78, 304-325.
- SIMMONS, E.C., LINDSLEY, D.H. and PAPIKE, J.J., 1974. Phase relations and crystallization sequence in a contact-metamorphosed rock from the Gunflint Iron Formation, Minnesota. *J. Petrology*, 15, 539-565.
- SMITH, J.V., 1959. Graphical representation of amphibole compositions. *Am. Miner.*, 44, 437-440.
- SMITH, J.V., 1974. *Feldspar minerals*, Vols. 1 and 2. Springer Verlag, Berlin, Heidelberg, New York.
- SMITH, J.V. and MUIR, I.D., 1958. The reaction sequence in larvikite feldspars. *Zeit. Krist.*, 110, 11-20.
- SMITH, P. and PARSONS, I., 1974. The alkali feldspar solvus at 1 kilobar water vapour pressure. *Mineral. Mag.*, 39, 747-767.
- SOBOLEV, U.S., BAZAROVA, T.Yu. and KOSTYUK, V.P., 1974. Inclusions in the minerals of some types of alkaline rocks. In Sørensen, H. (Ed.), *The alkaline rocks*, 389-401. John Wiley and Sons, London.
- SOBOLEV, V.S., BAZAROVA, T.Yu., SHUGAROVA, N.A., BAZAROV, L. Sh., DOLGOV, Yu.A. and SØRENSEN, H., 1970. A preliminary examination of fluid inclusions in nepheline, sorensenite, tugtupite and chkalovite from the Ilimaussaq alkaline intrusion, South Greenland. *Bull Grønlands geol. Unders.*, 81.
- SOOD, M.K. and EDGAR, A.D., 1970. Melting relations of undersaturated alkaline rocks. *Meddr. Grønland*, 181, 12.
- STEENSTRUP, K.J.V. and KORNERUP, A., 1881. Beretning om expeditionen til Julianehaabs distrikt; 1876 *Meddr. Grønland*, 2, 1.

- STEPHENSON, D., 1972. Alkali clinopyroxenes from nepheline syenites of the South Qôroq Centre, South Greenland. *Lithos*, 5, 187-201.
- STEPHENSON, D., 1973. The petrology and mineralogy of the South Qôroq Centre, Igaliko complex, South Greenland. Unpubl. Ph.D. thesis, University of Durham.
- STEPHENSON, D., 1974. Mn and Ca enriched olivines from nepheline syenites of the South Qôroq Centre, South Greenland. *Lithos*, 7, 35-41.
- STEPHENSON, D., 1976. A simple shear model for the ductile deformation of high level intrusions in South Greenland. *J. Geol. Soc. Lond.*, 132, 307-318.
- STEWART, J.W., 1964. The earliest Gardar igneous rocks of the Ilimaussaq area, South Greenland. Unpubl. Ph.D. thesis, University of Durham.
- STEWART, J.W., 1970. Precambrian alkaline-ultramafic/carbonatite volcanism at Qagssiarssuk, South Greenland. *Bull. Grønlands geol. Unders.*, 84, also *Meddr. Grønland*, 186.4.
- STORMER, J.C., 1973. Calcium zoning in olivine and its relationships to silica activity and pressure. *Geochim. Cosmochim. Acta*, 37, 1815-1821.
- STORMER, J.C. and CARMICHAEL, I.S.E., 1971. The free-energy of sodalite and the behaviour of chloride, fluoride and sulphate in silicate magmas. *Am. Miner.*, 56, 292-306.
- SUTHERLAND, D.S., 1969. Sodic amphiboles and pyroxenes from fenites in East Africa. *Contr. Mineral. Petrol.*, 24, 114-135.
- SUTTON, J., 1973. Some changes in continental structure since early Precambrian times. In Tarling, D.H. and Runcorn, S.K. (Eds.), *Implications of continental drift to the earth sciences*, 1071-1081. Academic Press, London and New York.
- SØRENSEN, H., 1962. On the occurrence of steenstrupine in the Ilimaussaq massif, S.W. Greenland. *Bull. Grønlands geol. Unders.*, 32, also *Meddr. Grønland*, 167,1.

- SØRENSEN, H., 1974. Alkali syenites, feldspathoidal syenites and related lavas. In Sørensen, H. (Ed.), The alkaline rocks, 22-52. John Wiley and Sons, London.
- THOMPSON, A.B., 1973. Analcime: free-energy from hydrothermal data. Implications for phase equilibria and thermodynamic quantities for phases in  $\text{NaAlO}_2\text{-SiO}_2\text{-H}_2\text{O}$ . *Am. Miner.*, 58, 277-286.
- THOMPSON, J.B. and WALDBAUM, D.B., 1969. Mixing properties of sanidine crystalline solutions. III. Calculations based on two-phase data. *Am. Miner.*, 54, 811-837.
- THOMPSON, R.N. and MACKENZIE, W.S., 1967. Feldspar-liquid equilibria in peralkaline acid liquids: an experimental study. *Am. J. Sci.*, 265, 714-734.
- THORNTON, C.P. and TUTTLE, O.F., 1960. Chemistry of igneous rocks: pt.1, Differentiation Index. *Am. J. Sci.*, 258, 664-684.
- TILLEY, C.E., 1954. Nepheline-alkali feldspar paragenesis. *Am. J. Sci.*, 252, 65-75.
- TILLEY, C.E., 1958. Problems of alkali rock genesis. *Quart. J. Geol. Soc. Lond.*, 113, 323-360.
- TUTTLE, O.F. and BOWEN, N.L., 1958. Origin of granite in the light of experimental studies in the system  $\text{NaAlSi}_3\text{O}_8\text{-KAlSi}_3\text{O}_8\text{-SiO}_2\text{-H}_2\text{O}$ . *Geol. Soc. Am. Mem.*, 74.
- TUTTLE, O.F. and SMITH, J.V., 1958. The nepheline-kalsilite system: pt.II, phase relations. *Am. J. Sci.*, 256, 571-589.
- UPTON, B.G.J., 1960. The alkaline igneous complex of Kûngnât Fjeld, South Greenland. *Bull. Grønlands geol. Unders.*, 27, also *Meddr. Grønland*, 123, 4.
- UPTON, B.G.J., 1964a. The geology of Tugtutôq and neighbouring islands, South Greenland. Part II. Nordmarkitic syenites and related alkaline rocks. *Bull. Grønlands geol. Unders.*, 44, also *Meddr. Grønland*, 169, 2.
- UPTON, B.G.J., 1964b. The geology of Tugtutôq and neighbouring islands. Part IV. The nepheline syenites of the Hviddal composite dyke. *Bull. Grønlands geol. Unders.*, 48, also *Meddr. Grønland*, 169, 3, 50-80.

- UPTON, B.G.J., 1971. Melting experiments on chilled gabbros and syenogabbros. *Ann. Rept. Geophys. Lab. Yearbook*, 70, 112-118.
- UPTON, B.G.J., 1974. The alkaline province of Southwest Greenland. In Sørensen, H. (Ed.), *The alkaline rocks*, 221-238. John Wiley and Sons, London.
- UPTON, B.G.J., THOMAS, J.E. and MACDONALD, R., 1971. Chemical variation within three alkaline complexes in South Greenland. *Lithos*, 4, 163-184.
- USSING, N.J., 1894. Mineralogisk-petrografiske Undersøgelser af Grønlandske Nefelinsyeniter og beslaegtede Bjaergarter. Anden del: De Kiselsyrefattige Hovedminerdes. *Meddr. Grønland*, 14, 1.
- USSING, N.V., 1912. Geology of the country around Julianehaab, Greenland. *Meddr. Grønland*, 38.
- VAN BREEMEN, O., AFTALION, M. and ALLAART, J.H., 1974. Isotopic and geochronological studies on granites from the Ketilidian mobile belt of South Greenland. *Bull. Geol. Soc. Am.*, 85, 403-412.
- VON ECKERMANN, H., 1948. The alkaline district of Alno island, *Sver. Geol. Unders.*, 36.
- WALTON, B.J., 1965. Sanerutian appinitic rocks and Gardar dykes and diatremes, north of Narssarssuaq, South Greenland. *Bull. Grønlands geol. Unders.*, 57, also *Meddr. Grønland*, 179, 9.
- WASHINGTON, H.S. and MERWIN, H.E., 1927. The acmitic pyroxenes. *Am. Mineral.*, 12, 233-252.
- WATT, W.S., 1966. Chemical analyses from the Gardar igneous province, South Greenland. *Rapp. Grønlands geol. Unders.*, 6.
- WEGMANN, C.E., 1938. On the structural divisions of southern Greenland. *Meddr. Grønland*, 113,2.
- WELLMAN, T.R., 1970. The stability of sodalite in a synthetic syenite plus aqueous chloride fluid system. *J. Petrology*, 11, 49-71.

- WHITTAKER, E.J.W., 1968. Classification of the amphiboles. Min. Soc. I.M.A. vol. (I.M.A. papers and proc. 5th gen. meeting, Cambridge 1966), 232-242.
- WIDENFALK, L., 1972. Myrmekite-like intergrowths in larvikite feldspars. Lithos, 5, 255-267.
- WILKINSON, J.G.F., 1965. Some feldspars, nephelines and analcimes from the square top intrusion, Nundle, N.S.W. J. Petrology, 6, 420-444.
- WINCHELL, A.N., 1951. Elements of optical mineralogy: pt.II, descriptions of minerals. John Wiley and Sons, London.
- WONES, D.R., 1972. Stability of biotite: a reply. Am. Miner., 57, 316-317.
- WONES, D.R. and EUGSTER, H.P., 1965. Stability of biotite: experiment, theory and application. Am. Miner., 50, 1228-1272.
- WOOLLEY, A.R., 1969. Some aspects of fenitization with particular reference to Chilwa Island and Kangankunde, Malawi. British Museum (Nat.Hist.) Bull. 2, 189-219.
- WOOLLEY, A.R., SYMES, R.F. and ELLIOTT, C.J., 1972. Metasomatized (fenitized) quartzites from the Borralan Complex, Scotland. Mineral. Mag., 38, 819-836.
- YAGI, K., 1953. Petrochemical studies on the alkali rocks of the Morutu district, Sakhalin. Bull. Geol. Soc. Am., 64, 769-810.
- YAGI, K., 1966. The system acmite-diopside and its bearing on the stability relations of natural pyroxenes of the acmite-diopside series. Am. Miner., 51, 976-1000.
- YODER, H.S., STEWART, D.B. and SMITH, J.R., 1957. Ternary feldspars. Ann. Rept. Geophys. Lab. Yearbook, 56, 206-217.

